THE DIFFUSION OF AVIATION FUEL AND WATER IN POLYSULPHIDE SEALANTS

A thesis submitted to the
Council for National Academic Awards
in partial fulfilment of the
requirements for the degree of
Doctor of Philosophy

by

M.M.S.Gick M.A., Grad.PRI

The London School of Polymer Technology
The Polytechnic of North London
Holloway Road
London

Collaborating Establishment:
Royal Aircraft Establishment
Farnborough
Hants

April 1988

PN 6215508 3

ABSTRACT

The diffusion of aviation fuel and water in polysulphide sealants

by M.M.S. Gick

The diffusion and permeation of aviation fuel (Avtur) and water in commercial and 'model' polysulphide sealants have been studied using simple gravimetric techniques.

For Avtur, the mass uptake behaviour is explicable in terms of normal, Fickian diffusion, and the diffusion coefficient determined has been found to be independent of the experimental method and concentration of the liquid.

Water, however, exhibits anomalous diffusion behaviour. Mass uptake by the polysulphides is high and equilibrium is not reached after several months. There is no correlation between the results of permeation, absorption and desorption experiments except at low water concentration.

These anomalies have been explained in terms of the formation of water droplets within the rubber. This study shows that the amount of water absorbed is dependent upon the amount and nature of the curing agent residues. The results have been analysed in terms of the osmotic and water vapour pressure and two equations have been derived which satisfactorily predict the amount of water absorbed at equilibrium.

It has been shown that the effect of the water droplets on permeation is negligible, and hence the diffusion coefficient found is a measure of the true rate of diffusion. In contrast, the effect of the droplets on mass uptake experiments is large and the apparent overall diffusion rate is greatly reduced. The apparent diffusion coefficient found is dependent upon the water concentration and the concentration of the water-soluble impurities. An equation has been derived showing the relationship between these variables.

The results of this work show that the elastic strength of the rubber has negligible effect in determining the water uptake at equilibrium and the apparent diffusion coefficient. However, deterioration in adhesive and cohesive strength occurs with water uptake. At high uptake some of this loss is irreversible. The deterioration in properties is mainly due to breakage of weak physical bonds and plasticisation effects.

Advanced studies undertaken in connection with the programme of research in partial fulfilment of the requirements of the degree:

1. a course of postgraduate lectures and tutorials on the following subjects:
   viscoelasticity
   rubber elasticity
   fracture mechanics
   adhesion

2. a course of guided study on diffusion

3. attendance at a conference, organised by Network Events, entitled Adhesives, Sealants and Encapsulants, held at the Kensington Exhibition Centre, London on 5-7th November, 1985

4. attendance at a conference, organised by the Plastics and Rubber Institute, entitled Diffusion Polymers, held at the City Conference Centre, London on 8-9th January, 1986.

ACKNOWLEDGEMENTS

Firstly, I should like to express my thanks to Dr. E. Southern, Dr. W.H. Burgar and Dr. P. Wilford for all their help and encouragement in this work.

I should also like to thank Dr. D.W. Aubrey for his patience and advice, particularly on problems of adhesion, and Dr. A. Haynes for many useful discussions.

I should like to thank all the technicians of L.S.P.T. for their assistance, with especial reference to the Research technician, Mr. Gayapersad, for his help in constructing equipment, and Miss Kotiyan for the microphotographs.

I should like to express my gratitude to the Procurement Executive, Ministry of Defence, for funding this project.

Lastly, I should like to thank my family for the cheerful way they have accepted a part-time wife and mother during the course of this work.

CONTENTS

CHAPTER 1: INTRODUCTION AND SURVEY OF THE LITERATURE

1.1. INTRODUCTION 1

1.2. POLYSULPHIDE RUBBERS 3

1.2.1. Introduction to polysulphide rubbers 3
1.2.2. Manufacture of polysulphides 4
1.2.3. Preparation of sealants 5
1.2.4. Curing of liquid polysulphides 6
1.2.5. Properties of cured liquid polysulphide rubbers 8
1.2.6. Labile linkages in cured polysulphide rubbers 8

1.3. SWELLING AND SOLUBILITY OF SOLVENTS IN RUBBER 9

1.3.1. Mechanism of swelling of rubber by solvents 9
1.3.2. Theory of swelling of rubber by solvents 10
1.3.3. Factors affecting solubility of solvents in rubbers 11
1.3.4. Swelling and solubility of solvents in polysulphide rubbers 13

1.4. DIFFUSION OF SOLVENTS IN RUBBERS 14

1.4.1. Introduction to diffusion of solvents in rubbers 14
1.4.2. Mechanism of diffusion of solvents in rubbers 14
1.4.3. Fundamental considerations of diffusion 15
1.4.4. Mathematics of diffusion 20
1.4.5. Types of diffusion coefficient 24

1.5. FACTORS AFFECTING THE DIFFUSION OF SOLVENTS IN RUBBERS 29

1.5.1. Effect of nature of diffusant on the diffusion of solvents in rubbers 29
1.5.2. Effect of nature of the rubber on the diffusion of solvents in rubbers 31
1.5.3. Effect of filler on the diffusion of solvents in rubbers 32

1.6. PERMEATION 33

1.7. DIFFUSION OF WATER IN RUBBER 34

1.7.1. Introduction to diffusion of water in rubbers 34
1.7.2. Mechanism of diffusion of water in rubbers 37
1.7.3. Theory of diffusion of water in rubbers 37
1.7.4. Factors affecting the rate of diffusion of water in rubbers 41
1.7.5. Factors affecting the equilibrium uptake of water 43
1.7.6. Water absorption by polysulphide rubbers 45

1.8. MEASUREMENT OF DIFFUSION AND PERMEATION COEFFICIENTS 46

1.8.1. Introduction to measurement of diffusion and permeation coefficients 46
1.8.2. Measurement of diffusion coefficients 47
1.8.3. Methods of determining permeation coefficients 48

1.9. THEORETICAL BACKGROUND TO SOME OF THE EXPERIMENTAL TECHNIQUES USED 48

1.9.1. Rubber elasticity 48
1.9.2. Stress relaxation 51

1.10. AIMS OF THIS PROJECT 53

CHAPTER 2: PROCEDURE

2.1. MATERIALS 54

2.1.1. Polysulphides 54
2.1.2. Curing agents 55
2.1.3. Solvents 56
2.1.4. Dessicants 57

2.2. SAMPLE PREPARATION 57

2.2.1. Preparation of samples from sealant solution 57
2.2.2. Preparation of PR1422 with filler removed 59
2.2.3. Preparation of test squares 59
2.2.4. Cold solvent extraction 59

2.3. MEASUREMENT OF MASS UPTAKE BY POLYSULPHIDES 61

2.3.1. Measurement of mass uptake of liquids by polysulphide films 61
2.3.2. Measurement of mass uptake of vapour by polysulphide films 62
2.3.3. Measurement of mass uptake of water by liquid polysulphides 63
2.3.4. Measurement of desorption of liquid from polysulphide films 63
2.3.5. Calculation of D from mass uptake measurements 64
2.3.6. Calculation of water concentration C_w 65

2.4. MEASUREMENT OF PERMEATION RATES 65

2.5. LAMINATE STACKS 67

2.6. BONDED SAMPLES 68

2.7. TESTING OF PHYSICAL PROPERTIES 69

2.7.1. Determination of moduli 70
2.7.2. Determination of peel strength 70
2.7.3. Determination of hysteresis 71

2.7.4. Determination of stress relaxation 71
2.7.5. Determination of resilience 71
2.7.6. Determination of glass transition temperature 71

CHAPTER 3: TRANSPORT OF AVIATION FUEL IN A COMMERCIAL POLYSULPHIDE

3.1. INTRODUCTION TO MASS UPTAKE EXPERIMENTS USING AVIATION FUEL 72

3.1.1. Presentation of data 72
3.1.2. Effect of sample thickness on aviation fuel uptake 73
3.1.3. Extraction of sheets of PR1422 75
3.1.4. Equilibrium swelling of PR1422 by Avtur 76
3.1.5. Determination of diffusion coefficient for aviation fuel in PR1422 79
3.1.6. Mass uptake of Avtur by nitrile rubber 83
3.1.7. Comparison of the uptake of Avtur with the uptake of other solvents in PR1422 85
3.1.8. Constrained samples 88
3.1.9. Effect of temperature on the mass uptake of aviation fuel in PR1422 89
3.1.10. Effect of filler on absorption of aviation fuel 92
3.1.11. Concentration profiles 96

3.2. PERMEATION OF AVIATION FUEL THROUGH PR1422 98

3.2.1. Permeation results 98
3.2.2. Correlation of diffusion and permeation data 101

3.3. SUMMARY OF THE RESULTS OBTAINED FOR THE TRANSPORT OF AVIATION FUEL IN PR1422 102

CHAPTER 4: PILOT STUDIES OF UPTAKE OF WATER FROM LIQUID AND VAPOUR PHASE BY VARIOUS POLYSULPHIDES

4.1. MASS UPTAKE OF WATER VAPOUR BY LIQUID POLYSULPHIDES 105

4.2. EXPERIMENTS ON THE MASS UPTAKE OF WATER BY POLYSULPHIDE RUBBERS FROM WATER 107

4.2.1. Mass uptake of water by polysulphides 107
4.2.2. Desorption of water from PR1422 111
4.2.3. Materials leached from PR1422 during immersion in water 113
4.2.4. Effect of filler on mass uptake of water by PR1422 115

4.3. SUMMARY OF RESULTS 117

CHAPTER 5: THE EFFECT OF WATER ON THE PHYSICAL PROPERTIES OF PR1422

5.1. INTRODUCTION 119

5.2. VOID FORMATION 119

5.3. DIMENSIONAL CHANGES AFTER PROLONGED WATER IMMERSION 121

5.4. EFFECT OF WATER ON SHEAR MODULUS 121

5.4.1. Changes in shear modulus, G, of PR1422 containing different amounts of absorbed water 123

5.4.2. Effect of water on Mooney Rivlin C_1 and C_2 for PR1422 (filler removed) and cumene hydroperoxide cured LP32 128

5.5. INITIAL EXPERIMENTS ON THE EFFECT OF WATER ON ADHESIVE STRENGTH 132

5.6. EFFECT OF HIGH WATER UPTAKE ON OTHER PROPERTIES OF PR1422 134

5.6.1. Effect of water immersion on hysteresis 134

5.6.2. Stress relaxation 136

5.6.3. Effect of water uptake on resilience 138

5.6.4. Effect of water immersion on glass transition temperature 139

5.7. SUMMARY OF RESULTS 141

CHAPTER 6: THE UPTAKE OF WATER FROM 1% SALT SOLUTION BY PR1422

6.1. INTRODUCTION 142

6.2. MASS UPTAKE OF WATER FROM 1% SALT SOLUTION AT 25°C. 142

6.2.1. Effect of sample thickness on water uptake 142

6.2.2. Measurement of diffusion coefficient and equilibrium uptake 145

6.2.3. Measurement of D from desorption experiment 147

6.3. EFFECT OF TEMPERATURE ON ABSORPTION OF WATER BY PR1422 FROM 1% SALT SOLUTION 150

6.4. CONCENTRATION PROFILES 152

6.4.1. Comparison of mass uptake of water by laminate stacks and single sheet of PR1422 152

6.4.2. Determination of concentration profile 155

6.5. SUMMARY OF RESULTS 155

CHAPTER7: PILOT STUDIES OF THE PERMEATION OF WATER THROUGH PR1422

7.1. EFFECT OF EXPERIMENTAL METHOD 158

7.2. CALCULATION OF PERMEATION RATE, TIME-LAG, TIME-LAG DIFFUSION COEFFICIENT AND WATER CONCENTRATION 158

7.3. CORRELATION OF DATA FROM DIFFUSION AND PERMEATION EXPERIMENTS FOR THE TRANSPORT OF WATER IN PR1422 161

7.3.1. Correlation of water concentrations 161
7.3.2. Correlation of diffusion coefficients 162
7.3.3. Correlation of R and DC_w 163

7.4. EFFECT OF THICKNESS OF SHEET ON PERMEATION RATE (R) 164

7.4.1. Single sheet 164

7.5. LAMINATE STACKS 166

7.5.1. Permeation rate in laminate stacks 166
7.5.2. Water concentration distribution within the rubber sheet at the steady state 167

7.6. SUMMARY OF RESULTS 169

CHAPTER 8: EFFECT OF VARYING WATER VAPOUR PRESSURE UPON DIFFUSION AND PERMEATION OF WATER VAPOUR IN PR1422

8.1. INTRODUCTION 171

8.2. MASS UPTAKE OF WATER BY PR1422 FROM SATURATED WATER VAPOUR 171

8.3. MASS UPTAKE OF WATER BY PR1422 FROM WATER VAPOUR AT REDUCED WATER VAPOUR PRESSURES 173

8.3.1. Mass uptake measurements 173
8.3.2. Calculation of D at reduced water vapour pressure 175
8.3.3. Equilibrium uptakes and solubility of water at reduced water vapour pressure 176
8.3.4. Discussion of effects of varying external water vapour pressure on amount of water present in droplet form 179
8.3.5. Relationship between D and C_w 181

8.4. EFFECT OF VARYING WATER VAPOUR PRESSURE ON PERMEATION OF WATER IN PR1422 182

8.4.1. Measurement of permeation rate (R) 182
8.4.2. Permeation rates at reduced water vapour pressure 182
8.4.3. Calculation of time-lag diffusion coefficient (D_{TL}) at reduced water vapour pressure 186

8.5. CORRELATION BETWEEN DIFFUSION COEFFICIENT FROM VAPOUR PHASE AND PERMEATION DATA 187

8.6. SUMMARY OF RESULTS 190

CHAPTER 9: INITIAL EXPERIMENTS WITH 'MODEL' LP32

9.1. INTRODUCTION 191

9.2. EFFECT OF HYDROPHILIC IMPURITIES OTHER THAN CURING AGENT ON MASS UPTAKE OF WATER FROM SODIUM CHLORIDE SOLUTIONS BY LP32 WITH VARIOUS ADDITIVES 191

9.2.1. Mass uptake of water from 2% NaCl solution using model polysulphide systems 191
9.2.2. Effect of azeotrope extraction on mass uptake of water by model compounds 195
9.2.3. Comparison of CHP+DPG cured LP32 and CHP+DPG cured LP32 with added epoxide resin 195
9.2.4. Comparison of CHP+DPG cured LP32 and CHP+DPG cured LP32 containing 1phr sodium chloride 196
9.2.5. Discussion of effect of added hydrophilic material to CHP+DPG cured LP32 196

9.3. EFFECT OF CURING AGENTS ON MASS UPTAKE OF WATER FROM SODIUM CHLORIDE SOLUTIONS BY LP32 197

9.3.1. Comparison of mass uptake of water by 7.5phr sodium dichromate cured LP32 and CHP+DPG cured LP32 197
9.3.2. Comparison of mass uptake of water by LP32 cured with different dichromate salts 197

9.4. EFFECT OF FILLER ON WATER UPTAKE BY MODEL POLYSULPHIDE 201

9.5. SUMMARY OF RESULTS 201

CHAPTER 10: EXPERIMENTS USING LP32 WITH DICHROMATE CURING AGENTS: EFFECT OF VARYING WATER VAPOUR PRESSURE (OSMOTIC PRESSURE)

10.1. INTRODUCTION 202

10.2. MASS UPTAKE OF WATER FROM THE VAPOUR PHASE BY 7.5phr SODIUM DICHROMATE CURED LP32 203

10.2.1. Results of mass uptake of water by sodium dichromate cured LP32 from the vapour phase at reduced water vapour pressure 203
10.2.2. Effect of varying external water vapour pressure on D 205
10.2.3. Effect of varying RH on C_w 206

10.3. MASS UPTAKE FROM THE LIQUID PHASE WITH VARIED EXTERNAL OSMOTIC PRESSURE 210

10.3.1. Introduction 210
10.3.2. Results of mass uptake of water by 7.5phr sodium dichromate cured LP32 from NaCl solutions of different concentration 210

10.3.3. Comparison of results of mass uptake of water from liquid and vapour phase by 7.5phr sodium dichromate cured LP32 212
10.3.4. Relationship between C_w and concentration of NaCl soaking solution 213

10.4. MASS UPTAKE OF WATER BY LP32 - EFFECT OF VARYING INTERNAL OSMOTIC PRESSURE 217

10.4.1. Results of mass uptake of water by LP32 cured with different amounts of sodium dichromate 217
10.4.2. Results of mass uptake of water by LP32 with different dichromate curing agents 219
10.4.3. Comparison of extrapolation of results of C_w obtained for 7.5phr calcium dichromate cured LP32 and C_w found from mass uptake of water by PR1422 220

10.5. ANALYSIS OF EQUILIBRIUM CONDITIONS 221

10.5.1. Relationship between water concentration and osmotic forces 221
10.5.2. Estimation of solubility (s_o) of water in polysulphide rubber 225
10.5.3. Estimation of molar quantities of impurities 225

10.6. RELATIONSHIP BETWEEN TOTAL WATER CONCENTRATION AND DIFFUSION COEFFICIENTS 227

10.6.1. Introduction 227
10.6.2. Considerations of the relationship between D and C_w: application of Southern and Thomas equation 230
10.6.3. Further considerations of relationship between D and C_w 235

10.7. PERMEATION OF WATER VAPOUR AT VARYING PRESSURE THROUGH 7.5phr SODIUM DICHROMATE CURED LP32 237

10.7.1. Introduction 237
10.7.2. Results of permeation experiments at varying relative humidity (RH) for sodium dichromate cured LP32 240

10.8. EFFECT OF FILLER ON PERMEATION RATES 244

10.9. EFFECT OF INCREASING RH ON THE PERMEATION COEFFICIENT 249

10.10. SUMMARY OF RESULTS OF EXPERIMENTS USING DICHROMATE CURED LP32 WITH VARYING WATER VAPOUR PRESSURE 252

APPENDIX 10.A 253

APPENDIX 10.B 257

CHAPTER 11: CONCLUSIONS AND SUGGESTIONS FOR FURTHER WORK

11.1. CONCLUSIONS ON THE TRANSPORT OF AVIATION FUEL IN POLYSULPHIDE RUBBERS 265

11.2. CONCLUSIONS ON MASS UPTAKE OF WATER BY POLYSULPHIDES 266

11.2.1. Mass uptake from distilled water 266
11.2.2. Effect of the mass uptake of water on the physical properties of polysulphide rubber 266
11.2.3. Mass uptake from sodium chloride solutions and the vapour phase 267
11.2.4. Permeation of water in polysulphides 270

11.3 SUGGESTIONS FOR FURTHER WORK 271

11.3.1. Effect of polar solvents on physical properties 271
11.3.2. Reaction products 272
11.3.3. Direct measurement of s, the amount of water in true solution, in polysulphide rubbers 272
11.3.4. Measurement of the relative importance of factors leading to an increase in P with increasing relative humidity 272

REFERENCES 274

CHAPTER 1. INTRODUCTION AND SURVEY OF THE LITERATURE

1.1. INTRODUCTION

Sealants are widely used in industry, in particular in the construction and transport industries. In order to be effective, a sealant must have good chemical resistance, high adhesive and cohesive strength and also flexibility over a wide range of service conditions. One important use of sealants is in the sealing of aircraft fuel tanks.

Long-range, high power aircraft require great amounts of fuel and both space and weight are at a premium. In the early days of aviation, fuel was carried in 'bag tanks', which were generally large bags of neoprene rubber and were self-sealing. Modern aircraft, however, store fuel in integral fuel tanks i.e. part of the metal structure of the aircraft. This latter development led to the need for efficient sealing of rivetted metal parts.

Polysulphides are used as sealants in aircraft integral fuel tanks because of their high resistance to aliphatic hydrocarbon solvents and their flexibility over a wide temperature range. Although their resistance to aviation fuel is excellent, their resistance to water is only moderate. It is known that traces of free water are frequently present in fuel tanks due to operational conditions and that the resultant water penetration tends to result in a deterioration of the adhesive and cohesive properties of the

sealants. Further, it is known that at high temperatures penetration of aviation fuel has a deleterious effect upon the sealants. In both cases there is only a limited knowledge of the extent of penetration with respect to time, distance and temperature.

The main aim of this project is to gain a greater understanding of the diffusion and permeation of both water and aviation fuel into polysulphide sealants in general current use. The mechanism of aviation fuel transport in polysulphides is thought to be fairly straightforward, following the classical pattern. However the diffusion behaviour of water in rubbers has been found to be anomalous.

The amount of liquid absorbed at equilibrium by a rubber depends upon the solubility of the liquid in the rubber; the time to reach that equilibrium depends upon the rate of movement of the liquid molecules. These in turn depend upon the nature both of the diffusant and the rubber molecules. This work is thus concerned with both the amount of liquid absorbed, the rate of penetration and those factors which affect both the solubility and diffusion process.

Firstly the nature of polysulphide rubbers will be discussed, then relevant aspects of diffusion and permeation and finally physical properties.

1.2. POLYSULPHIDE RUBBERS

1.2.1. Introduction to polysulphide rubbers

An excellent review of polysulphide rubbers has been published by Bertozzi[1].

Current theories of water transport in rubbers stress that the amount of hydrophilic impurities play a major role in determining both the rate of diffusion and also the amount of water absorbed at equilibrium[2,3,4].

Since polysulphides are manufactured by suspension polymerisation, there may be residual impurities present from this process. Moreover, the curing agents for the polysulphides used in aircraft sealant formulations are based upon metal dichromates and chromates [5]. Therefore there will be a relatively large amount of hydrophilic material present in the cured system due to excess curing agent and curing agent residues. Further, sealants contain adhesion promoters (often epoxide or phenolic resins) which are generally polar, low molecular weight materials.

Because of the importance of the effect of impurities on the diffusion process in rubbers a brief outline of the manufacture, preparation and curing of polysulphide sealants is given in the next sections.

1.2.2. Manufacture of polysulphides

The liquid polysulphides used in sealants are almost exclusively based upon bis(2-chloroethyl)formal, $Cl\text{-}C_2H_4\text{-}O\text{-}CH_2\text{-}O\text{-}OC_2H_4\text{-}Cl$, as the main monomer. This is reacted with sodium polysulphide, Na_2S_x, in aqueous suspension to produce a polysulphide of high molecular weight[6]. A surfactant and a nucleating agent, generally magnesium hydroxide, are added to control the reaction.

$$nCl\text{-}R\text{-}Cl + nNa_2S_x \longrightarrow (\ \text{-}R\text{-}S_x\text{-}\ )n + 2nNaCl$$

where R is $C_2H_4\text{-}O\text{-}CH_2\text{-}O\text{-}C_2H_4$

The above polysulphide is then 'split', or desulphurised[7] to give the lower molecular weight liquid polymers. This process employs sodium sulphite and sodium hydrogen sulphide, which reduce some of the polysulphide groups to thiol and disulphide groups.

$$\sim RSSSR\sim + Na_2SO_3 \longrightarrow \sim RSSR\sim + Na_2S_2O_3$$

$$\sim RSSR\sim + NaSH \longrightarrow \sim RSH + NaSSR\sim$$

$$\sim RSSNa + Na_2SO_3 \longrightarrow \sim RSNa + Na_2S_2O_3$$

The result of the above process is to produce a polymer with RSNa terminal groups. The amount of reducing salts added determines the molecular weight of the resultant polymer. The

low molecular weight fraction is soluble in the aqueous phase but the higher molecular weight fraction forms a dispersion.

The mixture is then acidified, causing coagulation of the dispersed polymer and precipitation of the soluble polymer, which then equilibriate by a process of mercaptan and disulphide interchange to produce a more uniform molecular weight distribution. This process continues during washing, drying and storage of the liquid polymer.

The incorporation of small amounts of a trifunctional monomer, 1,2,3-trichloropropane, $C_3H_5Cl_3$, in the formulation leads to the formation of a branched chain polymer. Because of branching, a crosslinked polymer can be formed with greater physical strength.

1.2.3. Preparation of sealants

Polysulphide sealants used in the aircraft industry are two part room temperature vulcanising systems, comprising

a) a base and

b) a curing agent.

a) The base generally contains the liquid polymer, fillers, solvents and adhesion promoters. The filler most commonly used is chalk. Pigments and a little carbon black, to absorb ultra-violet radiation, are also commonly added.

Adhesion promoters most commonly used are phenolic resole

resins with active methylol groups and low molecular weight epoxide resins. These can slowly react with the mercaptan groups on the main chain. For example the epoxide may react as follows:

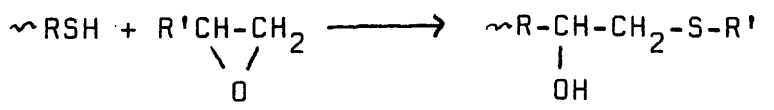

In general reactions of this type only occur to any extent at high temperature.

b) The curing agent is commonly a metal dichromate or chromate salt.

1.2.4. Curing of liquid polysulphides

The liquid polysulphides are cured to elastomeric solids by oxidation of the thiol terminal groups, commonly by the use of inorganic oxidising agents. Simplistically the cure reaction can be represented as:

The process of oxidation of the terminal thiol groups results in high molecular weight polymer chains. The various curing systems in common use have been discussed by Panek[8].

The development of dichromate curing agents has led to their

preferential use for cases where resistance to high temperatures is required, since they give efficient cross-linking without the formation of metal mercaptides, which block the reactive thiol terminal groups[9]. A recent study by Averko-Antonovich et al.[10], on dichromate cured systems, suggests that in addition to more effective cross-linking of low molecular weight fractions, co-ordination bonds are formed by complexing of chrome to sulphur or oxygen atoms in the main polymer chain. Sodium, potassium,calcium, zinc and ammonium chromates and dichromates are used in commercial sealants, generally in a paste with clay, dimethyl formamide and a little water.

The reaction mechanism is unclear, with several competing reactions. One reaction believed to be involved is:

$$6RSH + Cr_2O_7^{--} \longrightarrow 3RSSR + Cr_2O_3 + 2OH^- + 2H_2O$$

$$Cr_2O_7^{--} \longrightarrow 2Cr_2O_2^- + 3[O]$$

The oxide $Cr_2O_3.xH_2O$, is insoluble in water, but can form a range of complex hydrates. An excess of curing agent is used to ensure optimum properties, and hence unreacted chromates and dichromates, will also be present. In addition a range of complex amine derivatives can be formed, since dimethyl formamide is used as the solvent.

1.2.5. Properties of cured liquid polysulphide rubbers

Polysulphide rubbers show high resistance to swelling by solvents, the extent of resistance being primarily dependent upon the nature of the solvent and the cross-link density of the polymer. Many other physical properties are poor compared to other rubbers but for practical use they are enhanced by the use of additives, such as fillers, plasticisers, adhesion promoters and anti-oxidants. Some of these additives, together with the residues of curing agents, are hydrophilic in nature and will affect diffusion, particularly of water, in these rubbers.

1.2.6. Labile linkages in cured polysulphide rubbers

In common with other rubbers, polysulphides undergo a loss of stress when subjected to a constant strain particularly at elevated temperatures. This 'permanent set' is particularly high for polysulphides. (The converse, creep, which is increase in strain when exposed to constant stress is also very high). Both stress relaxation and creep are due to the viscous component of visco-elastic materials. See Section 1.9.

Tobolsky et al.[11,12,13] have shown that this is due to the labile nature of polysulphide linkages. For metal dioxide cured polysulphides the relaxation of stress was mainly due to mercaptide-disulphide interchange. With purified elastomers of known sulphur rank (the value of x in S_x) it

was found that the disulphide-disulphide bond was more stable than tri- and tetra-sulphidic crosslinks. Breakdown of disulphide linkages only occurred to a great extent at temperatures above 130°C.

However, studies of different curing systems showed that trisulphidic and tetrasulphidic links, (which were estimated from kinetic studies to be about 6% of the total polysulphidic linkages), were responsible for chemical stress relaxation at relatively low temperatures (about 90°C) in polysulphides with mainly disulphide bonds and no mercaptides[12].

It is believed that this bond lability will have an effect upon diffusion rates and the equilibrium uptake of liquids.

1.3. SWELLING OF RUBBER AND SOLUBILITY OF SOLVENTS IN RUBBER

1.3.1. Mechanism of swelling of rubber by solvents

Unlike linear polymers, crosslinked rubbers do not dissolve in solvents unless a breakdown of the structure occurs. They do however swell. Liquid/polymer interactions expand the chains from their unperturbed dimensions to an extent dependent upon the strength of these interactions. Gee[14] has suggested that swelling is due to a swelling pressure, akin to osmosis, which extends the three-dimensional network until the stresses are large enough to resist any further uptake of solvent. At this point equilibrium is reached and

no further swelling occurs.

1.3.2. Theory of swelling of rubber by solvents

Hildebrand and Scott[15] defined a solubility parameter, ∂, such that

$$\partial^2 = E/V \qquad (1.1)$$

E is the energy of vaporisation and V is the molar volume

They showed that in the absence of specific interactions, for example, hydrogen bonding,

$$\Delta H = V_m(\partial_1 - \partial_2)^2 \Phi_1 \Phi_2 \qquad (1.2)$$

where ∂_1 and ∂_2 are the solubility parameters and Φ_1 and Φ_2 are the molar volume fractions of the solvent and polymer respectively. V_m is the total volume of the mixture.

ΔH will approach zero as ∂_1 approaches the value of ∂_2. Mixing is thus more likely, as the process is then entropy driven.

Flory and Rehner [16] applied the theory of high polymer solutions and the statistical theory of rubber elasticity to relate the equilibrium volume swelling with the structure of the rubber. With a correction for entanglements[16a], then

$$\ln(1-v_2) + v_2 + \chi v_2^2 = NV_1(v_2^{(1/3)} - v_2/2) \qquad (1.3)$$

where V_1 is the molar volume of the solvent, χ is the solvent/polymer interaction parameter, N is the number of effective network chains per unit volume and v_2 is the

volume fraction of rubber in the swollen gel.

1.3.3. Factors affecting solubility of solvents in rubbers

There are three main factors affecting the solubility of solvents in rubbers. These are a) the solubility parameter of the rubber, b) the presence of filler and c) the effect of temperature.

a) solubility parameter

Generally rubbers swell more in solvents with a similar solubility parameter than in solvents of dissimilar one. Factors affecting the solubility parameter of a polymer include molecular weight, crystallinity, degree of crosslinking, polarity, chain flexibility, and branching. In this work the rubber used has a solubility parameter of 9.3-9.4 hildebrand[17] and hence swelling is greatest in solvents with a similar range, such as methyl ethyl ketone and chloroform. Aviation fuel which is predominantly aliphatic hydrocarbons of much lower ∂ would be expected to swell polysulphides only to a small extent.

b) filler

Filler content can have different effects. Most work has been done on the effect of filler on uptake of gases in rubbers. For natural rubber, with mineral fillers and non-reinforcing blacks, it has been found that no absorption of gas by the filler occurs and swelling by gases is related simply to the volume fraction of rubber present in the compound [18].

Barrer et al [19,20] accounted for changes in the uptake of propane by zinc oxide filled natural rubber by the presence of vacuoles at high loadings. At volume fractions of filler (zinc oxide) up to 0.2 they found a linear relationship between volume fraction of filler and the solubility of butane in a silicone rubber.

For liquids, however, the presence of filler has been found to suppress swelling of the rubber component. For hydrocarbon solvents, Kraus[21] studied the effect of carbon black on swelling of natural rubber and found that the volume swell of the filled rubber was related to the volume swell of the unfilled rubber by a factor involving the square of the volume fraction of filler.

Porter[22] studied uptake of decane by NR and compared the effect of different carbon black loadings. He determined the values of the constants a and b in a relationship derived by Lorenz and Parks[23]

$$v_{ro}(1-v_r)/v_r(1-v_{ro}) = a\,e^{-z} + b \qquad (1.4)$$

in which z is the weight of black per unit weight of rubber and a and b are constants. v_r and v_{ro} are volume fraction of rubber with respect to filler and solvent respectively.

c) temperature

The effect of temperature on the amount of swelling of rubbers by liquids depends mainly upon the heat of solution.

The heat of solution is due to both the heat of condensation and the heat of mixing. The former is the latent heat of vapourisation, and the heat of mixing can be estimated from the Hildebrand and Scott equation (1.2). Where the heat of solution is negative, as for many vapours, solubility decreases with rising temperature. For most liquids solubility increases with temperature, as the heat of mixing is the decisive factor and this is usually positive, and in most cases this solution effect outweighs any effect due to increases in elastic forces resisting swelling.

1.3.4 Swelling and solubility of solvents in polysulphide rubbers

Stout has studied the effect of fuel on polysulphide sealants[24] and found that at high temperature 'sponging' of the rubber occurred.

Ramaswamy and Achary [25] have recently studied the effect of varying curing agents on the aviation fuel uptake of polysulphide sealants. They found that there was negligible difference in swelling at 30°C between manganese dioxide, lead dioxide and ammonium chromate cures. They concluded that the major factor in determining fuel resistance was the presence of sulphur in the main chain of the polymer which led to a high solubility parameter. They also concluded that small changes in cross-link density had negligible effect on hydrocarbon uptake.

Mueller [26] found that the solubility of a hydrocarbon fuel in a polysulphide rubber, Thiokol ST, increased with increasing temperature.

1.4. DIFFUSION OF SOLVENTS IN RUBBERS

1.4.1. Introduction to the diffusion of solvents in rubbers

Diffusion is the process by which matter is transported from one part of a system to another as a result of random molecular motion. Transport of a liquid or vapour through a polymer membrane takes place through a number of stages. Firstly penetrant molecules are sorbed at the surfaces to establish a concentration gradient throughout the membrane which leads to diffusion of the penetrant into the membrane. Equilibrium is set up rapidly between the external liquid or vapour and that in solution at the surface so that the rate controlling stage is the diffusion process.

1.4.2. Mechanism of diffusion of solvents in rubbers

The mechanism of diffusion for a compatible, low molecular weight solvent in rubber is well-understood [27]. Molecules can penetrate the rubber only after forming a true solution (and here the rubber is behaving like an organic liquid). Brownian motion of both the penetrant and segments of the rubber molecules are involved in the process of solution and diffusion. Movement of the solvent into the polymer occurs because of a concentration gradient.

It is assumed that, as a result of energy fluctuations within the rubber, 'holes' are being continuously formed and destroyed. The rate of diffusion (as expressed by D, the diffusion coefficient) will depend on the concentration of 'holes' large enough to receive penentrant molecules. A Boltzmann distribution of 'hole' size is assumed.

It is possible that immobilisation of the penetrant at a specific site for periods of time which are longer than a diffusion step and clustering of molecules can occur. The degree of immobilisation and the extent of clustering depends on the magnitude and nature of the interactive forces. Thus extra energy is needed for the penetrant molecules to break free from the cluster. This effect will tend to slow down the apparent diffusion rate, as found from D, and increase the amount of penetrant absorbed at equilibrium. The transport of water is an extreme example of this phenomenon and will be discussed in detail later.

1.4.3. Fundamental considerations of diffusion

In 1855 Fick, by analogy with Fourier's treatise on heat transfer[28], established the fundamental equations known as Fick's First and Second laws of diffusion[29]. The First Law is based on the premise that the rate of transfer of diffusant across a unit cross-sectional area, the flux , F, depends only upon the concentration gradient normal to the section. This can be expressed as:

$$F = -D dc/dx \qquad (1.5)$$

The Second Law expresses concentration, c, in terms of time, t, and distance, x. For one dimension it can be expressed thus:

$$dc/dt = D\ (d^2c/dx^2) \qquad (1.6)$$

The constant of proportionality, D, is known as the diffusion coefficient. D gives a measure of the rate at which concentration changes with time and distance.

For any particular problem Fick's laws need to be solved for the particular initial and boundary conditions. Crank [30] has determined solutions to these equations for a wide range of sample geometries and experimental conditions, these conditions, by analogy with solutions obtained for heat transfer by Carslaw and Jaeger[31]. Those relevant to this work are discussed later, in Section 1.4.4.

The diffusion coefficient has been defined as the constant of proportionality in $F=-Ddc/dx$. However, the diffusion coefficient is also a measure of the number of successive jumps of a molecule in unit time from one equilibrium position to another.

A complete theory of diffusion would give the magnitude of the diffusion coefficient as a function of concentration and temperature. Additionally, the diffusion coefficient should be in terms of the molecular dimensions of the components of the system or other easily measurable properties. Einstein[32] formulated two expressions for the diffusion

coefficient, D, in terms of the jump distance, ∂, the jump frequency, ψ, and the molecular friction constant, ξ.

$$D = \partial^2 \psi \qquad (1.7) \qquad\qquad \text{and} \quad D=RT/\xi \qquad (1.8)$$

The latter expression, using Stoke's law to calculate ξ, led to the Stokes/Einstein Equation

$$D = kT/6\pi\,\eta_m r \qquad (1.9)$$

where k is Boltzmann's constant, T is absolute temperature, η_m is the viscosity of the medium and r is the radius of the diffusant molecule.

This assumed that the diffusing molecules were like spheres and were small compared to the molecules in the medium.

Eyring [33] applied the theory of rate processes to diffusion to calculate the jump frequency. Using an expression derived for viscosity he obtained a similar relationship to the Stokes/Einstein equation, but pointed out that η should be the viscosity of the mixture.

The jump from one position to another can be regarded as the same as the passage of the system over a potential energy barrier. The probability (for one degree of freedom) that a molecule has sufficient energy to pass over this barrier is exp(-E/RT) where E is the potential energy. Modification of equation 1.7 to allow for 3 dimensions, together with probability considerations, have led to several theories,

based on energy or free volume considerations. Since all of them are mostly concerned with the effect of temperature (activation energy) they are only dealt with briefly below.

Eyring et al.[33] used energy considerations to obtain an expression for D in terms of the jump distance, ∂, and G^* the free energy of activation. One translational degree of freedom was assumed. This expression could then be related by the basic laws of thermodynamics to give the entropy of activation, S^*.

Assuming values of the jump distance to be equal to the diameter of the diffusant molecule, d, the values of S^* calculated were large and positive. Eyring attributed this to severing of intermolecular forces during the activation process.

Barrer disagreed with this and put forward the alternative explanation that the high entropies were due to large disturbances of the polymer matrix in the formation of the transition state. This explanation led to the development of a kinetic/statistical theory of diffusion usually referred to as the 'activated zone theory'.

This theory assumes that the activation energy for a jump is shared with the chain segments involved in the diffusion step as well as by the diffusing molecules. Hence more degrees of freedom are involved and these characterise the zone of activation. Barrer and Skirrow evaluated the number of

degrees of freedom for several gas/elastomer systems[34] and found values of the order of 20, showing that a large zone of activation is needed for one diffusion step.

Brandt[35] extended the theory to include intermolecular and intramolecular interactions in the diffusion step.

Another theory is based upon free volume considerations and is derived from applications of Bueche's fluctuating density theory[36], developed by Wilkens and Long[37] and later by Fujita et al[38,39].

An expression for the diffusion coefficient, which eliminates ξ in equation 1.8, depends upon the concentration of the diffusant in terms of the total free volume average per unit volume, the fractional free volume of the diluent and a measure of the minimum size of hole required for the diffusant molecule to move into. This diffusion coefficient is the thermodynamic diffusion coefficient.

Many of these quantities have not been measured for rubber.

Meares[40] utilised free volume theory to relate the activation energy with the cohesive energy density (CED) by assuming that the former is the energy needed to produce a cylindrical hole of cross-sectional area $\pi d^2/4$ large enough to accommodate a molecule of diffusant, of diameter d.

$$E_D = \pi d^2/4.No.CED \qquad (1.10)$$

No is Avogadro's number

1.4.4. Mathematics of diffusion

The solutions to Fick's laws detailed here are for the particular geometries and boundary conditions used in this thesis viz mass uptake by a plane sheet and permeation through a membrane.

a) diffusion in a plane sheet

$$dc/dt = D\, d^2c/dx^2 \qquad (1.6)$$

is the relevant form of Fick's second law, as the process of absorption can be considered one-dimensional; the bulk of the absorption takes place through the major surfaces and the direction of penetration is normal to these.

The sheet occupies the region $-\ell < x < \ell$ (here ℓ is half the total sheet thickness and x is 0 at the centre of the sheet) and is initially at uniform liquid concentration of c_0. The surfaces of the sheet are maintained at a diffusant concentration of c_∞. There are two alternative forms of the mathematical solution for these conditions.

<u>Solution 1a</u> gives c_t/c_∞ in the form of error functions. Integration from $x = -\ell$ to $x = +\ell$ and replacement of concentrations by the amount of liquid absorbed at time t (M_t) and infinite time (M_∞) gives:

$$M_t/M_\infty = 2(DT/\ell^2)^{\frac{1}{2}}[\pi^{-\frac{1}{2}} + 2\sum_{n=0}^{n=\infty}(-1)^n \text{ierfc } n\ell/(Dt)^{\frac{1}{2}}] \qquad (1.11)$$

At short times the infinite series in equation 1.11 is small

compared to $1/\pi^{\frac{1}{2}}$ so can be ignored. The expression then simplifies to:

$$M_t/M_\infty = 2(Dt)^{\frac{1}{2}}/\ell\pi^{\frac{1}{2}} \qquad (1.12)$$

It can be seen from equation 1.12 that a plot of M_t/M_∞ versus root time enables a value of D to be calculated.

<u>Solution 2a</u> gives c_t/c_∞ in terms of an exponential series, which on integration and replacement of concentration by the amounts of liquid absorbed becomes:

$$M_t/M_\infty = 1 - \sum_{n=0}^{n=\infty} 8/(2n+1)^2\pi^2 \quad \exp\left[-D(2n+1)\pi^2 t/4\ell^2\right] \qquad (1.13)$$

At long times the series converges rapidly so the expression can be simplified to:

$$M_t/M_\infty = 1-(8/\pi^2)\exp[-(\pi/4\ell^2)Dt] \qquad (1.14)$$

taking logarithms of both sides of equation 1.14 this becomes

$$\ln(1-M_t/M_\infty) = \ln(8/\pi^2) - Dt\pi^2/4\ell^2 \qquad (1.15)$$

Thus D can be found from a plot of $\ln(1-M_t/M_\infty)$ versus time using data from long time absorption.

Crank and Park[41] used the first 2 (n=0 and 1) terms of equation 1.13 to calculate the time to half the equilibrium uptake ($t_{0.5}$). They obtained the equation:

$$D = 0.1976\ell^2/t_{0.5} \qquad (1.16)$$

If equation 1.12 is used to obtain the value of the constant term then 0.1963 is found. This close agreement indicates that the simplifications taken in deriving equation 1.12 are not unreasonable.

If equation 1.14 is differentiated and logarithms taken, then a further method of determining D, utilised by Twiss and Carpenter[42], is obtained. A plot of $\ln(dM_t/dt)$ versus time is linear with slope $-D\pi^2/4\ell^2$. This has the advantage that M_∞ does not need to be determined, but does require a large amount of long term data in order that the gradient of the original mass uptake versus time plot is accurately determined.

b) diffusion in a semi-infinite medium

This entails the determination of D from initial stages of swelling of an infinite block of rubber. The rubber occupies the region $x>0$; the surface $x=0$ is maintained at a concentration c_∞ and the concentration of liquid in the rubber is initially c_0. The solution is:

$$M_t = 2(c_\infty - c_0)(Dt)^{\frac{1}{2}}/\pi^{\frac{1}{2}} \qquad (1.17)$$

where M_t is mass of liquid, per unit area, absorbed at time t

Since M_∞ is equal to $\ell(c_\infty - c_0)$, this is identical to equation 1.12. In the early stages therefore, uptake by plane sheet can be considered the same as that of an infinite block of rubber i.e. the thickness of the sheet has no effect on the mass uptake in the early stages of absorption.

c) diffusion coefficient from permeation measurements

The amount Q_t which passes through a membrane of thickness ℓ in time t is:

$$Q_t/\ell c_2 = Dt/\ell^2 - 1/6 - 2/\pi \sum_{1}^{\infty} (-1)^n/n^2 . \exp -Dn^2\pi^2 t/\ell^2 \qquad (1.18)$$

As t approaches infinity this reduces to approaching the line

$$Q_t = Dc_2(t-\ell^2/6D)/\ell \qquad (1.19)$$

A plot of Q_t against time asymptotes to a straight line with

i) an intercept on the time axis of L (time-lag), where $L=\ell^2/6D$, and

ii) a slope of Dc_2/ℓ.

Since c_2 is the concentration at the wet side of the membrane, it is the amount taken up by free sheet at equilibrium ie the amount of liquid soluble in the rubber. Hence D can be found by dividing the slope by the solubility.

Rogers et al.[43] have used

$$\ln(t^{\frac{1}{2}}Q_t)=\ln[2c(D/\pi)^{\frac{1}{2}}]-\ell^2/4Dt \qquad (1.20)$$

to determine diffusion coefficients from the non-steady state portion of the curve, by plotting $\ln(t^{\frac{1}{2}}Q_t)$ versus 1/t.

1.4.5. Types of diffusion coefficient

a) mutual and intrinsic diffusion coefficients

For any diffusion experiment measurements are made by finding the transference of diffusant across a particular section or by finding the concentration distribution with respect to a particular section.

In the classical experiment of measuring the interdiffusion of two liquids the volume on either side of the initial boundary remains constant. Crank calls this diffusion coefficient the mutual diffusion coefficient. For a sheet of rubber in a diffusant liquid the surfaces of the sheet form natural boundaries. Measurements are made relative to a section on one of which is the whole rubber component. The diffusion coefficient measured in this way, D_1^r is related to the mutual diffusion coefficient, D^v, and the volume fraction of the rubber, v_r, by:

$$D_1^r = D^v . v_r^2 \qquad (1.21)$$

Hartley and Crank[44] have proposed a more fundamental diffusion coefficient which takes into account 'mass flow' effects. These occur in any two component system if the molecules of component A are different in size to those of component B. Because of this, the transfer of molecules caused by purely random thermal motion, across a fixed frame of reference from component A will not be exactly the same as

that from component B. Since the volume of a section fixed relative to the apparatus is constant there must be a compensating mass flow of the whole solution. The intrinsic diffusion coefficient D_i is defined relative to a section across which no mass flow occurs. Then the values for the two components are related to D^V by

$$D^V = (1-v_r)(D_{iB}-D_{iA}) + D_{iA} \qquad (1.22)$$

where A and B are the two components.

Hartley and Crank suggest that for a polymer the intrinsic diffusion coefficient D_{iB} can be reasonably assumed to be negligible compared to the liquid so that D_{iB} is zero.

Several workers have suggested that intrinsic diffusion coefficients are no more fundamental than mutual diffusion coefficients[45-47].

b) thermodynamic diffusion coefficients

It has been suggested by a number of workers[44,48,49] that the driving force for diffusion is not the concentration gradient as proposed by Fick but the chemical potential gradient. For two immiscible liquids there is obviously a concentration gradient but no diffusion, and in some systems[50,51] there is evidence for diffusion against a concentration gradient. The diffusion coefficient defined in terms of the chemical potential is known as the thermodynamic

diffusion coefficient D_T.

Although Park[48] has pointed out that a thermodynamic diffusion coefficient cannot be used to explain the concentration dependence of the measured diffusion coefficient for polymer/solvent systems, the concept has been used successfully to explain the effect of crosslink density changes on the concentration dependence of the measured diffusion coefficient for some rubber/solvent systems[52].

Modern theories of the diffusion of water in rubbers rely heavily upon use of a thermodynamic diffusion coefficient to explain the anomalous diffusion behaviour[3].

The relation between the thermodynamic diffusion coefficient D_T and the measured diffusion coefficient D is:

$$D_T = D\ (d\ln c/d\ln a) \qquad (1.23)$$

here a is the activity of the diffusant and c is the concentration of the diffusant in mass per unit overall volume[48].

c) concentration and time dependent diffusion coefficients

The diffusion coefficient, D, discussed in sections 1.8.1. is a constant factor and independent of factors such as concentration, the polymer's pre-history and time. In addition, the frames of reference used in the calculation of D are constant and generally utilise movement of diffusant

through a unit cross-section normal to the plane of movement.

In practice, it is found that the diffusion of liquids in rubbers generally depends upon the concentration of the diffusant. This can perhaps be best understood in terms of free volume theory. As solvent enters the polymer plasticisation occurs; there is more free volume available for the chain segments which therefore can move more freely. Solvent molecules can thus move faster through the matrix and in general the concentration dependency is of the type that the diffusion coeffient increases as the concentration increases. Desorption is slower than absorption in this case.

In these instances the solution of the diffusion equation 1.35 has to be carried out by numerical means. Crank and Park[41] have developed a method for doing this and the subject has been reviewed by Crank[30], where many solutions are given for common forms of concentration dependency.

Boltzmann[53] has shown that even when D is a function of concentration the amount of diffusing material (M_t) is still proportional to the square root of time in the early stages of absorption. If equations 1.11-1.16 are used then in these cases the value of D found is an average over the range of concentration used. The differential diffusion coefficient (the diffusion coefficient between small changes of concentration) can be calculated from this average but for slight concentration dependency the difference between

differential and average diffusion coefficients is often very small[54].

Often where great concentration dependency is found the fundamental theoretical diffusion coefficient $D_{c=0}$ is determined by extrapolation of concentration versus diffusion coefficient data to zero concentration. Unfortunately this gives little help in predicting behaviour at higher concentration or of comparing different systems under practical conditions.

Most studies on swelling sheet or membrane ignored lateral swelling. This probably holds during the early stages when the unswollen centre of the sheet maintains area relatively constant. Hartley and Crank[44] related the the diffusion coefficient found to the mutual diffusion coefficient by :

$$D = D^{v} v_{r}^{2} \tag{1.24}$$

At high swelling, nearer to equilibrium, assuming isotropic swelling, Garrett and Park[55] suggested that the relationship was better represented by

$$D = D^{v} v_{r}^{2/3} \tag{1.25}$$

Unfortunately, this allows only for the change in surface area and not the accompanying changes in surface concentration.

For many rubbers where equilibrium uptake is high anomalous sigmoid curves have been noted in the early stages. Southern and Thomas[56] have shown that this is best explained in terms of a non-constant surface concentration and of variable stresses set up during swelling. Restraint of the samples eliminates these anomalies. The anomalous behaviour of very thin films has also been explained in terms of boundary layer resistance[57].

Time-dependent diffusion coefficients have been incorporated into approaches which envisage the diffusion process as controlled either by relaxation or diffusion rates[58]. If these are of the same order then anomalies result which have to some extent been satisfactorily corrected by incorporating one or more terms of the relaxation spectrum. For most rubbers this effect is noticeable only at high swelling. For polysulphide rubbers the labile nature of the main chain bonds[12] can lead to relaxation effects.

1.5. FACTORS AFFECTING THE DIFFUSION OF SOLVENTS IN RUBBERS

1.5.1. Effect of nature of the diffusant on the diffusion of solvents in rubbers

In general, it has been found that the diffusion coefficient decreases as the size of the diffusing molecule increases. Van Amerongen[18] measured diffusion coefficients for a wide range of vapours in rubbers, and found that this was so but was unable to obtain any quantitative relationship.

For a wide range of liquids in natural rubber it has been found[52] that there is excellent correlation between the diffusion coefficients and the viscosity of the liquid. A modified form of the Stokes/Einstein equation (1.9) is used:

$$\ln D = \ln(kT/6\pi r\eta_\ell) - v_r(\ln\eta_r - \ln\eta_\ell). \qquad (1.26)$$

η_ℓ and η_r are viscosity of the liquid and rubber respectively.

Prager and Long[59] found, for a series of paraffins in polyisobutylene, that an increase in branching and size of the molecule lowered the diffusion coefficient, the former more than the latter. They explained this in terms of minimum hole size. Aitken and Barrer[60] found a similar relationship for natural rubber and polyisobutylene ie that the addition of a methyl side group to the diffusant reduced the diffusion coefficient more than if tthe group was added to the end of the main chain. Auerbach et al.[61] found for a range of diffusants in several rubbers (NR,IIR, CR and NBR) that for the straight chain hydrocarbons the diffusion coefficient varied inversely as the molecular weight of the diffusant.

The solubility of the liquid has been found to have little effect on the diffusion rate, but a marked effect on permeability.

The viscosity (internal) of the rubber is generally reduced in the presence of compatible liquids. Hence diffusion increases with increasing concentration of diffusant since

the mobility of the rubber molecules is increased. The magnitude of these effects depends upon the temperature of the experiment and the glass transition temperature T_g of the rubber. This effect is slight at temperatures greater than 20°C above T_g where segmental mobility is already high, but most work on rubbers has been done at low concentration to minimise concentration dependent effects. Garrett and Park[55] have studied the diffusion of benzene at all concentrations in natural rubber, Buckley and Berger[62] have looked at a range of solvents at all concentrations in butyl rubber. In both these cases it was found that as diffusant concentration increased so did the diffusion coefficient.

Mueller[26] found that permeability of a range of solvents in Thiokol rubber increased with temperature. He found that the more hydrophilic solvents had a lower permeability coefficient than hydrocarbons.

Recently Koszinowski[63] has related the diffusion coefficients of n-alkanes in polyolefins, including EPDM, to the molar volumes of the alkanes.

1.5.2. Effect of nature of the rubber on the diffusion of solvents in rubbers

Free volume theory leads to the conclusion that the more segmental mobility possessed by the polymer chain, then the faster will be the diffusion rate. Since factors affecting

chain mobility, eg chain stiffening groups, bulky side groups and polar side group reactions, are factors affecting T_g it is perhaps not surprising to find that rubbers with a high T_g have lower diffusion coefficients than rubbers with low T_g for the same diffusant. Van Amerongen [64] has published the diffusion coefficients for decane in a wide range of rubbers and related these to $T-T_g$. Barrer et al.[20] have suggested that methyl side groups lead to a decrease in the rate of diffusion, whilst Auerbach et al.[61] have shown that the presence of double bonds in the rubber leads to an increase in the diffusion coefficient. Barrie and Platt[65] showed that rubbers which strain crystallised gave lower diffusion rates. The effect of the original molecular weight of the rubber has been found to be negligible[60]. The effect of increasing cross-linking has, as expected, been found to have a slight effect on the diffusion coefficient. Auerbach et al.[61] found that the diffusion coefficient decreased linearly as the inverse of the molecular weight between cross-links. Gan[66] related increasing crosslink density to a slight decrease in the uptake of hydraulic fluids in polysulphide rubbers.

1.5.3. Effect of filler on the diffusion of solvents in rubbers

The effect of filler on the diffusion coefficients is two-fold. If there is interaction of the diffusant with the filler particles then diffusion can be slowed[64]. If no interaction occurs then the main effect is to increase the

path length for diffusion hence slowing down rate by tortuosity. A review of diffusion in heterogeneous media[68] gives a rigorous mathematical treatment of the effect of fillers. For many cases a simple formula by Maxwell[69], which considers the filler particles as spheres, has been used to calculate the structural or tortuosity factor

$$D_f = D_o \left(2/(3-v_r)\right) \tag{1.27}$$

Work by Barrer[19] and Van Amerongen[18] has confirmed this formula for the diffusion of gases in rubbers where there is no gas absorption by the filler. Other structure factor relationships have been derived by Fricke[70], Bruggeman[71] and Meares[72] .

1.6. PERMEATION

Wroblewski [73] applied Fick's laws to the diffusion of gases in rubber and formulated a permeability equation relating the quantity of gas, Q, transmitted in unit time, across a membrane thickness 2ℓ, separating gases at pressures p_1 and p_2, to D and solubility, S:

$$Q = DS\,(p_1-p_2)/2\ell \tag{1.28}$$

Later a more fundamental relationship was derived[30],

$$P=DS \tag{1.29}$$

where P is the permeation coefficient.

D is a measure of the rate at which matter is transported and S the amount absorbed at equilibrium. Because permeation in rubbers depends upon both these factors it is not unusual to find instances where the diffusion coefficient for a particular liquid is relatively low but the permeation coefficient is high, and vice versa. A recent review of permeation in polymers details this [74].

Salame[67] has developed a structure/property correlation model for predicting the permeability of several gases in polymers.

Mueller [26] found that the permeability of a range of solvents, including benzene, was very low in Thiokol ST compared to CR, SBR and NBR rubbers. In all cases, he found that the permeability was proportional to the solubility squared.

Gan[66] studied the transport of hydraulic fluid in Thiokol ST with a range of curing agents and related crosslink density changes to permeation rates. Very slight differences were found.

1.7. DIFFUSION OF WATER IN RUBBER

1.7.1. Introduction to diffusion of water in rubbers

The anomalous diffusion behaviour of water has been noted since the late 19th century, when Obach [75] found that the

uptake of water by rubber and gutta percha from sea water was less than from fresh water. However, no meaningful explanation was proposed until 1927, when Lowry and Kohman[76] examined the effect of varying the vapour pressure of the external solution by means of saturated salts.They found that this was the major factor determining the amount of water taken up by the rubber. They found that plots of vapour pressure against mass uptake were linear up to about 65% relative humidity, whereafter deviations occurred and Henry's Law was no longer obeyed ie solubility was not directly proportional to vapour pressure at high vapour pressure. They therefore postulated that water, at high uptake levels, was present in two forms. Part of the water was in true solution as shown by the linear relationship with vapour pressure, and part was present in a non-soluble form. They also studied the effect of washing out impurities and of adding sodium chloride to a pre-washed sample. As expected, the washed samples took up less water.

Later, Taylor, Herriman and Kemp[77] extended this work by measuring concentration profiles of plied sheets of natural rubber. Using a gravimetric technique, they found that the concentration of water in the rubber decreased rapidly from the side exposed to saturated water vapour and then became linearly related to distance from the middle of the sheet to the dry side. Using Lowry and Kohman's data, they were able to show that their experimental concentration/distance curve was in agreement with the assumption that the water vapour pressure dropped linearly across the composite membrane.

Following this, Daynes[49] proposed that since water absorption by rubber containing impurities did not follow Fick's Laws, then the solutions to the diffusion equations were inappropriate. He suggested that osmotic pressure gradient rather than concentration gradient should be used in Fick's equations. However, since Lowry and Kohman had shown previously that d(RH)/dc was not constant this rendered solution of the problem complex.

However, later workers studying concentration dependent coefficients have used the solutions to Fick's equations and numerical methods have been developed to obtain the diffusion coefficient as a function of concentration from average diffusion coefficients[30].

Tester[78] was successful in obtaining a rate equation for the absorption of water by natural rubber in a nitrogen atmosphere. He pointed out that the effect of oxidative aging was to increase the the water uptake.

Current theories of the diffusion of water in polymers are based on considerations of the water soluble impurities present within the rubber. Natural rubber and emulsion polymerised synthetic rubbers contain hydrophilic impurities. In addition , vulcanising agents, fillers and other compounding ingredients can also lead to hydrophilic material being present within the rubber.

1.7.2. Mechanism of diffusion of water in rubbers

The mechanism is based on two assumptions:

1) the impurities are present in particulate form and evenly dispersed throughout the rubber

and

2) a small proportion of water is in true solution within the rubber.

When a rubber is immersed in water, the water is transported through the rubber via the mechanism outlined in section 1.5.1. for solvent diffusion. Water, on reaching the hydrophilic impurities, forms droplets of solution. The droplets act as sinks, which reduce the rate of diffusion but increase equilibrium uptake of water in the rubber. However, the rate is still diffusion controlled since diffusion only takes place in the rubber phase. Strong evidence for this can be found from studies showing that bound water at hydrophilic sites does not affect the steady state permeation flux[79,80]. The driving force is the osmotic pressure gradient and an apparent diffusion coefficient is obtained.

1.7.3. Theory of diffusion of water in rubbers

The above mechanism implies there is a non-uniform water distribution throughout the rubber prior to equilibrium uptake being reached. This is shown in Figure 1.1.

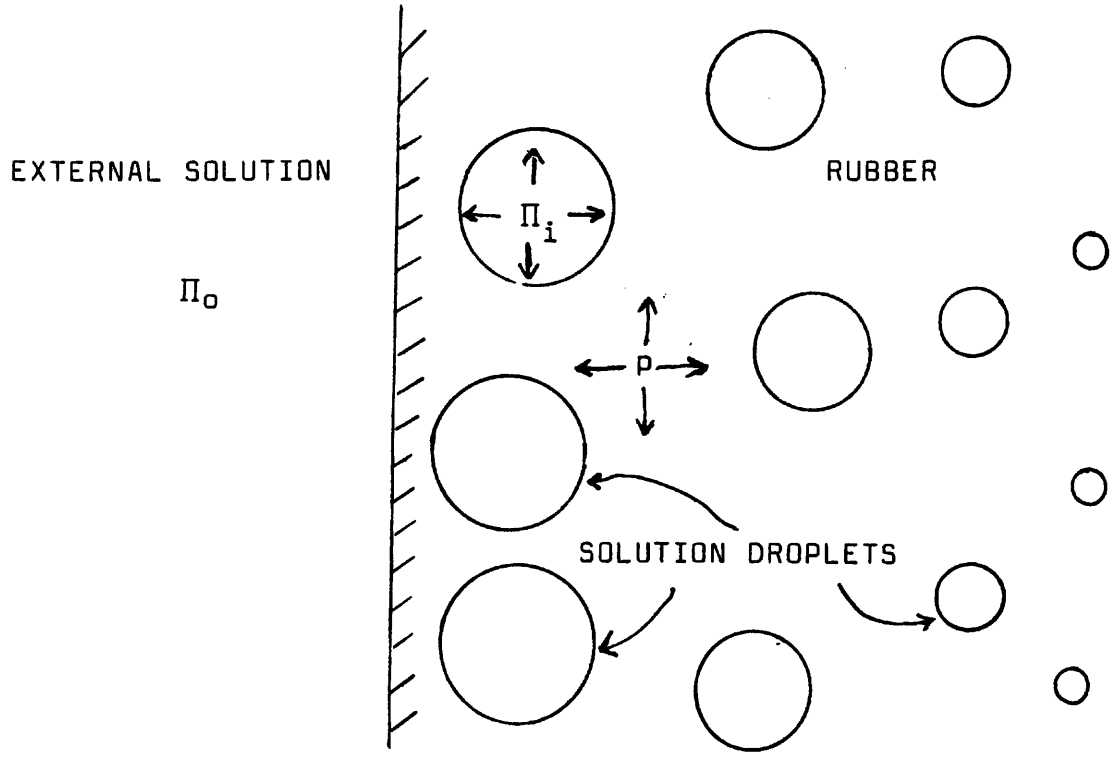

FIGURE 1.1

Showing forces within water droplet.

The rubber in the region surrounding the droplets is at a greater stress level compared with rubber containing no such droplets. Once solvation of a hydrophilic particle has occurred, water will continue to enter the droplet of solution until there is a balance between the elastic forces resisting expansion of the droplet and the osmotic forces tending to expand the droplet. The osmotic forces result from the difference in osmotic pressure between the external water phase and the droplet of solution within the rubber.

Briggs et al.[81] studied the high temperature absorption of water for a range of elastomers, including cis-polybutadiene. With this latter rubber they were able to quantify the effects of impurities on water uptake. Using cryogenic

techniques they proved the existence of water present in droplet form and estimated droplet size from depression of water freezing point. They proposed that the balance of forces at equilibrium could be represented by:

$$\pi_o = \pi_i - p \qquad (1.30)$$

where π_o and π_i are the osmotic pressures of the external and internal solutions respectively and p is the elastic pressure resisting droplet expansion.

Briggs used the inflation of a thick walled balloon as a model to predict the rubber pressure,p. However,although the balloon model does allow for a decrease in pressure at high extension and hence can qualitatively account for cases where no equilibrium is reached, later workers have tended to use solutions which more realistically model the droplet situation.

Solutions to the problem of enlargement of a spherical cavity in an infinite block of rubber have been given by Gent and Lindley[82] as:

$$p = G/2 \,.(5 - 4/\lambda - 1/\lambda^4) \qquad (1.31)$$

Hence

$$\pi_o = \pi_i - (G/2)(5-4/\lambda - 1/\lambda^4) \qquad (1.32)$$

where G is the shear modulus of the rubber, and λ is the extension ratio of the strained rubber around the droplets.

Equation 1.32 is only useful for extensions up to $\lambda \approx 3$.

Southern has used this theory to explain the water absorption of natural rubber[2] and has extended the theory to give an expression for the diffusion coefficient in terms of concentration of the occluded impurities.

$$D = D'S'\alpha C_i/(C_i+C_w)^2 \qquad (1.33)$$

where D' and S' are the diffusion coefficient and solubility for a rubber containing no impurities

C_i is the concentration of impurities in g/cc rubber

C_w is the concentration of water in g/cc rubber

α is an arbitrary constant

This assumes a linear dependence of the water concentration in the rubber on the concentration of occluded impurities. The equation also implies an inverse relationship between the diffusion rate and the square of the concentration of water (ignoring the concentration of impurity, C_i term on the denominator).

Recently a more rigorous treatment has been given by Thomas and Muniandy[3] which expresses both the kinetics and the equilibrium conditions in terms of the extension ratio.

Initially the impurity is present as particles of dry salt and osmosis does not play a part. In this case the rate of diffusion is fast as it is controlled solely by the transport throughout the rubber matrix. Subsequently water is absorbed by the salt particles to form droplets of solution. In the

early stages, the solution in the droplets will remain saturated with constant osmotic pressure and here the overall diffusion rate (as found from the apparent diffusion coefficient) is reduced as water enters the droplets rather than proceeds through the rubber. As the solution becomes more dilute (all impurity dissolved) the overall rate is reduced still more as now the elastic forces increase.

The theory satisfactorily predicts diffusion rates and equilibrium uptakes for water in natural rubber to which sodium chloride was added as a water-soluble impurity.

Evidence that the bulk of the water absorbed does not take part in the transport can be found in the work of Barrie, Machin and Nunn[80] who studied the steady state permeation of water in cis polyisoprene and natural rubbers seeded with salt. There was a large increase in water uptake compared to the unseeded samples but little change in the steady-state flux.

1.7.4. Factors affecting the rate of diffusion of water in rubbers

Factors which affect the diffusion coefficients for solvents in rubbers will also affect the rate of diffusion for water in a similar fashion e.g. higher crosslink density will lead to a lower rate of diffusion. However, in the case of diffusion of water in rubbers, these factors will be outweighed by even small amounts of water-soluble impurities. In general, the

diffusion coefficient of water is of the order of $10^{-14} m^2 s^{-1}$ for a wide range of rubbers.

The marked dependence of the diffusion coefficient upon the concentration of water in the rubber, of the type as water concentration increases, diffusion rate decreases, has been noted by several workers[2,3, 79]. In general, it has been found that reducing the vapour pressure of external soaking solutions leads to an increase in the diffusion coefficient and uptake of water from sea water is faster than from fresh water[76]. However, Patrick and Cassidy have found that for chloroprene the reverse is true[83].

Barrie and Machin [80] studied the steady state flux of water through silicone rubbers with and without added sodium chloride and found that the presence of impurities has little effect on diffusion rates as measured from permeation experiments. These reflect the transport of water through the matrix, since they are measured once a steady state is reached. Helander and Tolley have determined water vapour transmission rates for a range of rubbers, and found butyl rubber to give lowest and silicone highest permeability[84].

If fillers are hydrophilic then the rate of water uptake will be increased. One example of this has been reported recently[85] where it was found that active carbon black particles increased the water uptake rate of polyethylene cable insulators. The diffusion rate was found to vary inversely with filler loading.

Because the transport is diffusion controlled temperature dependence follows an Arrhenius type of equation.

1.7.5. Factors affecting equilibrium uptake of water

There is a very slight effect of factors which effect the equilibrium swelling of solvents such as T_g, polarity etc but again these are outweighed by factors due to the presence of impurities. For example, Briggs et al.[81] found that natural rubber and styrene butadiene rubber (which is emulsion polymerised and hence contains soaps etc) absorbed about 30 times as much water as solution polymerised EPDM and cis-polybutadiene.

The theory outlined in Section 1.7.3 implies that the equilibrium uptake will depend upon the osmotic forces, determined by the nature and amount of impurities present in the rubber, and the elastic forces. These latter depend upon the elastic modulus, G, of the rubber and the extension ratio of the rubber around the droplet at equilibrium, λ. This latter can be related to the concentration of water at equilibrium (C_w) and the concentration of impurities (C_i) thus:

$$\lambda^3 - 1 = \rho_i(C_w - s)/C_i \qquad (1.34)$$

here s is the amount of water truly soluble in the rubber and ρ_i is the density of the impurity.

Fedors[4] has published a method of predicting the

equilibrium uptake of water by rubbers based on knowledge of the modulus and solubility in water of occluded impurities. An osmotic approach has again been taken and Gent and Lindley's equation, equation 1.31, used to calculate pressure.

Temperature has very little effect on the equilibrium uptake. This may be due to the large contribution of the heat of vapourisation on the heat of solution, but considerations as in section 1.4.1. only describe the behaviour of the water in true solution in the rubber. From dilute solution theory the osmotic pressure is given by:

$$\pi = CRT/M \qquad (1.35)$$

where C is concentration of the solute in water, R is gas constant, T is absolute temperature and M is molecular weight of solute.

Substituting equation 1.35 for π, and rearranging, equation 1.32 becomes

$$C_o/M_o = C_i/(C_w - s)M_i - (G/2RT)(5 - 4/\lambda - 1/\lambda^4) \qquad (1.36)$$

Since $G = NkT$ the only temperature dependency is on s, the small amount of water in true solution, and the overall effect is negligible change with temperature.

In general uptake is lower from salt solutions, as has been reported from several studies[76,77] although Patrick and Cassidy have reported the reverse at certain temperatures from studies of chloroprene and nitrile rubber in sea water[83].

1.7.6. Water absorption of polysulphide rubbers

Only a little work has been published on the absorption of water by polysulphide rubbers. The effect of different curing systems over a range of temperatures has been studied by Russian workers[86], who found chromate cured polysulphides absorbed more water than manganese dioxide cured systems, which in turn absorbed more water than lead dioxide cured polysulphides. A study of the effect of hydrostatic pressure on similar systems has also been carried out[87]. In general the diffusion rate increased with increasing hydrostatic pressure.

Gan[66] has also studied the transport of water in a polysulphide rubbers, Thiokol ST, with a range of different curing agents, and determined activation energies for water diffusion at varying concentrations. He found the relationship between diffusion coefficient and concentration was complex, but in general the diffusion coefficient decreased with increasing water vapour pressure. He also found a very high water uptake on mass uptake experiments. In some cases no equilibrium uptake could be found. He attributed the low diffusion rates to clustering of water.

Recently, several papers have been published by the Australian Ministry of Defence[88,89] attributing the lack of attainment of equilibrium swelling to hydrolysis of the polysulphides. Various curing systems were studied over a range of temperatures.

1.8. MEASUREMENT OF DIFFUSION AND PERMEATION COEFFICIENTS

1.8.1. Introduction to measurement of diffusion and permeation coefficients.

Mass uptake diffusion experiments lead to determination of diffusion coefficients and solubility. Permeation experiments can lead to the determination of the diffusion coefficient, D, the permeation coefficient, P, and the solubility, S. In addition, the latter experiments can give two values of the diffusion coefficient by using

a) steady state data to give P and determining D from the relationship P=DS where S is found from a soaking experiment or the literature.

b) finding D from the time-lag (transient state data).

In theory, diffusion coefficients from mass uptake techniques and both sets of data from permeation experiments should be equal. In practice they often differ [27] and this difference can throw light on the visco-elastic behaviour of the polymer and on the type of concentration dependence present. For example, Barrer and Ferguson[90] found that the diffusion coefficient determined from a transient experiment was less than that found from a steady state measurement. They attributed the discrepancy to relaxation effects in the rubber. Similar differences have been found by others and for the case of hydrophilic liquids differences of orders of magnitude have been noted[27].

1.8.2. Measurement of diffusion coefficients

These have been reviewed[27,64,74], so only brief descriptions are given here. Transient methods are most commonly used. Much of the early work on the diffusion of vapours and gases in natural rubber [64] used the transient state data from membrane experiments. Concentration/ distance curves were used by Taylor et al.[77] who used a composite sheet of 8 rubber layers and a gravimetric technique. Gillespie and Williams used a similar method to study water absorption in cellulose[91]. Interferometer, Lamm scales and Moire fringes[58,92,93,94] have all been used to find concentration distance curves for transparent materials. Radiotracer methods have also been used[61]. Light intensity measurements using a simple inorganic dye have also been used for natural rubber[95]. Recently, fluorescence spectra[96] and small angle neutron scattering techniques have been carried out[97].

Several investigators have used absorption methods which used the extension of a quartz spring when exposed to vapour[98,99]; others have observed the changes in sample lateral dimensions on exposing sheet to liquid or vapour[62]. This method is not suitable for transparent rubbers, nor is it suitable when anisotropic swelling is present.

For a liquid, perhaps the easiest method is to obtain the amount absorbed by direct weighings and this is the main

method used in this work. This technique is widely reported in the literature[64,27]. Problems caused by sample thickness swelling and changing surface area associated with this technique have been discussed in Section 1.4.5.

1.8.3. Methods of determining permeation coefficients

These have been reviewed[27,74,100], so will be only briefly discussed here. The methods fall into two main categories - the permeation cell and the cup methods. Both are concerned with steady state transmission of vapour through a membrane.

In the permeation cell method changes in pressure on one side of the barrier membrane are monitored by pressure gauges and the flux recorded as a function of time.

In the cup method the amount of vapour transmitted is measured gravimetrically with respect to time, either by recording weight loss of liquid/vapour or by monitoring increase in weight of dessicants.

1.9. THEORETICAL BACKGROUND TO SOME OF THE EXPERIMENTAL TECHNIQUES USED

1.9.1. Rubber elasticity

Rubbers do not obey Hooke's law, except at very low strain, and stress/strain plots are not linear[101]. The Gaussian and

Mooney-Rivlin approaches are both attempts to explain the deviations from classical stress strain relationships.

The Gaussian theory was developed by Kuhn and is based, with several assumptions, on the statistical properties of randomly jointed chains undergoing deformation together with thermodynamical considerations of the entropy of individual chains and the free energy of deformation. For Gaussian plots, stress (force per unit area) plotted against $(1-1/\lambda^2)$, gives a straight line up to high extensions. λ is the extension ratio i.e. stretched length/original length. The slope of such a plot is G, the shear modulus. Deviations due mostly to entanglements (apparent extra cross-links) and the finite length of the chains occur at very high extension.

The Mooney-Rivlin theory is a phenomenological theory developed from the work of Mooney prior to the appearance of the Gaussian theory. Mooney derived from mathematical considerations of symmetry (assuming incompressibility and isotropy) a strain energy function expressed in terms of λ, and containing two constants C_1 and C_2. For simple extension differentiation with respect to λ then gives force/unstrained area in the form

$$f=2(\lambda-1/\lambda^2)(C_1+C_2/\lambda) \qquad (1.37)$$

A plot of $f/2(\lambda-1/\lambda^2)$ against $1/\lambda$ gives a straight line of slope C_2, intercept C_1. $G = 2(C_1 + C_2)$ at low strain. Since Rivlin expanded the work of Mooney to include all types of

strain the theory is generally known as Mooney-Rivlin.

Stress/strain testing can give details of cross-link density changes from analysis of Mooney-Rivlin plots since $G = NkT$, where N is the number of network chains per unit volume. At high strain it is thought that $G=2C_1$ rather than $G = 2(C_1+C_2)$ gives more realistic values. At high swelling ratios C_2 decreases almost to 0. Under these conditions it was thought that at low strain C_1 was the constant associated with cross-link density and C_2 was a measure of the deviations from ideality. It was thought that C_1 and C_2 were material constants. This is not now thought to be correct since the constants are not the same in compression. In this work both C_1 and C_2 are used to give estimate of G, the shear modulus, whilst C_1 and C_2 indicate the chemical and physical crosslinking respectively.

A straightforward stress/strain plot can give information about changes in Young's modulus and also hysteresis changes in rubbers.

By using the Flory-Rehner equation (equation 1.3) estimates of crosslink density can be obtained from swelling data if χ is known. Orwoll[102] has reviewed the methods of determining χ, and an equation derived by Bristow and Watson[103] can be used:

$$\chi = b + V_1/RT. (\delta_1 - \delta_2)^2 \qquad (1.38)$$

where b is a constant (0.34 for many rubbers), V_1 is the molar volume of the solvent and δ_1 and δ_2 are the

solubility parameters of the solvent and rubber respectively.

The modified form of the Flory-Rehner equation is

$$\ln(1-v_2) + v_2 + \chi v_2^2 = V_1 \rho / M_c \qquad (1.39)$$

M_c is the molecular weight between crosslinks

V_1 is molar volume of solvent

v_2 is volume fraction of rubber and ρ is the density

Alternatively, M_c can be found from stress/strain data, since N, the number of network chains per unit volume, is ρ/M_c and N can be found from G, since $G = N\kappa T$.

1.9.2. Stress relaxation

If a viscoelastic material is held at a fixed elongation then the stress decreases. An explanation of this can be made by considering separately the viscous and elastic components of viscoelasticity and postulating models incorporating both these. The simplest model is the Maxwell model with a spring and dashpot in series. A model consisting of several Maxwell elements in parallel approximates well to the behaviour of a real system and is shown schematically in Figure 1.3.

For one element, at constant elongation the stress on the system reduces as the dashpot, considered as a Newtonian fluid with a viscosity, η, slowly relieves stress.

$$\sigma = \eta d\epsilon/dt \qquad (1.40)$$

σ = stress

ϵ = strain

E = modulus

η = viscosity

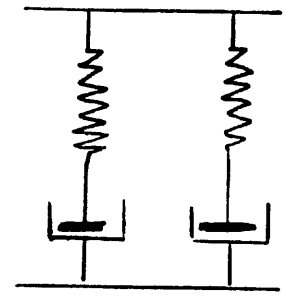

$E = \sigma_1/\epsilon_1$

$\eta = \sigma_2/(d\epsilon_2/dt)$

FIGURE 1.3. MAXWELL MODEL

Considering one element of Figure 1.3, since strain is constant, then

$$d\epsilon/dt = 0 \text{ and} \tag{1.41}$$

$$d\epsilon_1/dt + d\epsilon_2/dt = 0. \tag{1.42}$$

$$E^{-1}\, d\sigma/dt + \sigma/\eta = 0 \tag{1.43}$$

hence stress as a function of time ($\sigma(t)$) is given differentiation as

$$\sigma(t)/\sigma_0 = -Et/\eta \tag{1.44}$$

and E(t), the time dependent modulus is given by

$$E(t) = \sigma(t)/\epsilon_0 = E \exp(-Et/\eta) \tag{1.45}$$

For the system of several of these elements $E_T(t)$ is the summation of each separate term

$$E_T(t) = \sum E_i \exp(-t/\theta_i) \text{ where } \theta_i = \eta_i/E_i \tag{1.46}$$

The relaxation time can be found from plotting $\sigma(t)/\sigma_0$, or E(t) against ln time where the slope is the relaxation rate and the time for stress $\sigma(t)$ to fall to 1/e of its original value is taken as the stress relaxation time. This is an empirical method developed by Tobolsky[12].

1.10 AIMS OF THIS PROJECT

The main aim of this project is to gain a greater understanding of the transport behaviour of both water and aviation fuel into polysulphide sealants in current use. It is intended to investigate such behaviour over a range of temperature and concentration, in order to determine the effect of these variables on the diffusion coefficient, equilibrium uptake, and permeation rate.

The mechanism of diffusion of aviation fuel in polysulphides is thought to be fairly straightforward, following the classical pattern. Analysis of the data should thus be relatively simple. However, as a survey of the literature shows, the diffusion of water in rubbers is anomalous. It is proposed to initially analyse results in the light of the theories currently available for water uptake by rubbers, with possible modifications to incorporate the effects of the labile polysulphide bond system.

It is intended to study the factors affecting dependency of the diffusion coefficient (D) upon water concentration, and if possible to determine the relationship between

a) equilibrium uptake of water and D

and

b) equilibrium uptake, D and other variables inherent to the polysulphide system.

CHAPTER 2. PROCEDURE

2.1. MATERIALS

2.1.1. Polysulphides

Several commercial polysulphide sealants were obtained from B and K Resins Ltd. One of these, PR1422 was used for the bulk of the preliminary investigation. This material is available in several variations, including brushing or filleting grades, denoted by an A or B suffix, and various pot lives, denoted by a number suffix (pot life in hours at room temperature). PR1422 A2 was used since this is in current use by the RAF as a brushing grade sealant. It consists of a liquid polysulphide of nominal molecular weight 4000 and 1.9% by weight mercaptan (SH) content, a mixture of fillers and pigments (chalk, iron oxides and carbon black), epoxide resin, phenolic resin, stearic acid, toluene and methyl ethyl ketone. Stearic acid is used as a retardant and pot life can be varied by different amounts of this.

PR1750B has also been used in this work. It is a filleting grade having a slightly higher filler loading and less solvent and is based on a polysulphide with higher mercaptan (SH) content.

A range of liquid polysulphides were obtained from Morton Thiokol Ltd. These included LP32, LP12 and LP2. Their specifications are given in Table 2.1.

TABLE 2.1

Specifications of LP polymers

	LP12	LP32	LP2
viscosity poise 25°C	410-525	410-525	410-525
moisture %	0.27 max	0.27 max	0.3 max
thiol wt%	1.5-2	1.5-2	1.5-2
crosslinking sites %	0.2	0.5	2

Another liquid polysulphide, LP32C, a clarified version of LP32 with less impurities was also used.

2.1.2. Curing agents

A commercial curing agent for PR1422 A2 was obtained from B and K Resins Ltd. The active ingredient consists of a mixture of chromates and dichromates, predominantly calcium dichromate, but with traces of magnesium and sodium

dichromates. The compound is supplied as a paste with china clay and a little carbon black in dimethyl formamide and water. A mixing ratio of 1 part curing agent compound to 10 parts (by weight) was used.

For PR1750B the curing agent was a commercial paste of activated manganese dioxide in water. A mixing ratio of 1 part curing agent to 7.5 parts (by weight) of PR1750B was used.

Cumene hydroperoxide, obtained as a 80% solution in cumene, was used with both Analar zinc oxide and diphenyl guanidine to cure the LP series. General purpose grades (GPR) of sodium, ammonium and potassium dichromate were used with LP32C. All the above reagents were obtained from Aldrich Chemical Co.

GPR grades of zinc dichromate and calcium dichromate were obtained from Kodak Ltd.

2.1.3. Solvents

Avtur and Jet A aviation fuels were supplied by the Royal Aircraft Establishment. Both are a mixture of aliphatic and aromatic hydrocarbons, in the range C_7 to C_{15}. Jet A contains less additives, whilst Avtur contained de-icing agents and inhibitors.

Other solvents used were GPR grades obtained from BDH.

2.1.4. Desiccants

Silica gel with a cobalt chloride indicator was used for general sample desiccation. For desiccant trays used with the permeation apparatus molecular sieves of diameter size 40nm (for water absorption) and 130nm (for absorption of paraffins) were used. In addition, activated charcoal was used in desiccators to absorb paraffins. All were obtained from BDH.

2.2. SAMPLE PREPARATION

2.2.1. Preparation of samples from sealant solution

The sealant solution was mixed with the curing agent by hand, taking care not to entrap an excessive amount of air by stirring very slowly with a spatula for at least 10 minutes. The sealants were then spread on polytetrafluoroethylene (PTFE) sheet and placed in a vacuum desiccator for a further 10 minutes, to remove air and some of the solvents. The temperature and relative humidity of the laboratory was noted, although previous work[104] had shown that cure times for dichromate cured sealants were much less dependent upon relative humidity variations than manganese or lead dioxide curing systems.

Two methods were used to prepare sheets, one for thin samples and the other for thicker samples.

Thin films, of thickness 0.1mm to 0.2mm were produced by first spreading the sealants on PTFE sheet. The films were then allowed to reach a tack-free state, with most of the solvent evaporated, and were then pressed between stainless steel plates in a hydraulic hand-press for 24 hours. After experimentation with various spacers, it was found that thickness could be modified by both the amount of sealant spread out (by weight) and the pressure applied. In general, 35 grams and a pressure of $10MN/m^2$ was used.

Thicker sheets, of thickness 1.0mm to 1.5mm were prepared using a technique developed at RAE, Farnborough. A picture frame spacer mould was placed on PTFE covered steel plates and the sealant was spread using a dried compressed air line. Degassing was done in a vacuum dessicator. The mould was covered with a second PTFE lined steel plate and placed under slight pressure (until the pressure dial gauge just registered) for 24 hours.

Full cure of PR1422 does not take place until at least 6 weeks after application. In order to speed up the process a cure process of 3 days at room temperature followed by a week at 50°C was used. The prepared sheets were cooled and stored in a blackened dessicator to eliminate possible surface oxidation effects.

Toluene swelling tests were carried out to check that this cure process gave a similar product to the longer term room temperature cure. Previous curing processes at elevated

temperatures were abandoned as anisotropic sheets were produced.

2.2.2. Preparation of PR1422 with filler removed

Filler was removed by a centrifugation technique. Firstly samples of PR1422 were diluted with an equal amount by weight of methyl ethyl ketone. The diluted sealant was then centrifuged and the top layer poured into an evaporation dish. The precipitated filler was washed with methyl ethyl ketone to remove adsorbed sealant. After recentrifuging the washings were added to the dish which was then left at room temperature in a fume cupboard for 48 hours to allow most of the excess solvent to evaporate. The requisite amount of curing agent to react with the original weight of filled base was added and cured sheet produced as described above.

2.2.3. Preparation of test squares

Sample squares (49mm x 49mm) of cured sheet were cut with a scalpel using a template. These samples were then dried in a desiccator over silica gel for at least 48 hours. The thickness was measured in at least 5 places to 0.005mm using a Mercer dial gauge.

2.2.4. Cold solvent extraction

Extraction of leachable impurities by a conventional Soxhlet technique resulted in samples which showed

permanent set and strain. Samples remained in a curled position several days after extraction. In order to minimise structural changes to the samples during extraction a cold solvent extraction technique, using apparatus as shown in Figure 2.1. was used. this was designed and developed by MRPRA. An azeotropic mixture, previously studied by Khan Khadim[105], of methanol, chloroform and acetone was used.

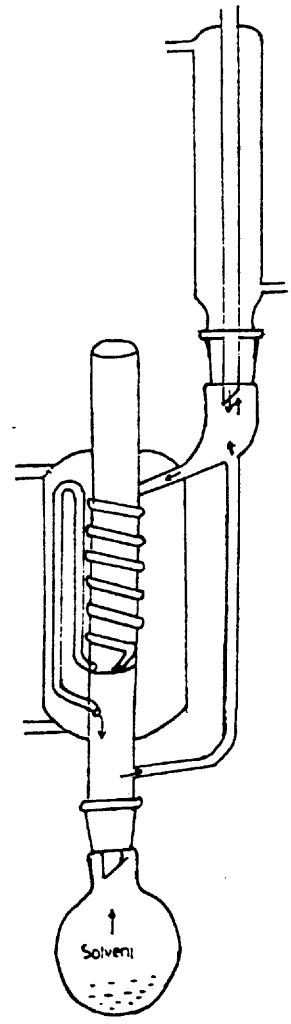

FIGURE 2.1

Cold extraction apparatus. Flow of solvent mixture is indicated by the arrows.

2.3. MEASUREMENT OF MASS UPTAKE BY POLYSULPHIDES

2.3.1. Measurement of mass uptake of liquid by polysulphide films

The diffusing liquids used in this work were a range of organic solvents, water and aqueous solutions. Test squares were immersed in the liquids under study in 175ml powder bottles, maintained at constant temperature in a water bath. Where noticeable leaching occurred, as shown by discolouration of the liquid, the liquid was changed every two days. Salt solutions were changed every two weeks as was distilled water and aviation fuel in long term tests. The bottles were kept tightly closed and shaken periodically.

The test squares were removed periodically from the soaking fluids, firmly dried between absorbant paper and their weight recorded using an electronic, analytical balance weighing to 4 decimal places. With practice, this procedure was effected in less than 10 seconds since a printer attachment was fitted to the balance and the weight automatically recorded. The time in which the sample was out of the liquid was thus kept to a minimum. Where very volatile liquids, eg. chloroform were used and/or uptake was high the samples were weighed using tared, stoppered weighing bottles. In other cases, where little or no evaporation was noted in the 3 seconds needed for the balance to reach stability it was found more convenient to weigh the samples directly on the balance pan.

2.3.2. Measurement of mass uptake of vapour by polysulphide films

For mass uptake data from the vapour phase, the samples were placed on small stainless steel mesh platforms supported above saturated aqueous solutions of various salts in 500ml wide-mouthed powder bottles. The salts used were known to give constant standard relative humidity values[106]. Care was taken to maintain the vapour above the salt solutions at constant relative humidity by checking that solid salts were present and that only a small vapour gap was present. The bottles were maintained at 30°C in a 'dry box' (see below). Prior to introduction of samples the bottles were kept in the dry box for at least 24 hours to ensure that liquid/vapour equilibrium was set up. The samples were removed periodically for weighing. Since opening the bottles to do this disturbed the equilibrium between liquid and vapour sample readings were done at less frequent intervals than for the liquid immersion tests and for all readings the time for which the bottle lid was removed was kept to a few seconds.

The 'dry box' was made from 10mm thick acrylic sheet with removeable trays in the base. The box was heated by a 100watt light bulb suspended in the centre of the box. Two centrifugal fans were placed such that the air flow was directly over a 30°C mercury contact thermostat which was midway between the fans and the light bulb. The position of the fans could be moved in order to maintain good temperature

control when bulky apparatus was placed in the box. Monitoring of temperature showed that constant temperature was maintained (±1°C) with a temperature gradient across the box of about 1°C.

2.3.3. Measurement of water mass uptake by liquid polysulphides

About 20 grams of each polymer were poured into weighed Petri dishes. These were placed in a humidity cabinet maintained at 100% relative humidity and 25°C. The samples were removed twice daily, weighed and monitored visually for opacity.

2.3.4. Measurement of desorption of liquid from polysulphide films

Desorption experiments were carried out by suspending sample sheets with their edges normal to the air flow from a centrifugal fan set up in a 'dry box' maintained at constant temperature. The floor of the box was filled with a mixture of fresh silica gel and 40nm diameter molecular sieve for water desorption and 130nm diameter molecular sieve and activated charcoal for hydrocarbon desorption. This ensured that desorption was the same from each surface and that, as far as possible, zero vapour concentration was maintained at the desorbing surfaces.

2.3.5. Calculation of D from mass uptake measurements

This was done in several ways using data from graphs similar to that shown in Figure 2.2.

a) D was calculated from the initial slope and the equilibrium absorption (M_{∞}%) using the equation:

$$M_t/M_{\infty} = 2(Dt)^{\frac{1}{2}}/\ell\pi^{\frac{1}{2}}$$

b) D was calculated from time to half equilibrium uptake ($t_{0.5}$) using the equation:

$$D = 0.1976\ \ell^2/t_{0.5}$$

c) Values of $\ln(1-M_t/M_{\infty})$ were calculated from Figure 2.2 and plots of this function against time were made. D was calculated from the slope of this straight line graph. The slope is $-D^2/4\ell^2$ and the intercept $\ln(8/\pi^2)$.

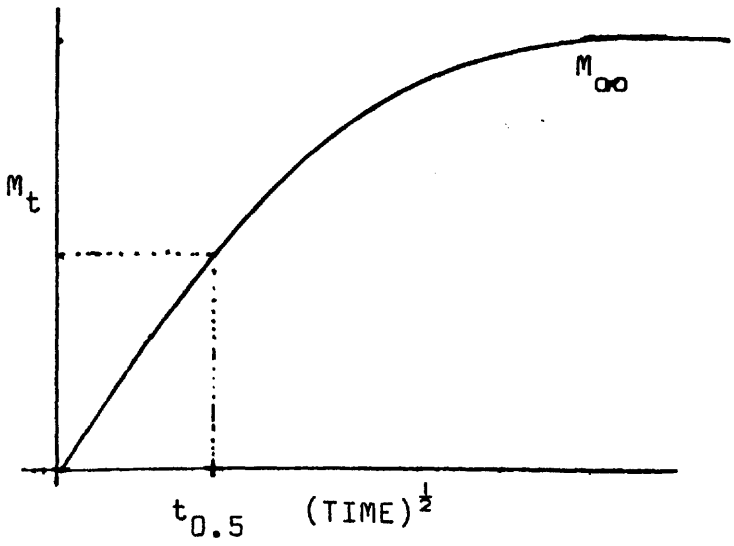

FIG.2.2

Typical mass uptake versus root time graph

2.3.6. Calculation of water concentration C_w

This was calculated from the equilibrium uptake, M_∞ and the density, p, of the rubber. In general M_∞ was found as a percentage of the weight of dry rubber compound. Thus

$$C_w = (M_\infty /100) \times \rho$$

where C_w is in gcm^{-3} of the rubber compound.

The density of the rubber, ρ, was found using a density bottle.

2.4. PERMEATION

Initially the permeability was determined to ASTM E96.66 using wax-sealed aluminium cups and thin film. 2 sheets were pressed together to minimise pin-hole effects. However, this method proved unsatisfactory in that inaccuracies in determining the time-lag (which was shorter than expected) occurred. Thicker samples were prepared and in addition an improved permeation cup was designed which enabled the liquid to be added after assembling and sealing the membrane (see Figure 2.3a). A similar apparatus was developed in which liquid, as opposed to vapour, was in contact with the membrane. This 'inverted cup' is shown in Figure 2.3b.

A comprehensive review by Newns[100] highlighted the possible errors of the cup method and attempts were made to minimise these. Sealing was effected by clamping the membrane between 2 ground glass flanges smeared with silicone high vacuum grease. The apparatus was checked for leakages by weighing with a 0.5mm thick PTFE membrane in place over water. No significant weight loss occurred in 48 hours. The apparatus was further checked with a polysulphide membrane in place inflated via the side arm with compressed air, and the apparatus coated with detergent. No bubbles were noted.

This apparatus also enabled the membrane to be checked in situ for loss of volatiles prior to exposure to vapour. Once the weight was stable liquid was introduced via the side arm and the apparatus placed in a desiccator over silica gel. This was then placed in the 'dry box' and maintained at 30°C.

Periodically the apparatus was removed and the desiccant tray containing molecular sieve was removed. The apparatus was then weighed and the weight loss recorded. Attempts to double check weight losses by weighing the desiccant trays were discontinued as the molecular sieve absorbed atmospheric moisture so rapidly that a stable reading could not be obtained in many cases.

For permeation experiments at reduced water vapour pressures standard salt solutions were made up as in section 2.3.1.

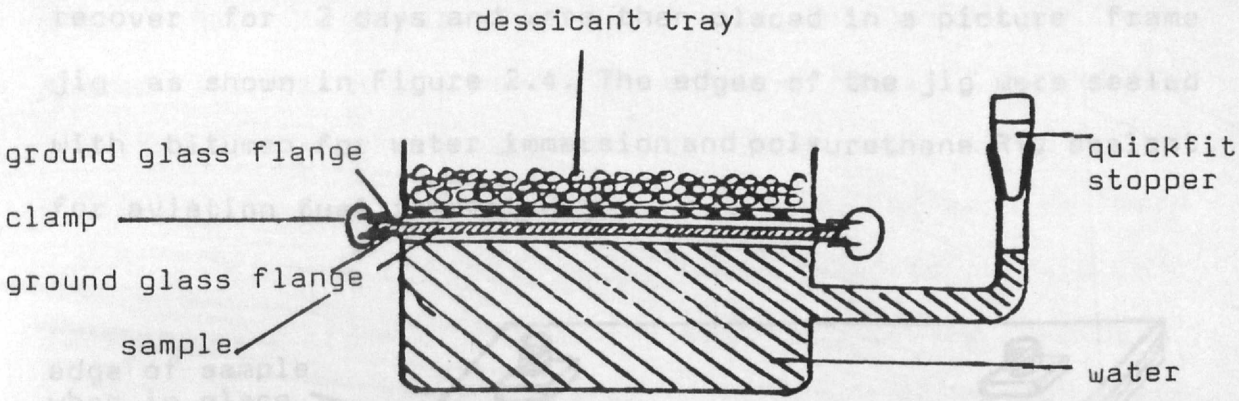

(a) CUP SCALE 1:1

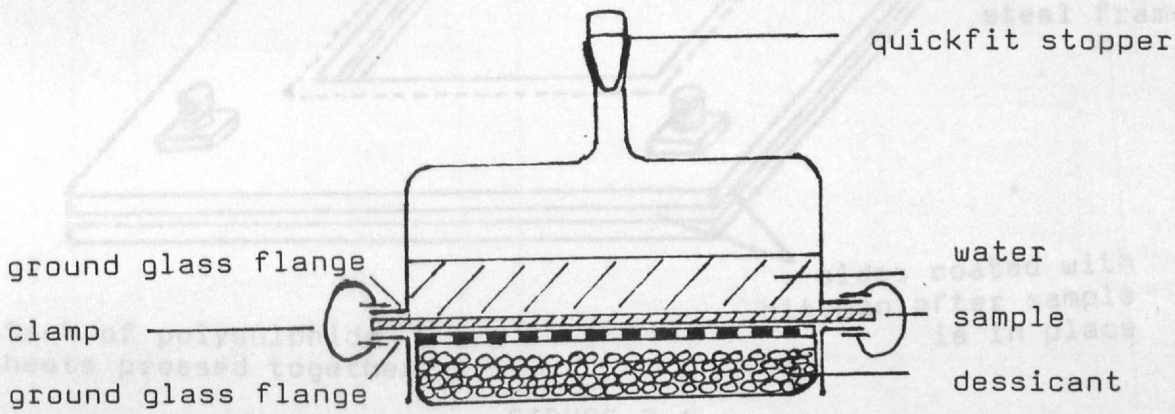

(b) INVERTED CUP SCALE 1:1

FIGURE 2.3

Permeation apparatus showing arrangements for determining permeation rate from vapours (a) and liquids(b)

2.5. LAMINATE STACKS

Ten squares, prepared as in 2.3.1., were placed one on top of each other and pressed together using a compression set apparatus overnight. The stacks thus formed were allowed to

recover for 2 days and were then placed in a picture frame jig as shown in Figure 2.4. The edges of the jig were sealed with bitumen for water immersion and polyurethane RTV sealant for aviation fuel immersion.

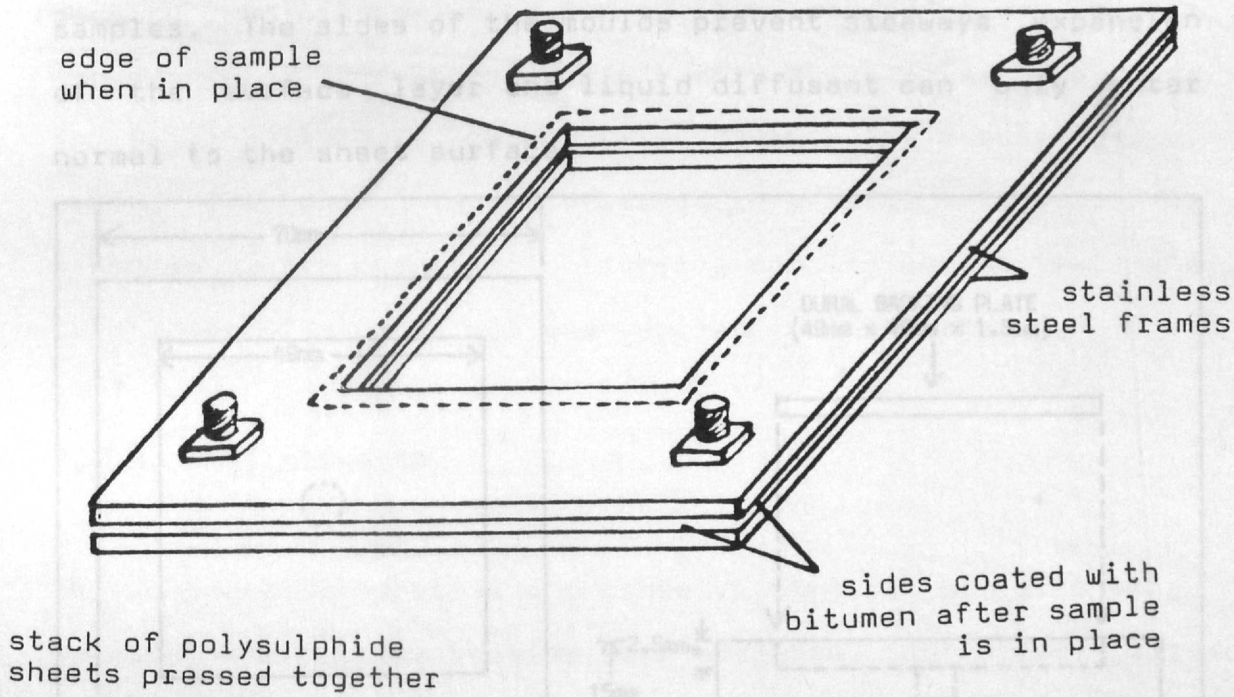

FIGURE 2.4

Laminate stack jig

SCALE 1:1

2.6. BONDED SAMPLES

One of the problems encountered in this work was that with some solvents very high swelling occurred. This caused changes in surface concentration and stresses from the underlying dry areas.

In an attempt to minimise these effects constrained samples

were made. Chrome-epoxide primed Dural backing plates were placed in PTFE cavity moulds as shown in Figure 2.5. Sealant was poured into the open mould, dried and cured under pressure. During solvent immersion tests, the samples were held in situ in the PTFE cavity moulds used to prepare the samples. The sides of the moulds prevent sideways expansion of the surface layer and liquid diffusant can only enter normal to the sheet surface.

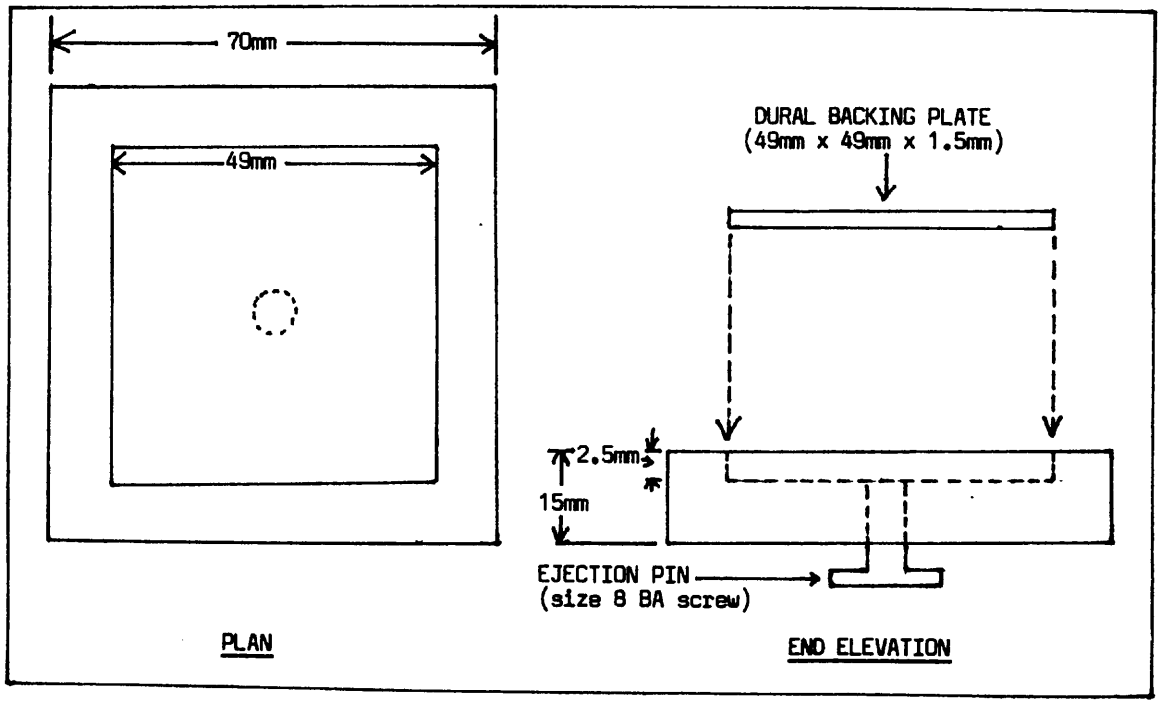

FIGURE 2.5

Cavity mould used for restrained sample

2.7. TESTING OF PHYSICAL PROPERTIES

In general, standard rubber testing techniques were used to BS903 (methods of testing rubber).

2.7.1. Moduli

Samples of sheet, 110mm x 4mm were cut from conditioned sheet using die stamping. These were then extended at a slow (5mm per minute) rate in an Instron Tensile testing machine until break. From the chart of stress versus strain Mooney-Rivlin and Gaussian plots were obtained as described in Section 1.10.1. The secant modulus (E_o) was obtained by taking the tangent to the curve at zero strain. In order to minimise water evaporation from the samples during testing a thin layer of mineral oil was applied to the surfaces.

2.7.2. Peel strength

The changes in adhesive and cohesive strength of films prior to and after water soaking were measured. Test pieces were made up coating the polysulphide solution onto chrome-epoxide primed Dural. A washed cotton tape was placed on the polysulphide film and the assembly cured under pressure. Cotton was chosen for its good water absorbing and wicking properties, to accelerate penetration of water to the sealant. Thickness control of the sealant was achieved by preparing all samples under pressure in a hydraulic handpress with a Dural spacer. Half the samples were immersed in water for 50 days. This time had been calculated from the determined apparent diffusion coefficient to be sufficient to enable penetration of water to the bondline. Testing was done using a jig, developed by Welding et al.[107], which kept the angle of peel at 90°.

2.7.3. Hysteresis

Tensile test samples were subjected to increasing followed by decreasing strain using an Instron and stress/strain charts were obtained. The enclosed area of the hysteresis loop obtained, ($area_2$), and the area under the original stress/strain curve, ($area_1$), were measured using a planimeter. Hysteresis was calculated, as the ratio of energy dissipated to the original work done and expressed as a percentage, thus:

$$\text{hysteresis} = 100(area_2)/(area_1)$$

2.7.4. Stress relaxation

This was determined from the changes in stress for samples held at constant 50% strain in an Instron Tensile testing machine. The theory is described in Section 1. 9.2.

2.7.5. Resilience

A steel ball was dropped onto polysulphide sheet and the rebound height was measured.The resilience was expressed as a ratio of rebound height to dropping height.
An average of ten readings was taken in each case.

2.7.6. Glass transition temperature

This was found using Perkin-Elmer DSC apparatus.

CHAPTER 3. TRANSPORT OF AVIATION FUEL IN A COMMERCIAL POLYSULPHIDE

3.1. INTRODUCTION TO MASS UPTAKE EXPERIMENTS USING AVIATION FUEL

The polysulphide rubber used in the following series of experiments was PR1422 and in the bulk of the experiments the soaking fluid was Avtur aviation fuel. Both of these materials are described in Section 2.1.1. Sheets of PR1422 were prepared as described in Section 2.2.

In order to find the equilibrium swelling and the diffusion coefficient, mass uptake experiments were carried out using the procedure described in section 2.3.1.

3.1.1. Presentation of data

Mass uptake data can be plotted in various ways; three such ways are shown in Figure 3.1. for the uptake of aviation fuel by samples of PR1422 of three different thicknesses.

A superficial inspection of the first two graphs suggests that the process of absorption is different for the three sheets. This is not so. The difference in the curves is only a consequence of the different methods of plotting.

Figure 3.1a is a plot of mass uptake /area versus root time. This graph suggests that the initial rate of uptake is the

same but the equilibrium uptake is different for the three samples.

Figure 3.1b shows the same data in the form of $M_t\%$ versus root time, where $M_t\%$ is mass uptake per unit mass of the dry rubber expressed as a percentage. Here it can be seen that the equilibrium uptake is the same, but that the initial portions of the curve differ.

Figure 3.1c, where $M_t\%$ has been plotted against root time divided the thickness, gives all the data on the same line. This plot thus compensates for thickness but gives a misleading representation of the time scale of a typical experiment.

To avoid confusion in this work it has been decide to adopt the following policy. In most experiments sheets of the same thickness have been used. In presenting these results plots of $M_t\%$ versus root time will be used. When sheets of different thickness are compared, $M_t\%$ versus root time/thickness will be used to compensate for the effect of thickness.

3.1.2. Effect of sample thickness on aviation fuel uptake

Figure 3.1a clearly shows that the change of concentration of aviation fuel in PR1422 with respect to root time is independent of the sample thickness, in the early stages of the experiment.This implies that the sheet acts as if it were

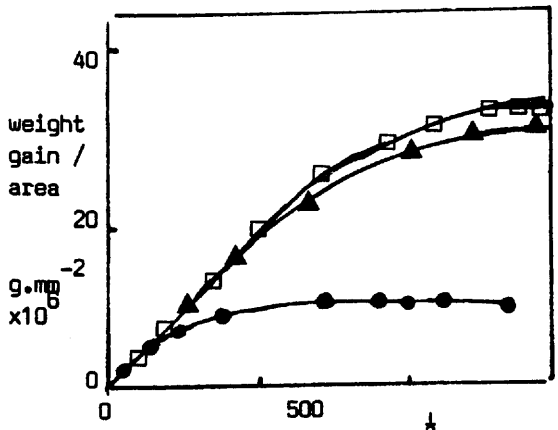

FIGURE 3.1a

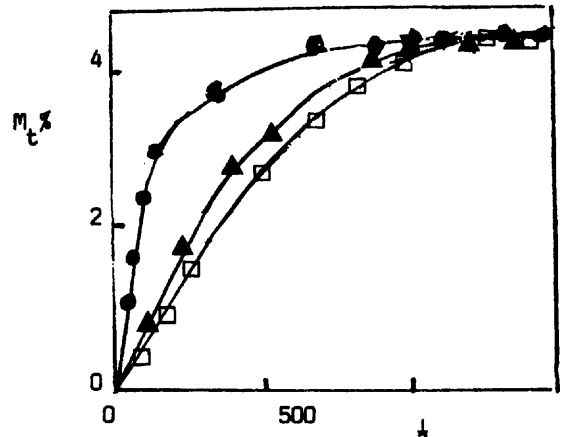

FIGURE 3.1b

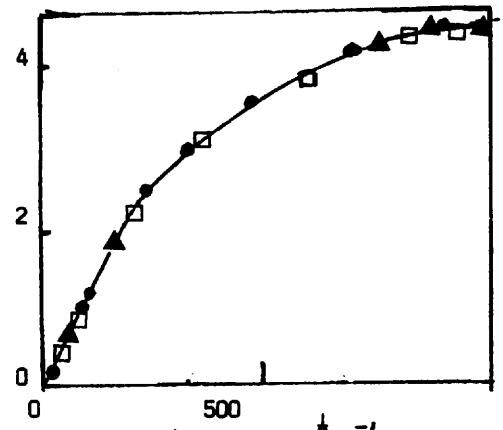

FIGURE 3.1c

FIGURE 3.1

Effects of plotting mass uptake of aviation fuel against root time in various ways for three samples of PR1422 of different thickness:

Figure 3.1a is weight gain per unit area against root time;

Fwgure 3.1b is M_t% against root time, and

Figure 3.1c is M_t% versus root time per unit thickness.

It can be seen that only in Fig.3.1c do the curves coincide.

Temperature = 30°C; area = 4800mm^{2}

KEY

● thickness = 0.27mm

▲ thickness = 1.40mm

□ thickness = 1.55mm

semi-infinite. This is one criterion of Fickian behaviour[108].

3.1.3. Extraction of sheets of PR1422

Sample sheets of PR1422 were extracted in various ways to remove soluble, low molecular weight materials. The conditions and the results of extraction are shown in Table 3.1.

TABLE 3.1.

Amount of material extracted from PR1422 using various techniques and conditions

method	weight loss %
a) acetone/methanol/ chloroform azeotrope at room temperature for 48 hours	7.5
b) toluene at 50°C for 48 hours	7.0
c) aviation fuel at room temperature for 6 months	2.2
d) water at room temperature for 3 months	1.4
e) aviation fuel at 30°C for 2 months	1.2

An infra-red spectrograph suggested that the material extracted by (a) and (b) includes the epoxide and phenolic adhesion promoters as well as low molecular weight

polysulphide. It has been reported that the adhesion promoters are extractable from the cured compound[109].

3.1.4. Equilibrium swelling of PR1422 by Avtur

The extracted sheets of PR1422 described above, together with non-extracted samples, were immersed in Avtur at 30°C and the mass uptake measured. The results are shown in Figure 3.2. It can be seen that the equilibrium uptake varies considerably.

A second method of determining the equilibrium uptake was to use the desorption technique described in Section 2.2.3. Figure 3.3 gives the desorption curves at 30°C for aviation fuel in PR1422.

Figure 3.2 shows that the equilibrium swelling of the differently prepared samples of PR1422 differs considerably in magnitude. The maxima in most of the curves suggest that leaching is taking place concomitant to solvent uptake.

Figure 3.3 tends to confirm this suggestion, in that the final percentage weight desorbed is approximately the same, i.e. each sample of rubber had approximately the same quantity of liquid in it prior to the desorption experiment.

On desorption, the weight loss of the non-extracted sample was found to be 3.8%. Comparing this with the uptake of 2.6% it appears that leaching occurred during the absorption experiment, resulting in the loss of 1.2% from the original

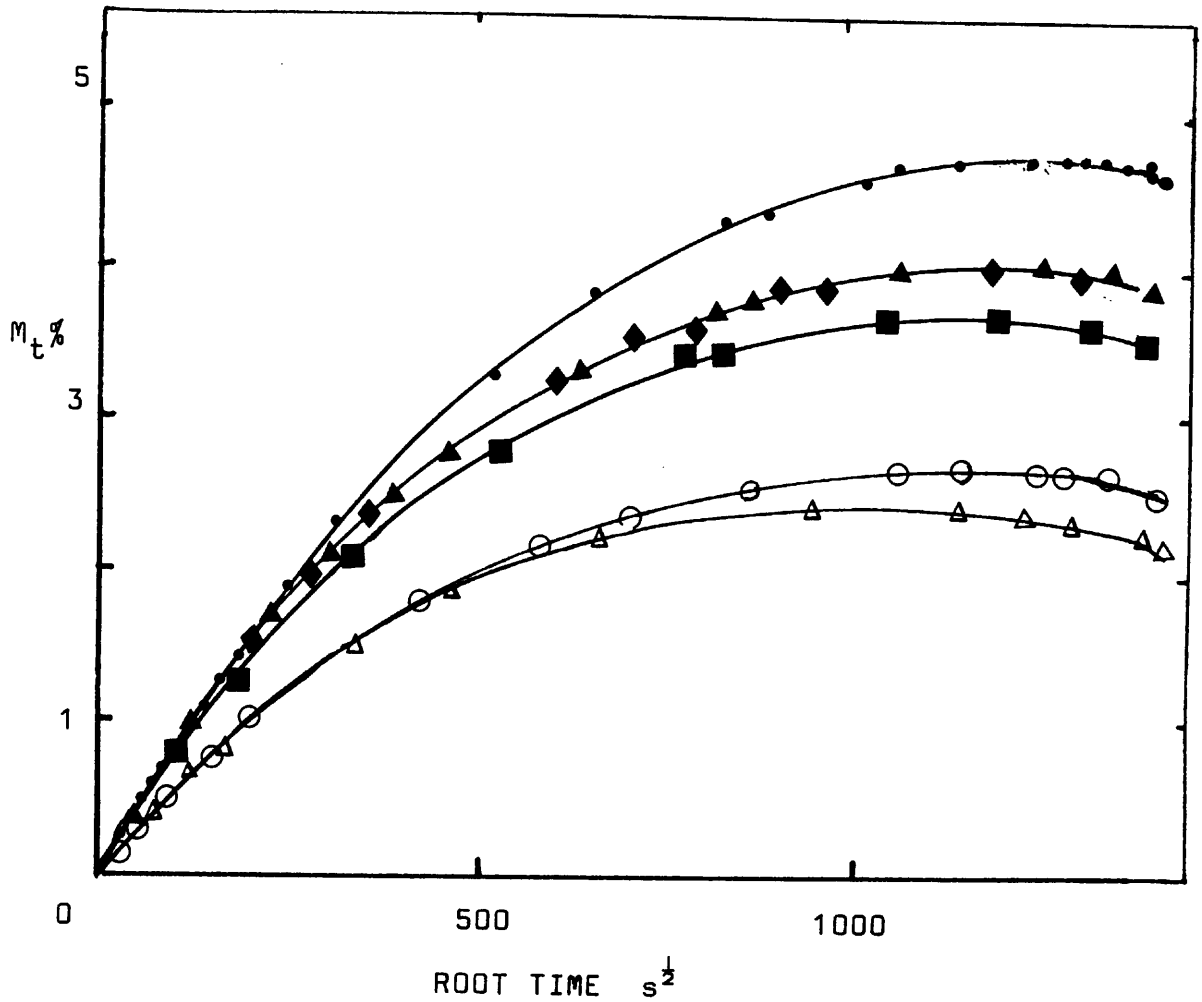

FIGURE 3.2

Plot of M_t% versus root time for mass uptake of aviation fuel (Avtur) by PR1422 at 30°C. M_t% is the weight of liquid absorbed per unit weight of dry sample (rubber plus filler). Total surface area of sample= 4800mm^2; thickness (2ℓ)= 1.54mm

KEY

- ● azeotrope extracted sample
- ▲ Avtur extracted sample
- ◆ toluene extracted sample
- ■ water extracted sample
- ○ non-extracted sample 1
- △ non-extracted sample 2

(see Table 3.1. for extraction conditions)

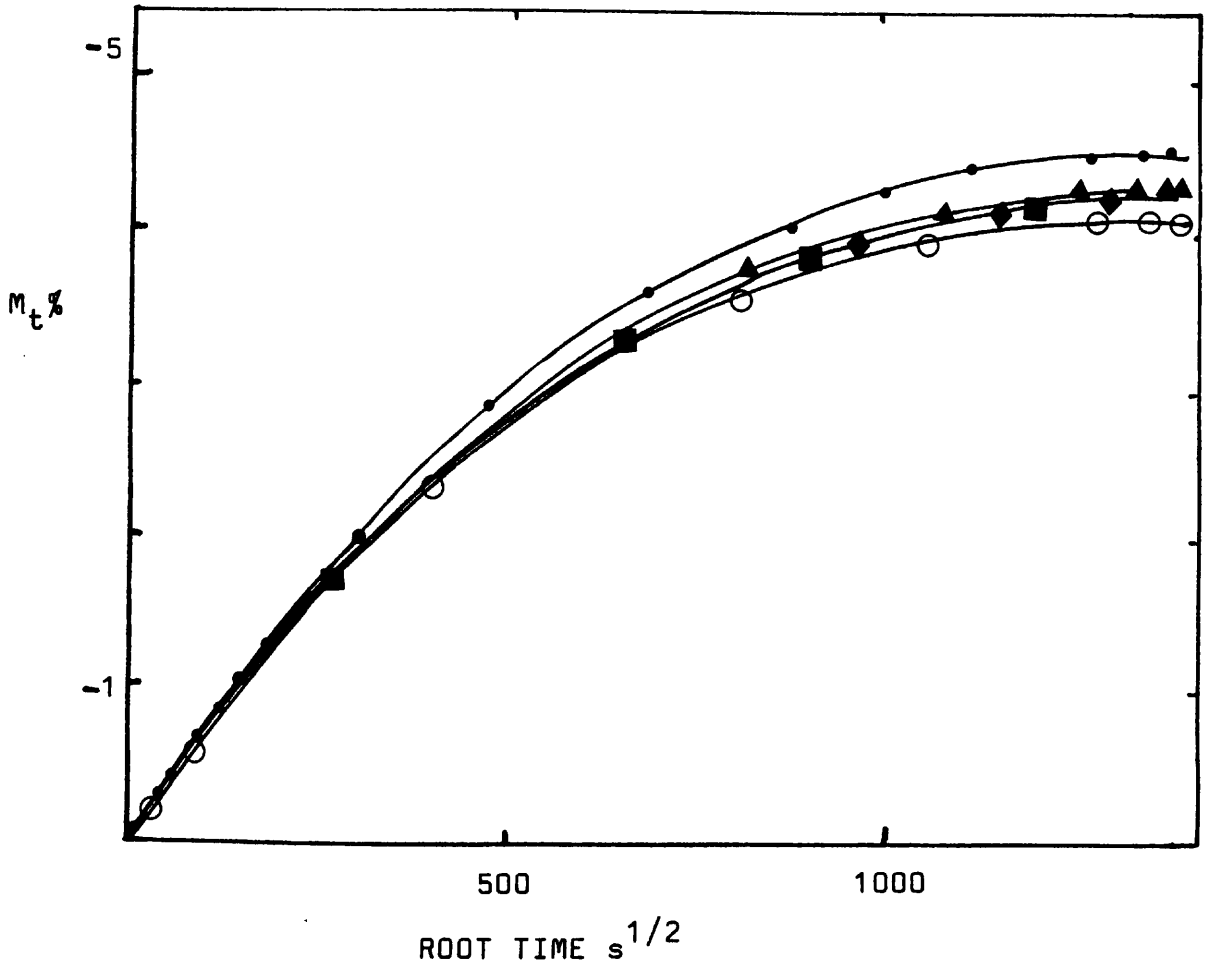

FIGURE 3.3

Plot of M_t% versus root time showing desorption of aviation fuel from PR1422 at 30°. The values on the M_t axis for this desorption experiment are presented in an unconventional way in order to allow comparison with the uptake curve of Fig.3.2. Total area of sample = 4800mm^2; thickness(2ℓ)=1.54mm

KEY

• azeotrope extracted sample

▲ Avtur extracted sample

♦ toluene extracted sample

■ water extracted sample

○ non-extracted sample 1

(see Table 3.1. for extraction conditions)

weight of the rubber.

Thus the true value of the equilibrium uptake in the absorption experiments is unclear for all the samples tested. This is a consequence of the simultaneous uptake of solvent and extraction of impurities. In the following section, where D is calculated, the value of M_{∞} for the absorption experiment is taken as the maximum value found in Figure 3.2.

3.1.5 Determination of diffusion coefficient for aviation fuel in PR1422

The diffusion coefficient was calculated for two samples only: a) azeotrope extracted sample and b) non-extracted sample. The three methods (detailed in section 2.3.4) were used to calculate D using data from Figures 3.2 and 3.3 for both absorption and desorption of the samples.

Briefly, the formulae used are:

Method A $M_t/M_{\infty} = 2(Dt)^{\frac{1}{2}}/(\pi^{\frac{1}{2}}\ell)$

Method B $D = 0.1976\,\ell^2/t_{0.5}$

Method C $\ln(1-M_t/M_{\infty}) = \ln(8/\pi^2) - 4Dt\ell^2/\pi^2$

where ℓ is half the sheet thickness

All three methods utilise the equilibrium uptake in the calculation of the diffusion coefficient, D.

Methods A and B both use the slope of the initial part of the curves in Figures 3.2 and 3.3.

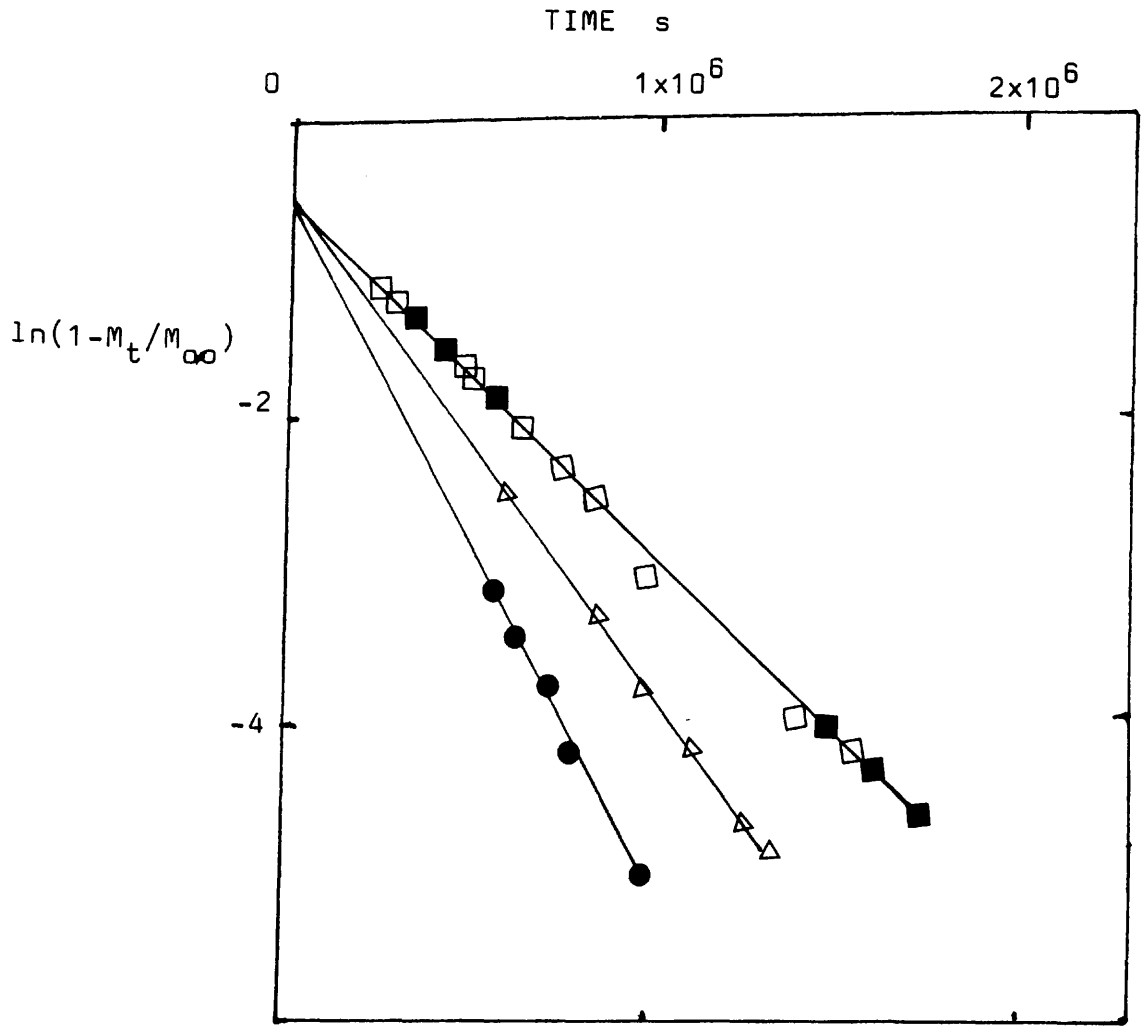

FIGURE 3.4.

Plot of $\ln(1-M_t/M_\infty)$ versus time showing linear relationship

Data is taken from Figures 3.2. and 3.3.

KEY

absorption data	desorption data
■ extracted	□ extracted
● non-extracted	△ non-extracted

Method C (plotting $(1-M_t/M_\infty)$ against time) uses only long term data. The graphs for method C are given in Figure 3.4.

The values of D calculated from the three methods are given in Table 3.2.

TABLE 3.2

Comparison of values of diffusion coefficient, D for different samples of PR1422

For azeotrope extracted sample M_∞ = 4.7%

For non-extracted sample M_∞ = 2.6% for absorption

and M_∞ = 3.8% for desorption

The values of D x 10^8 (cm^2s^{-1}) are shown for both the absorption (D_a) and desorption (D_d) experiments.

	azeotrope extracted sample		non-extracted sample	
calculation method	D_a	D_d	D_a	D_d
A) short term	1.03	1.06	1.61	1.52
B) half time	1.04	1.07	1.64	1.50
C) long term	0.77	0.77	1.08	0.92

The results shown in Table 3.2 indicate that

a) the two short term methods of calculation (A and B) give similar results. The long term (method C) calculated values of D are lower; this is probably a consequence of the inaccuracies in the long term data. In future calculations, only methods A and B will be used to calculate D.

b) leaching of the non-extracted sample affects the magnitude of D compared with that for the extracted sample. However, the differences in values found are not large.

c) Concentration dependence appears to be negligible, since there is very little difference between the desorption and absorption diffusion coefficients, for both the extracted and non-extracted samples.

Perusal of the literature gave no comparison values of the diffusion coefficient of aviation fuel in polysulphide rubbers. However an estimation can be made based on literature values of the diffusion coefficients of hydrocarbons in other rubbers and the glass transition temperatures of these rubbers [27,64].

For example, the values found, of about $10^{-8} cm^2 s^{-1}$ are an order of magnitude lower than for a range of hydrocarbons in gum stock natural rubber[27], but this is not unreasonable considering the higher T_g of the polysulphides (-53° compared to natural rubber with a T_g of -70°C).

The values of the diffusion coefficients for the non-extracted samples, although less accurate, are possibly a better indicator of the rate of diffusion of aviation fuel into the commercial sealant, which contains adhesion promoters.

3.1.6. Mass uptake of Avtur by nitrile rubber

It was decided to compare the diffusion coefficients of aviation fuel in polysulphide and a nitrile rubber at 30°C. Nitrile rubber is a polar rubber, with known good resistance to solvent swelling. The nitrile rubber chosen contained 30% acrylonitrile and had a 65% carbon black loading, based on the weight of the rubber. This gave a volume fraction of filler of approximately 0.25, which is the volume fraction of filler in PR1422.

A plot of M_t% versus root time is shown in Figure 3.6. The equilibrium uptake was 15% and the diffusion coefficient found was $4 \times 10^{-8} cm^2 s^{-1}$. This indicates that the order of magnitude found for the diffusion coefficient in the polysulphide is reasonable. Moreover, this result indicates that PR1422 has better resistance to aviation fuel than the nitrile rubber investigated. This is shown by both the lower equilibrium uptake and lower diffusion rate for PR1422 compared to the nitrile.

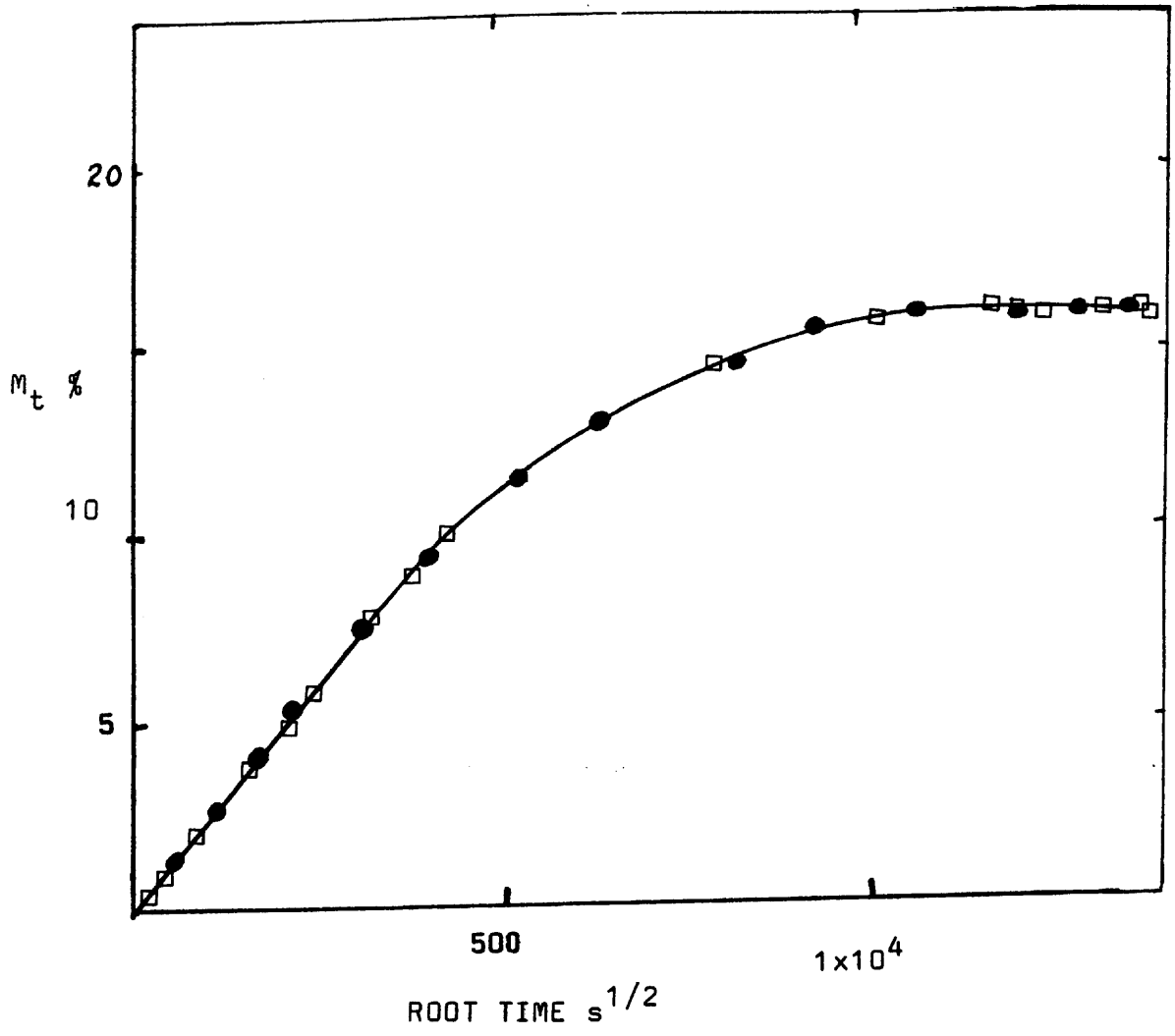

FIGURE 3.5

Plot of M_t % versus root time for the uptake of aviation fuel by nitrile rubber at 30° C.

area = 4800mm^2 thickness = 1.25mm

KEY

● sample 1

□ sample 2

3.1.7. Comparison of the uptake of Avtur with the uptake of other solvents by PR1422

To gain further information on solvent diffusion mass-uptake plots were obtained of PR1422 in hexane, decane, toluene and chloroform. The results are shown in Figures 3.6 and 3.7 in the form of M_t% plotted against root time. Abnormal shaped curves were noted in all cases, and the diffusion coefficient was found from the time to reach half the equilibrium absorption. The values of D obtained are summarised in Table 3.3.

TABLE 3.3

Values of D and equilibrium uptake for various solvents in PR1422

	uptake %	$Dx10^8$ cm^2s^{-1}
PR1422 in hexane	1*	2 *
decane	0.3*	1.8 *
Avtur	2.6	1.6
toluene	58	19
chloroform	360	50

* estimate only as heavy leaching occurred

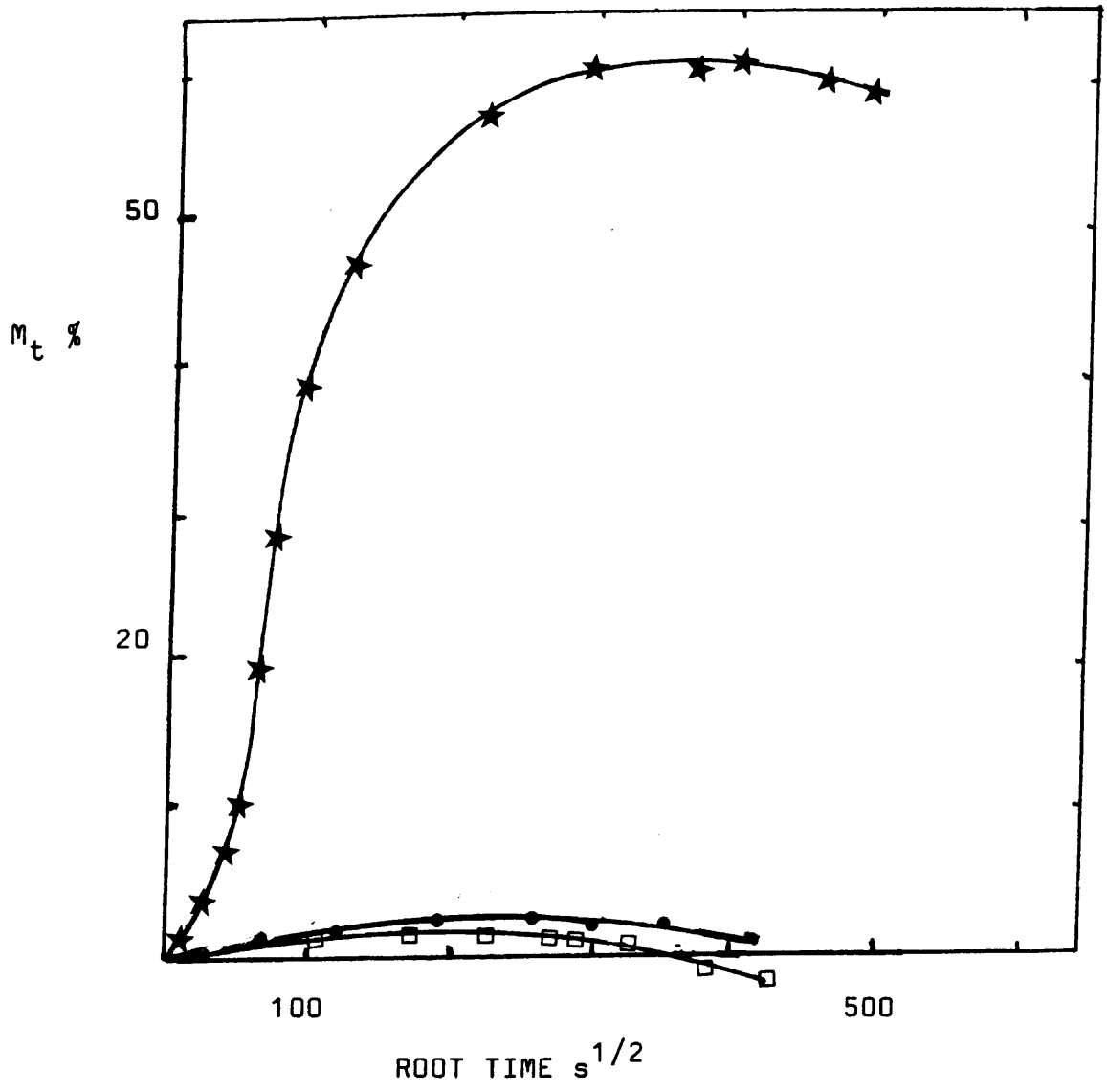

FIGURE 3.6

Plot of M_t % versus root time for the mass uptake of hydrocarbons by PR1422, showing very high uptake by the aromatic hydrocarbon,toluene and very low uptake by aliphatic hydrocarbons at 30° C.

sample area $4800mm^2$ thickness =1.54mm

KEY

★ toluene

⊡ decane

● hexane

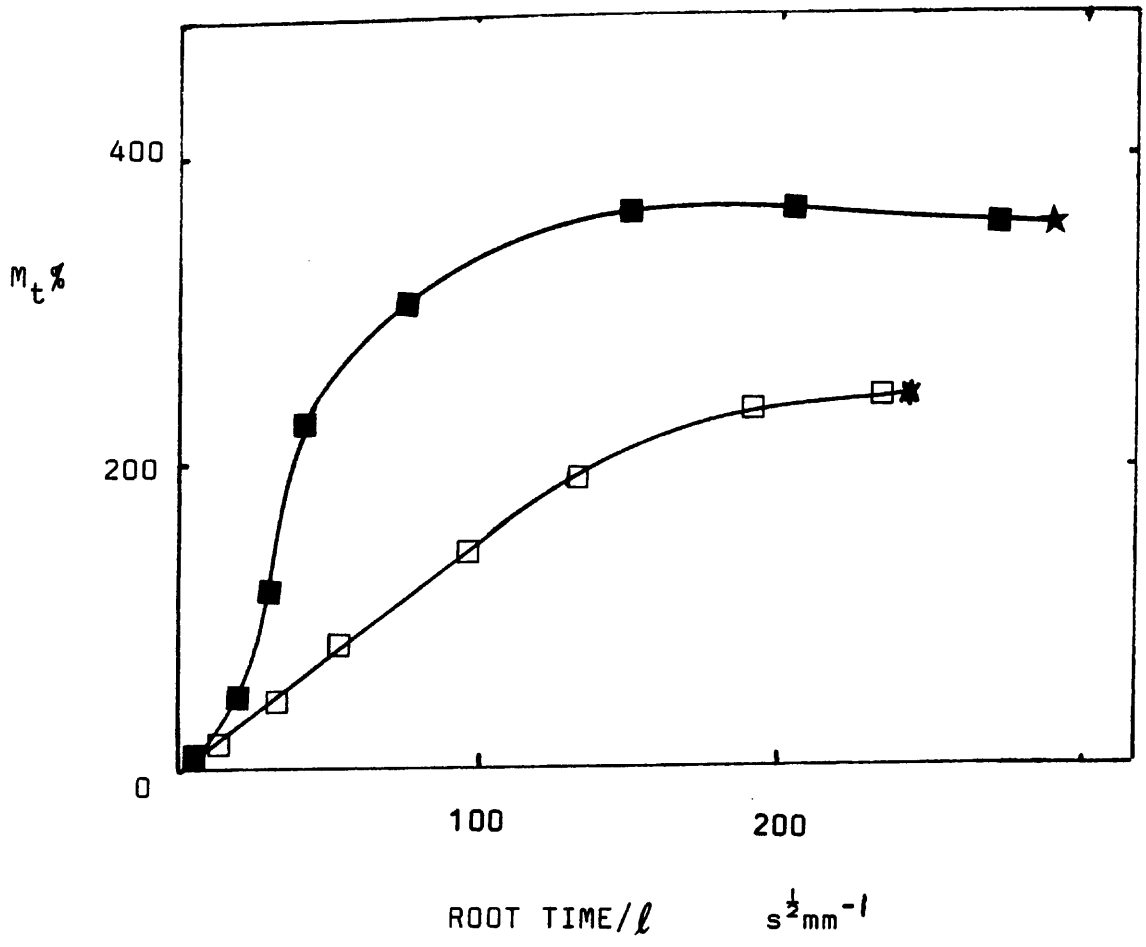

FIGURE 3.7

Plot of M_t% versus root time/ℓ for the mass uptake of chloroform by PR1422 at 30°C.

KEY

■ non-restrained sample: thickness(2ℓ)=1.31mm; area = 4800mm²

□ restrained sample: thickness (ℓ) = 0.47mm; area = 2500mm²

✱ sample broke

For details of restrained sample see Section 2.6.

It can be seen from Figure 3.6 that for the straight chain paraffins leaching occurred so that it was only possible to estimate the diffusion coefficients. The values of the diffusion coefficients found for toluene and chloroform were an order of magnitude greater than those for Avtur and the aliphatic hydrocarbons.

Although these results are not very accurate they do indicate that the order of magnitude for the diffusion of aliphatic hydrocarbons in polysulphide rubber is the same as for aviation fuel. This allows some comparison with other rubber/solvent systems in the literature.

3.1.8. Constrained samples

It has been postulated that anomalous sigmoidal curves shown in Figures 3.6 and 3.7 are a consequence of both the changing surface concentration and stresses from the dry underlying rubber regions when swelling is high [56]. To investigate whether this was the case constrained samples, prepared by the method described in section 2.6, were soaked in chloroform. The results are shown in Figure 3.7 where it can be seen that constraining the sample eliminates the sigmoidal shape of the mass uptake curve. This strongly suggests that the effect is mainly due to changes in surface concentration, as a result of the relaxation of swelling stresses during the experiment.

3.1.9. Effect of temperature on the mass uptake of aviation fuel in PR422

In these experiments D was found at different temperatures. These experiments were carried out on non-extracted samples of PR1422. The weight gain (M_t%) with respect to root time is shown in Figure 3.8. The decrease in equilibrium uptake with increasing temperature is small and is probably due to leaching being more pronounced at higher temperature.

TABLE 3.4.

D at different temperatures for aviation fuel in PR1422

Temperature °C	25	30	50	70
D x 10^8 cm^2s^{-1}	0.9	1.6	11	29

The diffusion coefficients shown in Table 3.4 were used to give the Arrhenius plot shown in Figure 3.9.

The straight line in Figure 3.9 allows the activation energy to be calculated from the slope. The value found of 14.5kcal/mole (6.1 x10^4 joules/mol) is of a similar order of magnitude as various hydrocarbons in rubbers. For example, Auerbach et al.[61] found 14kcal/mole (59 kJ mol^{-1}) for the activation energy for the diffusion of octadecane in nitrile rubber; Frensdorff[123] found 10.6-19.8 kcal/mole (45-83 kJ mol^{-1}) for benzene in ethylene-propylene copolymers.

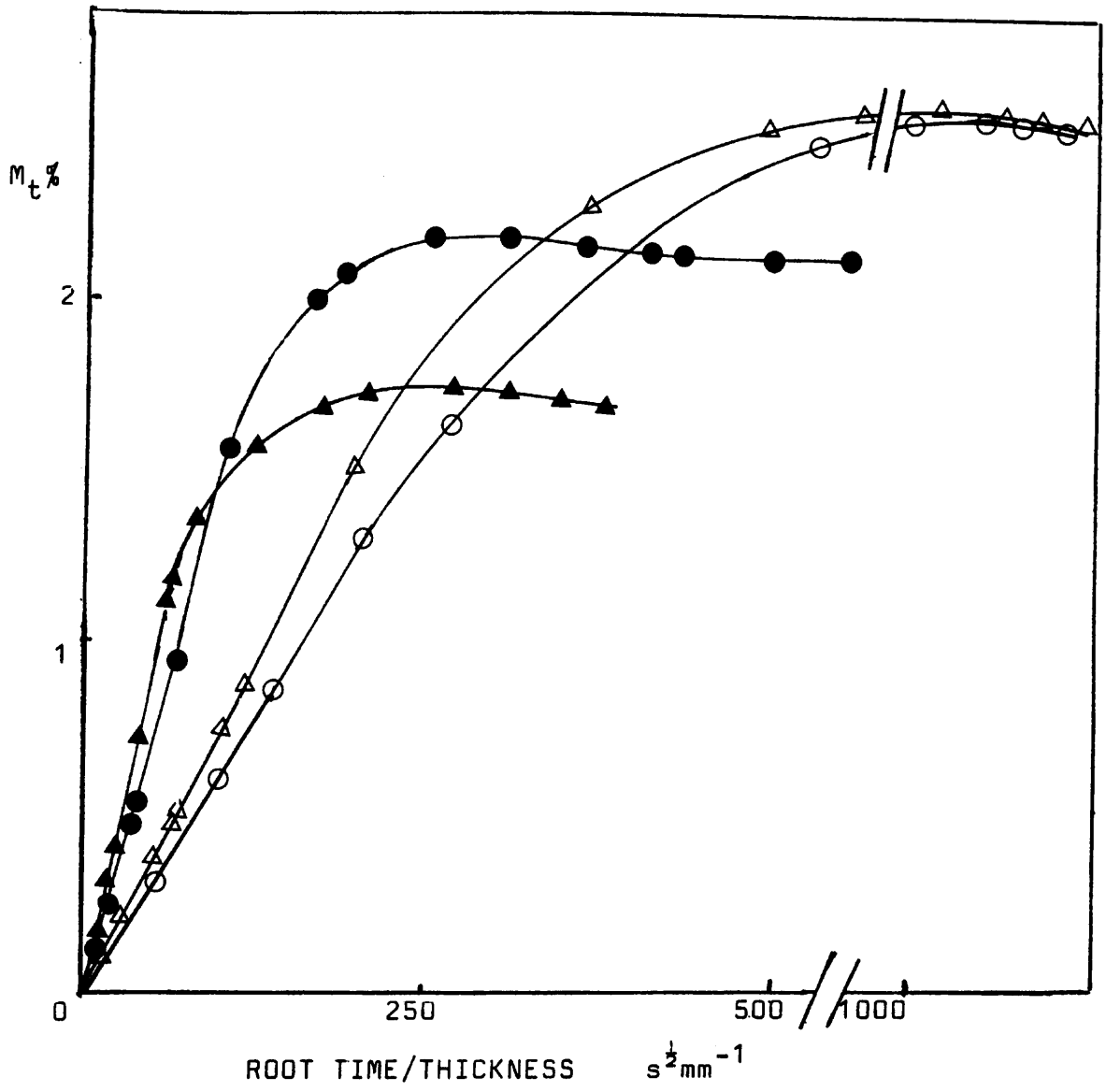

FIGURE 3.8.

Plot of M_t% versus root time/thickness for mass uptake of aviation fuel in PR1422 at different temperatures.

area = 4800mm^2 for all samples. Thickness = 2ℓ

KEY

○ 25°C thickness = 0.22mm

△ 30°C thickness = 1.46mm

● 50°C thickness = 1.60mm

▲ 70°C thickness = 1.36mm

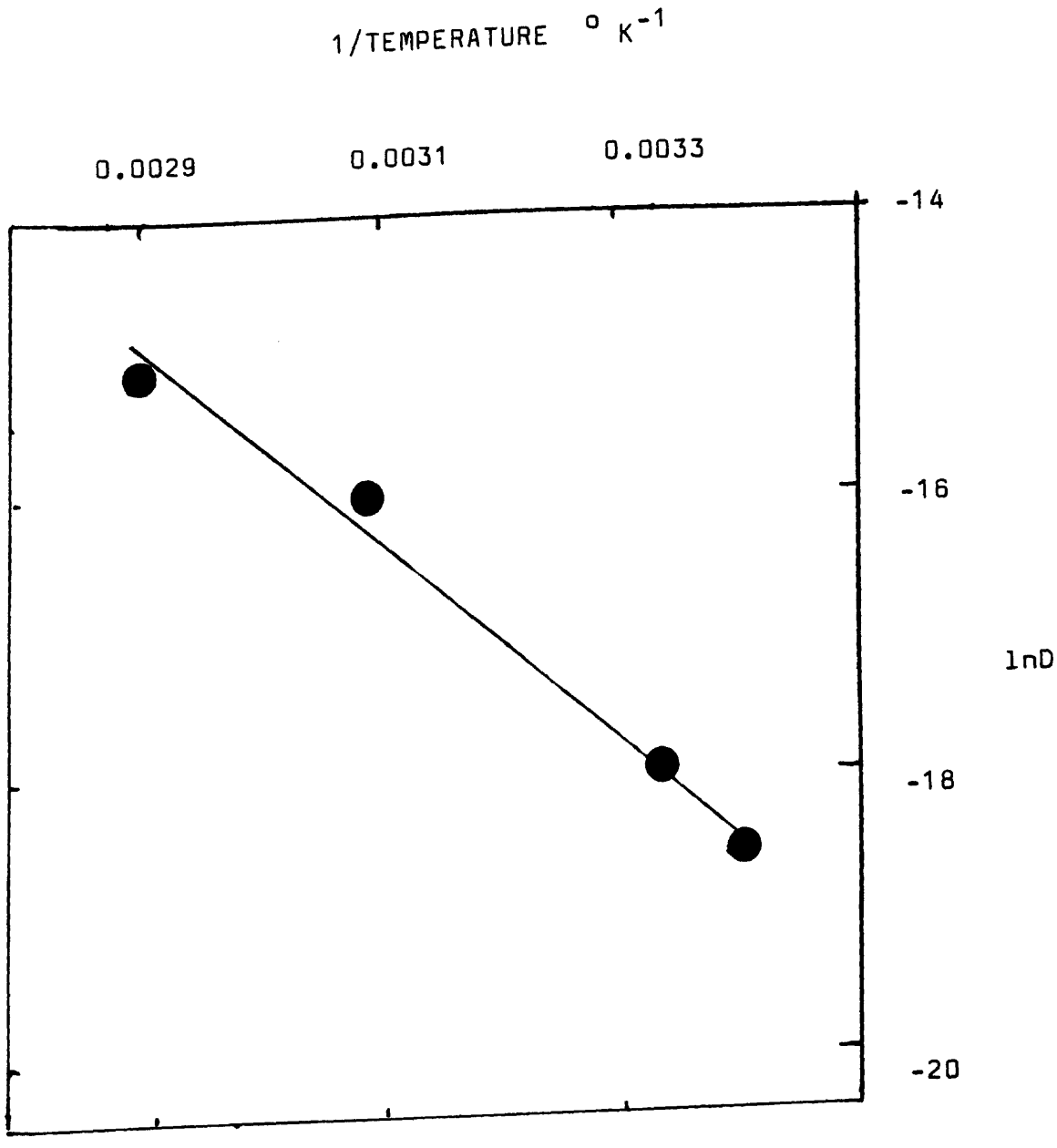

FIGURE 3.9

Plot of lnD versus reciprocal absolute temperature for uptake of aviation fuel by PR1422. The data is taken from Table 3.4. The straight line illustrates an Arrhenius relationship.

The slope = -7.5×10^{3} degrees K

Hence activation energy, E, = 6.1×10^{4} joules/mole

Considering the possible sources of error in the experiment the value found for the activation energy for the diffusion of aviation fuel in polysulphide rubber is not unreasonable.

3.1.10. Effect of filler on absorption of aviation fuel

In order to determine the effect of filler on mass uptake of aviation fuel, samples of PR1422 with filler removed were prepared as described in section 2.2.2. The results for mass uptake of aviation fuel by PR1422 with filler removed are presented in Figure 3.10.

A similar plot for PR1422 is included for comparison purposes, together with results obtained for a model compound, LP32 polysulphide (which is the main basis of PR1422) cured with 7.5% sodium dichromate.

From Figure 3.10 it can be seen that uptake is faster and the equilibrium uptake is higher for both the PR1422 (filler removed) and LP32 compared to the PR1422 sample (containing filler).

The data calculated from Fig. 3.10 is tabulated in Table 3.5.

Table 3.5 shows that the diffusion coefficients are higher for the PR1422 (filler removed) and the LP32 compared to the PR1422 containing filler.

There is good agreement between the diffusion coefficients

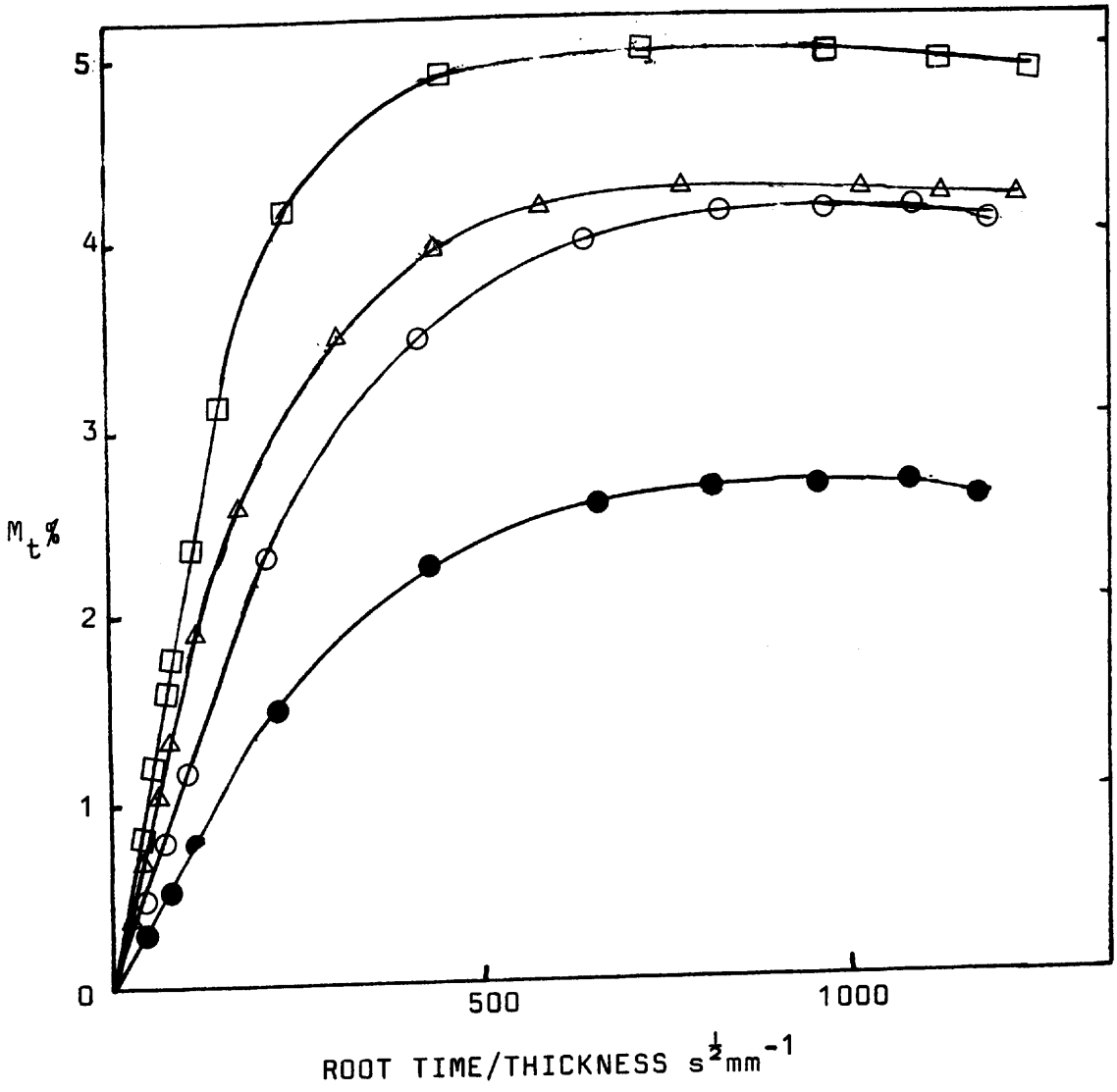

FIGURE 3.10

Plot of M_t% versus root time/thickness, showing differences in absorption of aviation fuel at 30°C for samples of PR1422, PR1422 (filler removed) and LP32. All sample areas = 4800mm²; thickness varied 1.1mm-1.54mm.

KEY

● PR1422

○ PR1422 corrected*

△ PR1422 (filler removed)

□ LP32

* M_t% adjusted to allow for filler by dividing by weight fraction of rubber (0.63)

for the LP32 ($D = 2.8 \times 10^{-8} cm^2 s^{-1}$) and the PR1422 with filler removed ($D = 2.6 \times 10^{-8} cm^2 s^{-1}$). The difference , of about 10%, is probably due to the error in estimating the equilibrium uptakes.

TABLE 3.5

Comparison of PR1422 and PR1422 (filler removed)

	PR1422	PR1422 filler removed	LP32
Equilibrium Uptake (%)	2.6	4.2	4.9
Filler content (% by weight)	37*	0	0
Rubber content (% by weight)	59	94**	100
resin content (% by weight)	4**	6**	0
M_∞ as %age of rubber	4.4	4.5	4.9
M_∞ as %age (rubber + resin)	4.1	4.2	4.9
$D \times 10^8 (cm^2 s^{-1})$	1.6	2.6	2.8

* filler content found from ash values.

** this estimate is based upon data in the patent[5] for PR1422 and data in Table 3.1 (extraction data), allowing for low molecular weight polysulphides.

Kraus, Lorenz and Parks and others[21-23] have shown that the restraining effect of the filler reduces the equilibrium uptake of filled samples relative to an unfilled sample. Table 3.5 indicates that this is not the case here. The presence of filler does not significantly reduce swelling as a percentage of rubber or rubber plus resin. However, the effect of changes in the elastic restraining forces caused by the addition of filler might be negligible in this case, since swelling is small.

The greater diffusion coefficients found for the samples containing no filler can perhaps be explained in terms of changes in the path distance travelled by the penetrant molecules i.e. tortuosity changes.

Maxwell's formula [69] is $D_f = 2D_u/(3 - v_r)$ (3.1)

where v_r is the volume fraction of the rubber in the filled rubber and D_u and D_f are the diffusion coefficients for unfilled and filled rubber respectively.

Substitution of 1.6 $\times 10^{-8} cm^2 s^{-1}$ for D_f in equation 3.1, suggests that D_u for the PR1422 with filler removed should be 1.8 $\times 10^{-8} cm^2 s^{-1}$, not the experimentally determined 2.6 $\times 10^{-8} cm^2 s^{-1}$ (PR1422 minus filler). Maxwell's formula has been used with some success for gaseous diffusion in a range of rubbers[18], and also for solvents in natural rubber[19] with small filler loadings, but other workers[68] have suggested that the discrepancy between diffusion rates for

solvents in filled and unfilled materials is often higher than that predicted by Maxwell's formula.

3.1.11. Concentration profiles

The results of the above sections appear to indicate that the absorption of aviation fuel by polysulphide rubber follows a well understood pattern of behaviour. If this is so, then it should be possible to predict the concentration profile with respect to distance, at any given elapsed time, for absorption by a simple geometric shape such as plane sheet. This theoretical profile can then be compared to an experimentally determined concentration profile.

In order to determine concentrations at various distances within the sheet, stacks of very thin sheet were prepared as described in section 2.1. These samples were then immersed in aviation fuel at 30°C and removed after 4 days. The stacks were disassembled and the separate sheets were weighed. The concentrations of aviation fuel in the individual sheets are shown in Figure 3.11.

Concentration is expressed as M_t/M_∞ where M_∞ is the equilibrium uptake of aviation fuel by PR1422.

As can be seen, agreement between the experimental results and the curve predicted from Crank's derivation is quite good considering the limitations of the experimental technique.

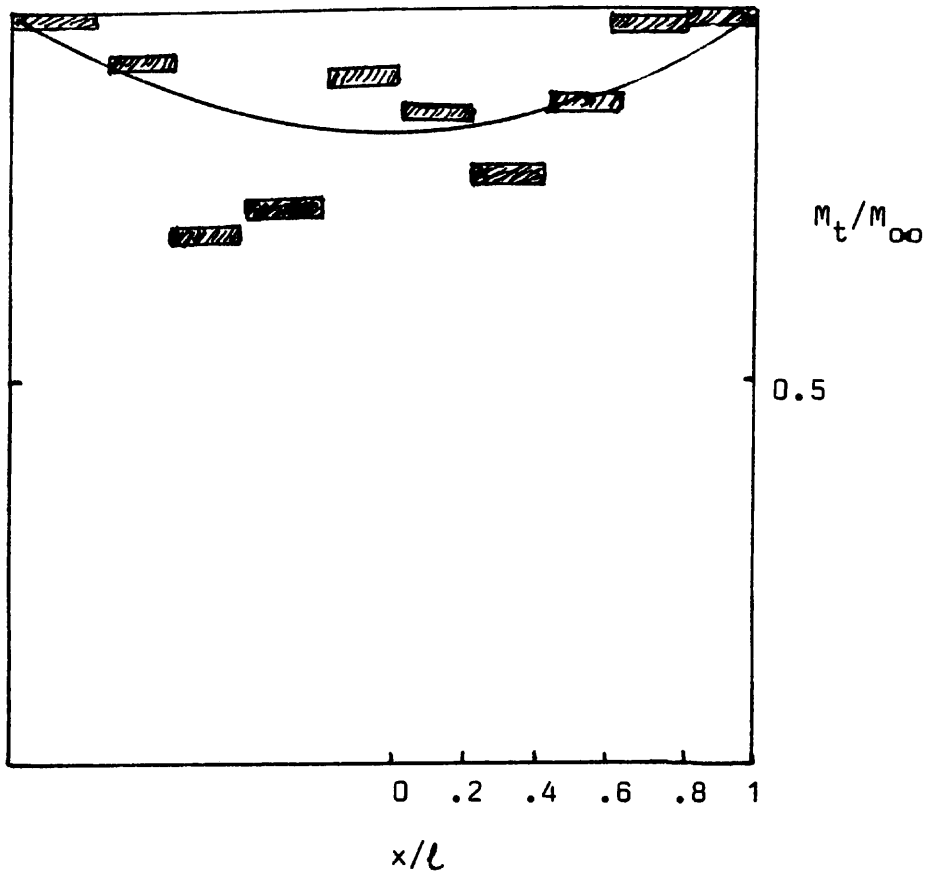

FIGURE 3.11

Plot of M_t/M_{oo} versus x/ to illustrate the concentration profile of aviation fuel in PR1422. The plot shows agreement between predicted (solid line) and experimentally determined (▨) concentrations at distances x/ℓ (where x is distance from the centre of the sheet and ℓ is half the composite sheet thickness). The theoretical curve (solid line) is derived from Crank[30] using the following data:

D taken as 1.6×10^{-8} cm^2s^{-1}

time (4 days) = 3.5×10^5secs

ℓ = half thickness of stack = 0.08cm

The theoretical curve is based on calculated Dt/ℓ^2 = 0.86

This agreement between the theoretical prediction and the experimental results again suggests that the aviation fuel is diffusing into the material in a normal, Fickian manner.

3.2. PERMEATION OF AVIATION FUEL THROUGH PR1422

3.2.1. Permeation results

The PR1422 samples were sealed in the permeation cups, as described in section 2.4 and the quantity of aviation fuel permeating through was measured with respect to time. The result of a typical experiment is shown in Figure 3.12.

The permeation experiment gives the permeation rate, R, at saturated liquid vapour pressure. In order to give the permeation coefficient, P, the value of R must be divided by the saturated vapour pressure (s.v.p.).

The derivation of R, P and D, from the data taken from Figure 3.12, is given in Table 3.6.

The value of the permeation rate ($R = 6.4 \times 10^{-10} gcm^{-1}s^{-1}$) is in good agreement with that obtained by Singh[114], who found the permeation rate of jet reference fluid through a blend of polysulphides to be $4 \times 10^{-10} gcm^{-1}s^{-1}$ at 25°C The value of R found in this work, also compares reasonably well with Mueller's value of 9.7×10^{-9} $gcm^{-1}s^{-1}$ for the permeation rate of SR6 gasoline in Thiokol ST polysulphide rubber at 55°C. He reported the rate to be negligible at 25°C[26].

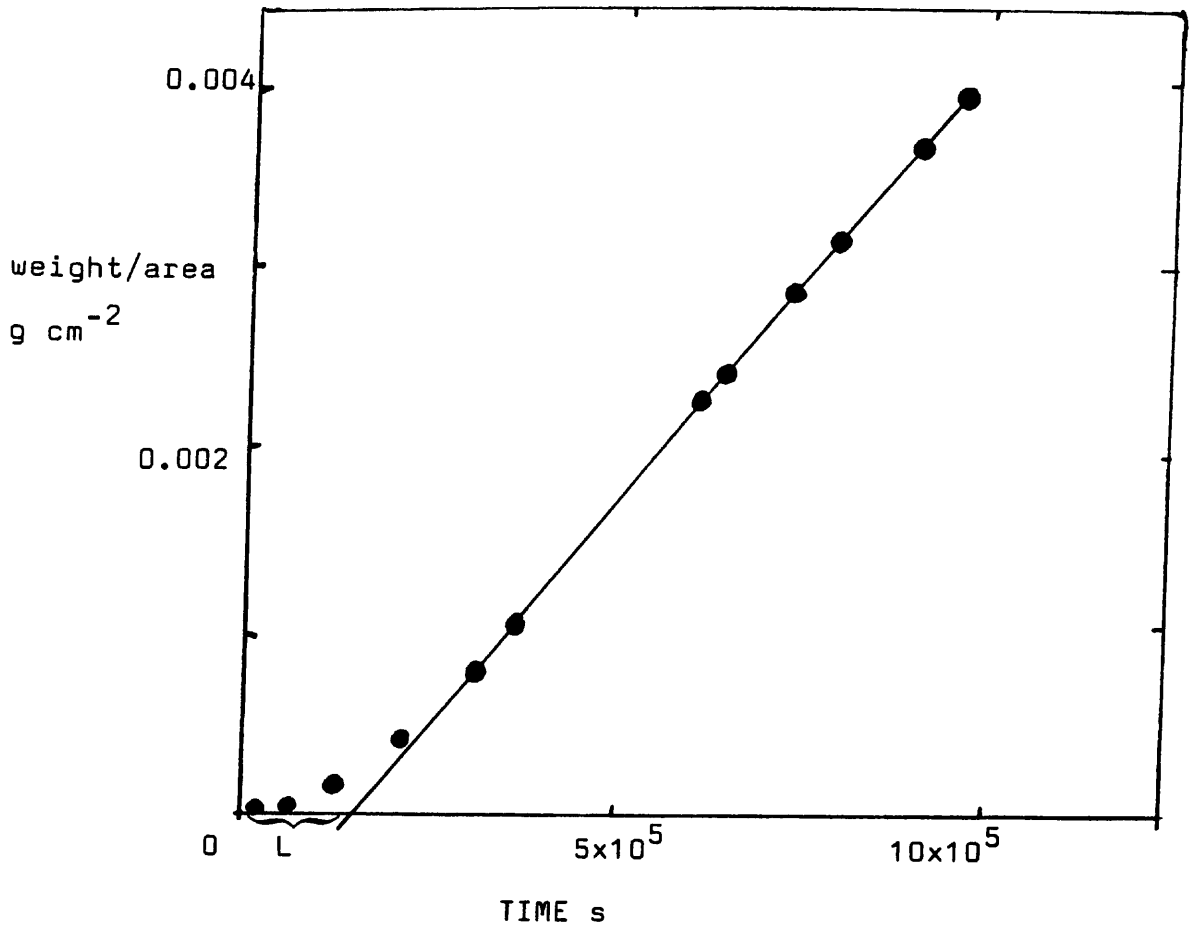

FIGURE 3.12

Plot of weight of Avtur per unit area transmitted through PR1422 with respect to time at 30°C. The plot asymptotes to a straight line.

thickness 1.35mm

area = 23.76 cm^2

slope = 4.75 x 10^{-9} g . cm^{-2}s^{-1}

time lag, L, = 1.5 x10^5 s

TABLE 3.6

Calculation of R, P and D from permeation experiment using Avtur aviation fuel at 30°C . Data from Figure 3.12 is used as the basis of these calculations.

A) permeation rate, R, = slope.thickness

slope (from Figure 3.12)= 4.75×10^{-9} g $cm^{-2}s^{-1}$

thickness = 0.135cm

Hence R = 6.4×10^{-10} $gcm^{-1}s^{-1}$

B) Permeation coefficient, P = R/(s.v.p. of Avtur)

s.v.p. = 0.456cm Hg at30°C *

Hence P = 1.42×10^{-9} g $cm^{-1}s^{-1}(cm\ Hg)^{-1}$

C) Time lag diffusion coefficient, $D_{TL} = \ell^2/6L$

ℓ = 0.135cm **

time lag (L) = 1.5×10^5s

Hence $D_{TL} = 2 \times 10^{-8} cm^2 s^{-1}$

* The saturated vapour pressure of Avtur has been estimated as 0.6kPa at 30°C from extrapolation of vapour pressure/temperature charts[111]. 1×10^5Pa = 76cm mercury.

** For permeation experiments ℓ is the sheet thickness

3.2.2. Correlation of diffusion and permeation data

The relationship

$$P=DS \qquad (3.2)$$

enables P to be calculated from the diffusion coefficient if the solubility is known. Equation 3.2 can be modified to R = DC as follows:

If Henry's Law is obeyed, then the concentration C, of aviation fuel in PR1422 is proportional to the vapour pressure.

$$C=Sp \text{ or } S = C/p$$

where S is the Henry's Law solubility for a system, p is the vapour pressure of the liquid, and C is the concentration of liquid in the rubber, in terms of mass per unit volume of rubber.

Since

$$P= R/p$$

a more convenient relationship can be derived by substituting for P and S in equation 3.2.

$$R/p = DC/p$$

$$\text{Hence } R = DC$$

where R is the permeation rate, D is the diffusion coefficient and C is the concentration.

Thus, if D and C are known, R can be calculated. D and C have been derived from the mass uptake experiment. The equilibrium uptake (M_{∞}) was converted to concentration of Avtur in PR1422 using the procedure described in Section 2.3.5. C is

calculated as follows (using the less inaccurate values obtained from the extracted samples):

The equilibrium uptake in PR1422 is 4.7g/100g rubber.
The average density of PR1422 was found to be 1.57g cm^{-3}.
Hence concentration (C) is $4.7g \times 1.57gcm^{-3}/100g = 0.074gcm^{-3}$
The diffusion coefficient (for the extracted samples) from mass uptake experiments is $1.0 \times 10^{-8} cm^2 s^{-1}$.

Hence the calculated permeation rate, R_{calc}, is given by:
$R_{calc} = 0.074 \times 1.0 \times 10^{-8} = 7.4 \times 10^{-10} gcm^{-1} s^{-1}$.

This value is in good agreement with the value for R of $6.4 \times 10^{-10} gcm^{-1} s^{-1}$ (shown in Table 3.6) which was obtained from the permeation experiment.

In addition, there is reasonable agreement between the diffusion coefficients from mass uptake experiments (D ranged from 0.8 to 1.6×10^{-8} $cm^2 s^{-1}$) and the permeation time lag diffusion coefficient ($D_{TL} = 2 \times 10^{-8} cm^2 s^{-1}$).

3.3. SUMMARY OF RESULTS OBTAINED FOR THE TRANSPORT OF AVIATION FUEL IN PR1422

The absorption of aviation fuel by PR 1422 is straightforward and appears to follows a classic, Fickian pattern. Evidence for this is

a) weight increase per unit surface area is independent of thickness in the early stages of uptake

b) weight increase is proportional to root time in the early stages

c) analysis of data at longer time shows $\ln(1-M_t/M_\infty)$ is proportional to time

d) the experimentally determined concentration profile is in reasonable agreement with the theoretical concentration profile.

e) Correlation between the experimentally determined permeation rate and that calculated from the solubility and diffusion coefficient is good.

f) There is reasonable agreement between the time lag diffusion coefficient ($2 \times 10^{-8} cm^2 s^{-1}$) and D obtained from mass uptake experiments (0.8 to $1.6 \times 10^{-8} cm^2 s^{-1}$).

There is some leachable material and removal of some of this results in a lower rate of diffusion and a higher equilibrium uptake.

Infra-red analysis indicated that the material leached from PR1422 was polysulphide plus epoxide resin and phenolic resin. Such material would probably be of low molecular weight and would act as a plasticiser for the bulk rubber. Hence the free volume available in the extracted samples is less after extraction of soluble material. This is indicated by the lower diffusion coefficient for the extracted samples

compared to the non-extracted samples.

The equilibrium uptake is about 3% by weight for the material prepared as the manufacturer's instructions.

The values of D obtained by the different mass uptake methods vary from 0.9 to 1.6 $\times 10^{-8} cm^2 s^{-1}$ for the non-extracted samples and from 0.8 to 1.1 $\times 10^{-8} cm^2 s^{-1}$ for the extracted samples.

The diffusion of many hydrocarbons in rubbers has been found to be concentration dependent[64,52]. However, in the case of aviation fuel in PR1422 there is no firm evidence for concentration dependency of the diffusion coefficient. The amount absorbed at equilibrium is relatively small and it is thus probable that the plasticisation effects which lead to the concentration dependency noted for other rubbers are absent.

Diffusion is faster in the unfilled material possibly due to a shorter path length for the diffusant.

The activation energy for the diffusion process is about 15 kcal/mole (62 kJ mol^{-1}).

The permeation rate is 6.4×10^{-10} g $cm^{-1} s^{-1}$.
The permeation coefficient is 1.42×10^{-9} $gcm^{-1} s^{-1} (cm\ Hg)^{-1}$.

CHAPTER 4

PILOT STUDIES OF UPTAKE OF WATER FROM LIQUID AND VAPOUR PHASE BY VARIOUS POLYSULPHIDES

4.1. MASS UPTAKE OF WATER VAPOUR BY LIQUID POLYSULPHIDES

A major part of this study is concerned with investigating the water uptake by commercial polysulphide sealants, in particular PR1422. It was decided, for comparison purposes, to determine the uptake of water by liquid polysulphides containing no additives (i.e. no filler, adhesion promoter or curing agent). The uncrosslinked liquid polysulphides that were investigated are shown in Table 4.1 together with some important structural properties.

The amount of water absorbed by liquid polysulphides exposed to an atmosphere of water vapour at 30°C was measured using the technique described in Section 2.3.2. All samples were maintained in a desiccator containing anhydrous calcium chloride for 1 week prior to exposure to the water vapour to remove any residual water. The weight changes are given in Table 4.1 in terms of M_t%, the weight of water absorbed as a percentage of the initial dry weight.

There appears to be no correlation between water uptake and the structural properties of the polymer (i.e. SH, crosslinking site concentration or viscosity).

All the uncrosslinked liquid polysulphides tested showed

TABLE 4.1

Composition and properties of commercial polysulphides and weight gains after exposure to water vapour at 100% RH at 30°C.

For all samples

exposed area of samples = 2400mm^2

approximate sample weights = 5g

approximate thickness = 5mm

Poly-sulphide	SH* %	Xlink* %	viscosity poise	M_t% after 1 hr	24 hrs	10days
LP 3	5.9-7.7	2.0	9.4-14.4	.15	.75	.85
LP 33	5 -6	0.5	15-20	.14	.48	.82
LP 2	1.5-2	2.0	410-525	.08	.38	.63
LP 32	1.5-2	0.5	410-525	.11	.45	.53
LP 12	1.5-2	0.2	410-525	not tested		
LP 31	1.0-1.5	0.5	950-1550	.14	.47	.76

* SH is the molecular weight percentage of thiol groups per molecular weight of polymer. Xlink refers to the crosslinking potential of the polymers. It is the percentage of branched molecules in the total number of molecules.

opacity after 48 hours exposure to water vapour. This opacity indicates that the water is not uniformly distributed. It is possible that water droplets form around impurities, or are caused by clustering of water through hydrogen bonding.

Since there is no correlation of water uptake with the number of thiol groups, it is concluded that the hydrophilic materials added during polymer manufacture (for example, latex stabilisers, soaps and reducing salts) may therefore be responsible for the bulk of the water absorption.

4.2. EXPERIMENTS ON THE MASS UPTAKE OF WATER BY POLYSULPHIDE RUBBERS FROM WATER

4.2.1. Mass uptake of water by polysulphides

The uptake of water by various cured polysulphide films was measured using the techniques described in Section 2.3.1. The samples tested were PR1422, PR1750, liquid polysulphides (LP2, LP12 and LP32) with different curing systems and uncured PR1422 (no curing agent added).

The results are shown in Figure 4.1 in the form of mass uptake, M_t%, versus root time/thickness plots.

In no case was an equilibrium weight increase reached; indeed the samples after soaking at 25°C for over 1 year were still gaining weight. Further, in the long term, anomalies are shown; the curves are concave to the abscissa. For both these

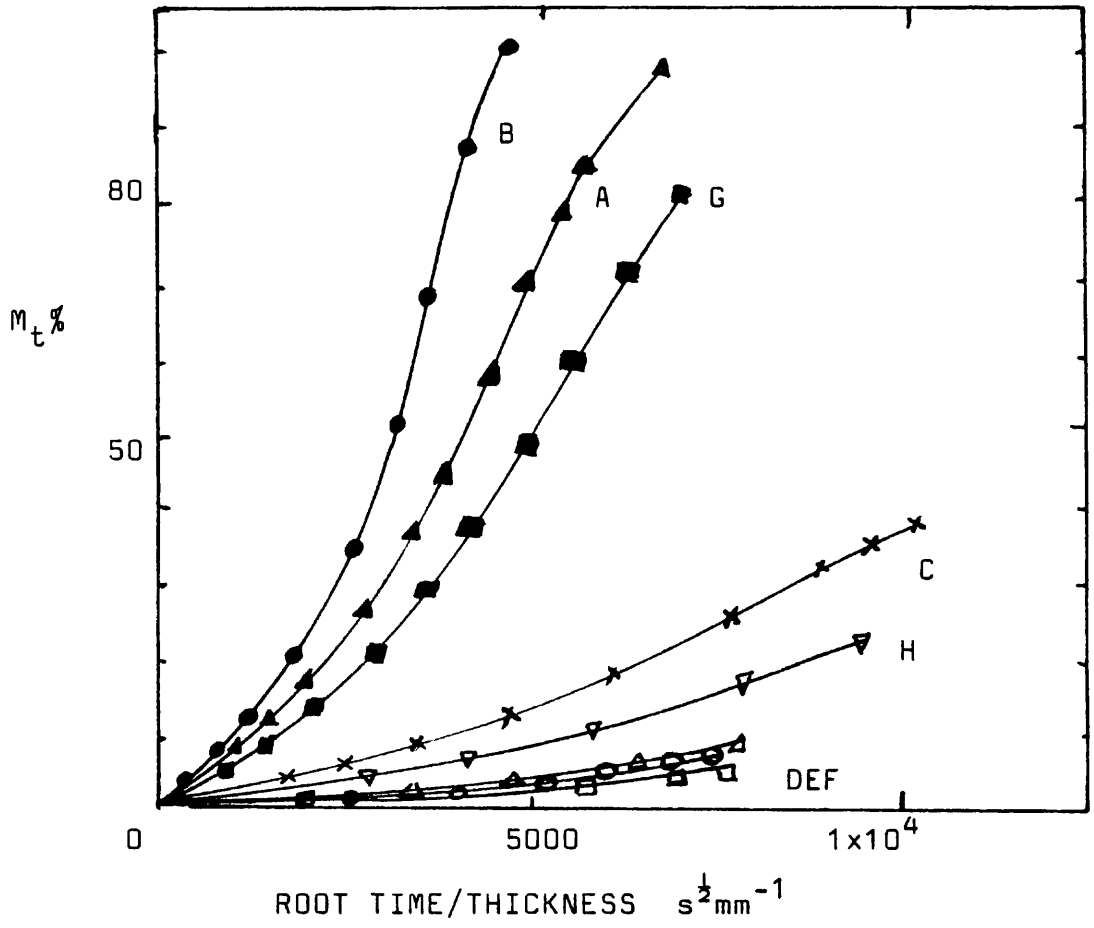

FIGURE 4.1.

M_t% versus root time/thickness for the absorption of water by various polysulphide rubbers with different curing agents. Temperature was 25°C for A,C,G & H; 30°C for B,D, E & F. Sample area=4800mm^2; sample thickness varied (0.28 to 2.9mm).

KEY

- ▲ A ... PR1422 + calcium dichromate
- ● B ... LP32 + 7% sodium dichromate
- × C ... LP32 + 7% cumene hydroperoxide (CHP) + 5% ZnO
- ⊙ D ... LP32 + 6% CHP + 1% diphenyl guanidine (DPG)
- △ E ... LP12 + 6% CHP + 1% DPG
- □ F ... LP2 + 5.5%CHP + 1%DPG
- ■ G ... PR1750 + manganese dioxide
- ▽ H ... PR1422- no curing agent

reasons, no attempt has been made to estimate diffusion coefficients.

There are marked differences in the rate of water uptake depending upon the type of polymer and curing agent used.

An important part of this work is to determine those factors that lead to these differences. Three obvious factors are:

a) the differences in crosslink density
b) the presence of curing agent and curing agent residues
c) the presence of impurities in the polymer (adhesion promoters etc)

a) importance of crosslink density in determining the magnitude of water uptake

Section 4.1 gave some indication of the rate of water uptake for the uncrosslinked materials. It might be expected that these would absorb water more quickly than the cured samples if crosslink density was important. However, after 1 hour these samples had absorbed on average about 0.1% In all cases the cured samples had absorbed a greater amount in this time: in the some instances orders of magnitude greater.

This suggests that crosslink density is not the predominant factor controlling the amount of water absorbed. The similar water uptakes by the cumene hydroperoxide cured LP polymers with different crosslink potential tends to confirm this.

b) importance of curing agent and curing agent residues in determining the magnitude of water uptake

Evidence for the importance of curing agent residues can be deduced from the difference of an order of magnitude between the amount of water absorbed by the sodium dichromate, calcium dichromate and manganese dioxide cured polysulphides and the cumene hydroperoxide cured samples. Polysulphides cured with totally organic systems appear to have the lowest water uptakes.It is thus possible that the water soluble residues from the curing agents are one of the causes of high water uptake.

Since most sodium salts are very soluble in water, it is to be expected that the sodium dichromate cure will result in a high proportion of water soluble residues and this is reflected in the highest water uptake. This is shown in curve B of Figure 4.1.

Curves A and G in Figure 4.1 describe the water uptake of samples of PR1422 and PR1750. (Hanela et al.[88] have shown that PR1422 and PR1750 both give similar crosslink densities when cured with their commercial curing agents. Both materials have a similar amount of filler and contain adhesion promoters. The major difference is that PR1422 is cured with calcium dichromate and PR1750 is cured with manganese dioxide. Calcium dichromate is readily soluble in water, whereas manganese dioxide is less soluble in water.

c) importance of impurities from sources other than curing agent in determining the magnitude of water uptake

Other obvious impurities which may contribute to the amount of water taken up by the polysulphides, are those due to:

a) materials present in the polysulphide base such as soaps and latex stabilisers (magnesium hydroxide is commonly used).

b) fillers

c) adhesion promoters

All the factors a,b and c are present in samples A',G and H. The greater uptake of water by the samples cured with inorganic salts,(A and G) relative to the PR1422 base with no curing agent added (curve H) show that the effect of different curing agents is much greater than the intrinsic impurities and hydrophilic additives in the base material.

It is concluded from the above observations that the effect of curing agent residues appears to be the major factor controlling the rate of water uptake. Of the curing systems studied, inorganic salts give higher water uptakes than organic, and the uptakes are in the order of the solubility of the cations formed.

4.2.2. Desorption of water from PR1422

A sample of PR1422 was soaked in water until it had absorbed more than 200% by weight. The desorption was carried out as described in section 2.3.3. The result is shown in Figure

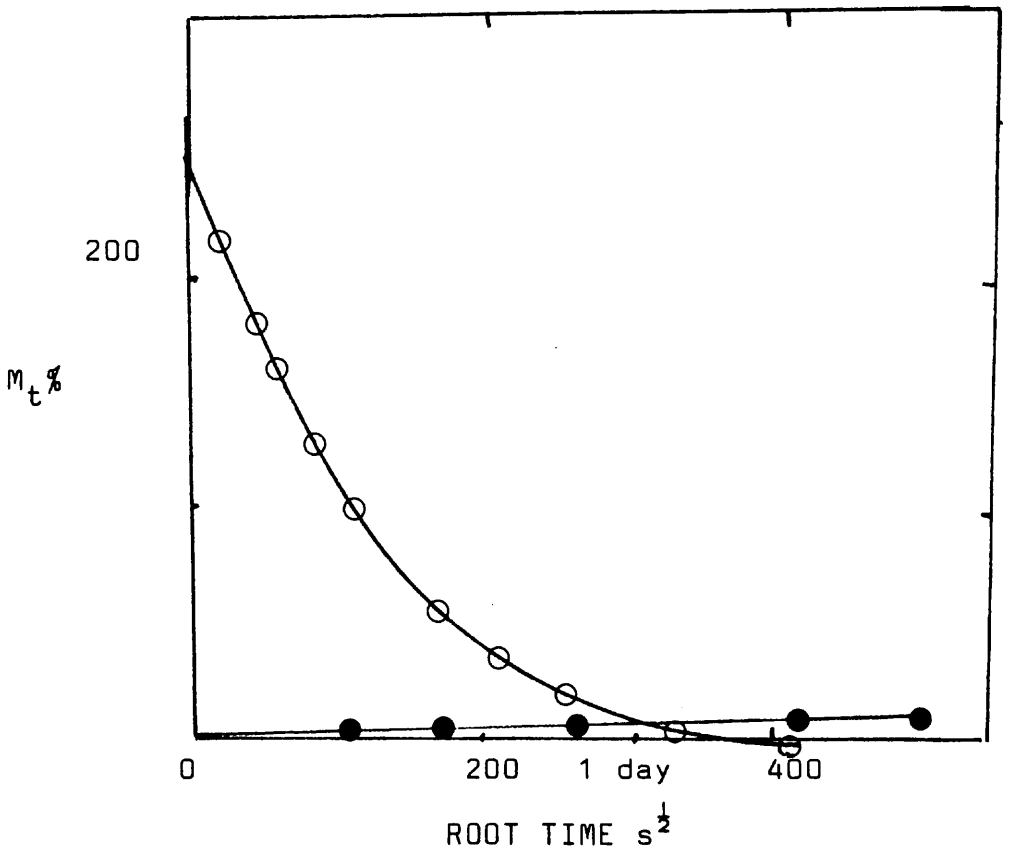

FIGURE 4.2

Plot of M_t% versus root time for the absorption at 25°C and desorption of water from PR1422 at 30°C, showing that desorption is fast relative to absorption of water.

Sample area = 4800mm^2: sample thickness = 0.105mm

KEY

● absorption

○ desorption

4.2. It can be seen that desorption is much more rapid than absorption.

The final $M_{t\%}$ for desorption is below zero. The weight loss of 4.5% indicates that some water soluble materials were leached out during the uptake of water.

Since the sample had not reached an equilibrium uptake during absorption, the desorption diffusion coefficient cannot be calculated from Figure 4.2. However, it is clear that the desorption diffusion coefficient must be appreciably greater than the absorption diffusion coefficient. This indicates that the diffusion coefficient is dependent upon the concentration of water. Concentration dependency has been found for diffusion of water in several rubbers[3,77].

4.2.3. Materials leached from PR1422 during immersion in water

The desorption experiment showed that material was lost through leaching during long time immersion. It was thought that a knowledge of the nature of the leached material would be important in understanding the process of water uptake.

In order to determine the nature of the water soluble materials, a sample sheet of PR1422 was cut into small pieces and sohxlet extracted for 48 hours using an acetone/water mixture. About 6.8% material was extracted.

Infra-red analysis of the extract showed the presence of polysulphide and epoxide/phenolic groups. There was no detectable qualitative difference between the toluene, azeotrope extracts (described in Section 3.1.3) and the water/acetone extracts.

It was concluded that the bulk of leached material was adhesion promoters and unreacted polysulphides of short chain length. Organic thiols are water-soluble [110]. Some calcium and chromium were detected by atomic absorption analysis of the water-leached material from PR1422. However, chromium was deduced to be low for the following reason. After 1 days immersion in water the dichromate cured PR1422 and LP32 caused discoloration of the water.

However, it was found (from dilution of standard solutions until the yellow coloration could not be seen) that the dichromate ion ($Cr_2O_7^{=}$) was visually detectable at levels as low as 10 parts per million. This implies that the yellow colour noted in the soaking water may be caused by leaching of very small amounts of dichromate. After 4 days, during which time the soaking water was changed daily, no further discoloration was noted. It was therefore concluded that the dichromate leached out in the early stages of immersion was present in (or on) the surface layer of the film.

In a separate experiment it was shown that there was no significant calcium loss from the chalk filler during water immersion.

4.2.4. Effect of filler on mass uptake of water by PR1422

A sample of PR1422 was treated to remove the filler, as described in Section 2.2.3. Mass uptake in distilled water at 25°C was monitored for samples of PR1422 and PR1422 (filler removed).

The results are shown in Figure 4.3. It can be seen that the PR1422 takes up a smaller percentage of water than the PR1422 (filler removed). A correction was carried out by calculating the weight uptake of water as a percentage of the weight of PR1422 only i.e. M_t% has been adjusted by dividing the values by 0.63, the weight fraction of rubber. However, this correction still does not account for the discrepancy between the amount absorbed by PR1422 and PR1422 (filler removed).

Qualitatively, this result is the same as for the early stages of the uptake of aviation fuel by PR1422 and PR1422 (filler removed) which is shown in Figure 3.10. As discussed in Section 3.1.10, there are two possible causes of the greater uptake of liquid by the PR1422 with filler removed:

a) effect of filler on modulus

b) tortuosity effects

a) Several authors [21-23] have found that the increase in modulus, due to an increase in filler content, leads to a reduction in swell of rubbers by solvents soluble in the rubber. In this work, an increase in modulus would also tend to a decrease in the amount of water present in droplet form.

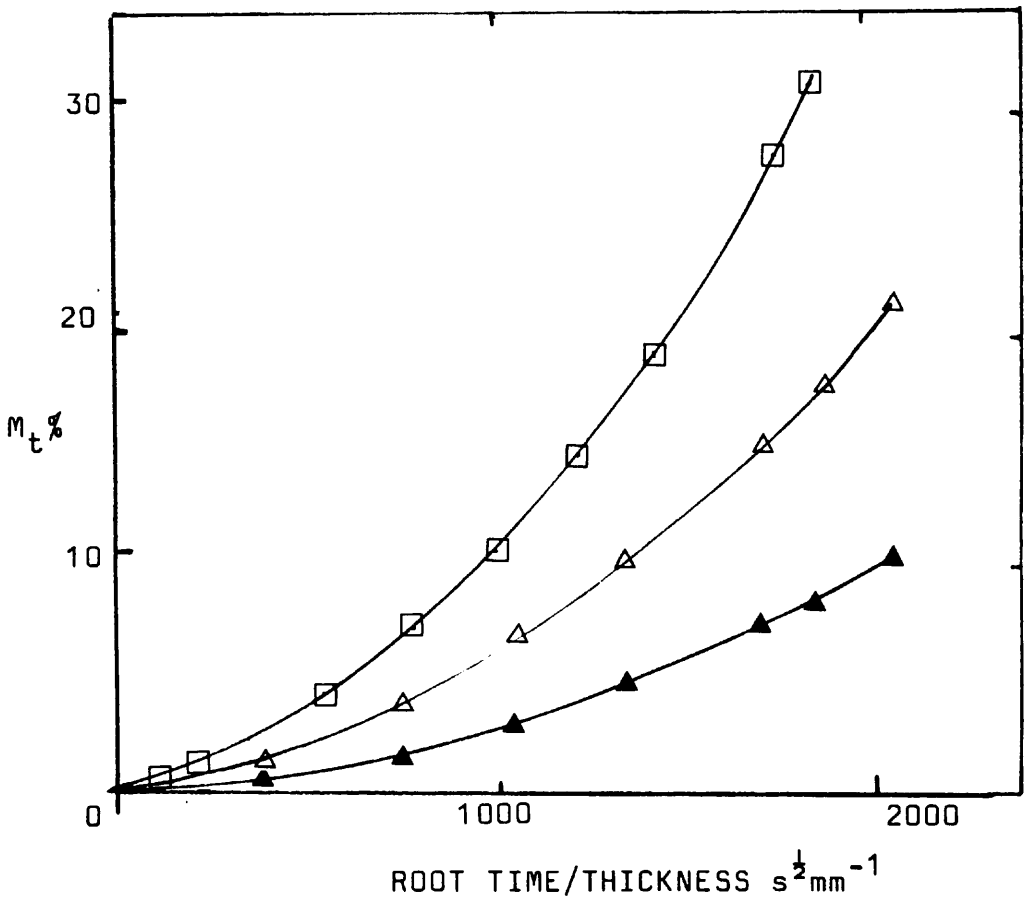

FIGURE 4.3

Plot of M_t% versus root time/thickness for the mass uptake of water by PR1422 and PR1422 (filler removed) at 25°C showing that removal of filler results in a higher water uptake.

All sample areas = 4800mm^2

KEY

	thickness
□ PR1422 filler removed	0.89mm
▲ PR1422	1.18mm
△ PR1422 adjusted *	1.18mm

* M_t% values have been divided by the weight fraction of the rubber (0.63)

Since swelling is high, the effect is presumably not negligible, as was found for the uptake of aviation fuel.

b) Because of a longer path length in the filled samples, the mobile water in solution would penetrate into the rubber more slowly. Hence the rate of uptake would be decreased for the filled samples.

The differences in water uptake between the filled and unfilled PR1422 are probably due to both modulus and tortuosity effects. Because of the lack of equilibria, it is not possible to distinguish between contributions due to either effect.

4.3. SUMMARY OF RESULTS

The mass uptake of water by polysulphides presents several difficulties of interpretation. Equilibrium is not reached within several months, even for very thin sheets. Further, abnormal curves (concave to the abscissa) result where uptake is especially rapid with respect to time.

The major factor affecting the rate of uptake of water. appears to be the type of curing agent added i.e. the amount of water soluble impurities present as curing agent residues. Crosslink density is not a major factor in determining water uptake.

For the commercial sealant PR1422, removal of the filler

increases the rate of uptake of water beyond that expected based on the fraction of filler present.

Desorption is noticeably more rapid than absorption, suggesting that the diffusion process of water in PR1422 is dependent upon the water concentration.

In order to make any progress with this study it is necessary to reach an equilibrium swelling of samples. A survey of the literature [2,3,75,76,77] has shown that this can be achieved by using common salt solution to increase the external osmotic pressure. This would lead to a reduction in the amount of water absorbed since the difference in internal and external osmotic pressure would be reduced. Therefore in subsequent chapters the soaking media will be salt solutions.

However, before discussing water uptake further it has been decided to discuss the effect of water uptake on physical properties, since this gives information that is relevant to an understanding of the mechanism of water uptake.

CHAPTER 5

THE EFFECT OF WATER ON PHYSICAL PROPERTIES OF PR1422

5.1. INTRODUCTION

The high uptake of water by polysulphide rubber samples (shown in chapter 4) would be expected to affect the physical properties of the rubber. For a sealant, reduction in either adhesive or cohesive strength can lead to its failure in service. Visual examination of thin samples of PR1422 after prolonged water immersion suggested that breakdown of the bond structure occurred in some cases. An investigation of the changes in physical properties of the commercial sealant, PR1422, was carried out using various techniques.

5.2. VOID FORMATION

Some thin (0.2mm) samples of PR1422 which had been soaked for over 1 year and had a water uptake of 180% by weight, showed voids.

A typical sample showing voids is shown in figure 5.1, together with a typical untreated sample from the same batch mix.

Void formation is possibly caused by permanent set of the rubber at high strain around large water droplets.

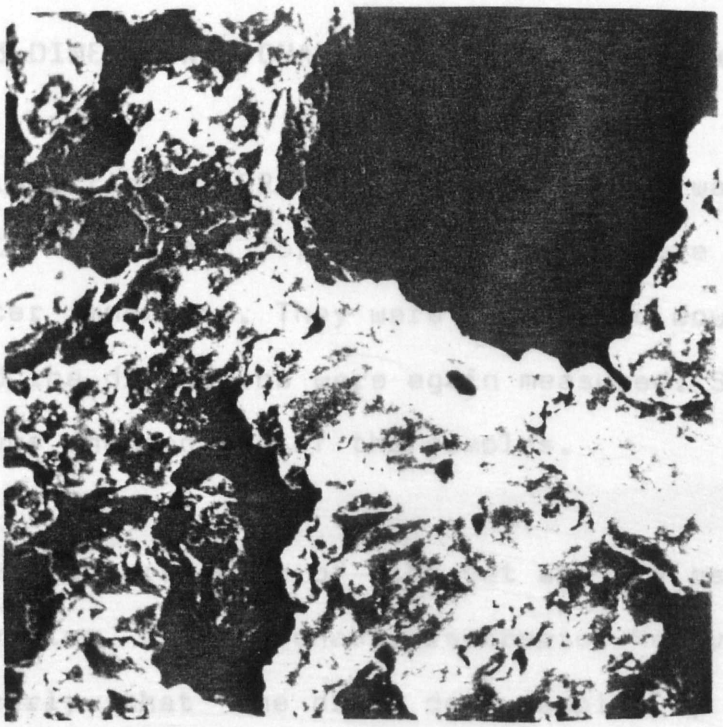

SAMPLE A

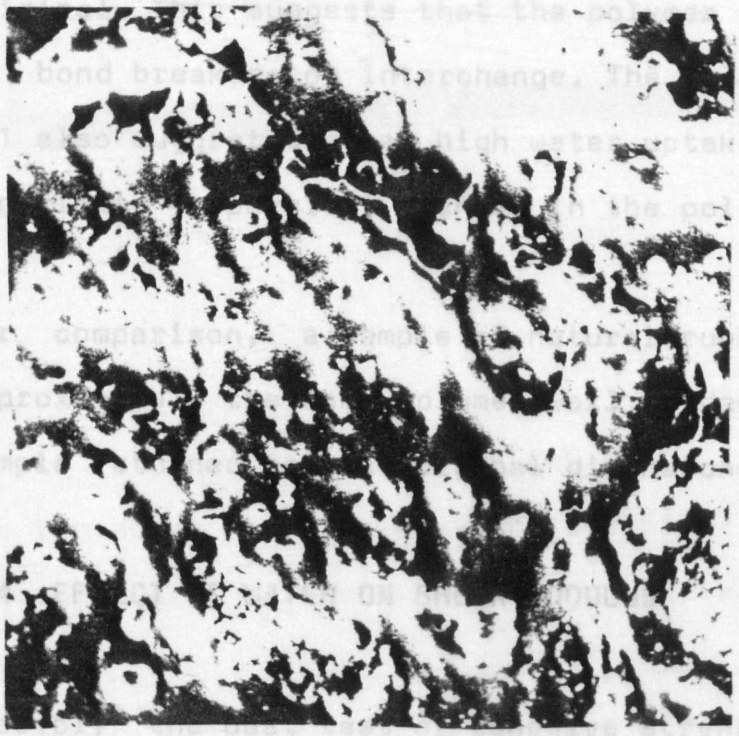

SAMPLE B

FIGURE 5.1

Samples of dry and water-soaked PR1422 examined x 1200 under electron transmission microphotography. Sample A, which was immersed in running water for 1 year, shows large voids. Sample B which has been kept dry in a desiccator does not show such voids.

5.3 DIMENSIONAL CHANGES AFTER PROLONGED WATER IMMERSION

Thin strips of PR1422 were immersed in water until the weight gain was about 75%. The dimensions were measured before and after immersion. They were then dried down to constant weight and the dimensions were again measured. See Figure 5.2, which shows photocopies of the samples.

The measurements of the wet and dry samples suggest that swelling is reasonably isotropic. However, it can be seen clearly that the dried down sample (3) is longer than the original. This suggests that the polymer structure is altered by bond breakage or interchange. The results shown in Figure 5.1 also suggest that at high water uptake void formation can contribute to physical changes in the polymer structure.

For comparison, a sample of natural rubber was swollen to approximately the same volume swell in decane. On drying, the sample returned to its original dimensions.

5.4 EFFECT OF WATER ON SHEAR MODULUS

Possibly the best test of cohesive strength of a material is the tear strength. However, this test tends to produce a wide range of scatter of results and requires the testing of a large number of specimens. In order to gain information quickly it was decided to test the shear modulus of the material as a measure of crosslink density and thus cohesive strength.

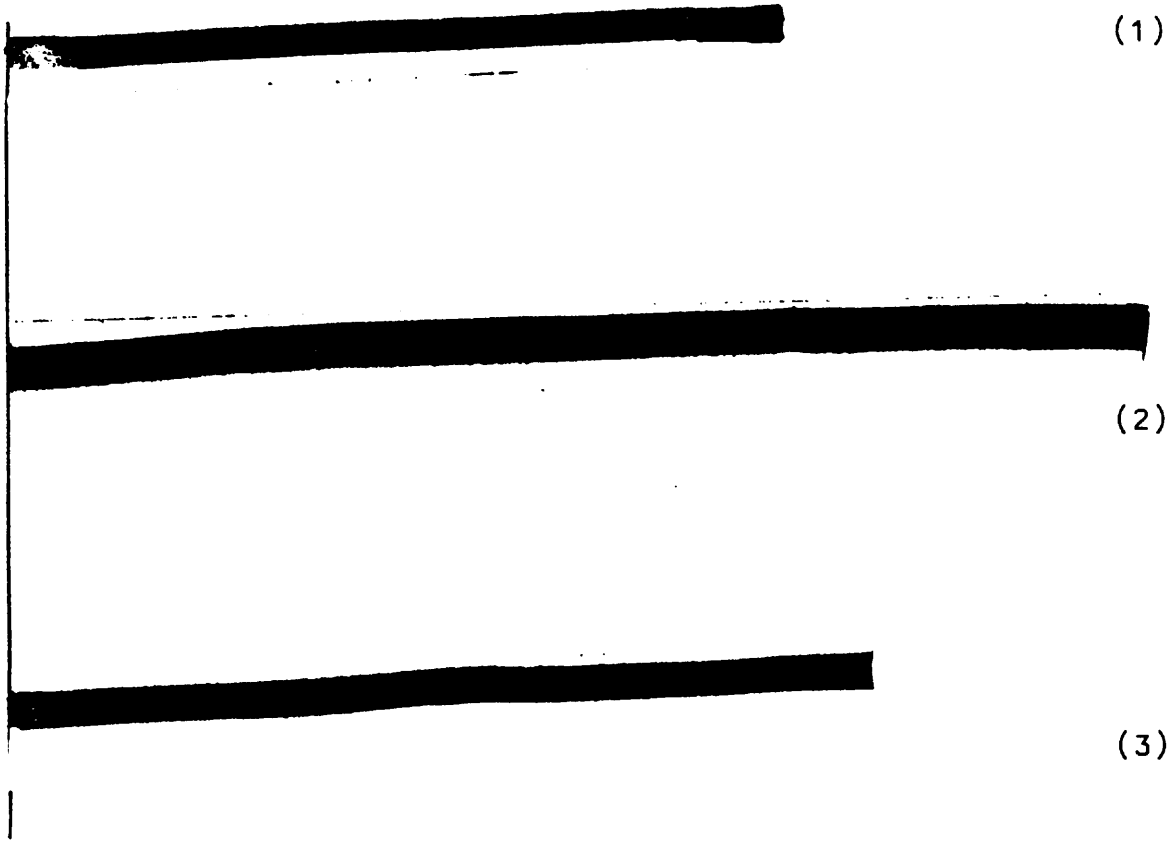

FIGURE 5.2

Photocopies of sample strips of PR1422, showing dimensional changes after prolonged immersion in water

KEY

	length mm	width mm	thickness mm
(1) Dry, original state	105	4.0	0.22
(2) wet: 75% water by weight	155	6.0	0.34
(3) wet, then dried out	117	4.2	0.20
% increase when wet	48	54	50

5.4.1. Changes in shear modulus, G, of PR1422 containing different amounts of absorbed water

Thin strips of PR1422 were immersed in water at 25°C for varying lengths of time. Strips having different water content were then tested on an Instron. Gaussian plots of stress versus $(\lambda - \lambda^{-2})$ were drawn. Stress was calculated on the basis of the unswollen, unstrained cross-sectional area of the specimens. λ is the extension ratio.

From the statistical theory of rubber elasticity,

$$G_{swollen} = G_{dry} v_r^{\frac{1}{3}} \qquad (5.1)$$

where $G_{swollen}$ and G_{dry} are swollen and dry shear moduli, v_r is volume fraction of rubber.

Thus, in theory, the only effect of swelling on shear modulus is to reduce the modulus by a factor of $v_r^{\frac{1}{3}}$.

Since equation 5.1. is derived from entropy considerations based upon an extension ratio referring to the unstrained **swollen** dimensions then the equation linking stress (f') to extension is

$$f' = G_{dry}\, v_r^{\frac{1}{3}} (\lambda - \lambda^{-2})$$

where f' refers to the swollen area. If the area used to calculate stress is the dry, unswollen area, then the relationship becomes:

$$f = G_{dry} v_r^{-\frac{1}{3}} (\lambda - \lambda^{-2})$$

where f is stress based on the dry, unswollen area.

Hence the slope of a plot of stress (f) against $(\lambda - \lambda^{-2})$ gives $G_{dry} v_r^{-\frac{1}{3}}$. Thus the slope multiplied by $v_r^{\frac{1}{3}}$ gives the theoretical dry modulus (G_{dry}) and changes in modulus other than those caused by the dimensional changes of swelling can be determined.

A plot of f versus $(\lambda - \lambda^{-2})$ for a sample of PR1422 before, during and after (dried down) water uptake of 70% is shown in Figure 5.3. Data taken from Figure 5.3 is given in Table 5.1.

TABLE 5.1

Data from Gaussian plots, of changes in shear modulus before, during and after water uptake of 70%

sample	G_{dry} Nmm^{-2}
dry	1.65
wet	0.82
wet, then dried	1.50 **

** based on final dry dimensions

For the dried out sample, it was noted that deviations from a straight line occurred at relatively low values of $(\lambda - \lambda^{-2})$ (about 0.5) compared to other rubbers[101].

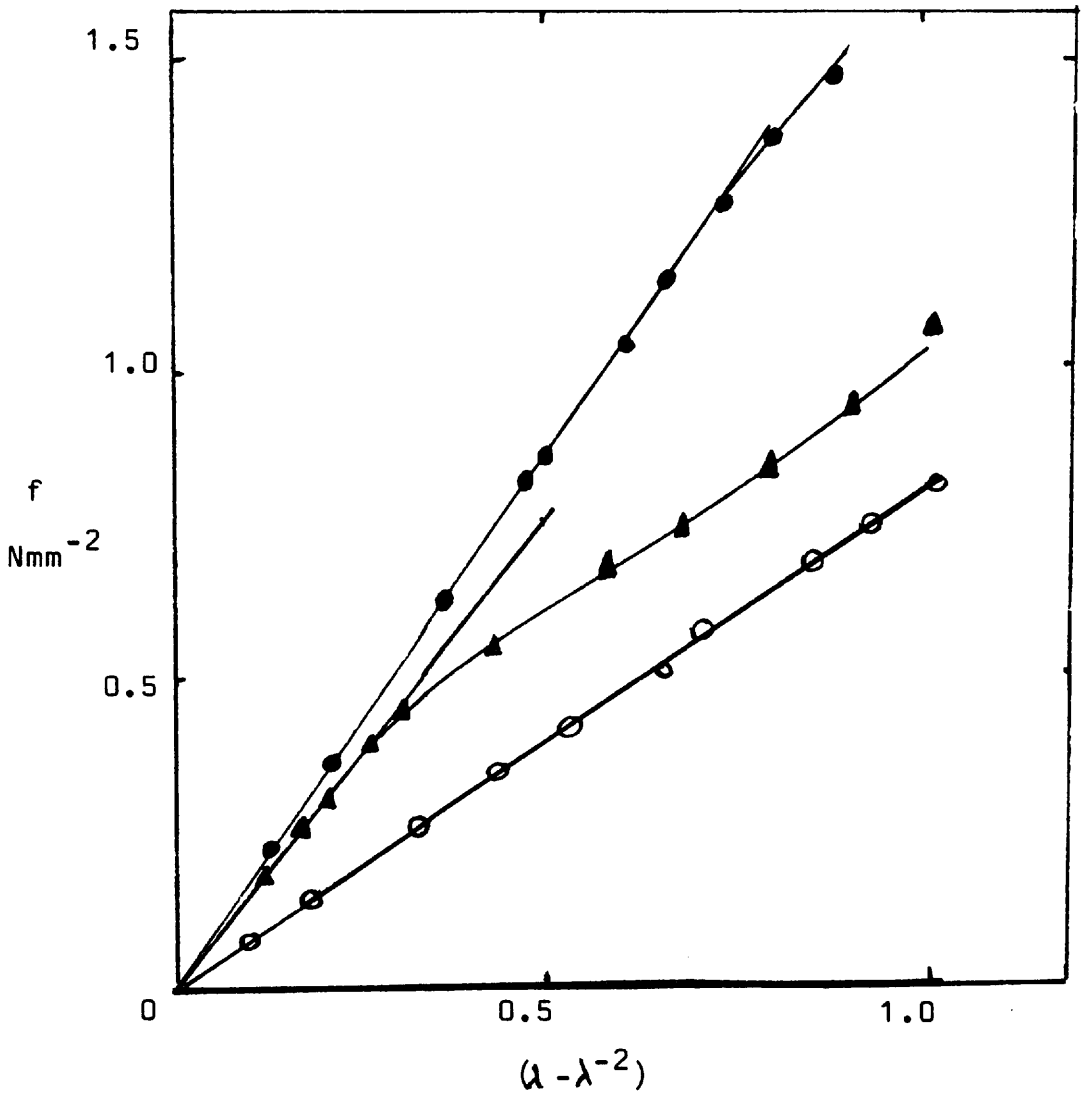

FIGURE 5.3

Gaussian plot of f versus $(\lambda - \lambda^{-2})$ showing difference in plot before, during and after water uptake by PR1422 of 70% by weight of water.

v_r is 0.48. f is based on dry cross- sectional area

KEY

● dry

○ wet

▲ wet, then dried

Table 5.1 shows that the loss in modulus after drying out is only about 10%. However, Figure 5.3 shows that the loss in stress is far greater than this at high extensions. This may be due to

a) possible void formation

b) reduction of strength through a decrease in the amount of effective physical crosslinking caused by entanglements and polar bonding, which on drying out do not reform to the same extent.

c) the effects of possible bond-interchange, leading to a change in bond configuration; the change in the shape of the Gaussian plot for the dried out sample may be evidence of bond-reformation in that there is greater deviation from a statistical configuration at lower extension for the dried out sample.

A plot of the shear modulus (G_{dry}) versus the the volume of water in swollen rubber/ volume of rubber (swell ratio) is shown in Figure 5.4.

It can be seen from Figure 5.4 that there is a marked lowering of the modulus after a relatively small water uptake. The marked drop in modulus on uptake of a relatively small amount of water is perhaps surprising, since allowance has been made for the volume of liquid in the calculation of G_{dry} but this effect has been noted for a range of sealants including polysulphides, polyurethanes and silicones [112].

It is possible that a large proportion of the effective

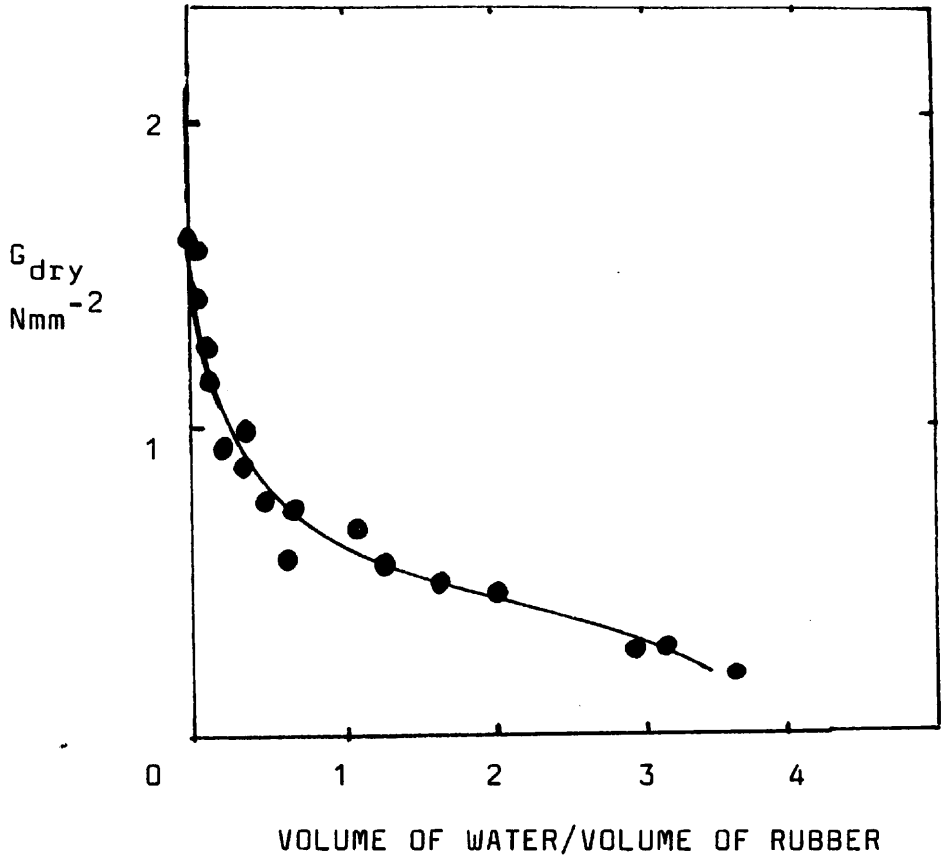

FIGURE 5.4

Plot of G_{dry} versus volume of water/volume of rubber, for PR1422 , showing effect of water on shear modulus G_{dry}. The plot shows the decrease in shear modulus with increasing water content.

The volume of water/volume of rubber is $(1/v_r - 1)$.

crosslinks in the polysulphide are physical crosslinks. These crosslinks, due to polar inter-chain bonds and chain entanglement, may be broken on swelling. A small amount of water would possibly be effective in decreasing polar bonding by a significant amount.

Figure 5.4 shows that the rate of change of modulus with increasing water content decreases at higher uptakes. In this region, the bulk of the water is present in droplet form and the number of chains involved with the droplets is relatively small. However, the stress on the rubber chains around the droplets will be very high indeed, and it is possible that breakage and reforming of these chains (bond interchange) can occur. Release of inbuilt stresses via a bond interchange mechanism[12], has been extensively studied for polysulphide rubbers.

The presence of voids, as indicated by Figure 5.1, can also contribute to the loss of strength found in this region. It is probable that void formation occurs due to permanent set of the strained rubber chains around large droplets.

5.4.2. Effect of water on Mooney-Rivlin C_1 and C_2 for unfilled PR1422 and cumene hydroperoxide cured LP32

Data from the stress/strain plots were converted to the form $fv_r^{1/3}/[2(\lambda-\lambda^{-2})]$ versus $1/\lambda$, to give Mooney-Rivlin plots. Mooney-Rivlin plots give some information about cross-link density. Mooney-Rivlin plots for PR1422, however, gave curves

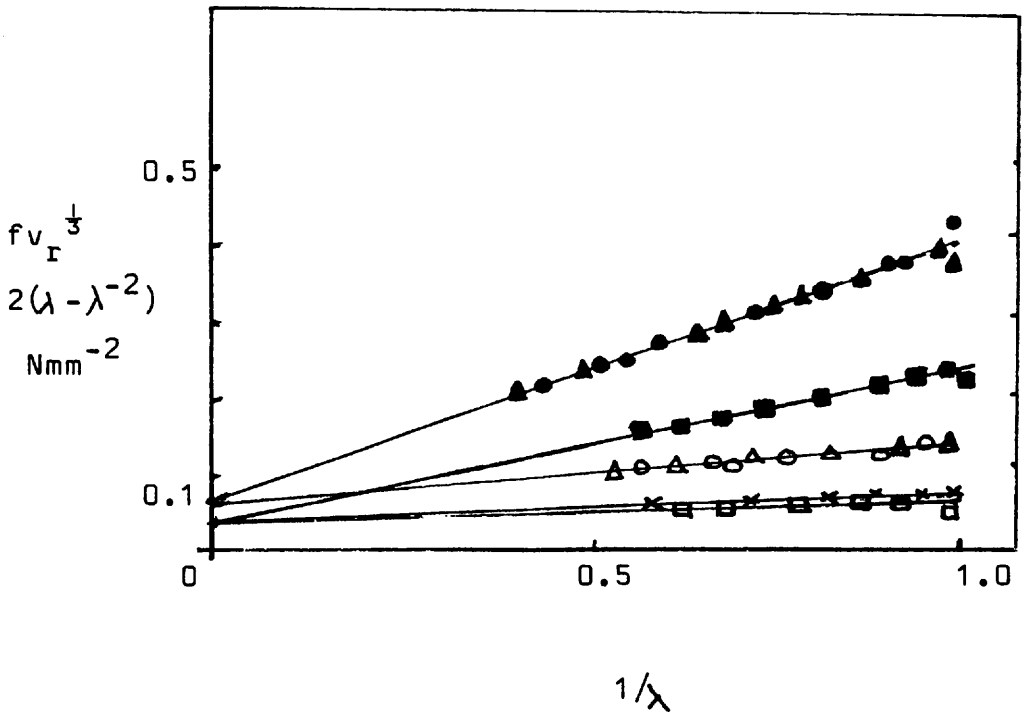

FIGURE 5.5

Mooney-Rivlin plots for PR1422 (with filler removed), 7% sodium dichromate cured LP32 and cumene hydroperoxide (CHP) cured LP32, showing that effect of water is to lower the slope (C_2). Toluene soaked cumene hydroperoxide cured LP32 is also shown, showing that the effect of water and solvent on C_1 and C_2 is similar. f is stress based on dry area. v_r is the volume fraction of rubber. C_1 is the intercept.

KEY

	v_r		
PR1422 (filler removed) water soaked	(.61)	wet ○	dry ●
LP32 + sodium dichromate water soaked	(.60)	wet △	dry ▲
LP32 + CHP water soaked	(.40)	wet □	dry ■
LP32 + CHP toluene soaked	(.38)	wet ×	dry ■

	C_1	C_2(dry)	C_2(wet)	
PR1422 (filler removed)	0.06	0.34	0.07	Nmm^{-2}
LP32 + CHP	0.04	0.18	0.02	

not straight lines. It was thus difficult to measure the intercept with any accuracy.

In order to obtain graphs which could give a reliable intercept stress /strain testing of PR1422 with filler removed was carried out.

Dry samples and wet samples containing 45% water by weight (v_r approximately 0.6) were tested. The resulting Mooney-Rivlin plots are shown in Figure 5.5. The results from samples of cumene hydroperoxide cured LP32, soaked in water and toluene, (v_r approximately 0.4), are also given for comparison, as are results from a sample of 7.5% sodium dichromate cured LP32.

It can be seen from Figure 5.5 that the change in C_1 after relatively high uptake of water is very small. This implies that there is negligible overall change in chemical crosslink density in the water soaked samples. There is strong evidence for bond interchange in polysulphide rubbers [11,12,13]. Bond interchange should not show as a change in C_1. Tobolsky has shown that the rate of formation is the same as the rate of breakage of bonds for this process[12], so the effective crosslink density remains the same.

There is, however, a marked decrease in the slope, C_2. Further, the ratio C_2 to C_1 (which can be deduced from Figure 5.5) is very high for the dry sample (approximately 6) when compared to published results for natural rubber[101] of less

than 1. This high C_2/C_1 ratio possibly indicates that the main strength of the sealant is due to entanglement, or physical bonding, rather than solely chemical linkage. C_2 is often regarded as measure of deviation from statistical, a Gaussian behaviour at high extension, and can be used as a measure of physical crosslinking due to entanglements and/or chain interactions.

The sample soaked in toluene shows the behaviour of a good swelling agent, compatible with the rubber. The effect appears to be the same as that of water.

For the case of toluene, all the amount absorbed is truly soluble. The mechanism of plasticisation by toluene is to solvate every polymer chain and results in a pushing apart of the polymer chain segments. This allows greater movement of the individual chain segments.

However, the amount of water soluble, in terms of molecular compatibility, is believed to be very small. It may be possible that the small amount of water truly soluble, since it is highly polar, has a much more marked effect on the free movement of the chain segments than a non-polar solvent. If this is so, then the implication is that there is a high degree of hydrogen-bonding (or other intra-molecular interactions) in the polysulphide.

A further explanation arises from the suggestion of the presence of co-ordination bonding in polysulphides cured

using dichromate curing systems[10]. It is possible that water would inhibit such coordination bonding and result in a reduction in modulus. However, peroxide cured LP32 also shows a high loss of modulus with relatively small amounts of water. It therefore seems unlikely that coordination bonding is an important cause of the reduction in modulus that arises in the presence of water.

5.5. INITIAL EXPERIMENTS ON THE EFFECT OF WATER ON ADHESIVE STRENGTH

A cursory examination of the effects of high water uptake on the adhesive properties of PR1422 was made. The following samples were prepared.

a) dry samples
b) wet samples with about 75% water uptake and
c) dried samples, previously soaked to the same water content as the wet samples

The relative peel strengths to primed Dural were measured as described in Section 2.7.2, and the results are shown in Table 5.2.

The adhesive failure to the cotton tape of the majority of the wet samples appeared (from visual examination during testing) to be due to crack formation at the wet cotton/PR1422 interface.

TABLE 5.2

Effect of 75% water content on peel strength of PR1422, bonded to Dural, at a peel rate of 10mm per minute.

sample	Peel strength Nmm^{-1}	type of failure (predominant)
dry	1.26	cohesive
wet	0.42	adhesive/cotton
wet, then dried	0.67	adhesive/Dural

It is seen that there has been some permanent loss of adhésive strength, on drying out of previously soaked samples. Normally, adhesive strength is strongly affected by the modulus of the adhesive. Since it was found that subsequent drying of a wet sample of PR1422 (see Table 5.1) had only a small effect on modulus, this, together with the change from cohesive to adhesive failure, suggests that full water penetration to the bond line has occurred.

The reduction in adhesive strength thus appears to be related to the partial destruction of the adhesive bond, not to changes within the adhesive.

5.6. EFFECT OF HIGH WATER UPTAKE ON OTHER PROPERTIES OF PR1422

The results from the modulus measurements suggest that some degree of plasticisation has occurred after water immersion. In order to see if this was correct various tests were carried out on wet and dry samples of PR1422.

5.6.1. Effect of water immersion on hysteresis of PR1422

Hysteresis was measured from stress/strain data at increasing and decreasing stress, as described in Section 2.7.3.

The results are shown in Table 5.3. which includes data from toluene swollen PR1422. In all cases the samples exhibited normal rubber behaviour in that on each successive cycle the strain dropped and the size of the hysteresis loop decreased. Because of limited time available none of the samples were subjected to more than two cycles.

Comparison of the effect of toluene swelling on hysteresis strongly suggests that qualitatively the effect of water swelling is similar to swelling in toluene. This is surprising. The effect of hydrocarbon swelling is readily explained in terms of plasticisation of the rubber. It appears that the effect of water swelling is the same, but this effect may be due to a different mechanism, since the bulk of the water uptake is presumed to be not in true solution. This result tends to confirm the suggestion put

forward in Section 5.4.2 as an explanation for the similar reduction in the slope of Mooney-Rivlin plots by toluene and water viz. that the small amount of water believed to be in true solution has the effect of destroying polar bonding between the polymer chains.

TABLE 5.3

Hysteresis of PR1422 and PR1422 (filler removed) films, showing reduction in hysteresis on water and toluene uptake. Strain = 60% in all cases.

			hysteresis **	
type of sample	solvent	wt%	% first loop	% second loop
filled	-	-	44	27
filled	water	12	37	20
filled	water	80	28	-*
unfilled	-	-	35	25
unfilled	water	50	26	23
filled	toluene	23	41	23

* sample broke on second application of strain.

2 further samples broke on application of first strain.

** Hysteresis is the amount of energy dissipated divided by the total work done

5.6.2. Stress relaxation

The following samples were tested for stress relaxation using the method outlined in Section 2.12.

a) dry samples

b) wet samples with about 75% water uptake and

c) dried samples, previously soaked to the same water content as the wet samples

Plots of f_t/f_o (stress at time t and zero respectively) versus the natural logarithm of time were made. The relaxation times were taken from the points where f_t/f_o was equal to 1/e, as shown in Figure 5.6. The relaxation times of the samples are shown in Table 5.4.

TABLE 5.4

Stress relaxation times of dry, wet (75% water by weight) and wet, then dried samples of PR1422, at 60% strain.

type of sample	relaxation time minutes	water content % by wt
(a) dry	66,000	0
(b) wet	5,500	75
(c) dried out	60,000	0

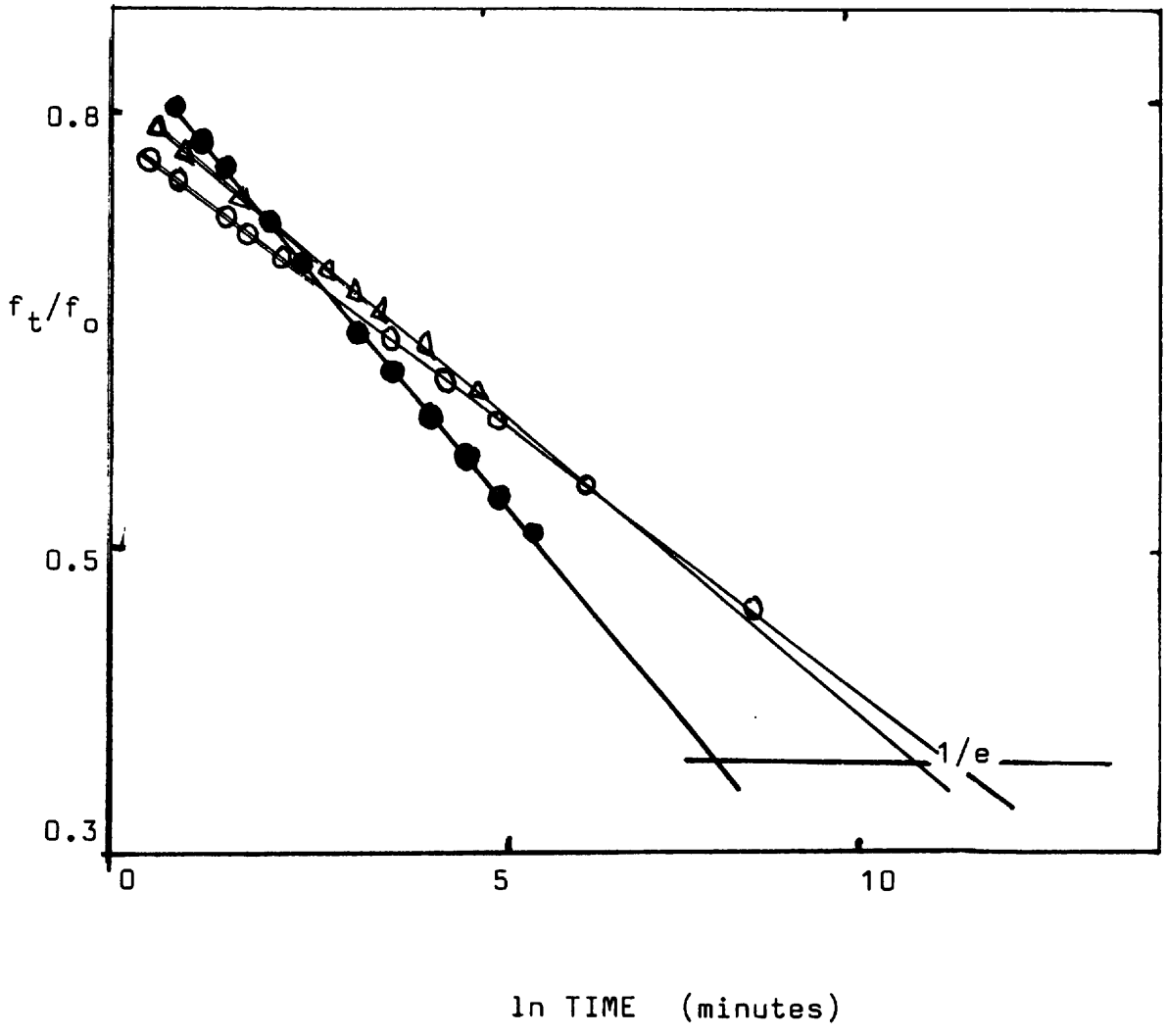

FIGURE 5.6

Plot of f_t/f_o versus ln time for samples of dry, wet and wet, then dried out PR1422, showing that stress relaxation at 25°C is faster for wet samples.

KEY

○ dry

● wet

Δ wet, then dried

The dry samples relax more slowly than the wet samples. The indicated increase in the rate of stress decay with a high water content suggests a decrease in the internal viscosity of the rubber when wet, i.e. a plasticisation effect by high water uptake. This is in general agreement with the reduction in hysteresis noted with increasing water content.

On drying out of the sample, the stress relaxation time values were appproximately the same as those of the untreated sample indicating a high degree of recovery. The slight difference noted may be due to changes in polymer structure as discussed in Section 5.4. As relaxation is slightly faster for the wet, then dried out sample than for the dry samples this tends to suggest that some reduction in intra-molecular forces has occurred.

5.6.3. Effect of water uptake on resilience

The resilience is related to hysteresis, in that resilience is the amount of the energy stored and hysteresis is the amount of energy dissipated, divided by the total work done upon deformation. The resilience was determined for wet and dry samples as described in Section 2. 7.5. Because thick specimens were needed, and these take a very long time to reach a high water uptake (about a year) only one set of samples has been tested. The results are shown in Table 5.5.

These results again suggest that some plasticisation of the rubber has occurred after prolonged water immersion. The

results confirm the trend already found from stress relaxation and hysteresis measurements.

TABLE 5.5

Resilience of dry and wet samples of PR1422, showing that resilience is increased on water soaking. The wet sample contained 120% water by weight.

Thickness of samples: 1.6mm dry and 1.9mm wet.

sample	Resilience %
dry	27
wet	37

5.6.4. Effect of water immersion on glass transition temperature (T_g)

If plasticisation had occurred then it was thought possible that a shift in the glass transition temperature (T_g) could occur after soaking. An attempt was made to detect this by measuring the T_g of wet (120% water by weight) and dry samples using DSC.

No detectable shift of T_g was found. The T_g was found to be between -53°C and -54°C for both wet and dry samples. This is in agreement with values in the literature for these materials[1,66].

Recently, Hinkley and Holmes[122] also attempted to correlate plasticisation of water-soaked chloroprene by DSC techniques. They also detected no lowering of T_g for the wet samples.

That no shift of T_g occurs may be because the T_g is toofar below the freezing point of water. Attempts to determine the effect of benzene on T_g of natural rubber have been reported in the literature, where a similar phenomenon occurs viz. no lowering of T_g is found and the solvent freezes out before the T_g is reached[52].

There were several major freezing peaks over the range 0 -20°C as the water (presumably in the form of concentrated solution) froze out. The multiple peaks suggest that a range of different molar solutions have been formed in the water.

5.7. SUMMARY OF RESULTS

The results from determining peel strength and moduli show tha, as expected, there is considerable loss in strength of PR1422 after prolonged immersion in water. The results consistently suggest that after high water uptake, this deterioration in physical properties is not completely reversible. The most interesting result is the marked decrease in modulus concomitant with relatively small water uptake. This is consistent with similar results noted for a wide range of sealant materials and requires further investigation in detail.

There is scant evidence for any change in chemical crosslink density.

Most interestingly, most of of the tests suggest that the effect of water uptake is similar to plasticisation effects by a solvent. This is surprising, since water is only slightly soluble in the rubber. However, the breakdown of polar effective crosslinks by water could account for the noted plasticisation effects.

CHAPTER 6

THE UPTAKE OF WATER FROM 1% SALT SOLUTION BY PR1422

6.1 INTRODUCTION

The pilot results of the water absorption experiments carried out in Chapter 4 gave only an indication of the relative rates of water uptake. Since no equilibria were obtained, it was not possible to estimate M_{∞} and hence D. Therefore 1% sodium chloride was used as the soaking medium in this section.

Throughout this chapter, tests were carried out on the commercial sealant PR1422 only. This material has already been described in Section 2.1.1.

6.2. MASS UPTAKE OF WATER FROM 1% SALT SOLUTION AT 25°C

The uptake of water from 1% sodium chloride solution was measured using the technique described in Section 2.3.1. Sample squares of various thickness were prepared as in Section 2.2.3.

6.2.1. Effect of sample thickness on water uptake

Mass uptake was measured, and the results are shown in Figure 6.1 as a mass/area versus root time plot. This shows that for sheet of thickness varying from 0.09mm to 0.24mm, mass uptake/area was reasonably constant during the early stages

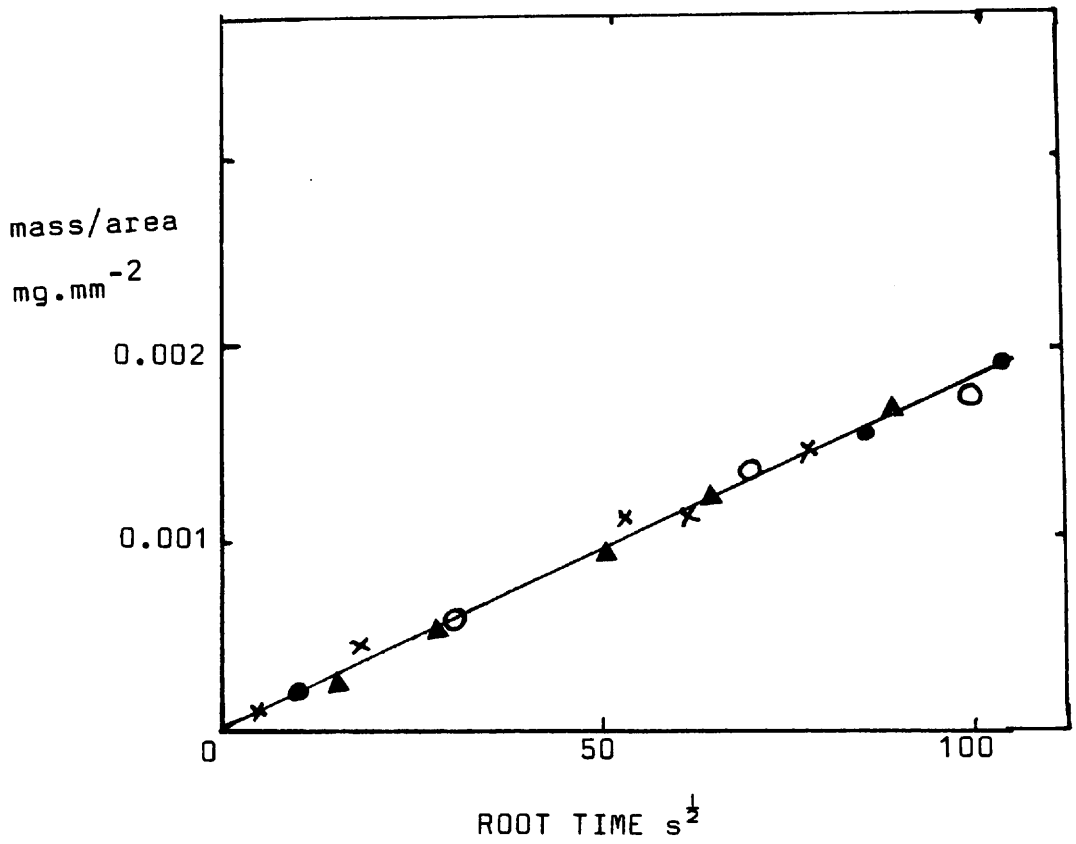

FIGURE 6.1

Plot of mass/area versus root time for the mass uptake of water by thin films of PR1422 from 1% NaCl solution at 25°C, This shows that at short times mass/area is independent of thickness when plotted against root time. Commercial PR1422 curing agent used is predominantly calcium dichromate.

All sample areas = 4800mm^2

KEY

		thickness
▲	sample 1	0.14mm
O	sample 2	0.18mm
X	sample 3	0.09mm
●	sample 4	0.24mm

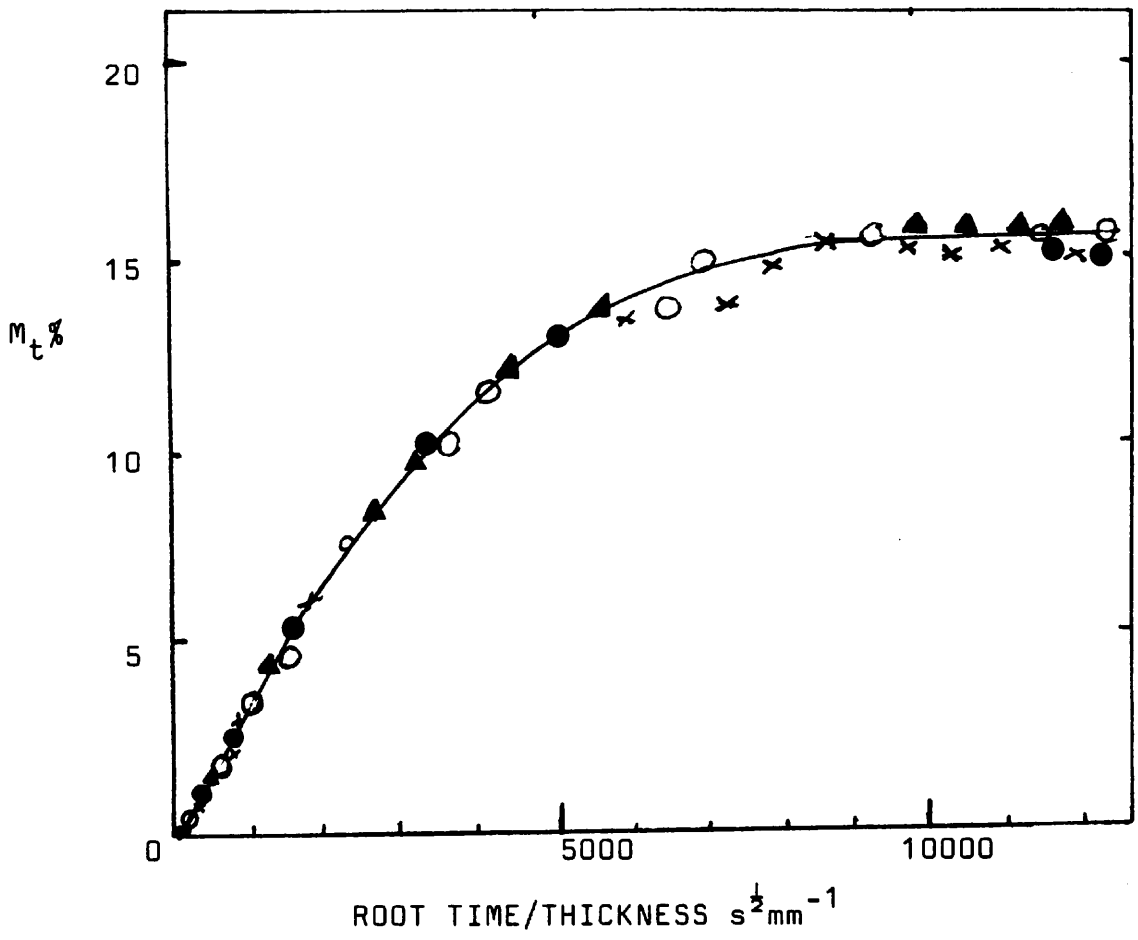

FIGURE 6.2

Plot of M_t% versus root time/thickness for the mass uptake of water by PR1422 thin films from 1% NaCl solution at 25°C. Commercial PR1422 curing agent used is predominantly calcium dichromate. Thickness = 2ℓ.

KEY

		thickness
▲	sample 1	0.14mm
○	sample 2	0.18mm
×	sample 3	0.09mm
●	sample 4	0.24mm

of absorption.

Figure 6.2 gives the M_t% versus root time/thickness plot. This shows that data from samples of different thickness fall on the same line.

Thus thickness variations can be allowed for by plotting M_t% versus root time/thickness.

It can be seen from Figure 6.2 that a normal, apparently Fickian uptake plot is obtained, as opposed to the the abnormal (increasing gradient) curves obtained in Chapter 4 (for the uptake of water from distilled water). This suggests that the very high water uptakes found in the latter case are primarily the cause of the abnormal shape of the curves.

Figure 6.3 shows $\ln(1-M_t/M_\infty)$ versus time for one sample and illustrates that the long term data follows Fickian diffusion.

6.2.2. Measurement of diffusion coefficient & equilibrium uptake

From the data shown in Figure 6.2, the value of the diffusion coefficient was found to be $1.3 \times 10^{-10} cm^2 s^{-1}$ ($1.3 \times 10^{-14} m^2 s^{-1}$).

All three methods of calculation were used (see Chapter 3, Section 3.1.5) and gave similar results. For the uptake of aviation fuel, method C gave consistently lower values of D. It

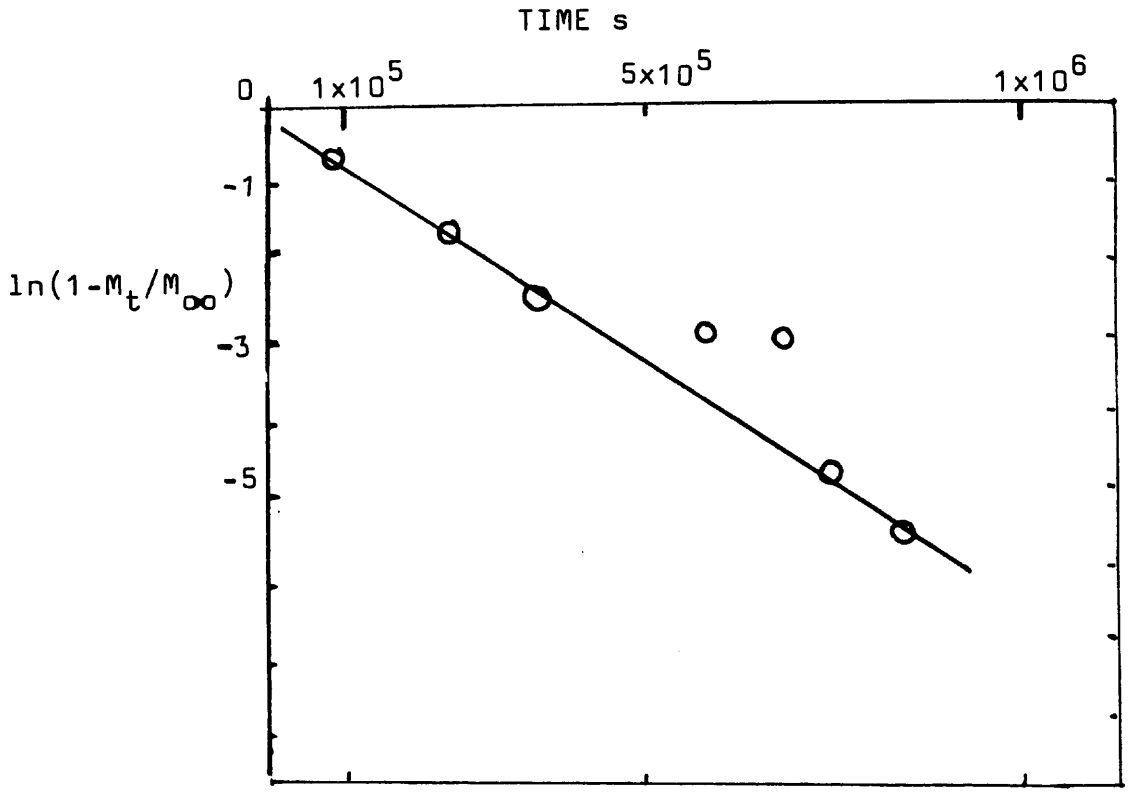

FIGURE 6.3

Plot of $\ln(1-M_t/M_\infty)$ versus time, showing linear relationship for mass uptake of water by PR1422 from 1% NaCl solution at 25°C. Commercial PR1422 curing agent used is predominantly calcium dichromate.

Data from sample 1 only

area = 4800mm^2 thickness = 0.14mm

$$\text{slope} = -D\pi^2/4\ell^2 = 6.25\times10^{-6}$$

$$D = 1.24\ \times^{-10}\text{cm}^2/\text{sec}$$

(ℓ is half thickness)

would appear that for aviation fuel, (where leaching is of the same order of magnitude as the equilibrium uptakes found) that leaching leads to error in the values of $(1-M_t/M_\infty)$ and thus affects the value of D found by this method to a significant extent. For the case of water, leaching is low (see Section 6.2.3) relative to the equilibrium uptake, and thus the error in $(1-M_t/M_\infty)$ is negligible.

The value found is in general agreement with values in the literature.

Gan [66], reported values of 1 to 3 x $10^{-10} cm^2 s^{-1}$ for the diffusion coefficients of water in a range of polysulphide rubbers, using mass uptake techniques. Further, diffusion coefficients of the order of $10^{-11} cm^2 s^{-1}$ have been reported for water in natural rubber[52] and $10^{-10} cm^2 s^{-1}$ for water and sea water in acrylonitrile butadiene rubber [125].

6.2.3. Measurement of D from desorption experiment

The rate of weight loss was measured using the technique described in section 2.3.3. and the results are shown in Figure 6.4.

The dried down weight showed a loss by leaching of 0.7%. This is small when compared to the equilibrium uptake, and further is within the range of M_∞ noted. Leaching thus will have negligible effect on the calculation of the diffusion coefficient.

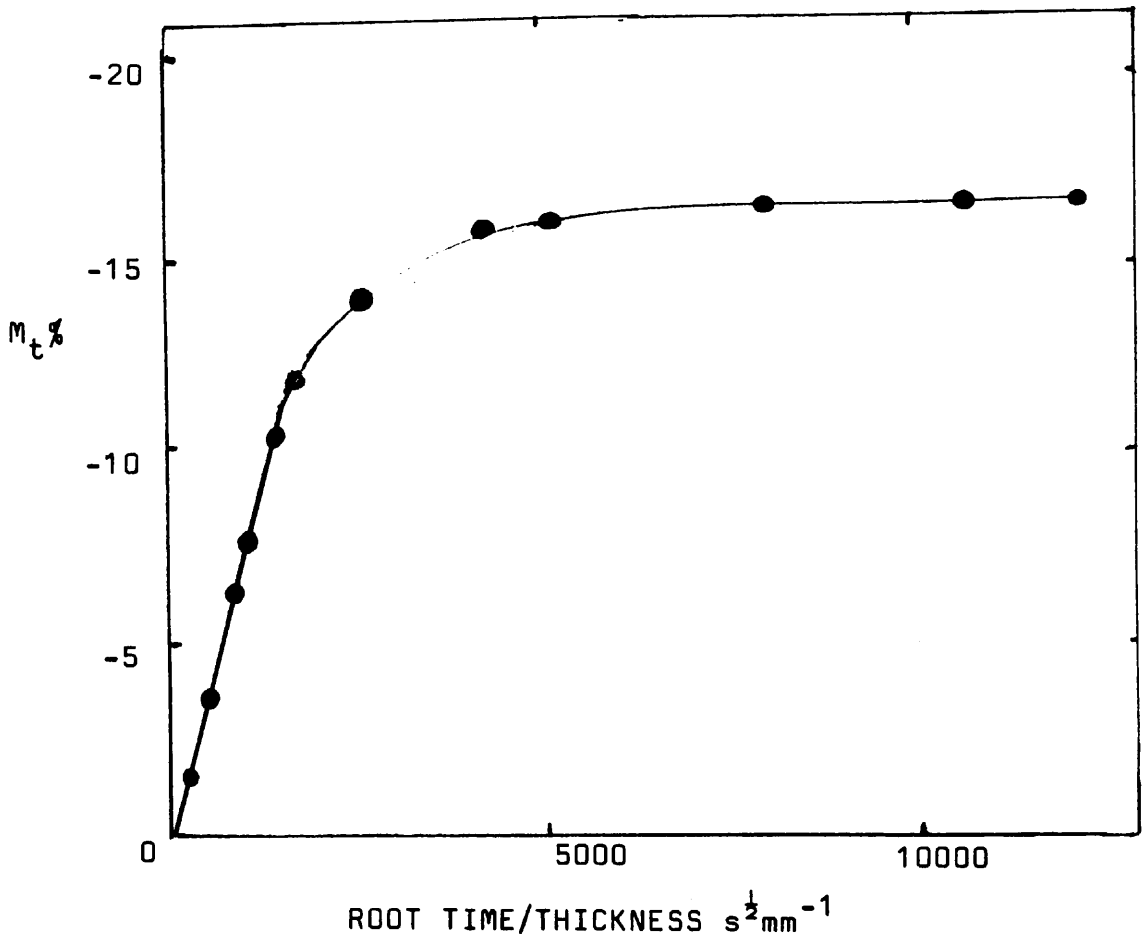

FIGURE 6.4

Plot of M_t% versus root time for the desorption of water from PR1422 thin film at 30°C. The values on the M_t% axis are presented in an unusual way in order to allow comparison with the uptake curve of Figure 6.2. Commercial PR1422 curing agent used is predominantly calcium dichromate.

thickness = 2ℓ = 0.018mm.

area = 4800mm^2

The desorption diffusion coefficient calculated, was found to be 8.7×10^{-10} cm^2s^{-1}. This is about 6 times greater than the absorption diffusion coefficient found at 25°C.

However, this difference in the absorption and desorption diffusion coefficients is in agreement with similar results found by Southern[52], who found a desorption coefficient 5 times greater than the absorption diffusion coefficient for water in natural rubber.

Crank[30] has shown that where the desorption diffusion coefficient is greater than the absorption diffusion coefficient, then this indicates:

a) concentration dependency of the diffusion coefficient

b) as concentration increases, the diffusion coefficient decreases.

The swelling in these experiments was fairly low prior to the desorption experiment. Therefore the faster rate of desorption is not due to a change in the structure of the PR1422, caused by high swelling (see Section 4.2), nor to leaching effects but is probably an effect of dependency of the diffusion coefficient on the concentration of water within the rubber.

6.3. EFFECT OF TEMPERATURE ON ABSORPTION OF WATER BY PR1422 FROM 1% SALT SOLUTION

Mass uptake of water by sheets of PR1422 in 1% salt solution was monitored at different temperatures.

Figure 6.5 shows the results in the form of M_t% versus root time plots, and the diffusion coefficients are given in Table 6. 1.

At 50°C and 70°C leaching was very pronounced and the scatter of results was high. Indeed, leaching is so high that it appears not to be leaching out of impurities so much as a breakdown of the polymer structure (and the rubber thus ceases to act as a semi-permeable membrane with respect to water). Chapter 5 showed that after long time water immersion at room temperature there was evidence of bond rearrangement. It is possible that this can occur at relative short times at raised temperature.

The diffusion coefficients given in Table 6.1 are thus estimates only. Extrapolation of the long term 'leaching' with respect to root time, to the point at which the line met the M_t% axis, gave a M_∞ of about 15% in each case, i.e. approximately the same M_∞ as that found at 25°C. This extrapolation method assumes that the rate of leaching remains constant. The calculated values of D were thus based upon a M_∞ of 15%.

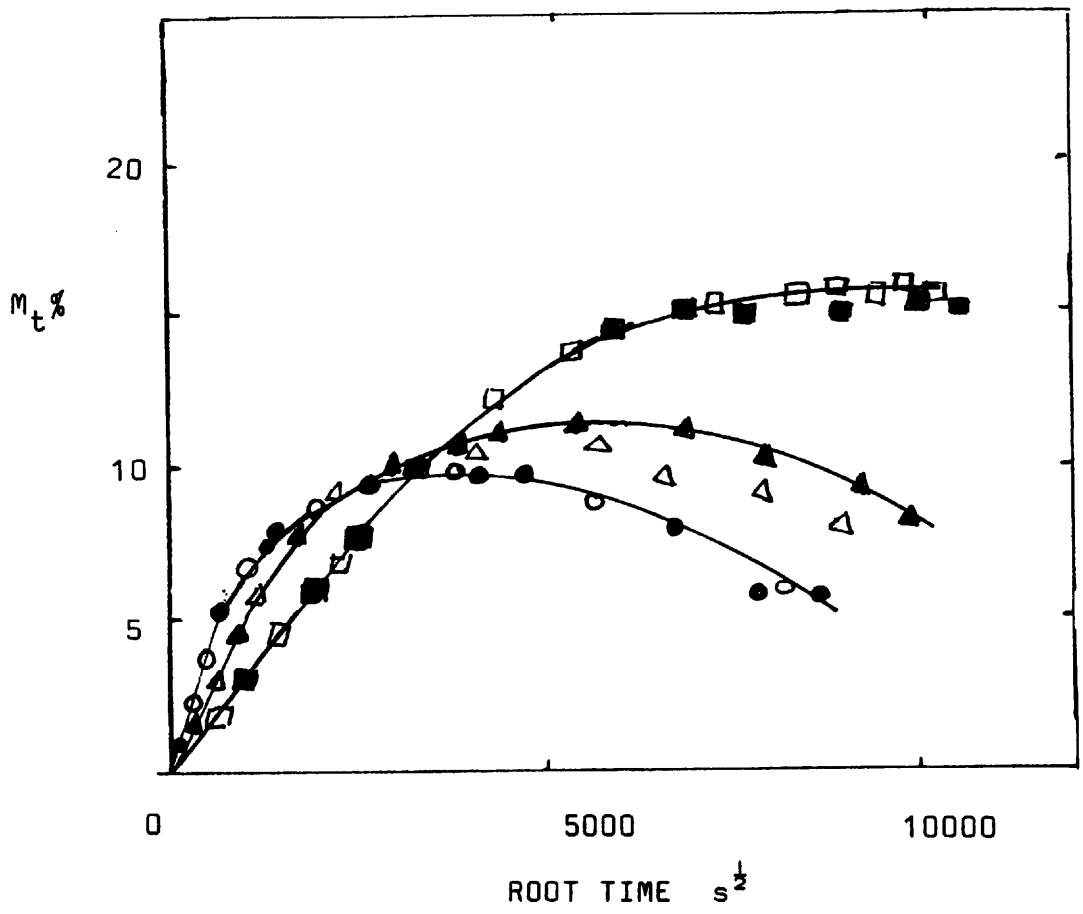

FIGURE 6.5

Plot of M_t% versus root time for the mass uptake of water by by thin film of PR1422 at elevated temperatures from 1% sodium chloride solution. Commercial PR1422 curing agent used is predominantly calcium dichromate.

all sample areas 4800mm^2 thickness= 0.11 mm

KEY

Temperature °C

25	50	70
■ □	▲ △	● ○ ×

TABLE 6.1

Calculated values of D at different temperatures, for the diffusion of water in PR1422 films. Soaking medium was 1% NaCl solution in each case. Commercial PR1422 curing agent used is predominantly calcium dichromate.

temperature °C	25	30	50	70
$D \times 10^{10}$ cm^2s^{-1}	1.3	1.8	2.6	6.8

An Arrenhius type plot of the data in Table 6.1. is shown in Figure 6.6. The activation energy of diffusion for water was calculated from the slope of the straight line as 7.3kcal/mole (3.1×10^4 joules/mol). This value is within the range reported for the diffusion of water in several rubbers[27].

6.4. CONCENTRATION PROFILES

6.4.1. Comparison of mass uptake of water by laminate stacks and single sheet of PR1422

In order to test the assumption that laminate stacks behaved as a single sheet, and that good contact between the separate layers was made, sample stacks were soaked in 1% salt solution and the mass uptake/root time curve compared to that for single sheet of similar thickness. The result, shown in Figure 6.7. shows agreement is excellent.

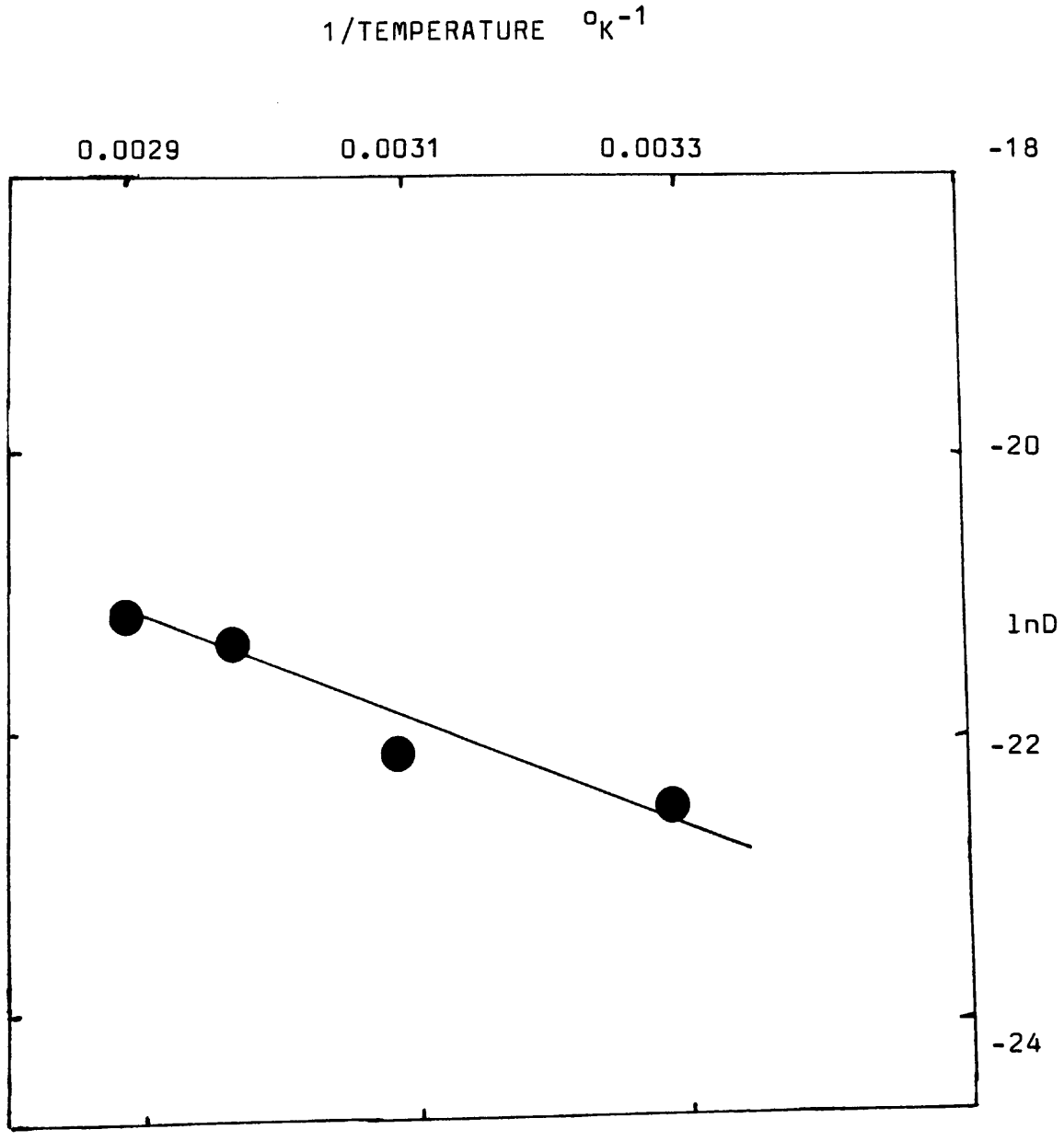

FIGURE 6.6

Plot of lnD versus reciprocal absolute temperature for uptake of aviation fuel by PR1422. The data is taken from Table 6.1. The straight line illustrates an Arrhenius relationship.

The slope = -3.7×10^3 degrees K

Hence activation energy, E, = 3.07×10^4 joules/mole

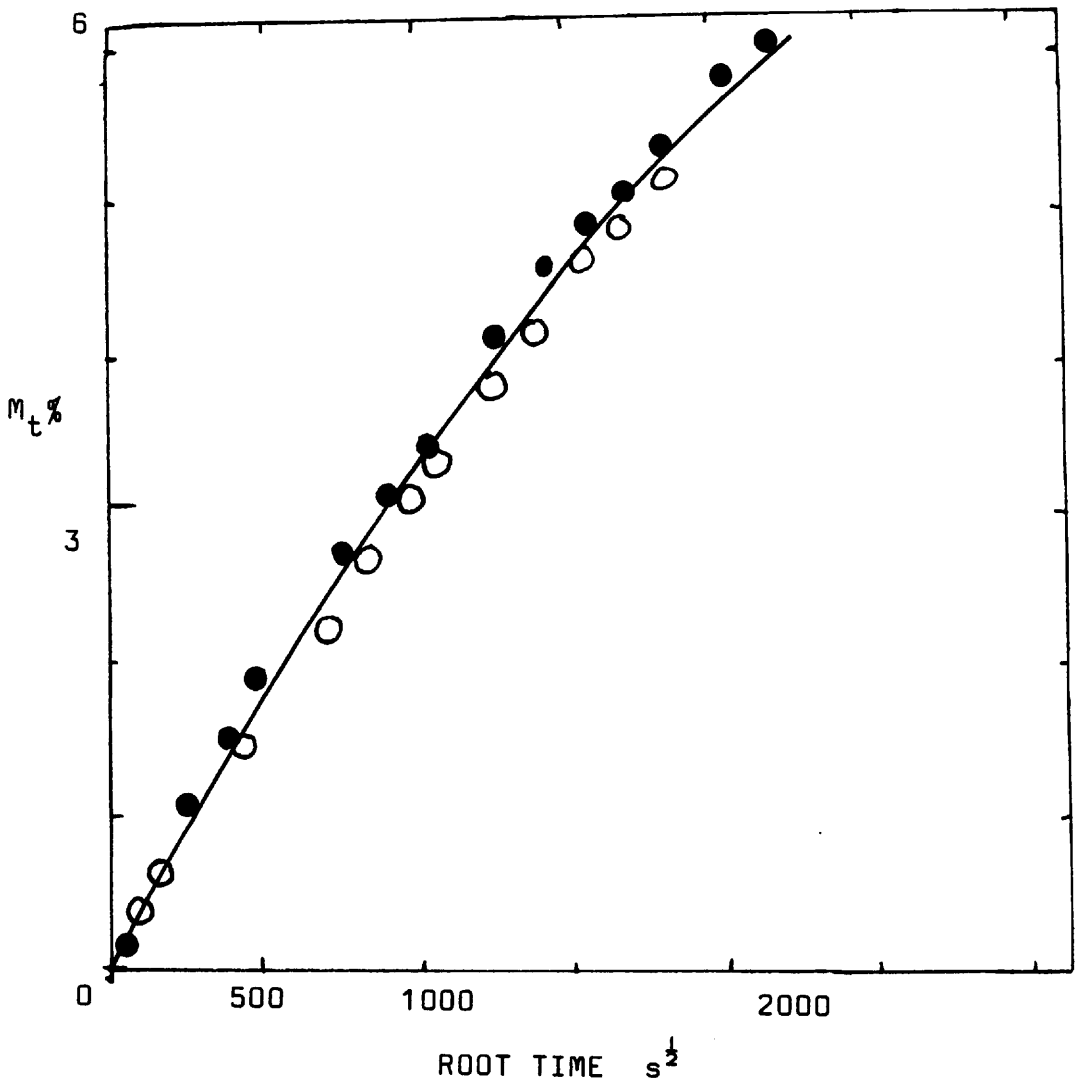

FIGURE 6.7

Plot of M_t% versus root time for PR1422 single sheet and laminate stack mass uptake in 1% NaCl solution at 25°C. There is excellent agreement.

Commercial PR1422 curing agent used is predominantly calcium dichromate.

all sample areas = 4800mm^2

KEY

○ single sheet thickness = 1.34mm

● 10 sheet laminate stack total thickness = 1.35mm

6.4.2. Determination of concentration profile

The water uptake by the separate sheets of laminate stacks of PR1422 (prepared as described in Section 2.5) was measured. The results of one such experiment are given in Figure 6.8. Experimentally determined values of M_t/M_∞ are compared to the theoretical values for various distances across the composite sheet. It is seen that the water penetration appears to be faster than the experimentally determined diffusion coefficient of $1.3 \times 10^{-10} cm^2 s^{-1}$ would suggest. The concentrations at the centre of the sheet are in approximate agreement with a theoretical diffusion coefficient of $10^{-9} cm^2 s^{-1}$, whilst the sheets at the edges are in agreement with a diffusion coefficient of 10^{-10} $cm^2 s^{-1}$ or less. It may be that leaching of impurities gives lower concentration values for the outer sheets.

6.5. SUMMARY OF RESULTS

The mass uptake curve suggests that in 1% salt solution the diffusion process appears to be Fickian. Evidence for this is that mass uptake with respect to root time is linear in the early stages and the long term results give a reasonable $\ln(1-M_t/M_\infty)$ plot versus time. This suggests a diffusion controlled process and is in agreement with the current theories of diffusion of water discussed in Chapter 1. The values of the apparent diffusion coefficient obtained, of the order of 10^{-10} $cm^2 s^{-1}$ are in agreement with values obtained

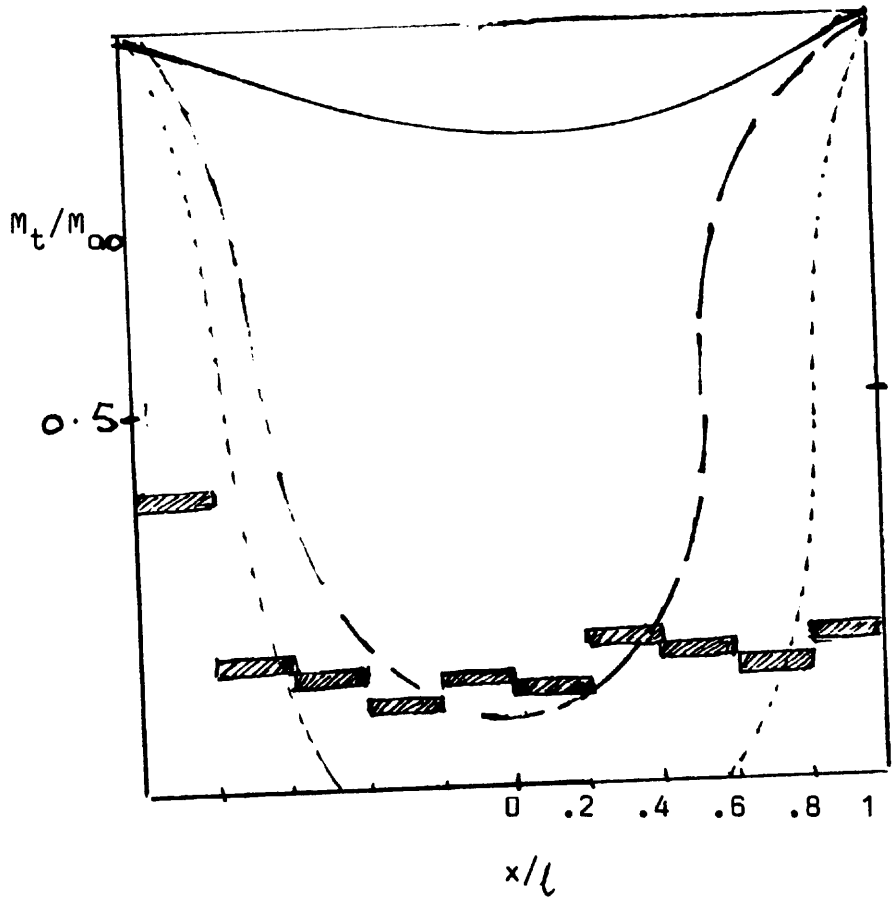

FIGURE 6.8

Concentration profile of water in PR1422 after immersion in 1%NaCl solution. The horizontal bars are the experimentally determined concentrations at distances x/ℓ (where x is the distance from the centre of the sheet and ℓ is half the composite sheet thickness). Concentration is shown as M_t/M_∞.

KEY

The curves indicate the theoretical concentration profiles derived for three values of D. The theoretical values are taken from Crank [30], using the following data:

time (3days) = 2.6×10^5s

half total thickness (ℓ) = 0.067cm

$D = 1.3 \times 10^{-10} cm^2 s^{-1}$: $D = 1 \times 10^{-9} cm^2 s^{-1}$: $D = 1 \times 10^{-8} cm^2 s^{-1}$

$Dt/\ell^2 = 0.0075$ ····· $Dt/\ell^2 = 0.06$ – – – $Dt/\ell^2 = 0.6$ ——

by Gan[66] for a range of polysulphides. Further, Southern[52] found a value of 5 $\times 10^{-11} cm^2 s^{-1}$ for the diffusion coefficient of water in natural rubber. The difference noted between the desorption and absorption diffusion coefficients indicate a concentration dependent diffusion coefficient.

Equilibrium is reached at about 15% by weight. This is equivalent to 0.23g/cc in terms of concentration of water per unit volume of rubber.

In 1% salt solution equilibrium was found at about 15% by weight after about 3 weeks. In water, after three weeks soaking the samples of thin sheet had gained 45% in weight. The dramatic decrease in the rate of water uptake obtained from using sodium chloride as the soaking medium is evidence of the contribution of osmotic forces to the diffusion process and will be discussed further in Chapter 10.

The results from the laminate stacks tend to suggest that a certain amount of the water penetrates more quickly than the apparent diffusion coefficient would predict.

Another method of determining diffusion coefficients is from permeation experiments. Diffusion coefficients can be calculated both from the time lag and, if solubility is known, from the permeation rate at steady state. This allows comparison to be made with the results of mass uptake experiments, and is the subject of the next chapter.

CHAPTER 7

PILOT STUDIES OF THE PERMEATION OF WATER THROUGH PR1422

7.1. EFFECT OF EXPERIMENTAL METHOD

Permeation experiments were carried out as described in Section 2.4 at room temperature, using both the cup and inverted cup methods.

The sheets were carefully checked for pinholes using a light box.

The cup method measures the permeation rate of water from the vapour phase and the inverted cup from the liquid phase. The results of the initial permeation experiments are shown in Figure 7.1. There is good agreement between the results of the two methods.

7.2. CALCULATION OF PERMEATION RATE, TIME-LAG, TIME-LAG DIFFUSION COEFFICIENT and WATER CONCENTRATION

The calculation of the permeation rate (R) and time-lag diffusion coefficient (D_{TL}) is shown in Table 7.1. In addition, the concentration of water in the rubber at the surface during the steady state (C_{ss}) has been calculated from R and D_{TL}. Values of the diffusion coefficient (D) and the total water concentration (C_w) obtained from the mass uptake experiment are given in Table 7.1. for comparison.

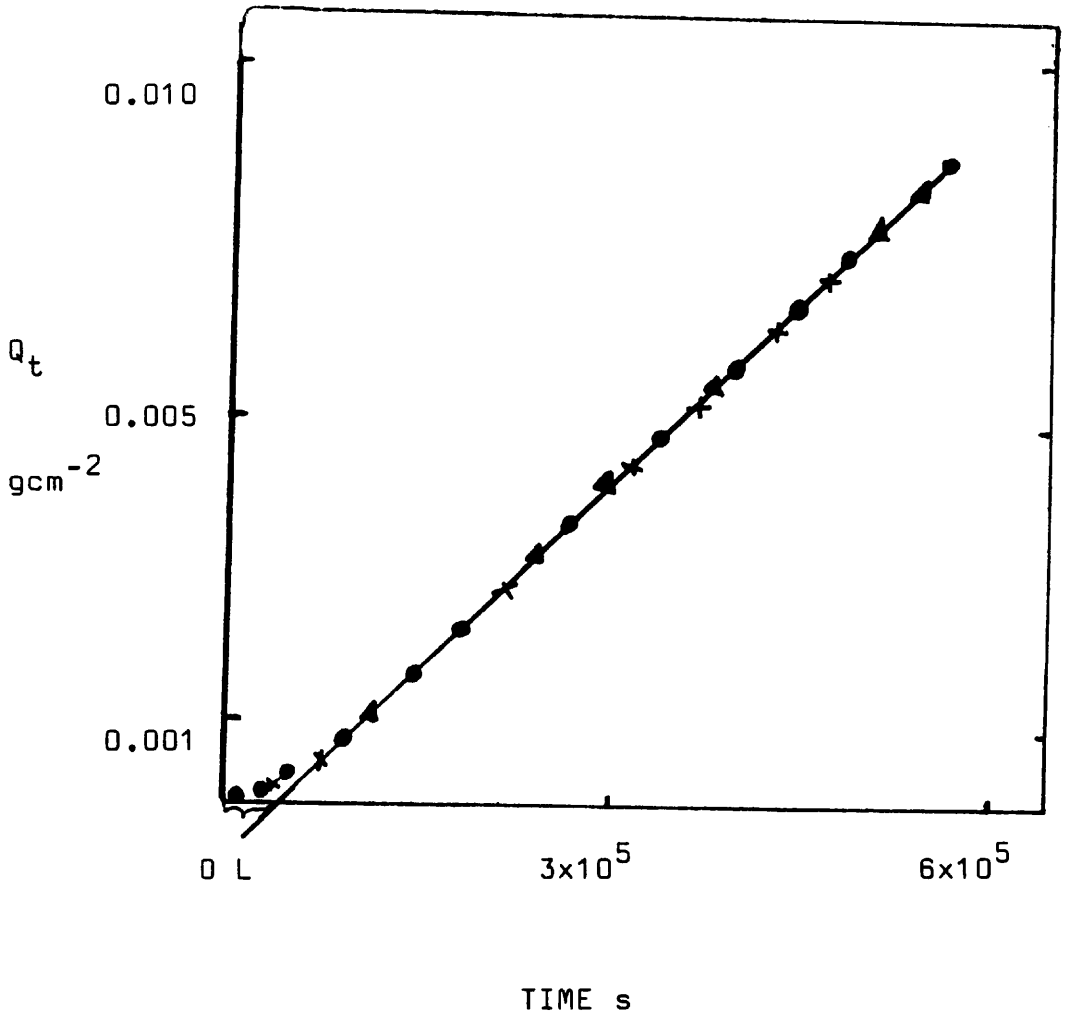

FIGURE 7.1

Plot of Q_t (weight transmitted per unit area) versus time showing permeation of water vapour through PR1422 at room temperature. The graph shows the small time-lag (L) found, and that the permeation rate for cup and inverted cup method is the same.

area of all samples is $23.76cm^2$.

thickness of samples 1.41mm

KEY

Sample 1	cup method	●
Sample 2	inverted cup method	x
Sample 3	cup method	▲

TABLE 7.1

Permeation rate (R), time-lag (L), time-lag diffusion coefficient (D_{TL}) and steady state concentration of water in the rubber (C_{ss}) for samples of PR4122 in contact with water vapour. Values are calculated from slope and intercept of the line in Figure 7.1.

$R \times 10^9$ $gcm^{-1}s^{-1}$	L seconds	$D_{TL} \times 10^{10}$ cm^2s^{-1}	$D \times 10^{10}$ cm^2s^{-1}	C_{ss} gcc^{-1}	C_w gcc^{-1}
2.23	48000	690	1.3	0.033	0.236

FROM THE PERMEATION EXPERIMENT

The permeation rate is found from the slope of the line, multiplied by the sample thickness. The time-lag (L) is the point of intersection of this line with the time axis.

$D_{TL} = \ell^2/6L$. ℓ = thickness = 0.141cm

C_{ss} has been found from substitution of R & D_{TL} in $R = D_{TL}C$

FROM THE MASS UPTAKE EXPERIMENT

D taken from absorption experiment (see Section 6.2.2).

C_w calculated from M_∞ and density (see Section 2.3.5).

The permeation rate of water in PR1422 of $2.2 \times 10^{-9} gcm^{-1}s^{-1}$ at room temperature is in good agreement with recently published work[113] on PR1422, where a value of $2.4 \times 10^{-9} gcm^{-1}s^{-1}$ at 25°C was found, and is in general agreement with permeation rates found for a range of polysulphide sealants[119] (at 20°C) of 2 to $3 \times 10^{-9} gcm^{-1}s^{-1}$.

7.3. CORRELATION OF DATA FROM DIFFUSION AND PERMEATION EXPERIMENTS FOR THE TRANSPORT OF WATER IN PR1422

7.3.1. Correlation of water concentrations

It can be seen from Table 7.1 that there is a discrepancy of an order of magnitude between the water concentration (C_w) calculated from the equilibrium mass uptake uptake and the calculated water concentration at the wet side of the sheet during the steady state (C_{ss}) from the permeation experiment. C_w includes both the water in true solution and the water present in droplet form. If the water in droplet form is presumed to be immobile then the value of C_{ss}, calculated from steady state permeation, may give a better indication of the concentration of water in true solution.

The calculation of C_{ss} is based on the assumptions that

a) $R = D_{TL} C_{ss}$

is valid. This is based on the assumption that there is a linear concentration drop through the rubber sheet. Fick's first law states

$F = -Ddc/dx$

where F is the flux, c is concentration, D is diffusion coefficient and x is distance. If ℓ is thickness of sheet. Integration of this from c=C at x=0 to c=0 at x = ℓ, gives $F.\ell = DC$, or R = DC or, in terms of the symbols used in the permeation experiment, $R = D_{TL}.C_{ss}$

b) D_{TL} is an accurate measure of the true rate of diffusion of the water.

As will be shown in Section 7.4, and following chapters, both assumptions may be incorrect. However. the results of this comparison support the view that the bulk of the water absorbed during the mass uptake experiment is not in true solution.

7.3.2. Correlation of diffusion coefficients

Table 7.1 shows that there are 2 orders of magnitude difference between the time lag diffusion coefficient (D_{TL}) and the diffusion coefficient found from the mass uptake experiment (D). D_{TL} is 690 $\times 10^{-10}$ as opposed to D = 1.3 $\times 10^{-10}$ cm^2s^{-1}.

Similar discrepancies of orders of magnitude greater for time lag diffusion coefficients compared to those obtained from mass uptake experiments have been reported in the literature[27] for hydrophilic polymers and polar solvents.

The discrepancy is possibly because D_{TL} reflects the

diffusion through the rubber phase only. D from mass uptake methods is calculated by considering the total water concentration (C_w) in the rubber, which includes soluble water and water in droplet form. Since the water in droplets is unlikely to contribute effectively to diffusion, the value of D will depend upon C_w.

It is concluded, therefore, that

a) diffusion of water takes place through the rubber phase

b) the diffusion coefficient (D) found from the mass uptake experiments is an apparent diffusion coefficient which is lower than the true diffusion coefficient.

7.3.3. Correlation of R and DC_w

Section 3.2.2 showed that there was good correlation between data from the permeation and mass uptake experiments for aviation fuel. For aviation fuel, it was found that R =DC, where D and C were values found from the mass uptake experiment and R from the permeation experiment.

However, substituting the values of C_w and D shown in Table 7.1 in

$R_{calc} = DC_w$,

where R_{calc} is the calculated value of R, gives:

$R_{calc} = 3.1 \times 10^{-11} gcm^{-1}s^{-1}$.

The permeation experiment gives $R = 2.2 \times 10^{-9} gcm^{-1}s^{-1}$

It is concluded that there is no correlation between the data from the two types of experiment and the discrepancy is two orders of magnitude.

It is not surprising that R_{calc} and R differ, since it has been seen that C_w is far greater than C_{ss} and also that D is not the true diffusion coefficient.

7.4. EFFECT OF THICKNESS OF SHEET ON PERMEATION RATE (R)

7.4.1. Single sheet

Using the cup method, the permeation rate of water through sheets of different thickness was measured. The results are shown in Figure 7.2.

There is a clear trend of increasing permeation rate with increasing thickness, allowing for experimental error.

In theory, the steady state permeation rate is independent of sample thickness (which enters into the calculation:- $R.l = Q_t/time$). However, there are several reports in the literature of permeation rates depending on sample thickness.

Taylor et al.[77] found a thickness effect at high concentration (as thickness increased, permeation rate increased) for the permeation of water in natural rubber. They attributed this to dependency of the diffusion coefficient upon water vapour pressure.

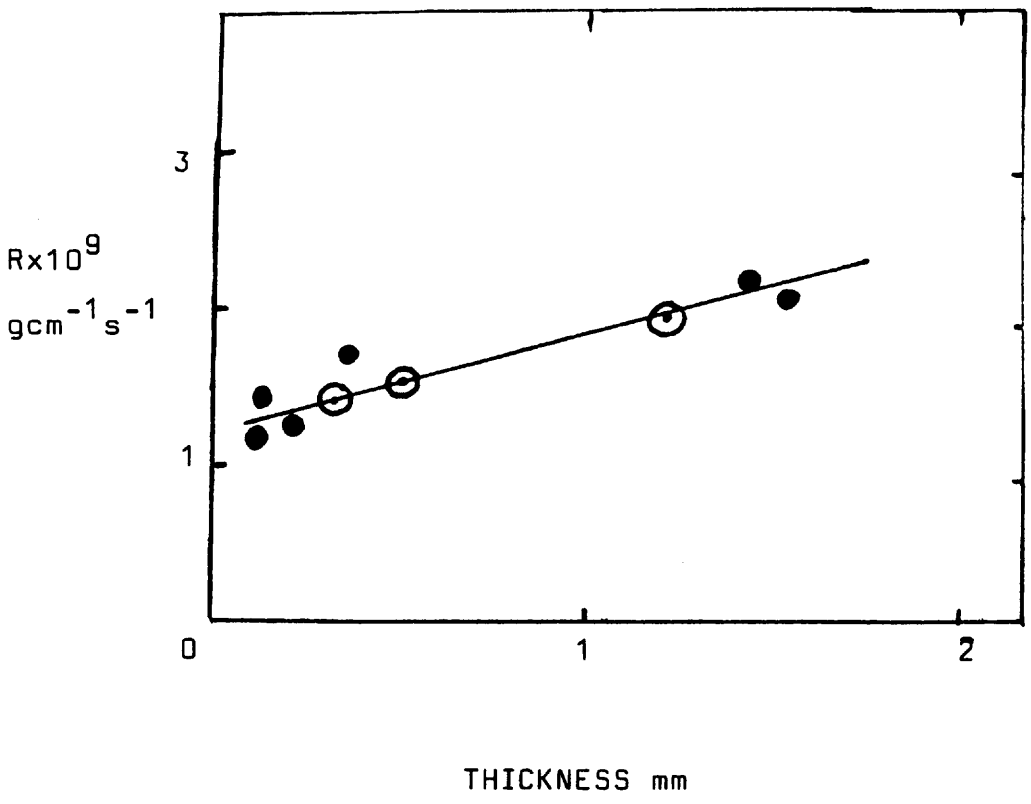

FIGURE 7.2

Permeation rate (R) of water vapour through PR1422 versus sheet thickness at room temperature. This shows that R increases with increasing thickness.

KEY

● single sheet

⊙ laminate sheet

Barrie[115] has shown that an increasing permeation rate with increasing sample thickness can be explained in terms of varying concentration at the sheet surfaces caused by poor vapour circulation.

Ito[116] has postulated that thickness effects may be due to stresses caused by plasticisation of the 'wet' side of a film.

Thickness effects would also be seen if the surface layers have been oxidised. If this is the case then permeation is through two regions of different permeability; the two surfaces and the inner bulk of the sheet.

The explanation for increasing R with increasing thickness in this work is unclear.

The dependence of permeation rate on sample thickness implies that the assumptions made in deriving the equations for permeation rate and time-lag are not correct, and further implies that there will be inaccuracies in the values of R and D_{TL} found.

7.5. LAMINATE STACKS

7.5.1. Permeation rates in laminate stacks

Thin sheet was prepared as described in Section 2.1.3. The permeation rate of water through multiple layers of sheet was determined, using the cup method. The results are shown in

Table 7.2, and data from this are included in Figure 7.2.

It can be seen from Figure 7.2 that the results for the

TABLE 7.2

Permeation rate (R) of water at room temperature through stacks of various numbers of thin sheet of varying thickness of PR1422

thickness mm	number of sheets	$R \times 10^9$ $gcm^{-1}s^{-1}$
0.298	2	1.43
0.494	4	1.52
1.115	5	1.93

laminated sheets fit the same line as for the single sheet. Since the laminated sheets have up to 12 surface layers incorporated in them, this suggests that surface oxidation of the rubber is not the cause of the observed effect of thickness on permeation rate.

7.5.2. Water concentration distribution within the rubber sheet at the steady state

At the end of the permeation experiment the laminate stacks were dismantled and individual sheets were weighed

individually. This gave the steady state concentration distribution. The results are shown in Table 7.3.

This experiment is of limited accuracy. However, the results

TABLE 7.3

Concentration distribution at steady state permeation (after 2 weeks) of water vapour in stack of 5 sheets of PR1422 at room temperature. Individual sheet thickness: 0.2mm

sheet number	concentration gcm^{-3}*
1 (wet side)	0.060
2	0.012
3	0.008
4	-0.004
5 (dry side)	0.007

* weight of water per cc of rubber.

in Table 7.3 show that the drop in overall water concentration throughout the sheet is not linear. However, this water concentration includes both water in droplet form and the water in true solution; certainly at high relative humidities (high external water concentrations) this will be so. The concentration for sheet 1, of $0.06gcm^{-3}$, is much lower than the concentration of $0.236gcm^{-3}$ found for the

equilibrium uptake on immersion in 1% NaCl solution. The laminae are relatively thick (about 0.2mm), and hence the result shown in Table 7.3 represents the average for that thickness i.e. in the first 0.2mm there has been a drop from $0.236 gcm^{-3}$ to a very low value to give the experimentally found average value. The discrepancy between the concentration found for the first sheet in this experiment and the equilibrium concentration found from mass uptake experiment is further confirmation that there is a very steep drop in the steady state concentration distribution with respect to distance from the 'wet' side.

The discrepancy between the results of the permeation and mass uptake experiments, as discussed in Sections 7.3.2 and 7.3.3, suggest that only part of the total absorbed water is in true solution. The extent to which the water in true solution and the water in droplet form affect diffusion will be discussed in later chapters.

7.6. SUMMARY OF RESULTS

The permeation rate (R) is dependent upon the sample thickness. Inadequate vapour circulation, plasticisation effects or a non-linear water concentration distribution throughout the sheet in the steady state may be the major cause of this.

The permeation rate is $2.3 \times 10^{-9} g/cm/s$ for 1.41mm thick sheet at room temperature.

There is no correlation between:

a) the time-lag diffusion coefficient(D_{TL}) and the diffusion coefficient (D) found from mass uptake experiments. The differences found are orders of magnitude.

b) The water concentration in the rubber at steady state calculated from D_{TL} and R and the water concentration found from the mass uptake experiment (C_w).

c) the calculated permeation rate from DC_w and the observed permeation rate.

If, as the results in general indicate, the lack of correlation is due to the presence of water droplets, which affect both the equilibrium uptake and the diffusion coefficient found from mass uptake experiments, but have less marked effects on permeation rate and D_{TL}, then mass uptake and permeation experiments at reduced water vapour pressure should lead to a reduction in the amount of water present in droplet form. Hence there should be better agreement between data from permeation and mass uptake experiments at reduced water vapour pressure, if the above explanation is correct.

Because of the possible effect of thickness of sheet, it was decided to carry out further permeation experiments using sheet of standard thickness and a controlled temperature of 30°C.

CHAPTER 8. THE EFFECT OF VARYING WATER VAPOUR PRESSURE UPON DIFFUSION AND PERMEATION OF WATER VAPOUR IN PR1422

8.1. INTRODUCTION

In an attempt to clarify the results found in the previous two chapters, experiments were carried out to measure the diffusion coefficient, equilibrium uptake and permeation rate from the vapour phase at varying water vapour pressures. The modified mass uptake technique is described in Section 2.3.2.

8.2. MASS UPTAKE OF WATER BY PR1422 FROM SATURATED WATER VAPOUR

A plot of M_t% versus root time is given in Figure 8.1 for a sample of PR1422 suspended above pure water.

It can be seen that the sample, after an initial weight gain, loses weight, then begins to increase in weight again. Several samples showed this initially puzzling behaviour.

In theory, mass uptake from the liquid and vapour phases should be identical. In practice, this is often not so. The phenomenon is known as 'Schroeder's Paradox'[117]. Various attempts have been made to explain this and it is now believed that the effect is due to the vapour not being fully saturated since small temperature gradients are set up within the vapour inducing condensation[118].

The result of soaking in 1% sodium chloride solution shown in

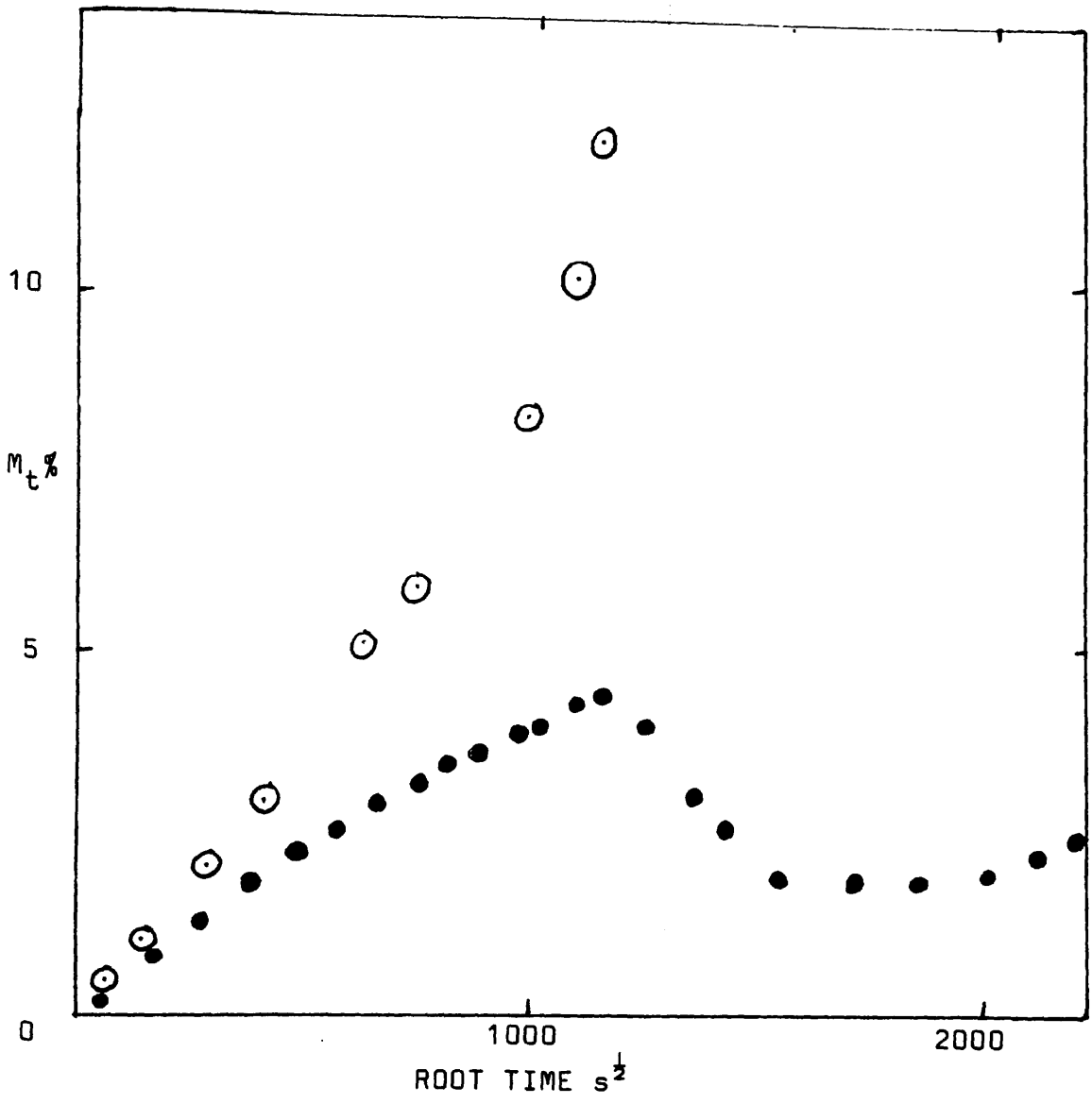

FIGURE 8.1

Plot of M_t% versus root time for the mass uptake of water by PR1422 from water vapour at 100% RH and from liquid water. In both cases temperature was 30°C.

Sample area = 4800mm^2.

KEY

	thicknes
⊙ water - liquid phase	1.35mm
● water - vapour phase	1.42mm

Chapter 6, indicate that reducing the vapour pressure of the water by a very small amount (1% NaCl solution reduces the vapour pressure of water from 23.75mm Hg to 23.61mm Hg at 25°C [120]) has a marked effect on reducing the amount of water absorbed. Thus these results suggest that saturated water vapour is not achieved by merely having the sample suspended above water.

Condensation droplets of water were noted on the sample and the apparatus indicating temperature variations.

Because of uncertainties about the value of the vapour pressure, and the equilibrium uptake, calculation of the diffusion coefficient was not made.

8.3. MASS UPTAKE OF WATER BY PR1422 FROM WATER VAPOUR AT REDUCED WATER VAPOUR PRESSURES

8.3.1. Mass uptake measurements

Reduced water vapour pressures of known nominal relative humidities were obtained by using salt solutions. Details of these, and the technique used are given in Section 2.3.2.

Results of mass uptake of water by PR1422 are shown in Figure 8.2 as M_t% versus root time plots. At relative humidities below that of pure water all the samples tested showed initial mass uptake linear against root time, and in all cases an equilibrium value of M_t% was reached.

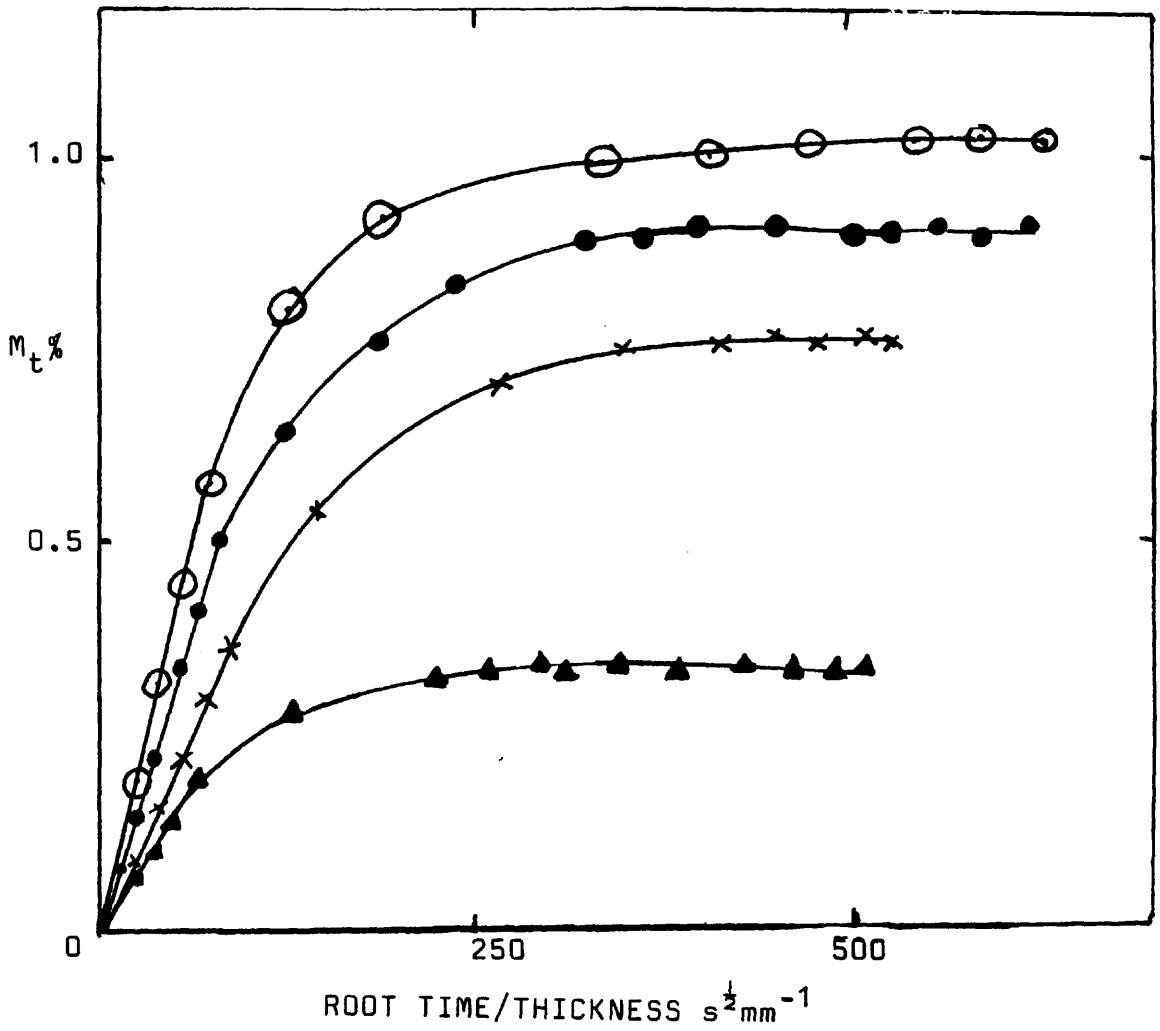

FIGURE 8.2

Plot of M_t% versus root time/thickness for the mass uptake of water by PR1422 from water vapour of varying vapour pressure at 30°C. All samples area = 4800mm^2.

KEY

nominal relative humidity		thickness
○	91%	1.28mm
●	84%	1.68mm
×	75%	1.65mm
▲	42 %	1.55mm

8.3.2. Calculation of D at reduced pressure

Table 8.1 gives the calculated D, M_{∞} and C_w values.

TABLE 8.1.

Calculated D and M_{∞} at varying RH for the uptake of water by PR1422 from vapour phase at 30°C. Data taken from Figure 8.2 and similar mass uptake plots.

RH %	D x10^7 cm^2s^{-1}	M_{∞} %	C_w* g/cc	C_w' g/cc
10	1.6	0.079	0.0012	0.0013
20	1.6	0.31	0.0048	0.0026
32	1.6	0.27	0.0042	0.0042
42	1.5	0.39	0.0061	0.0055
52	1.5	0.44	0.0069	0.0068
75	1.2	0.75	0.0118	0.0100
84	1.4	0.89	0.0140	0.0113
91	1.3	1.01	0.0158	0.0122
96.5	1.2	1.13	0.0177	0.0130
99.5**	10^{-10}	15.0	0.236	0.0134

* C_w is grams of water per cc of rubber. Here the rubber is filled and the volume includes the filler volume.

** from 1% NaCl solution for comparison

C_w' calculated using Henry's Law

A plot of D versus RH (Figure 8.3) shows clearly that D increases to a limiting value as RH decreases.

The marked increase in the diffusion coefficients (of $10^{-7}cm^2s^{-1}$) found, relative to the D found from the experiment of mass uptake from the 1% NaCl solution ($10^{-10}cm^2s^{-1}$) and the time-lag diffusion coefficient, D_{TL}, ($7x10^{-7}cm^2s^{-1}$), will be discussed later, in Chapter10.

8.3.3 Equilibrium uptakes and solubility of water in PR1422 at reduced water vapour pressure

One of the difficulties of this study is the problem of distinguishing between water that is soluble in the rubber and water that is in droplet form. An attempt is made below to make such a distinction.

For an ideal system, solubility varies linearly with vapour pressure (Henry's Law).

The plot of C_w against RH is given in Figure 8.4. It can be seen that the plot is approximately linear below relative humidities about 50%, suggesting that Henry's Law can be taken to apply in this region. Above 50% RH Henry's Law is not obeyed at all.

At this stage, it is assumed that at relative humidities below about 50%, the amount of water absorbed is in solution within the rubber. The amount absorbed thus is solely

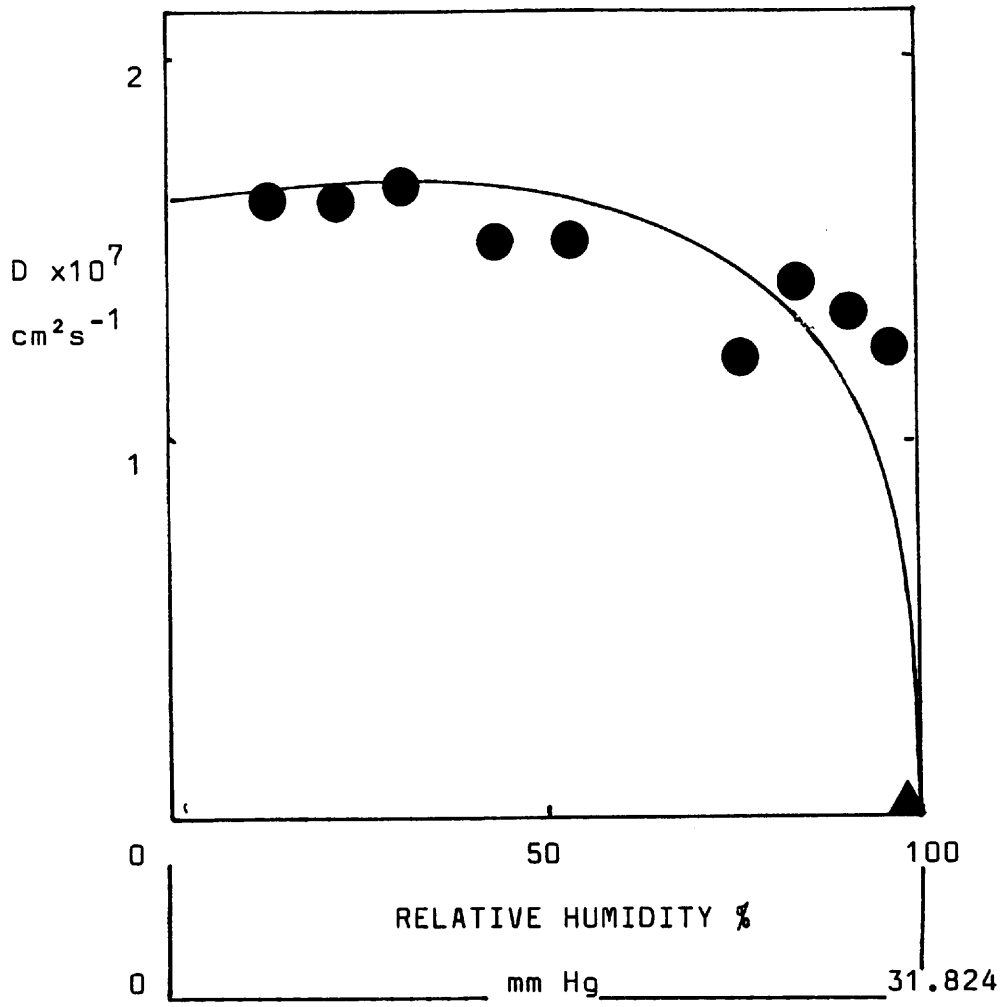

FIGURE 8.3

Plot of D versus relative humidity, showing variation of the diffusion coefficient with relative humidity at 30°C . The RH values have also been converted to mm of mercury. Saturated water vapour pressure taken from Int. Crit. Tables as 31.824mm Hg at 30°C[120].

KEY

● from vapour phase ▲ from 1% NaCl solution

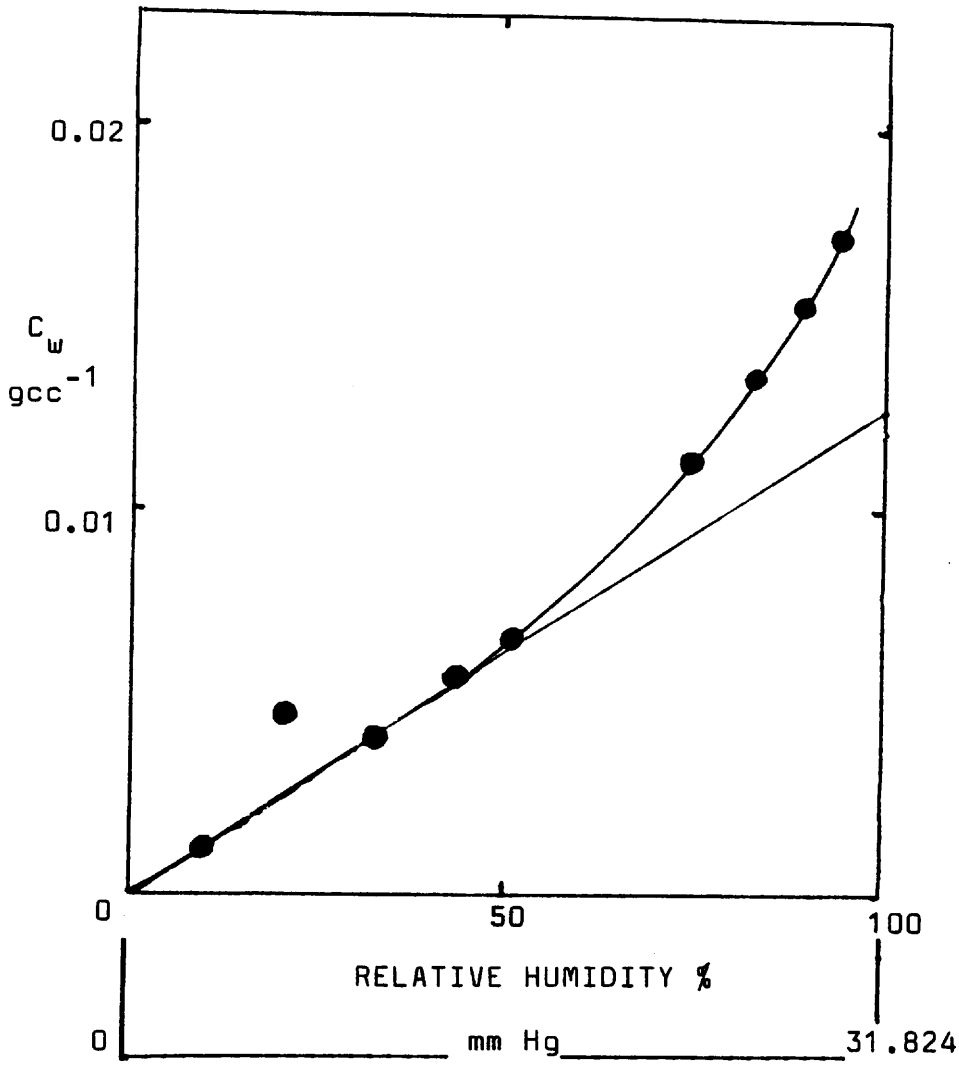

FIGURE 8.4

Plot of C_w versus relative humidity for water vapour uptake at reduced water vapour pressures for PR1422 at 30°C. The nominal relative humidities of the vapour above the salt solutions have been converted to mm of mercury. Saturated water vapour pressure taken from Int. Crit Tables as 31.824mm Hg at 30°C.

C_w is based on total rubber volume and includes filler

dependent on the relationship between solubility and vapour pressure (Henry's Law). The effect of elastic forces restricting swelling (Flory-Rehner). are negligible in the vapour pressure region studied, (See Section 1.8.3) as swelling is very low.

Extrapolation of the straight line shown in Figure 8.4 gives an intercept at 100% RH of C_w = 0.0125gcm^{-3} rubber compound. This is taken as the concentration of water in true solution in the rubber compound at 100% RH.

8.3.4. Discussion of effects of varying external water vapour pressure on amount of water present in droplet form

In the region below about 50% RH the impurities in the rubber are assumed not to absorb water i.e. the absorbed water is soluble only in the rubber and the impurities remain dry. This is plausible since as water enters the rubber and reaches the impurity sites, the first molecule of water absorbed by the impurity will form a saturated solution of a certain vapour pressure. If this is above the vapour pressure of the external water vapour there is no thermodynamic driving force to cause more water to solvate the impurity. Thus no more water is absorbed by the impurities.

At higher RH than about 50%, it is possible that the external water vapour pressure is above that of a saturated solution of the impurities. Hence it is possible that the impurities

absorb water to give droplets of solution.

An estimation of the minimum water vapour pressure (RH) at which droplet formation occurs can be made using Raoult's Law. This gives the lowering of vapour pressure of pure water by a saturated solute in solution as proportional to the molar fraction of the solute in that solution.

$$(p_o-p)/p_o = x_2 \qquad (8.1)$$

where p_o is the vapour pressure of pure water and p is the vapour pressure of the solution at the same temperature. x_2 is the molar fraction of solute.

Then, since p/p_o is RH,

$$(100-RH)/100 = n_iC_i/M_i/(n_iC_i/M_i+C_w/M_w) \qquad (8.2)$$

where C is concentration in gms per cm^3 of rubber, M is molecular weight and n is the number of ions in solution. The subscripts i and w refer to impurity and water respectively. For convenience the amount of water in true solution (s) has been ignored in equation 8.2.

Equation 8.2 can also be used to give the RH of a saturated solution of any given impurity. In this case, $C_w = 1gcm^{-3}$ rubber and C_i is numerically equal to the solubility of the impurity (in gcm^{-3} water).

Hence for calcium dichromate, the RH of a saturated solution can be estimated thus:

The solubility of calcium dichromate (found experimentally) was 1.5 g/cc water.

M_i =256; C_i = 1.5; n_i = 2 ; C_w = 1; M_w = 18

hence (100-RH)/100 = 0.17

thus the RH of a saturated solution is approx 83%.

Above this RH it is possible that water will be present in droplet form. The experimental curve of C_w versus RH (Figure 8.4) shows deviation from linearity at RH values below 83%. This is probably due to traces of other, more soluble impurities (e.g. sodium salts) which give droplet formation at lower RH values than the 83% RH estimated.

The possibility of high osmotic forces being present, and their implications for predicting the amount of water absorbed at equilibrium, will be discussed later in Chapter 10.

8.3.5. Relationship between D and C_w

Table 8.1 shows that, for relative humidities above 42% RH, there is a slight trend of decreasing D with increasing C_w Between 96.5% RH and 99.5% RH the trend noted becomes marked. Because of difficulties in maintaining constant high relative humidities (discussed in Section 8.2) this experiment gives insufficient data for the high RH region.

It is concluded that the diffusion coefficient is dependent upon the total concentration of water in the rubber, but lack of data precludes any suggestions about the relationship between D and concentration at this stage.

8.4. EFFECT OF VARYING WATER VAPOUR PRESSURE ON PERMEATION OF WATER IN PR1422

8.4.1. Measurement of permeation rate (R)

The effect of varying water vapour pressure on the permeation rate was studied at 30°C using the cup method and saturated salt solutions, as described in section 2.3. The results in the form of weight loss/area with respect to time are shown in Figure 8.5 and Table 8.2 shows the calculated R values.

8.4.2. Permeation rates at reduced water vapour pressure

Figure 8.6 shows that at RH below about 50% R varies linearly with RH.

This is a similar qualitative trend to the results obtained with natural rubber by Taylor at al[77]. They found that at relative vapour pressures below 0.75 (75% RH) the permeation rate varied linearly with wvp.

A limiting value of the permeation coefficient can be calculated, from the slope of the linear part of Figure 8.6 using the water vapour pressure scale. This gives a permeation coefficient (P) of $8.3 \times 10^{-10} g.cm^{-1}s^{-1}(cm\ Hg)^{-1}$.

The **increase** in R at high relative humidities is a puzzling result, since this increase implies either

a) D increases with increasing concentration of the

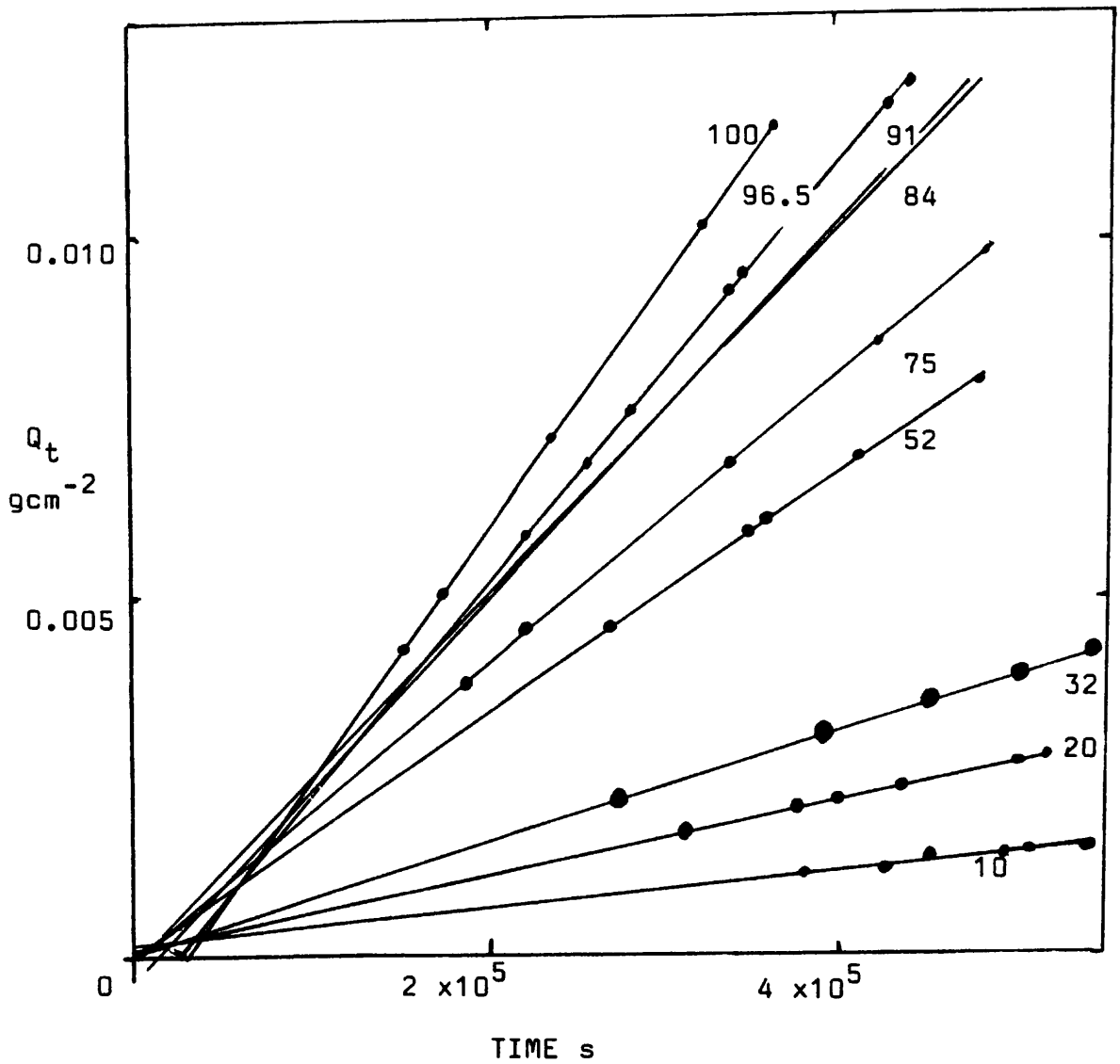

FIGURE 8.5

Plot of Q_t (weight of water transmitted per unit area) versus versus time for the permeation of water from the vapour phase through PR1422 at 30°C. The slope of the graph is a measure of the permeation rate. Numbers on the lines are the nominal relative humidities of vapour over the salt solutions used. The reduced slope of the lines shows that the permeation rate is lower at reduced water vapour pressure. All samples are of area 23.76cm^2 and thickness 0.105cm. Some of the points have been removed for clarity. The experiments were carried out over a longer time scale than that shown with no change in slopes.

TABLE 8.2.

Relative humidity values (RH) and permeation rates (R) calculated from data from Figure 8.5, and similar plots, for the permeation of water through PR1422 at 30°C. Sample thickness 1.05mm.

RH %	R $\times 10^9$ $gcm^{-1}s^{-1}$
10	0.25
20	0.5
32	0.8
42	1.1
52	1.7
75	2.1
85	2.6
91	2.8
96.5	3.0
98	3.3
100	3.6

This data is shown graphically in Figure 8.6.

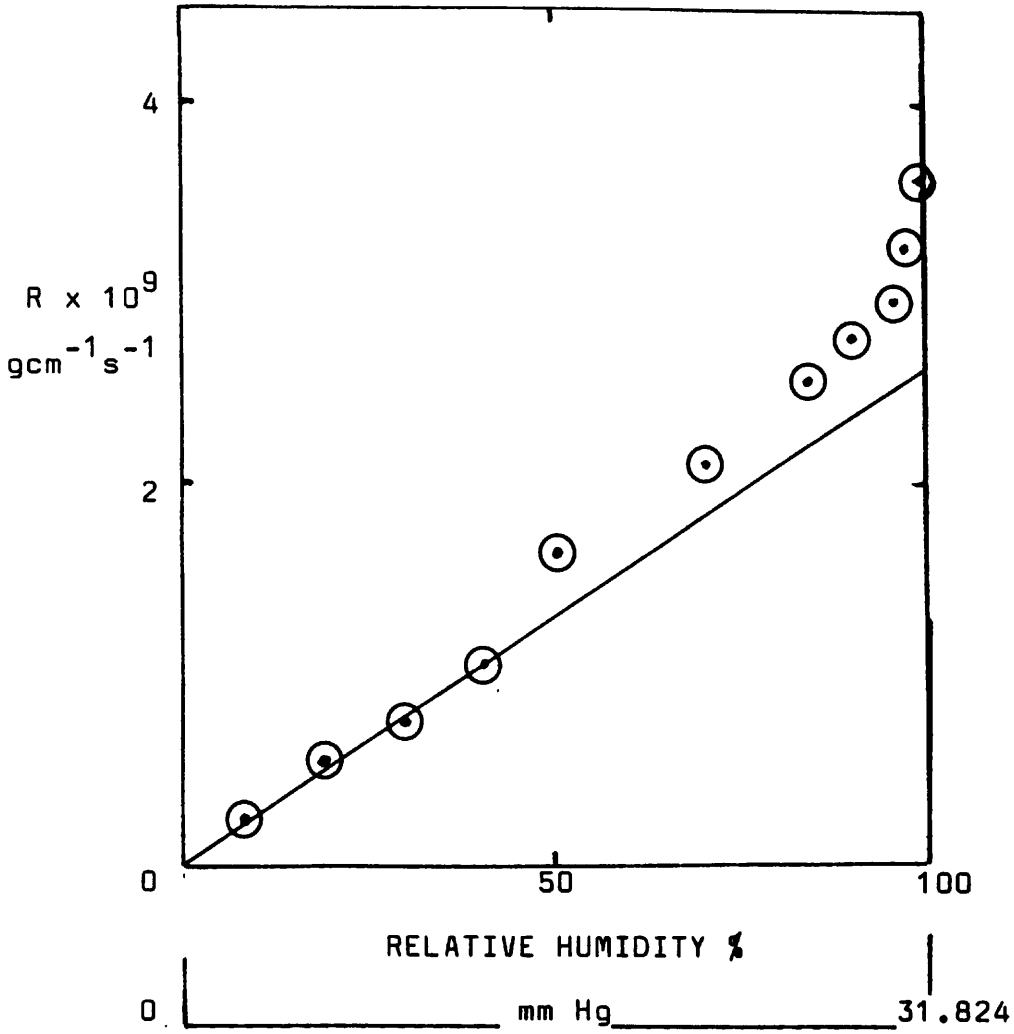

FIGURE 8.6

Plot of permeation rate (R) for water through PR1422 at 30°C versus relative humidity showing that permeation rates, become linear with respect to relative humidity at low levels of relative humidity (low water vapour pressure). Saturated water vapour pressure taken from Int. Crit. Tables as 31.824mm Hg at 30°C.

water in true solution.

b) solubility increases over and above the expected increase due to the Henry's Law increase of the amount of water in true solution with increasing water vapour pressure.

An attempt to explain the increase in R with increasing RH is made later, in Chapter 10, in the light of further results.

8.4.3 Calculation of time-lag diffusion coefficients (D_{TL}) at reduced water vapour pressure

Figure 8.5 gives some indication of the problems found in estimating the time-lags in these experiments. At low vapour pressures, no time-lag was found. Many samples showed negative intercepts. This is because the vapour pressure was below that of the laboratory, and during filling of the apparatus water vapour entered the membrane. It was thus not possible to measure time-lag diffusion coefficients from these experiments. At 91% and 96.5% RH reproduceable time-lags were found and these are shown in Table 8.3, together with D_{TL} values.

It can be seen from Table 8.3 that the time-lag diffusion coefficients give the correct order of magnitude when compared to diffusion coefficients obtained from vapour uptake experiments at water vapour pressures below saturated water vapour pressure. A discrepancy of two orders of magnitude is noted at 100% RH (see Section 7.3.1).

TABLE 8.3

Time-lag diffusion coefficients found at various water vapour pressures at 30°C, compared with D from mass uptake from the vapour phase for PR1422.

RH %	L $\times 10^{-4}$ seconds	D_{TL} $\times 10^{7}$ cm^2s^{-1}	D $\times 10^{7}$ cm^2s^{-1}
91	1.01	1.8	1.3
96.5	2.38	0.8	1.2
100	2.6	0.7	0.001

$$D_{TL} = \ell^2/6L$$

ℓ = thickness of sheet = 0.105cm

8.5. CORRELATION BETWEEN DIFFUSION COEFFICIENT FROM THE VAPOUR PHASE AND PERMEATION DATA

The values of D calculated from the mass uptake of water from the vapour phase are shown in Table 8.1.

The equation R=DC can also be used to calculate D if R and C are known. R values are shown in table 8.2 and C values (i.e. C_w) are shown in Table 8.1.

The experimentally determined (R and C_w) and the theoretical values (R' and C_w') have been used to calculate the D' values

shown in Table 8.4.

It can be seen that there is excellent agreement between D (from mass uptake data), D_{calc} and D'_{calc} (from permeation data) at low RH values. Values in all three cases are constant at low RH. This suggests that at low RH the diffusion of water is approaching ideal, Fickian behaviour. Further, the value of D is independent of the method of determination i.e. there is agreement at low RH between D found from the mass uptake experiment and D found from the permeation experiments.

This contrasts strongly with the discrepancies found when comparison is made of the results of permeation experiments for water vapour at 100% RH and the soaking experiments in 1% NaCl. The progressively increasing discrepancies between the two methods as RH increases suggests that the formation of droplets seriously distorts the values of D.

Changes in physical properties (Chapter 5) suggest that the uptake of water leads to plasticisation of the rubber. This might be expected to lead to an **increase** in D at higher RH, where plasticisation would be greater. Table 8.4 shows, if anything, that the reverse is so. It is thus concluded that any plasticisation effects on the value of D are negligible.

It is concluded that the true value of D is of the order of $1.5 \times 10^{-7} cm^2 s^{-1}$.

TABLE 8.4.

Comparison of data from mass uptake of water from the vapour phase and water permeation experiments for PR1422 at 30°C. The results were obtained at known water vapour pressures. Since C_w and C_w' are based on total rubber volume, these values divided by v_r give concentrations based on rubber alone. v_r = 0.75.

RH %	R $\times 10^9$ $gcm^{-1}s^{-1}$	D $\times 10^7$ cm^2s^{-1}	C_w gcc^{-1}	D_{calc} $\times 10^7$ $\simeq Rv_r/C_w$ cm^2s^{-1}	R' $\times 10^9$ $gcm^{-1}s^{-1}$	C_w' gcc^{-1}	D'_{calc} $\times 10^7$ $\simeq R'v_r/C_w'$ cm^2s^{-1}
10	0.25	1.6	.0012	1.6	0.25	.0013	1.4
20	0.50	1.6	.0048	0.8	0.50	.0026	1.4
32	0.80	1.6	.0042	1.4	0.80	.0042	1.4
42	1.1	1.5	.0061	1.4	1.05	.0055	1.4
52	1.7	1.5	.0069	1.8	1.3	.0068	1.4
75	2.1	1.2	.0118	1.3	1.9	.0100	1.4
84	2.6	1.4	.0140	1.4	2.1	.0113	1.4
91	2.8	1.3	.0158	1.3	2.3	.0122	1.4
96.5	3.0	1.2	.0177	1.3	2.4	.0130	1.4
99.5	3.6	0.001*	.236*	0.11	2.5	.0134	1.4

* results from mass uptake from 1% NaCl solution

C' taken from extrapolated straight line in Figure 8.4;

R' taken from extrapolated straight line in Figure 8.6.

8.6. SUMMARY OF RESULTS

A dramatic change in the order of magnitude, of both the diffusion coefficient and the equilibrium uptake was noted, when comparing the results of water uptake from the vapour phase and those obtained from the liquid phase.

The diffusion coefficient, as calculated from the mass uptake experiments, increased with decreasing concentration of water in the rubber, until a limiting value was reached of $1.6 \times 10^{-7} cm^2 s^{-1}$ at 30°C. This is in close agreement with that calculated from the permeation rate, R, and concentration of water in true solution in the rubber phase. It is thus assumed to be the true diffusion coefficient.

An estimation of the amount of water in true solution at 100%RH gives a value of $0.0125 gcm^{-3}$ rubber compound.

Because of the complications of filler, and the possible effects of adhesion promoters, it was decided to carry out further work using a model rubber, with no additives other than curing agent.

CHAPTER 9. INITIAL EXPERIMENTS WITH'MODEL' LP32

9.1. INTRODUCTION

As explained earlier, PR1422 contains additives and it is not clear what contribution these make to the results of the mass uptake and permeation studies described above. Additives which are hydrophilic substances may increase water uptake. These materials may be conveniently divided into

a) epoxide and phenolic adhesion promoters,emulsifiers etc.

b) curing agents

c) fillers

The effect that these have on water uptake is the subject of this chapter.

9.2 EFFECT OF HYDROPHILIC IMPURITIES OTHER THAN CURING AGENT ON MASS UPTAKE OF WATER FROM SODIUM CHLORIDE SOLUTIONS BY LP32 WITH VARIOUS ADDITIVES

9.2.1 Mass uptake of water from 2% NaCl solution using model polysulphide systems

In order to separate some of the variables inherent in the commercial system, two model systems were studied:

Model 1: LP32 cured with 8phr cumene hydroperoxide and 1phr diphenyl guanidine (LP32 + CHP + DPG).

Model 2: LP32 cured with various dichromate salts

Model 1 was used to give a product with minimal hydrophilic impurities whilst Model 2 gave a more realistic simulation of the commercially available sealants which are cured with dichromate salts.

Both non-extracted and extracted (using the cold azeotrope technique described in Section 2.2.4) samples of Model 1 and Model 2 were studied.

To test whether the adhesion promoter affects water uptake, samples of Model 1 were prepared containing 5phr of epoxide resin, Epikote 1001.

To test for the effect of added hydrophilic material, 1phr NaCl was added to Model 1.

To test the effect of filler, varying amounts of dried chalk (Winnofil S) were added to both Model 1 and Model 2.

Water mass uptake experiments were carried out on the two types of model compound, both with and without additives, using the method described in Section 2.3 and 2% NaCl solution as the soaking medium.

The results in the form of M_t% versus root time/thickness plots are shown in Figure 9.1. The values of D and C_w calculated from Figure 9.1 are given in Table 9.1, together with the amount of extractable material.

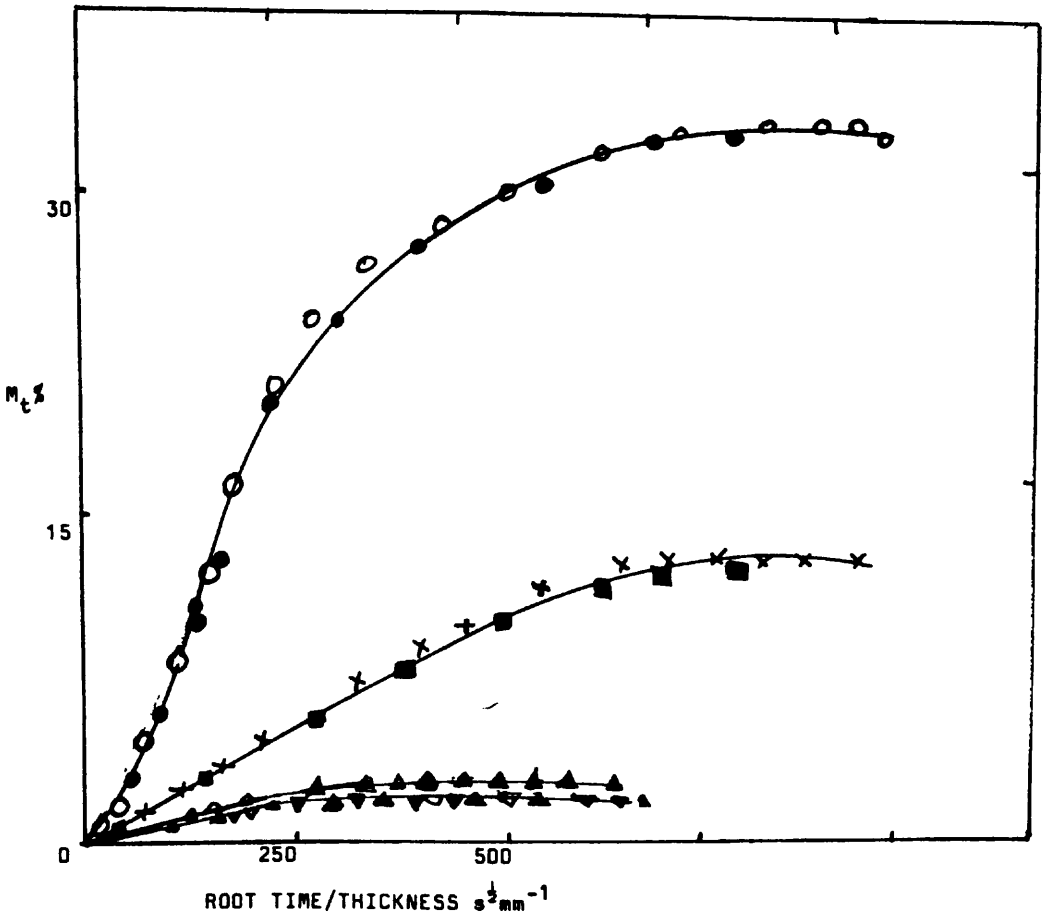

FIGURE 9.1

Plot of M_t% versus root time/thickness, for the mass uptake of water from 2% NaCl solution for samples of 7.5phr sodium dichromate cured LP32 and 8phr CHP+ 1phr DPG cured LP32 at 30°C, with and without additives.

All sample areas = 4800mm^2: thickness = 2ℓ

	KEY		thickness mm
LP32 + sodium dichromate	● extracted	○ non-extracted	1.85
LP32+CHP+DPG	▲ extracted	▼ non-extracted	1.64
LP32+CHP+DPG+1phr NaCl	■ extracted	X non-extracted	1.65
LP32+CHP+DPG+5phr epoxide	▽ extracted	△ non-extracted	1.31

TABLE 9.1

D and C_w values for the mass uptake of water from 2% NaCl solution at 30°C by:

a) LP32 cured with 8phr CHP + 1phr DPG

b) LP32 cured with 8phr CHP + 1phr DPG plus additives.

c) LP32 cured with 7.5phr sodium dichromate.

Additives: 1phr salt or 5phr epoxide resin

material	amount extracted %	$D \times 10^7$ $cm^2 s^{-1}$	C_w gcc^{-1}
extracted LP32+CHP+DPG	4 to 7	2.5	.0159
non-extracted LP32+CHP+DPG	-	2.1	.0154
extracted LP32+ CHP+ epoxy	11 to 12	2.3	.0157
non extracted LP32+ epoxy	-	1.9	.0175
LP32+CHP +DPG + salt **	5 to 7	0.08	.1800
LP32+$Na_2Cr_2O_7$ **	5	0.03	.4307
LP32 +$CaCr_2O_7$	-	0.1*	.16*

* estimate from extrapolated data obtained by soaking in stronger salt solutions

** both extracted and non-extracted samples gave similar results

9.2.2 Effect of azeotrope extraction on mass uptake of water by model compounds

The results shown in Figure 9.1 and Table 9.1 suggest that, with the exception of the samples containing epoxide resin, extraction has negligible effect on water uptake. The effect of extraction on the samples containing epoxide resin is discussed later.

9.2.3. Comparison of LP32 + CHP + DPG and LP32 + CHP + DPG with added epoxide resin

Addition of epoxide to CHP+DPG cured samples increases water uptake slightly, but extracted samples (initially containing epoxide) give similar uptake to samples containing no epoxide. For the extracted samples, it is probable most of the additive is removed during soxhlet extraction. It has previously been reported that the adhesion promoters are removable by extraction procedures[109]. The greater amount of extractable material from the samples containing epoxide, as shown in Table 9.1, tends to support this view.

For the unextracted samples, the differences in both mass uptake at equilibrium and diffusion coefficient are very slight and can perhaps be explained in terms of more hydrophilic sites in the samples containing epoxide resin, leading to a higher water uptake. Moreover this immobilisation of water should slow down the rate of diffusion, as found in this experiment.

9.2.4. Comparison of CHP + DPG cured LP32 and CHP + DPG cured LP32 containing 1phr sodium chloride

Addition of sodium chloride to the CHP+DPG cured samples increases water uptake and decreases the diffusion coefficient, by an order of magnitude compared to the samples without added NaCl. Again, this confirms the trend of increased water uptake for samples with an increased amount of hydrophilic impurity.

9.2.5. Discussion of effect of added hydrophilic material to CHP + DPG cured LP32

The effect of added hydrophilic material is to increase the amount of water absorbed at equilibrium and to decrease the diffusion coefficient.

The effect of added epoxide resin is very small; however, the effect of 1phr NaCl is very noticeable. This confirms the trend already noted in Chapter 4, where it was seen that inorganic salts had a much more pronounced effect on water uptake than organic hydrophilic curing systems.

It would be expected, therefore, that the use of dichromate curing agents (which are very water soluble inorganic salts) would lead to an increase in water uptake and a decrease in the diffusion coefficient.

9.3. EFFECT OF CURING AGENTS ON MASS UPTAKE OF WATER FROM SODIUM CHLORIDE SOLUTIONS BY LP32

9.3.1. Comparison of mass uptake of water by 7.5phr sodium dichromate cured LP32 and CHP + DPG cured LP32.

It can be seen from Table 9.1 that the difference is two orders of magnitude greater for the diffusion coefficient and for the equilibrium water uptake for the sodium dichromate cured LP32 compared to the CHP +DPG cured LP32. The effect is more pronounced than the addition of 1phr of NaCl to LP32 cured with CHP + DPG. This suggests that the LP32 samples cured with 7.5phr sodium dichromate contains a larger amount of hydrophilic material remaining as curing agent residues.

Problems were encountered in extracting the sodium dichromate cured LP32 samples, in that some of the samples showed signs of permanent set, and in a few instances surface blistering was noted. For this reason, and the negligible effect of extraction on water uptake, the majority of further tests on the dichromate cured samples (Sections 9.3.2 and the experiments described in Chapter 10) were carried out using non-extracted samples.

9.3.2. Comparison of mass uptake of water by LP32 cured with different dichromate salts

This mass uptake experiment was carried out in 20% NaCl solution, in order to reach equilibrium quickly. The results

shown in Table 9.2 are thus not strictly comparable with those of Table 9.1. However, it is clearly seen that D is inversely related to C_w.

TABLE 9.2

D and C_w calculated from mass uptake experiments carried out in 20% NaCl solution at 30°C, for LP32 cured with different dichromate salts. 20% NaCl solution is approx. equivalent to 88% RH.

dichromate cation	$D \times 10^7$ cm^2s^{-1}	C_w gcm^{-3}
Na	0.32	0.099
K	0.8*	0.04 *
NH_4	0.90	0.029
Ca	1.68	0.018

* estimate only as leaching noted.

The main reaction for dichromate curing of polysulphides is thought to be:

$$6 \sim RSH + Cr_2O_7^{=} \longrightarrow Cr_2O_3 + 2OH^- + 2H_2O + 3 \sim RSSR \sim \qquad (9.1)$$

Cr_2O_3 is insoluble in water but the hydroxides as well as unreacted dichromates are soluble to different extents. Table

9.3 gives estimates of the solubility, in grams per 100grams of water of the dichromates used, together with the respective hydroxides; C_w is also shown.

TABLE 9.3

Estimated solubilities of possible reaction residues for dichromate cured polysulphides at 30°C. Values are taken from literature[120] and temperature adjusted.

cation	solubility g/100g hydroxide	solubility g/100g dichromate	C_w g/cc
Na	119	223	.099
K	125	30	.04
NH_4	57(gas)	89	.029
Ca	0.15	100*	.018

* experimentally determined.

The proportion of metal hydroxide and unreacted dichromate can be estimated from the main reaction equation (9.1), using sodium dichromate as an example. The molecular weight of the LP32 used was found to be 3600 from vapour pressure osmometry measurements. Since this contain 2RSH groups, and 1mole of dichromate is equivalent to 6RSH, then 1mole of sodium

dichromate (262g) is equivalent to (3600/3)g LP32. Hence the stoichiometric amount of sodium dichromate for 100g LP32 is

$$(262 \times 100)/(3 \times 3600) = 2.5g$$

An excess of dichromate is used (7phr), as the reaction is very inefficient.

Thus unreacted dichromate will be (7g-2.5g) or 4.5g.

From equation 9.1, 2.5g $NaCr_2O_7$ gives (2.5 x2x40)/262g NaOH = 0.76gNaOH.

For the other samples of dichromate cured LP32, similar calculations give 0.72g $Ca(OH)_2$, 0.69g NH_4OH and 0.95g KOH.

The hydroxides may react further, and additional side reactions may also occur. However, it can be seen from Table 9.3 that there is reasonable correlation between the amount of water absorbed by the polysulphide and the average of the dichromate and hydroxide solubilities.

The results shown in Table 9.2 again show that the nature of the curing agent residues is the major factor in determining the magnitude of D and C_w.

A more detailed explanation, and an attempt to quantify this effect will be discussed later, in Chapter10.

9.4. EFFECT OF FILLER ON MASS UPTAKE OF WATER BY MODEL POLYSULPHIDES

Several attempts to produce samples of the two model systems with varying amounts of chalk (dried WinnofilS) were made. In all cases there were problems in producing consistent degrees of cure. Mass uptake results were non-reproduceable. Examination of the samples under a microscope (x200) showed voids and agglomerates of filler. This section of the work was therefore abandoned.

9.5. SUMMARY OF RESULTS

There is only a small effect on both the diffusion coefficient (D) and the amount of water absorbed (C_w) by addition of an epoxide adhesion promoter. Addition of 1phr NaCl resulted in a large change in C_w. Change of curing agent type has a large effect on both D and C_w. For different dichromate system the main factor seems to be the solubility of the possible reaction products.

In all the different mass uptake experiments, as the amount of water absorbed increases, the diffusion coefficient decreases. This confirms the trend noted for PR1422 (see Section 8.3.1) that D depends upon (C_w). A more detailed study of the relationship between D and C_w can be made by varying the osmotic pressures of the external solutions by using different soaking solutions, and this is the subject of the next chapter.

CHAPTER 10.

EXPERIMENTS USING LP32 WITH DICHROMATE CURING AGENTS: EFFECT OF VARYING WATER VAPOUR PRESSURE (OSMOTIC PRESSURE)

10.1. INTRODUCTION

The results of the experiments of varying water vapour pressure on PR1422 detailed in Chapter 8, present three major problems of interpretation. These are:

1) reconciling the differences in the D and C_w found from the mass uptake from the vapour phase experiments and those found from the soaking experiment. The results of Chapter 8 suggest that, for PR1422, a large change in both D and C_w occurs over a small change in relative humidity (from about 96%RH to 100%RH);
2) determining the relationship between D and C_w, which appears to be different to that found for other rubbers;
3) explaining the increase in R at high RH values.

In this chapter, an attempt has been made to explain the above mainly in terms of changes in osmotic pressure of solutions in droplet form within the rubber.

The commercial curing agent of the PR1422 used was predominantly calcium dichromate. However, the bulk of the experiments described in this chapter were carried out using sodium dichromate cured LP32, for the following reasons.

The relative solubilities of the hydroxide and dichromate

(see Table 9.2) for calcium and sodium, and the implications of Raoult's Law detailed in 8.3.4 suggest that for calcium dichromate the range over which droplets predominate is much smaller than for sodium dichromate. An estimate of the droplet range for calcium dichromate cured systems has been given (in Section 8.3.4) as 83%RH to 100%RH. The vapour pressure of a saturated solution of sodium dichromate is 52%RH[120]. Hence sodium dichromate cured LP32 will have water predominantly in droplet form for the range 52%RH to 100%RH.

Further, the mass uptake of water (at all relative humidities) is greater for sodium dichromate, and hence changes in C_w, with changing external relative humidity, are more readily detectable for sodium dichromate cured LP32 than for calcium dichromate cured LP32.

10.2. MASS UPTAKE OF WATER FROM THE VAPOUR PHASE BY 7.5phr SODIUM DICHROMATE CURED LP32

10.2.1. Results of mass uptake of water by sodium dichromate cured LP32 from the vapour phase at reduced water vapour pressure

Mass uptake from the vapour phase was carried out using the technique described in Section 2.3.1. Mass uptake curves are given in Figure 10.1. The diffusion coefficients (D) and water concentrations at equilibrium (C_w), calculated from Figure 10.1, are given in Table 10.1.

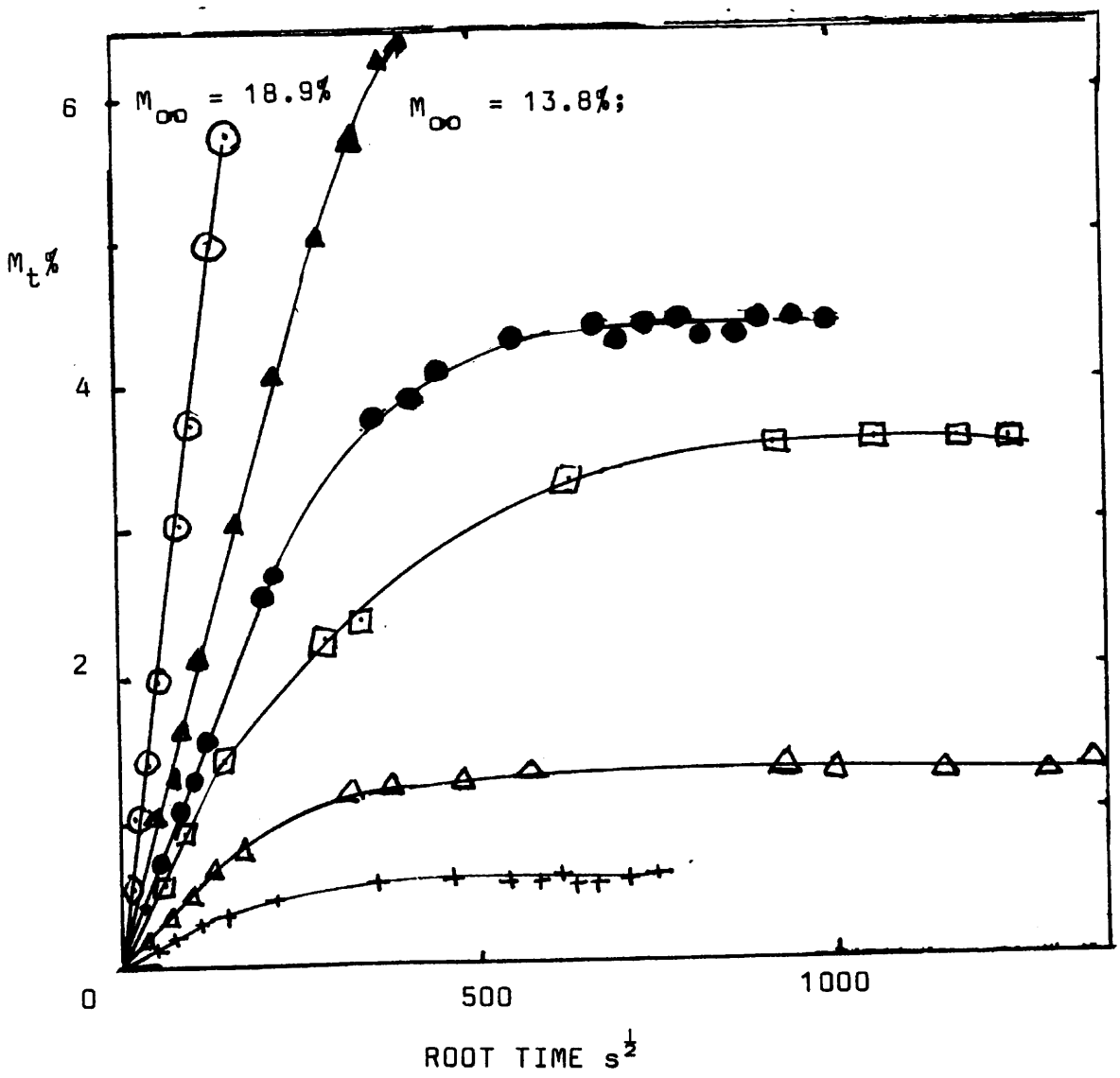

FIGURE 10.1

Plot of M_t% versus root time for the mass uptake of water from the vapour phase at varying water vapour pressure (relative humidity) by 7.5% sodium dichromate cure LP32 at 30°C. All samples: area = 4800mm^2 thickness = 1.62mm

KEY

Relative humidity of external water vapour

+	32%	75%	●
△	42%	91%	▲
□	52%	96.5%	○

TABLE 10.1

D and C_w calculated from Figure 10.1 for the mass uptake of water from the vapour phase by 7.5phr sodium dichromate cured LP32 at 30°C and various relative humidities (RH).

RH %	$D \times 10^7$ cm^2s^{-1}	C_w gcm^{-3}
32	2.2	.0041
42	.84	.0162
52	.52	.0436
75	.30	.0560
91	.16	.1565
96.5	.098	.2520

In several instances condensed water droplets in the region of the sample would tend to give a higher RH than nominal.

10.2.2 Effect of varying external water vapour pressure on D

Table 10.1 shows that, in line with previous results, as C_w increases D decreases. A more detailed analysis of the relationship between D and C_w is given later in Section 10.3.

10.2.3. Effect of varying RH on C_w

A plot of C_w versus RH, with values taken from Table 10.1 is given in Figure 10.2.

The results of Section 9.3.3 show that sodium dichromate curing agent residues are very soluble. It is known[120] that the vapour pressure of a saturated solution of sodium dichromate is 52%RH. If the conclusion reached in Section 9.3.3 is correct, then above an external water vapour pressure of 52%RH there will be a large proportion of the total water concentration, C_w, present in droplet form.

Assuming that the droplets absorb water until the vapour pressure of the solution is approximately equal to the external vapour pressure. The elastic forces resisting swelling are assumed in the case of polysulphides to be relatively weak (since previous experiments carried out in Chapter 5 have shown a high degree of physical bonding, and in addition polysulphides are known to have labile bonds[12]) and thus can be ignored.

Then, using Raoult's Law,

$$(p_o-p)/p_o=(100-RH)/100=(n_iC_i/M_i)/(n_iC_i/M_i+C_w/M_w) \qquad (10.1)$$

where p_o and p are the vapour pressures of water and solution respectively, C is concentration in gms per cm^3 of rubber, n is the number of ions formed and M is molecular weight. The subscripts i and w refer to impurity and water respectively.

For convenience the amount of water in true solution (s) has been ignored in equation 10.1.

Let $n_i C_i / M_i = k$, then equation 10.1 reduces to

$$(100-RH)/100 = k/[(k+ C_w/M_w)] \qquad (10.2)$$

This further reduces to

$$RH/(100-RH)=C_w/(kM_w)$$

or

$$C_w = (KM_w)RH/(100-RH) \qquad (10.3)$$

k was estimated from the probable amounts of unreacted dichromate (4.5g per 100g rubber) and hydroxide (0.8g per 100g rubber) shown in Section 9.3.2. 100g of LP32 has a volume of $75cm^3$.

This gave $kM_w = (4.5x3x18)/(75x262) + (0.8x2x18)/(75x40) = 0.02$

Hence the the theoretical C_w,($C_w$calc), can be calculated.

Sample values are given in Table 10.2 and included in Figure 10.2. It can be seen from Figure 10.2 that agreement between C_w and $C_w$calc is good.

Equation 10.3 is similar to an isotherm derived for natural rubber by Tester[78]. Tester's isotherm is

$$p/p_o = (RH/100) = w/(w+a)$$

where a is a constant and w is the weight of water absorbed.

$100/RH = 1 + a/w$; then $100/RH-1 = a/w$, $(RH/(100-RH) = w/a$

TABLE 10.2.

Calculated values of C_w using equation 10.3 at various RH values

RH %	$C_w$calc gcm^{-3}	RH %	$C_w$calc gcm^{-3}
40	0.013	70	.046
50	0.020	80	.080
60	0.028	90	.180
65	0.036	95	.380

It is concluded that, for sodium dichromate cured LP32,

a) the bulk of the water is in droplet form above about 52%RH.

b) an approximate relationship exists of the form

$$(kM_w)RH/(100-RH) = C_w$$

where k is primarily dependent upon the molar concentration of impurity within the rubber.

Since

$$RH = p/p_o$$

then C_w can easily be related to the osmotic pressure of an external soaking solution, since

$$\pi = (RT/V)\ln(p_o/p)$$

where R is the gas constant, T is absolute temperature and V is the partial molar volume of water in the solution.

The effects of changing the external water vapour pressure,

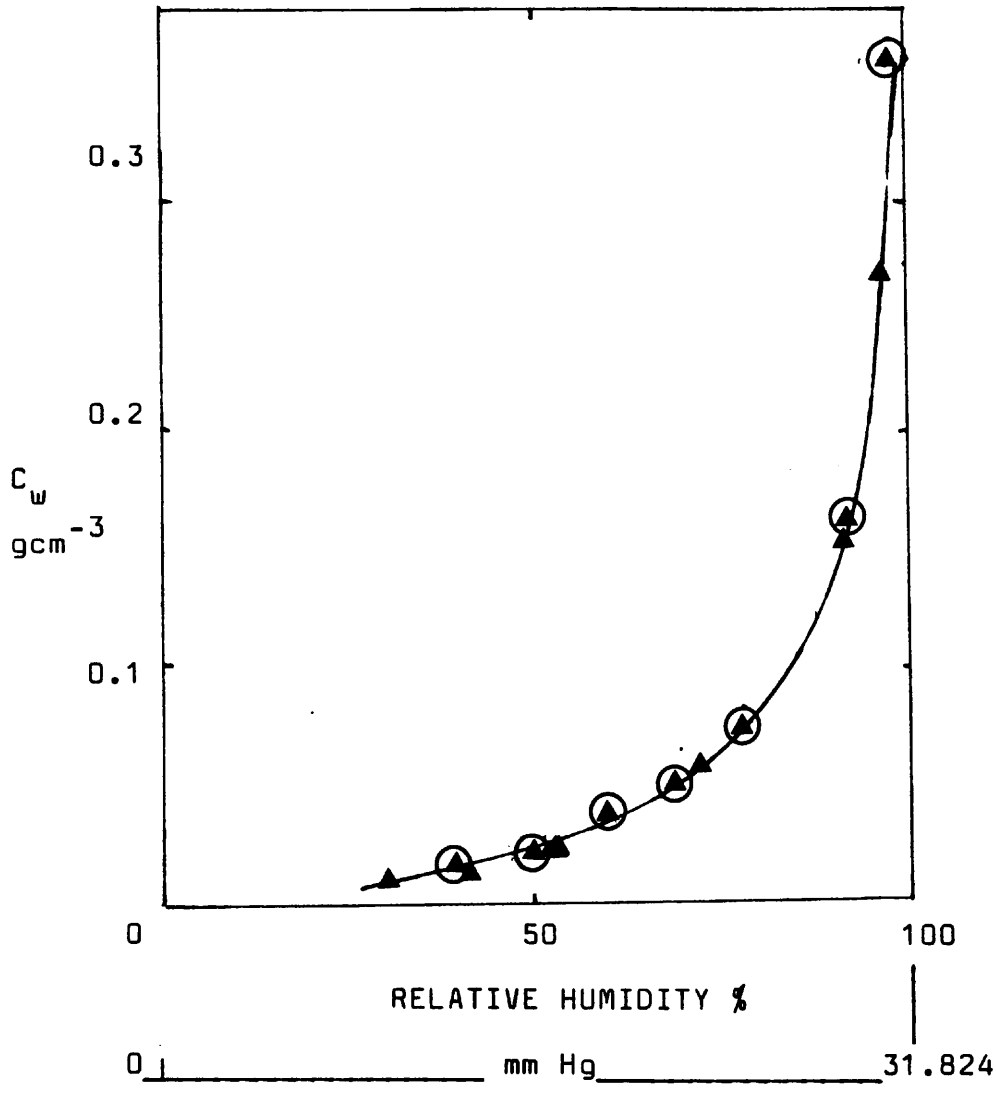

FIGURE 10.2

Plot of C_w versus RH for 7.5phr sodium dichromate cured LP32. Data taken from mass uptake of water from the vapour phase at 30°C. Circled points from data calculated using equation 10.3.

KEY

▲ 7.5phr sodium dichromate cured LP32

Ⓐ Calculated values using equation 10.3.

and the correlation with solubility of reaction products, suggested that osmosis played a dominant part in the process. It was therefore decided to attempt to quantify the osmotic effects on water uptake. Experiments to effect this this are the subject of the next sections.

10.3 MASS UPTAKE FROM THE LIQUID PHASE WITH VARIED EXTERNAL OSMOTIC PRESSURE

10.3.1. Introduction

The external osmotic pressure was varied by using different strength NaCl solutions as soaking media. Changes in the internal osmotic pressures of the solutions formed in the water droplets were made by varying the type and amount of dichromate curing agent added to LP32.

Mass uptake experiments were carried out using the method described in Section 2.3.1.

10.3.2. Results of mass uptake of water by 7.5phr sodium dichromate cured LP32 from NaCl solutions of different concentration.

Typical mass uptake curves are shown in Figure 10.3. Table 10.3 shows the diffusion coefficients (D) and equilibrium water uptake (converted to C_w) calculated from these curves. It can be seen that as the strength of the external salt solution increases D increases and C_w decreases.

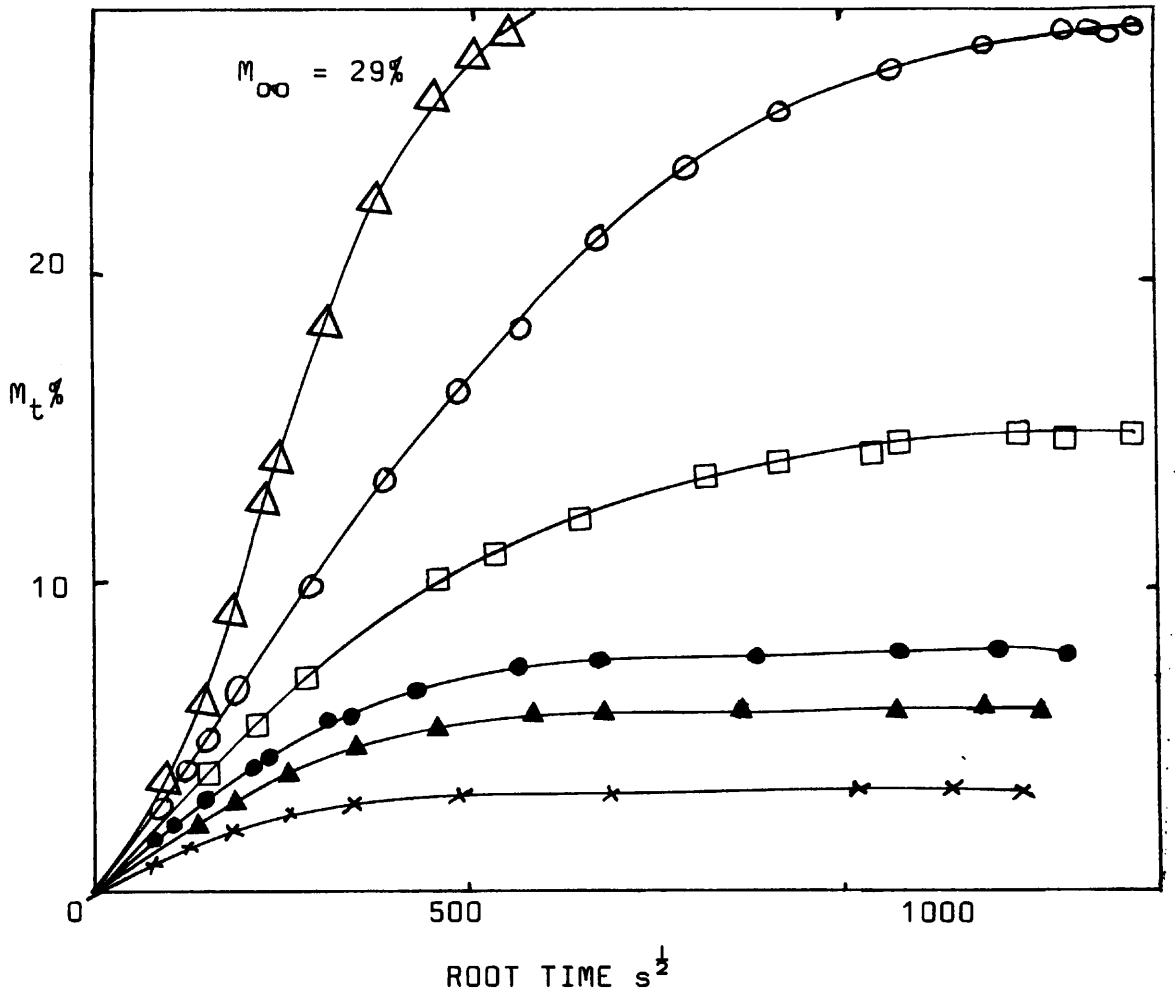

FIGURE 10.3

Plot of M_t% versus root time for the mass uptake of water by 7.5phr sodium dichromate cured LP32 in various soaking solutions at 30°C. The plots show that equilibrium uptake is decreased, and the rate of uptake increased, with increasing strength of the external soaking solution. All sample areas = 4800mm^2; thickness (2ℓ) = 1.31mm

KEY

soaking solution 2% sodium chloride	△
5%	○
10%	□
20%	●
30% sodium chloride	▲
saturated sodium dichromate	×

TABLE 10.3

D and C_w for the mass uptake of water by 7.5phr sodium dichromate cured LP32 from various NaCl solutions at 30°C. Data calculated from Figure 10.3.

external soln g_{Na} (g NaCl/cc water)	D x10^8 cm^2s^{-1}	C_w gcm^{-3}
.02	0.27	.4307
.05	0.32	.3691
.10	1.30	.1862
.20	3.2	.0990
.30	4.8	.0630
sat. $Na_2Cr_2O_7$	7.1	.0395

10.3.3 Comparison of results of mass uptake of water from liquid and vapour phase by 7.5phr sodium dichromate cured LP32

For the mass uptake of water from the vapour phase experiments, the relative humidity of the external vapour was controlled by using a variety of different salts. To allow comparison of the results of this experiment (shown in Table 10.1) with the results of mass uptake from NaCl solutions (Table 10.3), the equivalent number of grams of NaCl per cm^3

of water to give water vapour of the relative humidities shown in Table 10.1 was required. For RH between 75% and 100%, values were taken from the literature[120]; other values were calculated, using Raoult's Law. The converted data, together with the results of D and C_w, is given in Table 10.4.

TABLE 10.4

C_w values obtained from vapour phase, with RH of external vapour converted, using data from Int. Crit. Tables, to g_{Na} (g NaCl.cm^{-3} water) for 7.5phr sodium dichromate cured LP32.

RH %	g_{Na} gcm^{-3}	$D \times 10^8$ cm^{2}s^{-1}	C_w gcm^{-3}
52	0.65	5.2	0.0436
75	0.35	3.0	0.0560
91	0.16	1.6	0.1565
96.5	0.06	0.98	0.2520

10.3.4. Relationship between C_w and concentration of NaCl soaking solution

Throughout this, and subsequent sections, C_w is the total water concentration in the rubber , s is the concentration of the water in solution in the rubber and C_i is the concentration of water-soluble curing agent residues in the rubber. All these are expressed as gcm^{-3} of rubber. g_{Na}

refers to the concentration of the external NaCl solution, expressed as grams of sodium chloride ADDED per cubic centimetre of water. M is molecular weight (the subscripts i,w and Na refer to impurity, water and NaCl respectively) and n_i is the number of ions formed in solution by the impurity.

Current theories of water absorption by rubbers[2,3,4] give the equilibrium condition as

$$\pi_o = \pi_i - (G/2)(5-4/\lambda-1/\lambda^4) \qquad (10.4)$$

where G is shear modulus and λ is the extension ratio of the rubber in the region of the droplets and π_o and π_i are the external and internal osmotic pressures.

For the unfilled polysulphides G is about $0.8 Nmm^{-2}$, but falls rapidly on absorption of water (see Section 5.4). The osmotic pressure of the soaking solutions used varied from $\simeq$ $7.5 Nmm^{-2}$ to $45 Nmm^{-2}$. This was estimated using Van't Hoff equation, PV=RT, and $0.1 Nmm^{-2}$ = 1 atmosphere pressure.

It can be seen that under the conditions of the mass uptake experiments, with relatively strong concentrations of salts in both the internal and external solutions, the pressure due to elastic forces can be neglected, relative to the osmotic pressures. Thus it is assumed that the internal osmotic pressure of the solution within droplets in the rubber is approximately equal to the osmotic pressure of the external soaking solution.

The equations relating osmotic pressure to concentration of a solution are given in Appendix A. An approximation of these shows that osmotic pressure of a solution is directly proportional to the molar fraction of the solute in the solution. Assuming that

a) the osmotic pressures of the internal and external solutions are equal,

b) for a given rubber compound C_i/M_i is a constant factor,

c) s is small relative to C_w and can be ignored,

d) both internal and external solutions deviate from ideality to the same extent,

then manipulation of the expressions for the internal and external osmotic pressures gives

$$C_w = K/g_{Na} \qquad (10.5)$$

where $K = (M_{Na} n_i C_i)/(2M_i)$

The derivation of equation 10.5 is given in Appendix A.

Thus a plot of ln C_w versus ln g_{Na} should be a straight line of slope = -1 if the initial premise (i.e. that the osmotic pressure of the internal solution in the droplets is equal to that of the external soaking medium) is true. A ln:ln plot of the internal water concentration ($\ln C_w$) against external salt concentration ($\ln g_{Na}$) is shown in Figure 10.4, where it can be seen that a linear relationship obtains. Further, the slope of -0.95 shows that, to a close approximation, the water

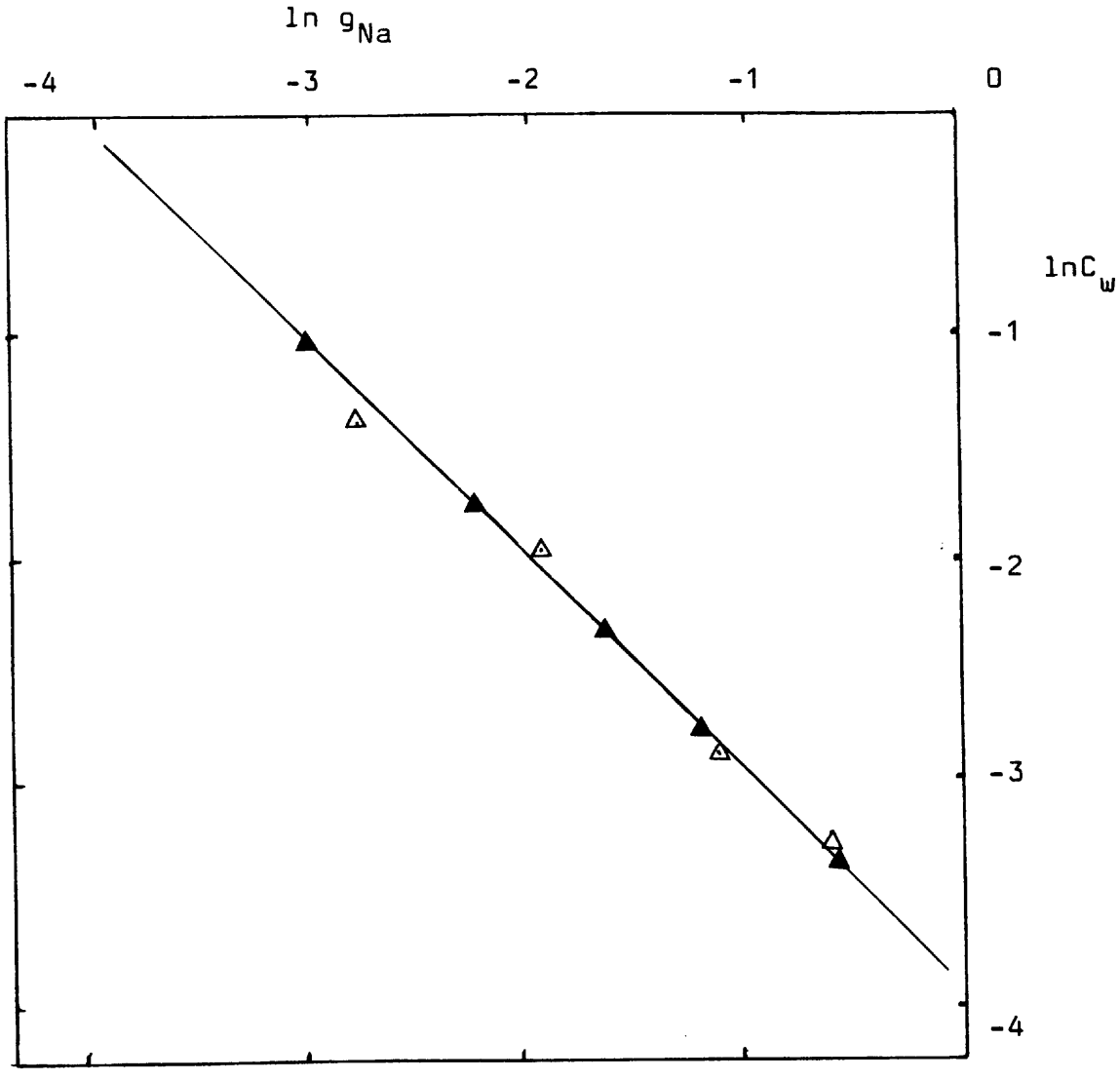

FIGURE 10.4

Plot of ln C_w versus ln g_{Na} showing linear relationship. The slope of the line is -0.95; hence, to an approximation, C_w is inversely proportional to g_{Na}. The plot also shows that converted data from the vapour phase fits the same line. Polymer used is LP32 cured with 7.5phr sodium dichromate.

KEY

C_w from liquid phase ▲

C_w from vapour phase △

g_{Na} is the number of grams of NaCl (or equivalent) added to $1cm^3$ of water as the external phase.

eoncentration, C_w, within the rubber is inversely proportional to the external concentration, g_{Na} of the NaCl in the soaking medium.

This substantiates the premise that the osmotic pressure inside the droplet solution is essentially equal to the osmotic pressure of the external soaking medium. This confirms that the elastic pressure is negligible compared to the osmotic pressures of the internal and external solutions.

The relationship between g_{Na} and C_w is discussed more fully later, in Section 10.5.1, in the light of further results.

10.4. MASS UPTAKE OF WATER BY LP32 - EFFECT OF VARYING INTERNAL OSMOTIC PRESSURE

Experiments were carried out with different amounts of impurities, in order to change the internal osmotic pressure of water in droplets. This was effected by

a) varying the amount of sodium dichromate curing agent.
b) using different dichromate curing agents

10.4.1. Results of mass uptake of water by LP32 cured with different amounts of sodium dichromate

Samples were prepared, of LP32 with 2.5, 7.5 and 14 phr sodium dichromate as curing agent. Mass uptake experiments were carried out with relatively high external osmotic

pressures to speed up the time to equilibrium. Soaking solutions were 10%, 20%, 30% sodium chloride solution and saturated sodium dichromate solution.

The results of equilibrium uptake (in the form of C_w) and the diffusion coefficient, D, are shown in Table 10.5.

TABLE 10.5

D and C_w, calculated from mass uptake experiments in various NaCl soaking solutions at 30°C, for LP32 cured with different amounts of sodium dichromate.

external solution g_{na} (g NaCl added to 1 cc water) *	phr dichromate					
	2.5		7.5		14	
	D *	C_w *	D *	C_w *	D *	C_w *
.05	-	-	0.33	.369	-	-
.10	2.1	.062	1.3	.186	-	-
.20	10.2	.032	3.2	.099	1.8	.199
.30	10.4	.026	4.8	.063	2.7	.146
** .6	-	-	7.1	.040	3.6	.074

* units are: g_{Na}, gcm^{-3}; D $x10^8$, cm^2s^{-1}; C_w, gcm^{-3}

** saturated $Na_2Cr_2O_7$ taken as equivalent to g_{Na} of approximately 0.6.

It can be seen from Table 10.5 that in all cases:

a) for each external solution, the samples containing most dichromate curing agent gave higher C_w values, and corresponding lower values of D.

b) as the strength of the external solution is increased, i.e. as its osmotic pressure is increased, then the value of D increases and the value of C_w decreases.

Since the overall effect appears to be due to the difference in internal and external osmotic pressures, this confirms the results found in Section 10.3.

10.4.2. Results of mass uptake of water by LP32 with different dichromate curing agents

7% calcium dichromate cured LP32 and 7% ammonium dichromate cured LP32 samples were also prepared, and mass uptake from 10%, 20% and 30% salt solution monitored.

The results are tabulated in Table 10.6 where a similar trend can be noted to that shown in Table 10.5 for the sodium dichromate cured samples viz. as the external salt solution becomes stronger, then C_w decreases and D increases.

This data is analysed further in Sections 10.5 and 10.6.

TABLE 10.6

D & C_w for ammonium and calcium dichromate cured LP32 calculated from the mass uptake of water from various NaCl solutions at 30°C.

dichromate type	external soln (g_{Na}) gcm^{-3} water	$Dx10^8$ cm^2s^{-1}	C_w gcm^{-3} rubber
ammonium	.20	7.76	0.0311
"	.30	12.5	0.0199
"	* .6	12.0	0.0139
calcium	.10	5.85	0.0333
"	.20	16.5	0.0183
"	.30	22.3	0.0131

* saturated $Na_2Cr_2O_7$ equivalent to g_{Na} = 0.6

10.4.3. Comparison of extrapolation of results of C_w obtained for 7phr calcium dichromate cured LP32 and C_w found from mass uptake of water by PR1422

Extrapolation of the results of C_w obtained for calcium dichromate cured LP32 to g_{Na} = 0.01 (equivalent to the 1% NaCl soaking solution used in Chapter4) gives C_w of $0.31gcm^{-3}$. If allowance is made for filler (v_r=0.75) then C_w for the filled model system = $0.23gcm^{-3}$. This is in excellent

agreement with the result obtained for PR1422 of $C_w = 0.24 gcm^{-3}$. This suggests that

a) filler has negligible restraining effect on water uptake and

b) the conclusion that curing agent residues are the major source of high water uptake is essentially correct

10.5. ANALYSIS OF EQUILIBRIUM CONDITIONS

10.5.1. Relationship between water concentration and osmotic forces

The results obtained in Sections 10.2 and 10.3, as shown in Figure 10.4, indicate that there is a linear relationship between the internal and external water concentrations.It has already been seen that the elastic forces are small relative to the osmotic forces and can be neglected.

In Section 10.3, where only sodium dichromate cured LP32 was considered, the amount of water in true solution (s) was neglected as small compared to C_w. However, Table 10.6 shows that the C_w values found for calcium and ammonium dichromate cured LP32 are appreciably smaller than those found for the sodium dichromate cured samples. It was thought possible that for these samples s was of the same order of magnitude as C_w and thus could not be neglected.

From the osmotic pressures of the external solution and the osmotic pressure of the solution within the water droplets an

equation has been derived, relating C_w to the concentration of the external solution, and including s as a function of s_o, the concentration of the water in true solution at 100%RH for a rubber containing no impurities.

The derivation of this equation is given in Appendix 10.A. The expression is:

$$C_w /f = 58.5n_iC_i/(2g_{Na}M_if) + s_o \qquad (10.6)$$

where C_w is the total water concentration, in gcm^{-3} of rubber, g_{Na} is the concentration of the external solution in gcm^{-3} of NaCl in water, C_i is the concentration of impurities in gcm^{-3} of rubber; n_I and M_i are the number of ions and molecular weight of the impurity, s_o is the solubility of the water in the rubber in gcm^{-3} and f is a factor to allow for variation in the amount in true solution with changes in vapour pressure.

Details of the determination of f, and a table of assumed values, is given in Appendix 10.A.

Thus a plot of C_w/f versus $1/(fg_{Na})$ should give straight lines with a common intercept of s_o and slopes of $(58.5n_iC_i)/(2M_i)$.

The data in Table 10.7 is derived from the primary data in Tables 10.1, 10.3 and 10.4. Figure 10.5 shows the plot of C_w/f versus $1/fg_{Na}$.

TABLE 10.7

C_w and g_{Na} data converted using f factor.

Dichromate type	$1/g_{Na}$	C_w gcm^{-3}	$1/(fg_{Na})$ cm^3g^{-1}	C_w/f gcm^{-3}
7phr Na	20	.369	20.6	.380
	10	.186	10.6	.198
	5	.099	5.6	.111
	3.33	.063	4	.075
	1.73	.0395	2.47	.056
2.5phr Na	10	.0619	10.6	.066
	5	.0321	5.6	.036
	3.33	.0256	4	.030
14phr Na	5	.199	5.6	.223
	3.33	.146	4	.173
	1.73	.0744	2.47	.105
calcium	10	.0333	10.6	.035
	5	.0183	5.6	.021
	3.33	.0131	4	.016
ammonium	5	.0311	5.6	.032
	3.33	.0199	4	.024
	1.73	.0139	2.47	.0196

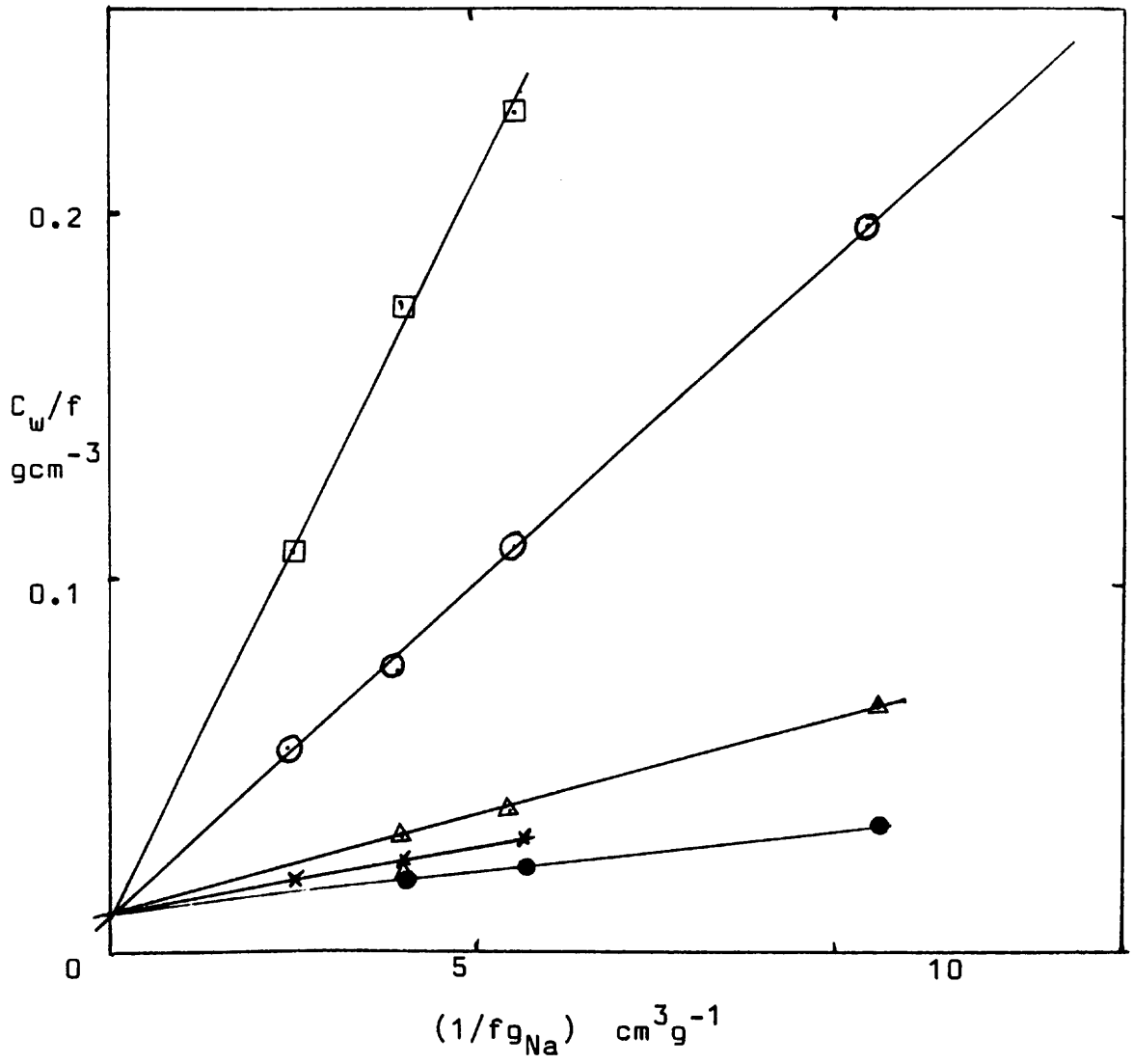

FIGURE 10.5

Plot of C_w/f versus $1/(fg_{Na})$ for LP32 cured with different types and amounts of dichromate salts. Data from Table 10.7. A linear relationship is found of intercept 0.01 gcm^{-3}.

KEY

14phr	sodium dichromate cured LP32	□
7.5phr	sodium dichromate cured LP32	○
2.5phr	sodium dichromate cured LP32	△
7phr	ammonium dichromate cured LP32	×
7phr	calcium dichromate cured LP32	●

10.5.2. Estimation of solubility (s_o) of water in polysulphide rubber

Figure 10.5 shows that all lines give the same intercept at about $0.01 gcm^{-3}$ and this is taken as the solubility of water en true solution within the polysulphides.
Previously, in Section 8.3.3, it was estimated that

$$s_o = 0.016 gcm^{-3}$$

for the solubility of water in PR1422. This value is in very good agreement with the value of $0.01 gcm^{-3}$ found here.

It is concluded that the solubility of water in the polysulphides studied is of the order of $10^{-2} gcm^{-3}$.

10.5.3 Estimation of molar quantities of impurities

Figure 10.5 shows that the samples with different dichromate curing agents, and/or different amounts of dichromate curing agent give lines of different slope. The slope is equal to $(58.5 n_i C_i)/(2M_i)$, and so reflects different molar concentrations of water-soluble residues. The slopes of the lines of Figure 10.5 are given in Table 10.8.

Table 10.8 also shows the concentration of added curing agent, $(n_i C_i / M_i)_o$, (in gram mol ions per cm^3 of rubber) and the experimentally determined curing agent residues. The difference in values indicates that the reaction products are

not completely soluble, or that the assumptions made concerning n_i, C_i and M_i are incorrect. It is known that insoluble Cr_2O_3 is formed which would account for some of the difference. Further, there may be side reactions, possibly leading to insoluble products. The incorporation of some of the chromium into the polymer chains via coordination bonding has also been reported[10].

TABLE 10.8

Slope of lines of Figure 10.5, and conversion to n_iC_i/M_i

n_iC_i/M_i is the experimentally determined value of curing agent residues.

dichromate type	slope	n_iC_i/M_i	$(n_iC_i/M_i)_o$
2.5% sodium	.005	.00017	.0004
7.5% sodium	.018	.00061	.001
14% sodium	.039	.00133	.002
7% calcium	.002	.00007	.0007**
7% ammonium	.0035	.00012	.001 ***

* $(n_iC_i/M_i)_o$ is the approximate amount of added curing agent converted to n_iC_i/M_i form assuming $n_i = 3, M_i = 250$

** for calcium, n_i is assumed to be 2

*** for ammonium, n_i is assumed to be 3

Units are gram mole ion/cc of rubber: slope = $29.25 n_iC_i/M_i$

There is a greater difference between n_iC_i/M_i and the amount of added curing agent for the ammonium and calcium dichromate

cured samples than for the sodium dichromate cured samples. In the case of the ammonium dichromate cured samples, possible reasons for the difference may be that organic complexes of limited solubility may be formed and/or the reaction residues may include ammonia. For the calcium dichromate cured samples, it is possible that much of the calcium dichromate has been converted to the relatively insoluble calcium hydroxide.

The number of moles of impurity per cc of rubber calculated from Figure 10.5 (n_iC_i/M_i) is plotted versus the number of moles of curing agent added per cc of rubber in Figure 10.6. It can be seen that for the sodium dichromate cured LP32, with varying amounts of the curing agent, there appears to be a linear relationship between the amount added and the amount of effective, i.e. water soluble, impurities as calculated from the slopes of the plots in Figure 10.5. The slope of the line in Figure 10.6 is 0.66, implying that 66% of the added sodium dichromate gives residues in a soluble form (including unreacted dichromate).

10.6. RELATIONSHIP BETWEEN TOTAL WATER CONCENTRATION & DIFFUSION COEFFICIENTS

10.6.1. Introduction

A plot of the diffusion coefficients (D) obtained by varying the osmotic pressure of both the internal (droplet) and external (concentration of NaCl) solutions versus total water

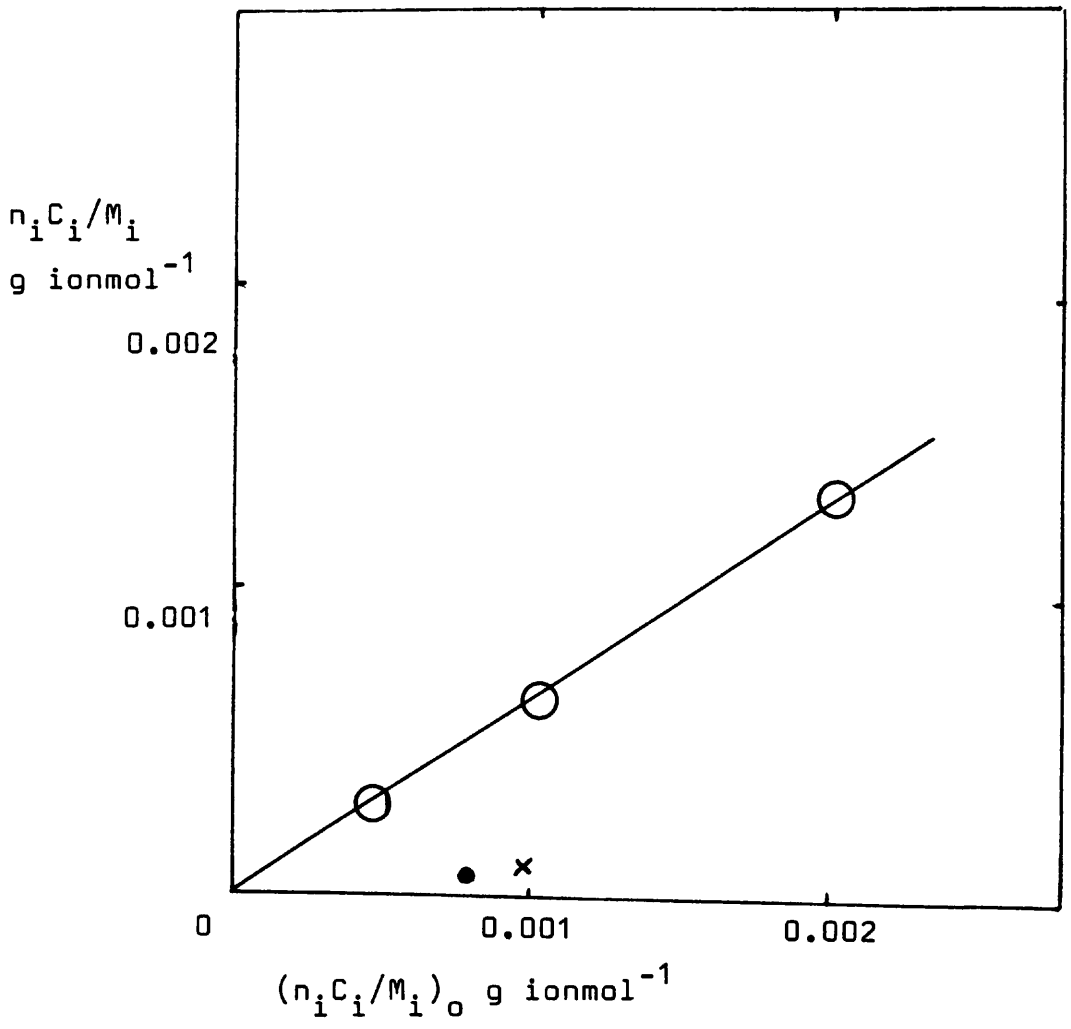

FIGURE 10.6

Plot of n_iC_i/M_i versus ($n_iC_i/M_i)_o$ (number of molar ions of a curing agent) showing that the number of moles of water soluble impurities calculated from the slopes of Figure 10.5. is related to the number of moles of dichromate added.

KEY

sodium dichromate ○

calcium dichromate ●

ammonium dichromate ×

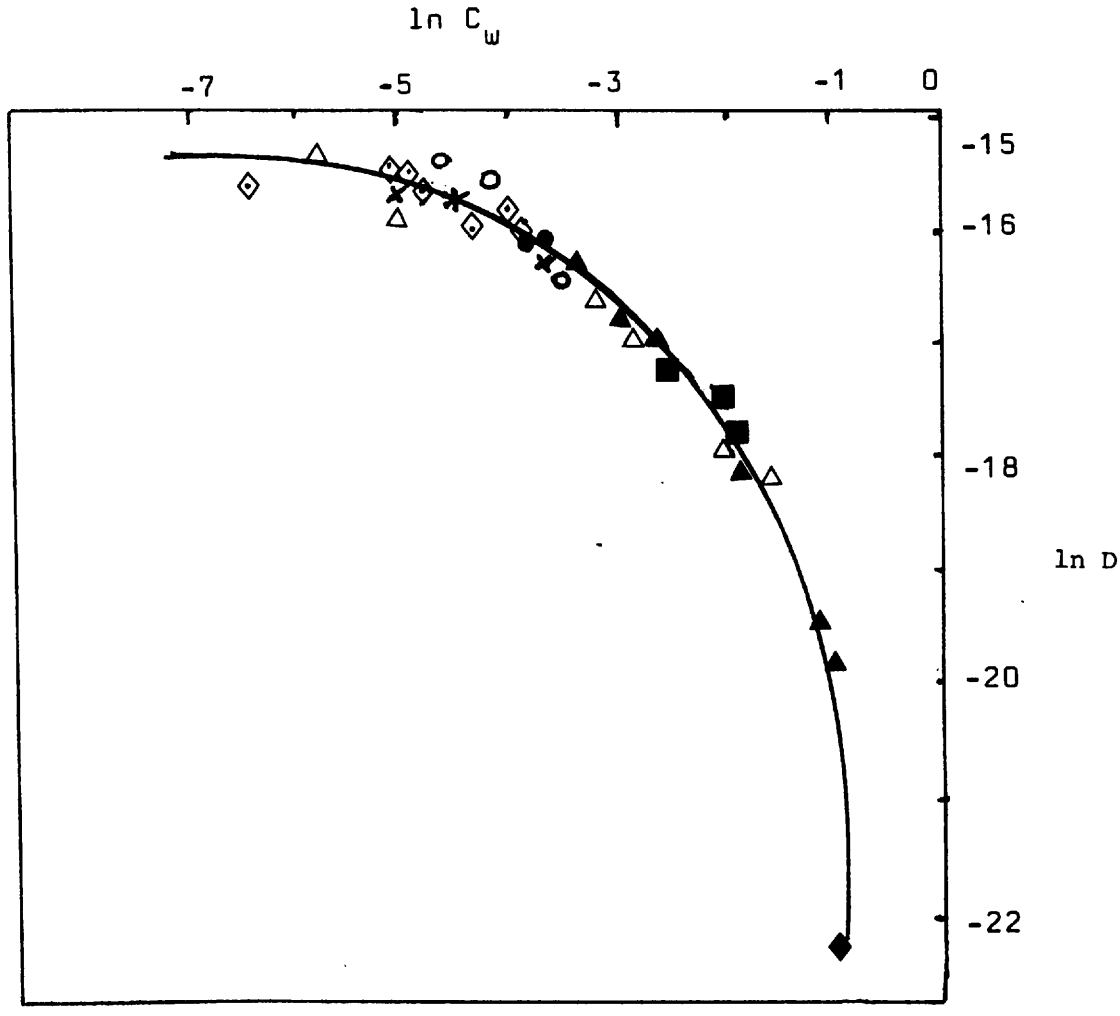

FIGURE 10.7

Plot of lnD versus $\ln C_w$ for various dichromate cured polysulphides.

KEY	mass uptake from liquid	mass uptake from vapour
PR 1422	◆	◇
14phr sodium dichromate	■	not tested
7.5phr sodium dichromate	▲	△
2.5phr sodium dichromate	●	not tested
7phr calcium dichromate	○	not tested
7phr ammonium dichromate	×	not tested

C_w values for PR1422 have been divided by 0.75 (V_r) to allow for filler volume.

concentration (C_w) is given in Figure 10.7.

Figure 10.7 shows that the diffusion coefficients obtained all have the same relationship to the total amount of water absorbed i.e. D is dependent upon C_w in the same way, even though D and C_w were determined under very different conditions viz.

a) at different water vapour pressures from the vapour phase
b) at different external osmotic pressures from the liquid phase and
c) using different amounts and type of curing agent

Further, data from the commercial sealant PR1422 is in agreement with the general trend noted for the model polysulphide rubbers.

It can be seen from Figure 10.7 that the concentration dependency is of the type that as the water concentration increases, the diffusion coefficient decreases.

Figure 10.7 suggests, however, that the relationship between D and C_w is neither linear, nor follows a power law.

10.6.2. Considerations of the relationship between D and C_w: application of Southern and Thomas equation

Southern and Thomas[4] found that the diffusion coefficient for water in natural rubber varied inversely as the square of

the water concentration in the rubber. They explained the concentration dependency noted by using the following empirical equation

$$D = D_o \; a \; s_o \; C_i/(C_w + C_i)^2 \qquad (10.7)$$

D is the experimentally determined diffusion coefficient, D_o is the diffusion coefficient when no impurities are present, s_o is the solubility at 100%RH and a is a constant.

If C_i is small relative to the water concentration, and can be ignored, then D is directly proportional to $1/C_w^2$.

In this work, the results for D and C_w, both for the model rubber and for PR1422, indicate that D does not vary in inverse proportion to the square of the total water concentration.

The main differences between natural rubber and dichromate cured polysulphide rubbers are that the polysulphide

a) probably has a greater amount of water in true solution
b) contains more impurities
c) has labile bonds.

For the case of water absorption by natural rubber, Southern and Thomas neglected the amount of water in true solution as neglible. The two experimental estimates of water in solution (s_o) in the polysulphide are approximately $10^{-2} gcm^{-3}$. C_w found varied from 10^{-2} to $10^{-1} gcm^{-3}$. Hence the water in solution cannot be ignored.

C_i in equation 10.7 cannot be ignored, since the concentration of added curing agent is of the same order of magnitude as the C_w values found. For example, the amounts of curing agent added varied from 0.03 to 0.18gcm^{-3} of rubber. This is commensurate with the C_w values found of from 0.07 to 0.4gcm^{-3} of rubber. However, if C_w in equation 10.7 is modified by the amount of water in solution and an estimate made of C_i in gcm^{-3} rubber then a plot of lnD versus $\ln(C_w-s+C_i)$ can be made.

C_i for all the samples cured with 7phr dichromate was taken as 0.09g/cc from (7/107)x 1.33. 1.33 g/cc is the average density of the cured samples. s was assumed to be constant and equal to 0.01g/cc i.e. s_o, and variations in the solubility of in the rubber due to Henry's law were ignored.

The tabulated data of $(C_w-s_o+C_i)$ and D is given in Table10.9 and a ln:ln plot of this data in Figure 10.8.

It can be seen that a linear relationship results, and that the slope is approximately -2, i.e. D is proportional to $1/(C_w-s_o+C_i)^2$.

The intercept, which is $\ln D_o a s_o$, gives $D_o a s_o$ as 5.08×10^{-10}.

The equation used is empirical and the constant a is a constant which needs to be determined empirically for different rubbers. Further, equation 10.7 expresses the concentration of impurities solely in weight terms, not as

TABLE 10.9

Data for Southern and Thomas plot, with C_w modified by C_i and the amount of water in solution in the rubber

s_o =0.01 and C_i =0.09 gcm^{-3} for 7phr dichromate

$Dx10^8$ cm^2s^{-1}	C_w g/cc	$(C_w-s_o+C_i)$ g/cc	$\ln(C_w-s_o+C_i)$	ln D
sodium				
.27	.4307	.5107	-0.67	-19.73
.32	.3691	.4491	-0.80	-19.56
1.3	.1862	.2662	-1.32	-18.16
3.2	.0991	.1791	-1.72	-17.26
4.8	.0630	.1430	-1.95	-16.85
7.1	.0395	.1195	-2.12	-16.46
calcium				
5.85	.0333	.1133	-2.18	-16.65
16.55	.0183	.0983	-2.32	-15.62
22.3	.0131	.0931	-2.37	-15.32
ammonium				
7.76	.0311	.1111	-2.20	-16.37
12.5	.0199	.0999	-2.31	-15.90
12.0	.0139	.0939	-2.37	-15.94

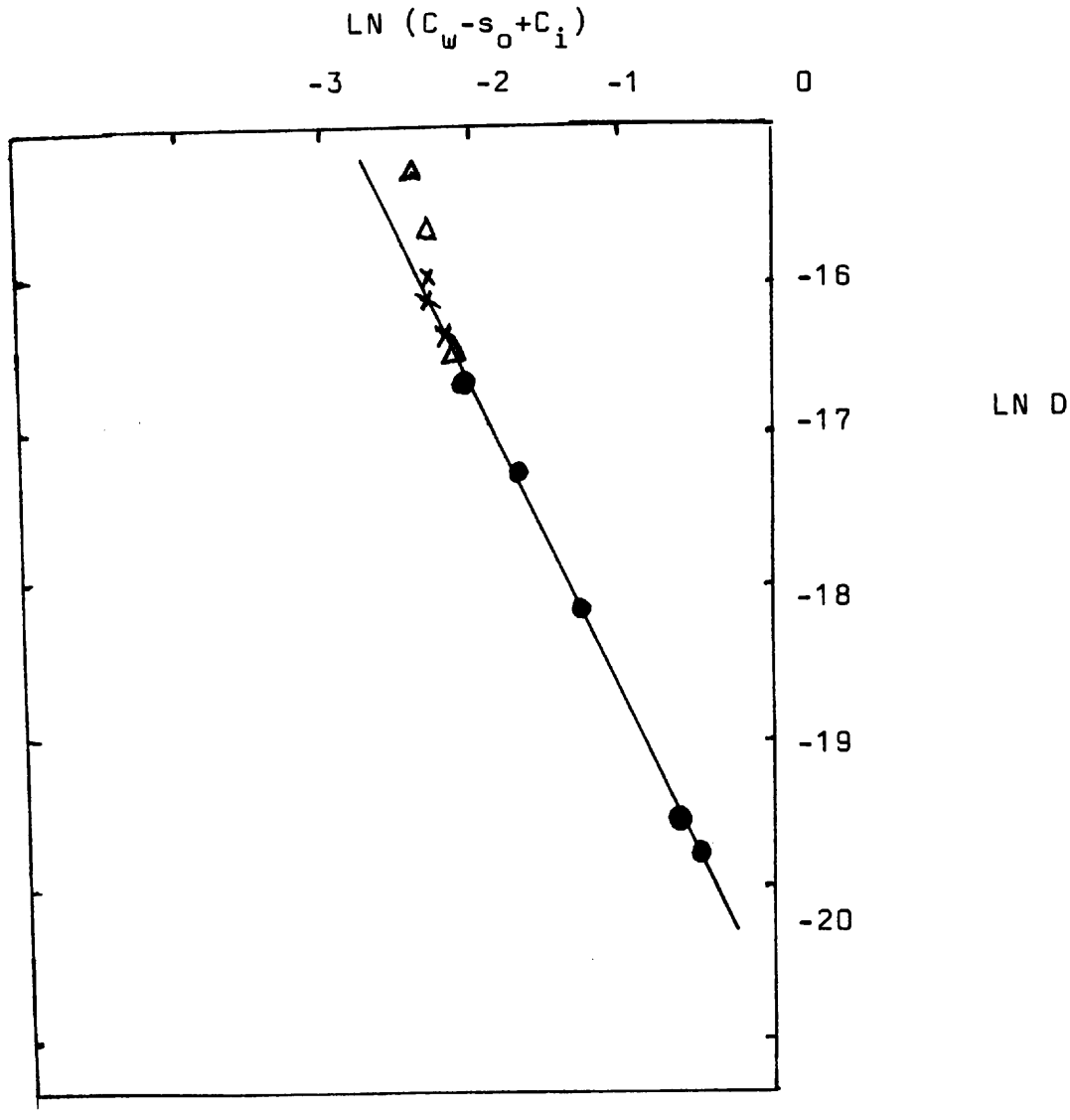

FIGURE 10.9

Plot of lnD versus ln(C_w-s_o+C_i) showing that D varies as (C_w-s+ C_i).

C_i = 0.09gcm^{-3}; s_o = 0.01gcm^{-3}.

KEY

sodium dichromate ●

calcium dichromate △

ammonium dichromate ×

molar concentrations. Evidence from most of the sections in this chapter of this work imply that C_w is dependent upon molar quantities of impurities. The data of Table 10.9 shows a good fit to equation 10.7 possibly because $(n_i C_i M_w)/M_i$ is of the same order of magnitude to C_i, since $n_i = 3, M_w = 18, M_i = 250$.

In order to obtain further information, the diffusion coefficient needs to be related to the water concentration using factors which can be determined from other properties of the impurity/rubber mix. An attempt to find such a relationship is carried out in the next section.

10.6.3. Further considerations of the relationship between D and C_w

A relationship between the observed diffusion coefficient, a constant thermodynamic diffusion coefficient, the amount of impurities and water absorbed at equilibrium is obtained (see Appendix B) by assuming

a) the water absorbed by the rubber obeys Henry's and Raoult's Laws.

b) the water in solution in the rubber surrounding the droplets and the water in the droplets are related by the change in chemical potential

c) all diffusion is through the rubber phase only

This gives the expression (ignoring the small elastic contribution):

$$D = D_T s_o [A/((C_w - s + A)^2 + A s_o)] \qquad (10.8)$$

where A is $n_i C_i M_w / M_i$

D is the observed, apparent diffusion coefficient, D_T is the thermodynamic diffusion coefficient for a rubber containing no impurities, C is concentration in g/cc of rubber, M is molecular weight, p is density. The subscripts i and w refer to impurity and water respectively. s is the solubility of water in the rubber at various external water vapour pressures, s_o is the solubility of water in the rubber at 100%RH. n is the number of ions produced by one mole of impurity. T is absolute temperature, R is gas constant , V is molar volume of water. All describe conditions at equilibrium.

Data calculated from such a relationship is shown in Table 10.10.

A plot of the reciprocal apparent diffusion coefficient against the function $(C_w - s + A)^2/A$ should give a straight line of intercept $1/D_T$ and slope $1/D_T s_o$.

A plot of $1/D$ against $(C_w - s + A)^2/A$ is shown in Figure 10.9. It can be seen that there is a reasonable fit to a straight line of slope 2.3×10^7.

The intercept was found to be 0.5×10^7 scm^{-2}.
Hence $D_T = 2 \times 10^{-7} cm^2 s^{-1}$ or $2 \times 10^{-11} m^2 s^{-1}$.
D_T found in this way is equivalent to the diffusion coefficient at zero water concentration. The value of D_T

found is in good agreement with the limiting value noted for PR1422 , of $1.6 \times 10^{-7} cm^2 s^{-1}$, and is in agreement with the diffusion coefficient found at low RH levels for sodium dichromate cured LP32 i.e. $2.2 \times 10^{-7} cm^2 s^{-1}$.

Unfortunately, the solubility found from the slope is more than an order of magnitude greater than those found from the extrapolation of low RH data and from Figure 10.5. This suggests that either

a) the approach is correct, but there is error in some of the values used. The most likely source of error is in the estimation of A.

b) the assumptions used in the derivation of the equation are invalid.

10.7. PERMEATION OF WATER VAPOUR AT VARYING VAPOUR PRESSURE THROUGH 7.5% SODIUM DICHROMATE CURED LP32

10.7.1. Introduction

It has been shown in Section 10.5 that the difference between the C_w values found for LP32 cured with different dichromate salts are due to the difference in the amounts of water-soluble reaction residues. The amount (and type) of water-soluble material dictates the relative amount of water which is in droplet form. These two factors, in turn, determine the observed, apparent diffusion coefficient found from a mass uptake experiment, since D is dependent upon C_w and C_i.

TABLE 10.10

$(C_w-s+A)^2/A$ and 1/D for various curing systems and LP32. A is $n_iC_iM_w/M_i$ calculated from the slopes of Fig.10.6, x18. s for each set of data was determined from fs_o (Appendix A)

curing agent (phr)	A gcm^{-3}	s gcm^{-3}	C_w gcm^{-3}	$(C_w-s+A)^2/A$ gcm^{-3}	1/D scm^{-2} $\times10^7$
sodium	.024	.0089	.1990	1.91	5.43
(14)		.0084	.1461	1.09	3.70
		.0070	.0744	0.35	2.78
sodium	.011	.0097	.3692	12.48	31.25
(7.5)		.0094	.1860	3.20	7.69
		.0089	.0991	0.93	3.13
		.0084	.0630	0.39	2.04
		.0070	.0395	0.17	1.42
sodium	.0032	.0094	.0620	0.97	3.44
(2.5)		.0089	.0323	0.22	0.98
		.0084	.0262	0.14	0.96
calcium	.0013	.0094	.0333	0.47	1.71
(7)		.0089	.0183	0.09	0.61
		.0084	.0131	0.03	0.45
ammonium	.0022	.0089	.0311	0.27	1.29
(7)		.0084	.0199	0.09	0.80
		.0070	.0139	0.04	0.83

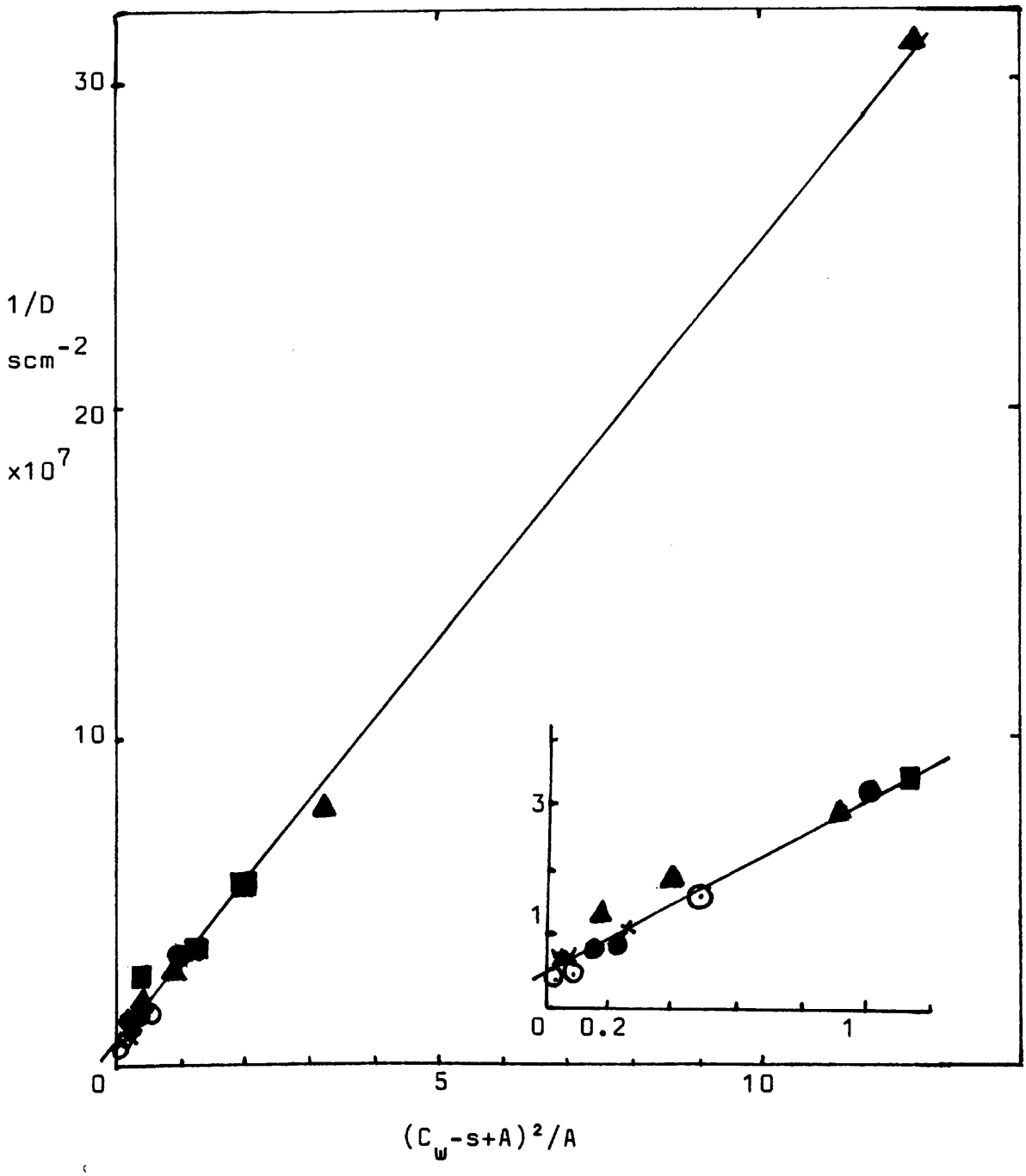

FIGURE 10.9

Plot of 1/D versus $(C_w-s+A)^2/A$ showing linear relationship

KEY

14% sodium dichromate	■
7.5% sodium dichromate	▲
2.5%sodium dichromate	●
7% calcium dichromate	○
7% ammonium dichromate	×

Permeation experiments, on the other hand, give data based primarily upon the movement of the amount of water in true solution. The water immobilised in droplet form plays only a minor role in the permeation process, once the steady state is reached.

10.7.2. Results of permeation experiments at varying relative humidity (RH) for sodium dichromate cured LP32

Permeation experiments were carried out as in section 8.2 using samples of 7.5% sodium dichromate cured LP32. Results of several experiments are given in Figure 10.10.

Permeation rates (R) were calculated from Figure 10.10 and the resultant R and relative humidity (RH) values. are given in Table 10.11.

A plot of R versus RH is given in Figure 10.11. As with PR1422 (see Section 8.6), it can be seen that at RH below about 50% there is a linear relationship between R and RH. Above about 50%RH, the increase in R with increasing RH is greater than extrapolation of the straight line.

TABLE 10.11

Permeation rates (R) at various relative humidities (RH) for 7.5% sodium dichromate cured LP32 at 30°C. Sample thickness 0.131cm and area 23.76cm^2 in all cases.

RH %	$R \times 10^9$ $gcm^{-1}s^{-1}$
20	0.82
32	1.4
42	1.8
52	3.4
75	4.1
84	4.2
91	5.2
96.5	5.7
100	6.2

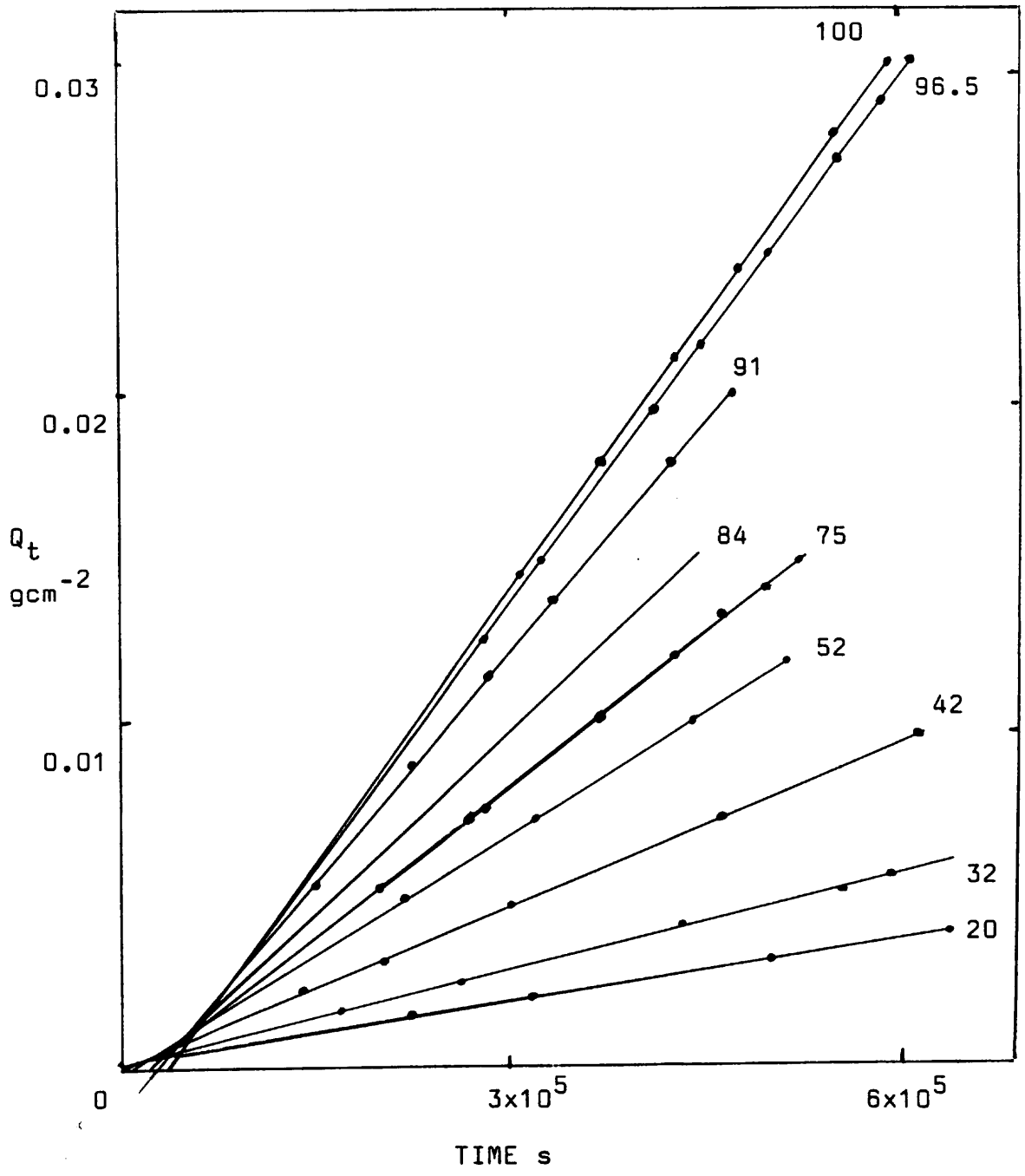

FIGURE 10.10

Plot of Q_t (mass transmitted per unit area) versus time for the permeation of water vapour through 7.5% sodium dichromate cured LP32 at various water vapour pressures at 30°C. Area of all samples = 2376mm^2. Thickness = 1.32mm. Numbers on lines refer to RH used. Some of the points have been omitted for clarity. In most cases experiments ran for 3 weeks.

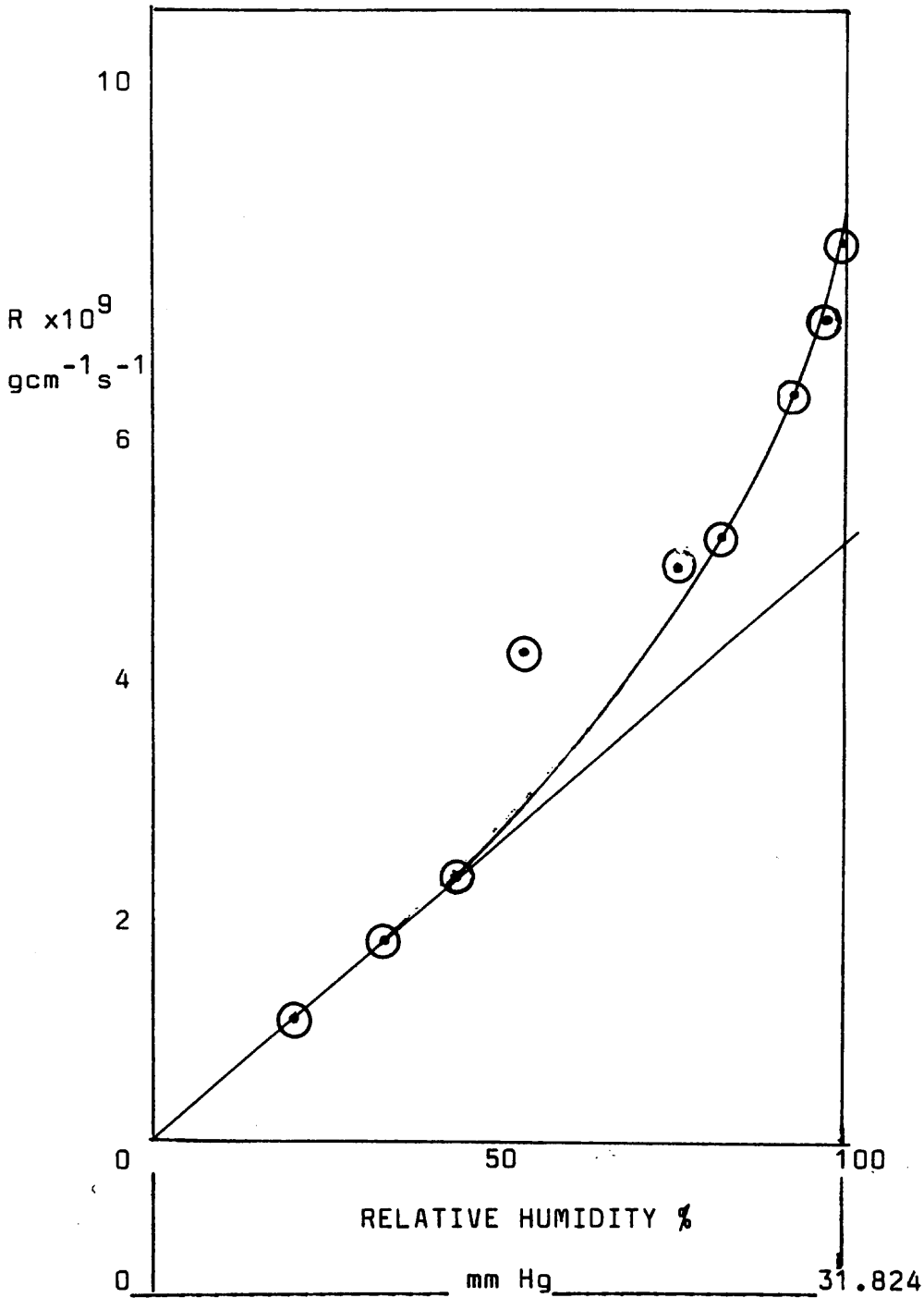

FIGURE 10.11

Plot of permeation rate (R) versus relative humidity (RH) at 30°C for 7% sodium dichromate cured LP32 showing that R is linear with respect to RH at low levels of RH.

10.8. EFFECT OF FILLER ON PERMEATION RATES

Since the experiments using different curing systems (Section 10.4) all give essentially the same s_o value, and the same relationship between D and C_w (Section 10.5), then there should be a relationship between the permeation rates of water through PR1422 and and those for sodium dichromate cured LP32 which is primarily attributable to the effect of filler on permeation.

Figure 10.12 shows a plot of the permeation rates (R) at the various relative water vapour pressures for PR1422 (R_f) plotted against the values for LP32 +7.5% sodium dichromate (R_u) for the same vapour pressures. It can be seen that a good straight line relationship is obtained, even at the higher water vapour pressures where deviations of R from linearity with respect to RH were noted for both materials.

The slope, R_f/R_u, of the line is 0.56.
The subscripts f and u refer to R of the filled and unfilled polysulphide respectively.

In the following hypothesis the same subscripts are used to denote water concentration and diffusion coefficient of the filled and unfilled polysulphide. v_r is the volume fraction of rubber in the filled samples; i.e. 1- volume fraction of filler.

It is postulated that filler has a two-fold effect on R.

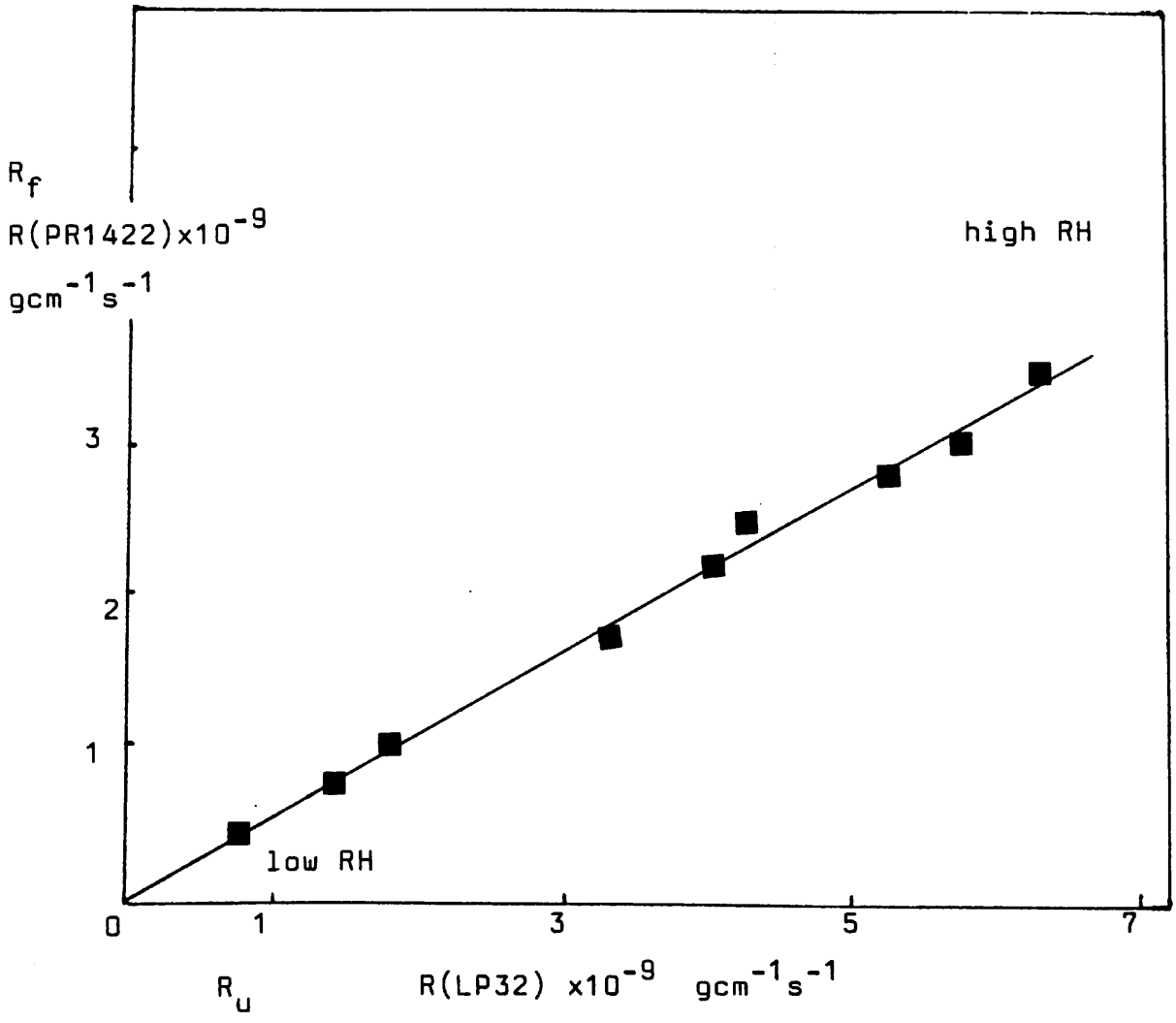

FIGURE 10.12

Plot of R(PR1422) versus R(LP32) showing that a linear relationship exists between permation data at the same relative vapour pressure for 7.5% sodium dichromate cured LP32 (no filler) and PR1422 (filled, and predominantly cured with calcium dichromate). All results obtained at 30°C and similar thickness sample. Each point on the graph represents the result obtained at the same relative humidity.

Since the permeation rate depends upon both the diffusion coefficient and the solubility, then filler will affect

a) the concentration of water in the rubber phase

b) the diffusion coefficient of the water in true solution only.

a) Effect of filler on concentration: since transport is through the rubber phase, it is assumed that major effect of filler on concentration of water in the rubber phase is, in effect to reduce the concentration of the water in true solution by the factor v_r, (modulus effects have been ignored). This is considering concentration in terms of grams of water per unit volume of the medium as a whole (i.e. including filler volume, where present, in that unit volume). This allows for changing area and distance travelled, less tortuosity effects.

Let s = water concentration (in true solution), then

$$s_f = v_r s_u \tag{10.7}$$

b) Effect of filler on diffusion coefficient: the presence of filler will reduce the diffusion coefficient because of tortuosity effects.

Using Maxwell's equation[69] then,

$$D_f = D_u(2/(3-v_r)) \tag{10.8}$$

c) Effect of filler on permeation rate: since

$$R = Ds, \tag{10.9}$$

then

$$R_f = s_f \times D_f \text{ and } R_u = s_u \times D_u \tag{10.10}$$

Hence

$$R_f = R_u v_r [2/(3-v_r)] \tag{10.11}$$

For PR1422, $v_r = 0.75$

Calculated value of R_f/R_u is 0.66

Experimentally found R_f/R_u is 0.56

Maxwell's formula assumes a filler of spherical shape, totally non-absorbant. The difference between the diffusion coefficients of aviation fuel in PR1422 and aviation fuel in PR1422 with the filler removed (chapter 3, section 3.1.11) was greater than Maxwell's formula would suggest. Similar formulae to Maxwell's have been proposed, using different filler shape factors [70-72].

Considering the assumptions made, agreement between the experimental value of R_f/R_u of 0.56 and the theoretical value of 0.66 (derived using Maxwell's formula) is surprisingly good.

Minor contributions to the differences noted may be due to

1) Crosslink density differences, with concomitant effects on both the diffusion coefficient and the amount of water in true solution,

and/or

2) possible effects on permeation rates caused by the presence of different amounts of water present in droplet form.

(1) is not very likely, since the Mooney-Rivlin plots discussed in Section 5.5 show that unfilled PR1422 and the sodium dichromate cured LP32 have essentially the same cross-link density.

(2) It has already been shown in Section 8.3.4 that at low RH it is highly unlikely that any water is present in droplet form. Since in Figure 10.12 the data at higher RH fits the line drawn through the data at low RH, this suggests that differences in the relative permeation rates due to different curing agents, (leading to differences in the relative amount of water in droplet form) are negligible i.e. if such differences had a large effect, it would be expected that deviation from the straight line in Figure 10.12 would occur at high RH.

It is concluded that, after allowing for the volume of filler, the major effect of filler on permeation rate is to reduce the diffusion coefficient by a tortuosity mechanism.

It is further concluded that if the crosslink density is the same, then the different curing agents, leading to different amounts of water in droplet form, do not strongly affect the relative permeation rates (since the difference can be accounted for by considering tortuosity effects).

10.9. EFFECT OF INCREASING RH ON PERMEATION COEFFICIENT

A plot of the permeation coefficient (P) for PR1422 and the LP32 samples versus relative humidity is shown in Figure 10.13. The permeation coefficient is the permeation rate divided by the vapour pressure.

The quantitative difference on the P axis between P(PR1422) and P(LP32) is probably due solely to filler effects, as discussed in Section 10.8. Qualitatively, the curves are similar. It can be seen that for both materials P is constant at low RH levels. However, in both cases between about 50% and 100% RH, it can be seen that P increases as RH increases.

This is the reverse of the trend noted for the diffusion coefficient, where there was a marked decrease in D with increasing RH.

The work of Barrie et al.[79,80] had shown that the presence of added impurities (sodium chloride) had no effect on permeation rate for silicone and polyisoprene rubbers. The rubbers with added salt would have water present in droplet form at high RH. For these materials, R was linear with respect to RH over the range 0 to 100% RH, for samples both with and without added NaCl. The plot of P versus RH (and R versus RH) shows that the water uptake behaviour of polysulphides differs from that of silicone and polyisoprene rubbers.

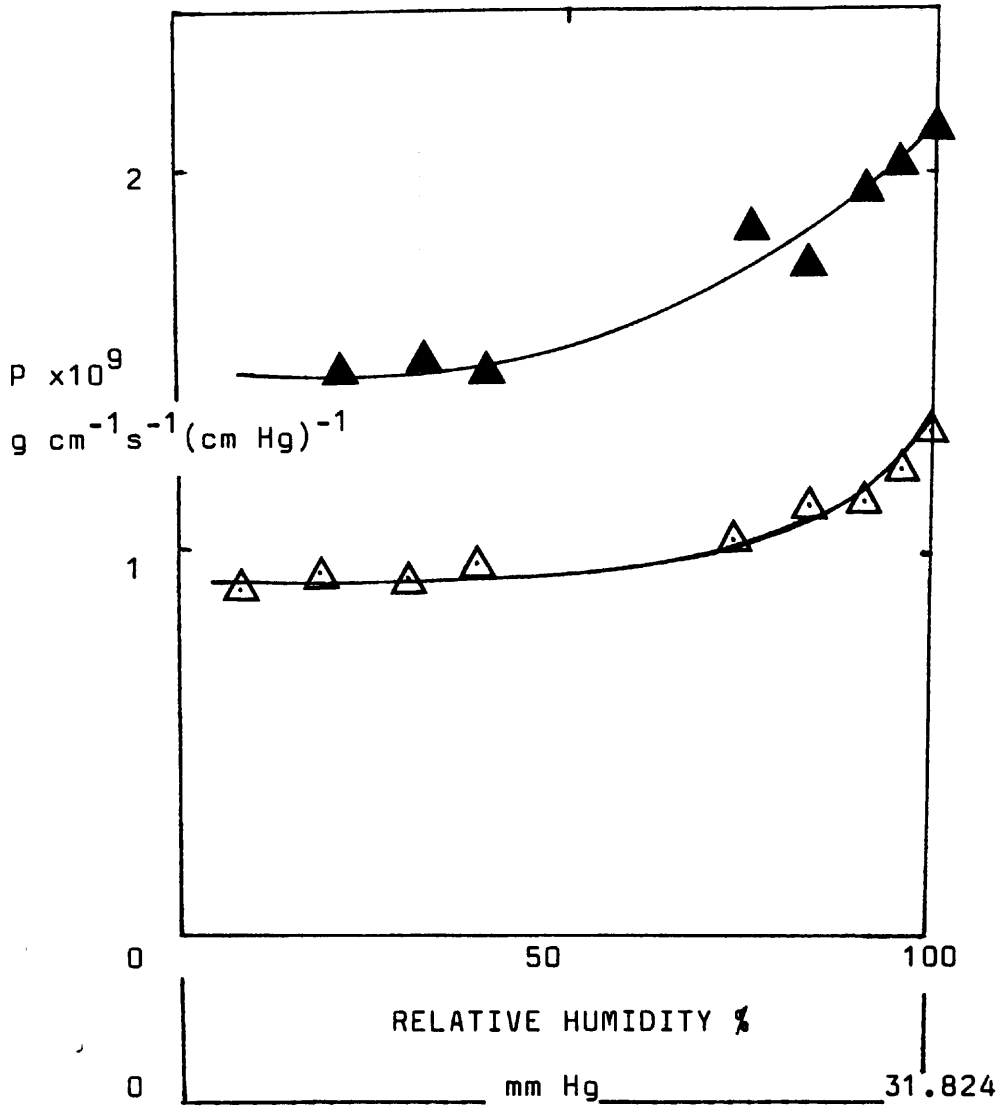

FIGURE 10.13

Plot of permeation coefficient (P) versus relative humidity (RH) for PR1422 and 7.5% sodium dichromate cured LP32 at 30°C showing that in both cases P increases from a constant level at high relative humidities.

KEY

▲ 7.5% sodium dichromate cured LP32

△ PR1422 (calcium dichromate cured)

This difference in behaviour is probably due to the higher solubility of water in polysulphide than in silicone and isoprene rubbers. For the latter, the amount of water in true solution was very low, of the order of 10^{-3} gcm^{-3}. For the polysulphide used in this work the amount of water in true solution is believed to be greater than this (of the order of $10^{-2} gcm^{-3}$). Further, the dichromate curing agents used in this work have greater solubilities than NaCl and are used in relatively large quantities.

Since it has been shown that permeation rate is dependent upon the rate of movement and the amount of water in true solution then the increase in P noted for the polysulphides must be due to:

a) an increase in the diffusion coefficient (true diffusion coefficient of the mobile water) possibly due to plasticisation of the rubber (evidence for plasticisation is given in see Chapter 5)

and/or

b) an increase in the concentration of water in true solution above that predicted by Henry's Law,

with increasing relative humidity.

The decrease in the observed D, as measured by mass uptake techniques, with increasing water concentration (increasing RH) has already been discussed. It was concluded that at high RH the presence of water droplets led to effective immobilisation of the water and hence to a reduced measured D. A slight tendency to an **increase** in D with increasing water concentration would be masked by this large effect.

It is thus concluded that there is no evidence from this work to decide which of these factors is predominant.

10.10. SUMMARY OF RESULTS OF EXPERIMENTS USING DICHROMATE CURED LP32 WITH VARYING WATER VAPOUR PRESSURE

An osmotic approach gives excellent correlation between the total amount of water absorbed at equilibrium and the difference in osmotic pressure of the internal solutions of impurities and the external soaking media.

The solubility of water in polysulphide rubbers based on LP32 is about $0.01 gcm^{-3}$.

As well as dependent upon C_w, D is also dependent upon C_i, the concentration of water-soluble reaction residues. D varies as the square of (C_w-s+A) where A is the molar concentration of impurities multiplied by the molecular weight of water.

The results of the permeation experiment suggest that tortuosity is a major factor leading to a decrease in permeation rate for the filled commercial sealant compared to unfilled sodium dichromate cured LP32.

The permeation coefficient increases at high relative humidities but the reasons for this are unclear.

APPENDIX 10.A

The osmotic pressure of a solution is given by

$$\pi = RT(\ln p_o/p)/V$$

which, using Raoult's Law, reduces to

$$\pi = RT \ln (1-x_2)/V$$

which, in dilute solutions, reduces to

$$\pi = RTx_2/V \qquad (10.A.1)$$

where x_2 is the mole fraction of solute in solution, T is absolute temperature and R is the gas constant, V is strictly the partial molar volume of water in the resulting solution, but can be approximated to the molar volume of water. The solutes involved are strong electrolytes, with high lattice energies, and here the volume on solution is not additive so this approximation is justified. Literature values for the volume of sodium chloride solutions support this view (120).

The equilibrium condition for water uptake is

$$\mu_o = \mu_i - p \qquad (10.A.2)$$

where subscripts o and i refer to the external solution and the internal solution in droplets and p is the elastic pressure.

Substituting for μ from 10.A.1 into equation 10.A.2. gives

$$x'_2RT/V = x_2RT/V - p$$

x'_2 and x_2 are the external and internal molar fractions of

solute respectively.

Rearrangment gives

$$x'_2 = x_2 - p\ V/RT \qquad (10.A.3)$$

$$\text{where } p = G/2\ (5-4/\lambda-1/\lambda^4)$$

If molar concentrations are used, then V/RT is.0073 taking R as 8.314: G is $0.8 Nmm^{-2}$. Hence pV/RT will be very small and can be neglected relative to molar fractions of about 0.1.

$$x'_2 = \frac{g_{Na}/58.5}{(g_{Na}/58.5 + 1/18)} \qquad (10.A.4)$$

$$= x_2 = \frac{C_i/M_i}{C_i/M_i + (C_w - s)/18} \qquad (10.A.5)$$

where g_{Na} is the number of grams of sodium chloride added to 1 g of water. The amount of water soluble in the rubber is s, (gcm^{-3} rubber) and C_w (gcm^{-3} rubber) is the total amount of water absorbed at equilibrium, C_i (gcm^{-3} rubber) and M_i are the concentration and molecular weight of impurity. Assuming that pV/RT can be neglected, then

$$x_2 = x'_2$$

Invertion of 10.A.4 and 10.A.5 gives

$$1 + 58.5/(18.g_{Na}) = 1 + [(C_w - s).M_i/(18.C_i)]$$

which reduces to

$$58.5/g_{Na} = (C_w - s).M_i/C_i \qquad (10.A.6)$$

To allow for the effect of the number of ions present, since strong electrolytes are involved, the molecular weights used should be divided by the number of ions (Van't Hoff factor)

then the equilibrium equation, neglecting elastic forces, becomes

$$58.5/2g_{Na} = (C_w - s)M_i/n_iC_i \qquad (10.A.7)$$

where n_i is the average number of ions produced by a mole of impurity

Unfortunately, s is a variable, dependent upon the water vapour pressure of the external solution.

Assuming that:

a) Henry's Law applies

b) Raoult's Law applies

c) the water vapour pressure within the droplets at equilibrium is the same as that of the external solution (true if osmotic pressure is the same i.e. elastic forces are negligible by comparison with osmotic forces)

Then s can be expressed thus

$$s/s_o = p/p_o = 1 - n/(n+N)$$

$$s/s_o = N/(n+N)$$

s_o is the solubility with no impurities, or the solubility at 100% RH, p and p_o here refer to water vapour pressure. n and N are the number of moles of solute and solvent respectively.

$$s = s_o\ N/(n+N) \qquad (10.A.8)$$

Let $s = fs_o$

equation 10.A.6 then becomes

$$58.5/2g_{Na} = (C_w - fs_o)M_i/n_iC_i$$

$$\text{or } C_w - fs_o = 58.5n_iC_i/(2g_{Na}M_i) \qquad (10.A.9)$$

dividing 10.A.9 through by f gives

$$C_w / f = 5850 n_i C_i / (2 g_{Na} M_i f) + s_o \qquad (10.A.10)$$

This allows s_o to be calculated if C_w and f are known.

C_w is found experimentally and f can be calculated from equation 10.A.8, for each set of data, from the strength of the external solutions.

$$f = \frac{100/M_w}{100/M_w + 2g_{Na}/58.5}$$

Table 10.A.1 shows f for the 5 solutions used.

TABLE 10.A.1

Showing conversion factor f for various salt solutions

grams of NaCl + 1g water	f
.05	0.970
.10	0.942
.20	0.890
.30	0.844
saturated $Na_2Cr_2O_7$	0.700

APPENDIX 10.B

This approach is similar to that used by Muniandy and Thomas[3], who used differentiation with respect to extension ratio. Here differentiation has been carried out with respect to water concentrations. This is because there are doubts about the restraining forces for a rubber with labile bonds.

Defining D_T as the thermodynamic diffusion coefficient for a rubber with no impurities, then the flux, F,[126] is given by:

$$F = (-D_T c/RT)(d\mu/dx)$$

where μ is the chemical potential and c is the concentration of the diffusant in terms of mass per unit volume of the rubber.

It is assumed that all diffusion takes place through the rubber phase, and hence c can be replaced by s, the concentration of the water in true solution.

$$F = (-D_T s/RT)(d\mu/dx) \qquad (10.B.1)$$

where s is the amount of water in true solution in the rubber phase, R is gas constant, T is absolute temperature, V is molar volume of water and

For one mole of water entering the droplet and going into

solution, the change in chemical potential is given by:

$$-d\mu = \mu - \mu_o = VdP \qquad (10.B.2)$$

where μ_o is the chemical potential of the water in the rubber, μ is the chemical potential of water in the droplet, P is the pressure difference, and V is the molar volume of water. This is negative, since the chemical potential of the water decreases if water is to go into the droplet from the rubber phase.

Assuming a large number of impurity sites, then the average chemical potential gradient per mole of water is

$$-d\mu u/dx = V\ dP/dx \qquad (10.B.3)$$

Substitution in 10.B.1. for $d\mu/dx$ gives

$$F = (D_T Vs/RT)(dP/dx) \qquad (10.B.4)$$

The apparent diffusion coefficient, D_a, is defined as the constant of proportionality relating the flux to the overall change in water concentration with respect to distance. Thus

$$F = -\ D_a\ dC_w/dx \qquad (10.B.5)$$

where C_w is the total amount of water absorbed per cc of rubber and includes water both in solution and in droplets. Equating 10.B.4 and 10.B.5. gives

$$D_a\ (dC_w/dx) = -(D_T Vs/RT)(dP/dx)$$

Hence

$D_a = -(D_T\ sV/RT)(dP/dx)(dx/dC_w = -D_T sV/RT(dP/dC_w)$

then $D_T cV/RT(dP/dx) = -D_a(dC_w/dx)$.

$$D_a = (-D_T sV/RT)(dP/dC_w) \qquad (10.B.6)$$

where dP/dC_w is the change in pressure with respect to total water concentration

The pressure (P) on the water in the region of the droplet is given by:

$$P = \pi_i - \pi_o - p' \qquad (10.B.7)$$

where p' is the elastic forces opposing growth of the droplet, and is $G(5-4/\lambda-1/\lambda^4)/2$. The subscripts i and o refer to the internal and external solutions.

Since the difference in osmotic forces $(\pi_i-\pi_o)$ is the +ve driving force, and p' is the force in the droplets resisting entrance of water

$$dP/dC_w = d\pi_i/dC_w - d\pi_o/dC_w - p'/dC_w \qquad (10.B.8)$$

manipulating dP/dC_w and dividing by ds gives:

$$dP/dC_w = dP/ds \times ds/dC_w$$

If it is assumed that the outside concentration remains constant, then π_o will be constant, and thus

$d\pi_o/dC_w = 0$

Therefore

$$dP/dC_w = d\pi_i/dC_w - dp'/dC_w$$

$$\pi_i = RT\ln(p_o/p)/V = RT\ln(s_o/s)/V$$

Since $p_o/p=s_o/s$ if Henry's Law is obeyed.

$d\pi_i/ds = d(RT/V\ (\ln s_o/s)/ds$

let $s_o/s = u$ $du/ds= -s_o/s^2$

$$d\pi_i/du = (RT/V)1/u$$

$d\pi_i/ds=d\pi_i/du \times du/ds$

$$= -s_o/s^2 \times (RT/V)1/u$$

$d\pi_i/ds=d\pi_i/du \times du/ds$

$$d\pi_i/ds = -s_o/s^2 \times (RT/V)s/s_o$$

$$d\pi_i/ds = -\ (RT/V)(1/s)$$

This is a negative quantity since π_i will decrease with increasing (1/s): as s decreases (1/s gets larger) more water is in droplet and osmotic pressure decreases

$$d\pi_i/dC_w = d\pi_i/ds \times ds/dC_w \qquad (10.B.9)$$

The above gives an expression for $d\pi_i/ds$; now need to know ds/dC_w.

Raoult's Law gives $(p_o-p)/p_o = n/(n+N)$ where n and N are the number of gram molecules of solute and solvent respectively and p and p_o are the vapour pressures of the solution and the pure solvent respectively.

Since Henry's Law gives $s/s_o = p/p_o$ then

$s/s_o = p/p_o = 1-n/(n+N) = N/(n+N)$

For 1cc of rubber (and assuming water density of 1g/cc)

$N = (C_w-s)/M_w$ and $n=n_iC_i/M_i$

$s/s_o = M_i(C_w-s)/(C_iM_w + M_i(C_w-s))$

Let $A = n_iC_i.M_w/M_i$

Then

$$s_o/s = 1 + A/(C_w-s)$$

Rearrange

$$C_w = As/(s_o-s) + s \qquad (10.B.10)$$

Differentiating C_w with respect to s

$$dC_w/ds = A.s_o/(s_o-s)^2 + 1$$

$$ds/dC_w = (s_o-s)^2 / [As_o + (s_o-s)^2]$$

where $A = n_iC_iM_w/C_i$

$$d\pi_i/dC_w = -RT/Vs \times (s_o - s)^2 /((s_o-s)^2 + As_o)$$

But, $s_o-s = s_oA/(C_w-s+A)$ hence substituting this

$$d\pi_i/dC_w = \frac{(-RT/Vs)\ (s_oA)^2}{(C_w-s+A)^2[(As_o + (s_oA)^2/(C_w-s+A)^2)]} \qquad (10.B.11)$$

****

Next to find dp'/dC_w

$$p' = G(5-4/\lambda - 1/\lambda^4)/2$$

$$dp'/ds = dp'/d\lambda \times d\lambda/ds$$

$$dp'/d\lambda = (G/2)(0 + 4/\lambda^2 + 4/\lambda^5)$$

$$dp'/d\lambda = 2G\ (1/\lambda^2 + 1/\lambda^5)$$

But

$$\lambda = [C_w - s)\rho_i/(\rho_w C_i) + 1]^{1/3}$$

where ρ_i is the density of the impurity and ρ_w is the density of water.

$$\text{let } \lambda = u^{1/3}$$

$$d\lambda/du = (1/3)u^{-2/3}$$

$$d\lambda/du = 1/(3\lambda^2)$$

$$d\lambda/ds = d\lambda/du \times du/ds$$

substituting $As/(s_o - s)$ for $C_w - s$ then

$$u = [As/s_o - s)\rho_i/(\rho_w C_i) + 1]$$

$$du/ds = (A\rho_i/C_i\rho_w)\ [s_o/(s_o - s)^2]$$

but $\quad dp'/ds = dp'/d\lambda \times d\lambda/du \times du/ds$

therefore

$$dp'/ds = 2G(1/\lambda^2 + 1/\lambda^5)(1/3)(\lambda^{-2})(A\rho_i/C_i\rho_w)[s_o/(s_o - s)^2]$$

let $\rho_i/c_i\rho_w = B$. Simplifying

$$dp'/ds = (2ABG/3)(1/\lambda^4 + 1/\lambda^7)(s_o/(s_o - s)^2)$$

this is +ve, since increase in p' depends on decrease in s

$$dp'/dC_w = dp'/ds \times ds/dC_w$$

$$ds/dC_w = (s_o - s)^2 / ((s_o - s)^2 + As_o)$$

Thus

$$dp'/dC_w = (2ABG/3)\ (s_o/(s_o - s)^2) \times [\lambda^{-4} + \lambda]^{-7}]$$
$$\times (s_o - s)^2 / ((s_o - s)^2 + As_o)$$

$$dp'/dC_w = (2ABG/3)\ (s_o/\ ((s_o-s)^2 + As_o)\ \times$$
$$\times\ [\lambda^{-4} + \lambda^{-7}]$$

$$dP/dC_w = d\pi_i/dC_w - dp'/dC_w$$

$$dP/dC_w = -RT/Vs \times (s_o - s)^2 /((s_o-s)^2 + As_o) -$$
$$[(2ABG/3)\ (s_o/\ ((s_o-s)^2 + As_o)$$
$$\times\ (\lambda^{-4} + \lambda^{-7})]$$

****

$$D_a = (-D_T sV/RT)(dP/dC_w)$$

$$D_a = (D_T)(s_0-s)^2/((s_o - s)^2 + As_o)$$
$$-$$
$$[(-D_T sV/RT)(2ABG/3)\ (s_o/(s_o-s)^2 + As_o)\ \times$$
$$(\lambda^{-4} + \lambda^{-7})]$$

$s = [s_o(C_w-s)]/(C_w-s+A)$ and $-(-) = +$

$$D_a = (D_T)(s_0-s)^2/((s_o - s)^2 + As_o)$$
$$+$$
$$(D_T V/RT)(2ABG/3)\ [s_o(C_w-s)]/(C_w-s+A)\ (s_o/(s_o-s)^2 + As_o)\ \times$$
$$[\lambda^{-4} + \lambda^{-7}]$$

last two terms are $(1/\lambda^4 + 1/\lambda^7)$ and C_w-s is $(1/B)(\lambda^3-1)$ from $\lambda^3-1 = (C_w-s)p_i/(p_w C_i)$

and B is $p_i/C_i p_w$

then $(1/B)(\lambda^3-1)(1/\lambda^4+1/\lambda^7) = (1/B)(1/\lambda - 1/\lambda^7)$

$$D_a = (D_T)(s_o-s)^2/((s_o-s)^2 + As_o)$$

$$+$$

$$(D_T V/RT)(2ABG/3)\ (1/B)\ s_o/(C_w-s+A)\ (s_o/(s_o-s)^2 + As_o) \times [\lambda^{-1} - \lambda^{-7}]$$

$$D_a = (D_T)(s_o-s)^2/((s_o-s)^2 + As_o)$$

$$+$$

$$[(D_T V/RT)(2AG/3)s_o]/(C_w-s+A) \times (s_o/(s_o-s)^2 + As_o) \times (\lambda^{-1} - \lambda^{-7})]$$

but $\lambda^3 = [(C_w-s)p_i/(p_w C_i)]+1 \quad = [(C_w-s)B]+1$ hence

$$D_a = (D_T)(s_o-s)^2/((s_o-s)^2 + As_o)$$

$$+$$

$$[(D_T V/RT)(2AG/3)(s_o/(C_w-s+A)] \times (s_o/(s_o-s)^2 + As_o) \times [[C_w-s)B+1]^{-1/3} - [C_w-s)B+1]^{-7/3}]$$

Since $s_o-s = s_o A/(C_w-s+A)$

$$D_a = D_T\ s_o A/[(C_w-s+A)^2 + As_o]$$

$$+$$

$$(2D_T AVG/3RT)[s_o{}^2/(C_w-s+A)] \times (C_w-s+A)^2)/(As_o(C_w-s+A)^2+(s_o\ A)^2) \times [(C_w-s)B+1]^{-1/3} - [C_w-s)B+1]^{-7/3}]$$

$$D_a = D_T\ s_o A/[(C_w-s+A)^2 + As_o]$$ Due to Osmotic Contribution

$$+$$

$$D_T(2VG/3RT)[s_o(C_w-s+A)]\ /[(C_w-s+A)^2+s_o A] \times [(C_w-s)B+1]^{-1/3} - [(C_w-s)B+1]^{-7/3}]$$ Due to elastic Contribution

where $B = p_i/C_i p_w$ and $A = n_i C_i M_w/M_i$

CHAPTER 11. CONCLUSIONS AND SUGGESTIONS FOR FURTHER WORK

11.1. CONCLUSIONS ON THE TRANSPORT OF AVIATION FUEL IN POLYSULPHIDE RUBBERS

The diffusion of aviation fuel in polysulphide rubbers cured with dichromate curing agents follows a straightforward Fickian pattern. For the commercial sealant PR1422 the value of D found was $1 \times 10^{-8} cm^2 s^{-1}$ and M_{∞} was about 4% by weight.

To a close approximation concentration dependency is negligible and the diffusion coefficients determined

a) by different methods

b) at different concentrations

are in agreement with each other. The concentration profile is in good agreement with that predicted from the theoretical equations. Temperature dependence of the diffusion coefficient is in accordance with an Arrhenius type equation. Since an increase in temperature does not lead to an increase in the amount of aviation fuel absorbed, it appears unlikely that there is any significant concentration dependency at raised temperatures. Further, there is close agreement between values of D and equilibrium uptake obtained for polysulphides with different curing agents.

For the case of aviation fuel, it is thus simple to predict the extent of penetration, time to equilibrium etc from the experimentally determined diffusion coefficient and the specimen geometry. Predictions of behaviour at different

temperatures can also be made, and changes in curing agent do not cause significant changes in the pattern of diffusion.

11.2. CONCLUSIONS ON THE MASS UPTAKE OF WATER BY POLYSULPHIDES

11.2.1. Mass uptake from distilled water

The diffusion behaviour of water in polysulphides differs from that of aviation fuel in several respects. Three main differences are

a) the amount of water absorbed is very high. For example, the mass uptake on immersion of PR1422 in water is greater than 200% for thin sheet.

b) Equilibrium is not achieved within a year. As a corollary to this, since the approach to equilibrium occurs over a long time, the inference is that the diffusion rate is very low. The molecular size of the water molecules is smaller than that of the aviation fuel, and it would be expected, therefore, that the rate of movement of water molecules would be greater than that of the molecules of aviation fuel.

c) desorption is faster than absorption.

11.2.2. Effect of the mass uptake of water on the physical properties of polysulphide rubber

The cohesive and adhesive strength of PR1422 fall on absorption of water and at high absorption the effects are

irreversible.

Small amounts of absorbed water lead to a large reduction in the shear modulus, G. For example, for PR1422 G is reduced from 1.7 Nmm^{-2} to 1.3 Nmm^{-2} after 5% water uptake.

The deterioration in physical properties on uptake of water appears to be due to plasticisation of the rubber. Evidence of this is that after uptake of water

a) the slope of Mooney-Rivlin plots (C_2) decreases

b) hysteresis decreases

c) stress relaxation times decrease

d) resilience increases.

Evidence from Mooney-Rivlin data suggests that much of the bonding is of a physical, as opposed to chemical, nature and it is these bonds which are weakened on uptake of water.

11.2.3. Mass uptake from sodium chloride solutions and the vapour phase

Mass uptake experiments were carried out, from both the liquid and vapour phase, on PR1422 (cured predominantly with calcium dichromate) and model rubbers based on the liquid polysulphide LP32 cured with different curing agents. For PR1422, in 1% NaCl solution, an equilibrium uptake of 15% by weight of water was reached within 3 weeks, enabling D to be calculated. The value found was 1.3 $\times 10^{-10} cm^2 s^{-1}$ at 25°C.

The reduction in the amount of water absorbed after immersion in salt solution is evidence for the importance of osmotic (vapour pressure) effects.

Compared to the results obtained for aviation fuel,

a) the amount absorbed at equilibrium is high and depends on the concentration of the soaking solution
b) D for desorption is greater than D for absorption
c) the diffusion coefficient, D, varies with the method of measurement (absorption, desorption or permeation experiment) and the conditions of the experiment
d) as found from mass uptake experiments, D varies inversely as C_w

Explanations for both the high equilibrium uptake (C_w) and the low diffusion coefficient have been made in terms of droplets of aqueous solution which form around occluded hydrophilic impurities within the rubber. The bulk of the absorbed water is within the droplets, not in true solution. It has been shown in this work that the main factor controlling the amount of water absorbed at equilibrium is the type and amount of curing agent residues. This factor determines the molar concentration of the solutions formed in the droplets. The elastic forces restraining the size of the droplets appear to be so small that they can be neglected. This is because polysulphide sealants contain labile bonds.
In this work, two equations have been derived to predict C_w, the total amount of water absorbed at equilibrium, expressed in terms of gcm^{-3} rubber.

i) For uptake from the vapour phase, at a given external vapour pressure, a modified form of Raoult's Law has been used to give an expression which relates C_w to the external vapour pressure (RH) thus:

$$C_w = (kM_w RH)/(100-RH) \qquad (11.1)$$

where $k = n_i C_i / M_i$

n is number of ions produced, C is concentration in gcm^{-3} of the rubber and M is the molecular weight. Subscripts i and w refer to water-soluble impurity and water. RH is relative humidity (%).

ii) For uptake from the liquid phase, an osmotic approach is more suitable. The equilibrium condition is given by

$$C_w = K/g_{salt} \qquad (11.2)$$

where $K = (M_{salt} n_i C_i)/(n_{salt} M_i)$

the symbols used are as above, and g_{salt} refers to the concentration, in gcm^{-3} water, of the salt in the external soaking medium.

b) The diffusion coefficient (D) of water in polysulphide rubbers, as determined from mass uptake measurements, shows strong dependency upon the concentration of the water within the rubber. There is a change of 3 orders of magnitude for D between results obtained at high concentration of water within the rubber and those obtained at low concentration. The concentration dependency is of the type that as C_w increases, then D decreases. For the mass uptake experiments the effect of droplets is to greatly slow down the apparent diffusion rate.

An equation has been derived, which shows that D is dependent upon C_w and C_i, the effective concentration of water-soluble curing agent residues. The expression used is;

$$D = D_T A s_o / [(C_w - s + A)^2 + A s_o)] \qquad (11.3)$$

where D is the observed diffusion coefficient, D_T is the thermodynamic diffusion coefficient, taken as equivalent to the diffusion coefficient of a rubber without water-soluble impurities i.e. equivalent to the diffusion coefficient at zero water concentration. s and s_o are the water in true solution at different RH levels and 100%RH respectively $A = n_i C_i M_w / M_i$

Equation 11.3 can be used to predict D for different impurity and water concentrations, if D_T and s_o are known. For the dichromate cured polysulphide rubbers used in this work, s_o was found to be $0.01 gcm^{-3}$ rubber, and D_T was found to be $2 \times 10^{-7} cm^2 s^{-1}$.

11.2.4. Permeation of water in polysulphides

The permeation coefficient was found to be of the order of $10^{-9} g.cm^{-1} s^{-1}$ (cm Hg)$^{-1}$ at 30°C and 100%RH.

There is a small increase in the permeation coefficient with increasing water concentration. There is insufficient evidence from this work to decide whether this is due to an increase in D with rising concentration and/or to the solubility not obeying Henry's Law.

The diffusion coefficients obtained from permeation experiments do not vary to any great extent with changing water concentration. This is because diffusion takes place primarily through the rubber matrix and hence the effect of droplets of solution on the observed diffusion rate is negligible for a permeation experiment.

The main effect of filler on permeation rates is to reduce the rate by a tortuosity mechanism.

11.3. SUGGESTIONS FOR FURTHER WORK

Although this work has clarified much of the puzzling behaviour and effects of high water uptake by polysulphide rubbers, there are still some areas where further work is required to either quantitatively explain some of the behaviour, or to decide on the relative importance of more than one effect.

11.3.1. Effect of polar solvents on physical properties

Confirmation of the results of tests on physical properties which point to plasticisation could be carried out using other polar, in particular, hydrogen bonding, solvents. The use of a solvent with a low freezing point, such as iso-propyl alcohol, could be used to determine whether there is a reduction of T_g after high absorption. This would be strong evidence for a plasticisation mechanism.

11.3.2. Reaction products

Chemical analysis of reaction products from dichromate salts with mercaptans of varying type and chain length could help to establish the reaction residues for polysulphides. More precise knowledge of the reaction residues, in particular their composition and solubility, could then be used to predict water uptake using equations 11.1 and 11.2.

11.3.3. Direct measurement of s, the amount of water in true solution, in polysulphide rubbers.

One major problem in this work is to distinguish between the amounts of water present in true solution and droplet form. Preparation of an ultra-pure polysulphide might produce a rubber in which droplets would not form. The preparation could be achieved by using a peroxide cured system, and repeated washing of the rubber in a suitable solvent. Such a rubber would possibly behave in an ideal fashion and mass uptake experiments from the vapour phase should establish whether the soluble water in the rubber obeys Henry's Law.

11.3.4. Measurement of the relative importance of factors leading to an increase in P with increasing relative humidity.

As described in Section 10.9, the increase in P with increasing relative humidity may be due to an increase in D with increasing water concentration. In this work any

tendency for D to increase with increasing concentration is masked by the effect of droplets (which cause a marked decrease in D with increasing concentration). However, two factors could lead to an increase in the diffusion coefficient

i) plasticisation of the rubber

ii) droplets of solution causing an easier pathway

i) Again by using a purified, peroxide cured polysulphide, measurement of D, from mass uptake experiments from the vapour phase, at various RH levels, would establish whether there was an increase in D with increasing RH for a rubber with water only in true solution. This would establish whether plasticisation was a major factor leading to an increase in D.

ii) Movement of water through the water droplets would be expected to cause a increase in D. There are thermodynamic restrictions on water entering and leaving droplets once a steady state has been set up, but the labile bond system of the polysulphide systems would allow for this possibility.

To establish whether (ii) is an important factor, further permeation experiments with varying known amounts of impurity (added to the purified sample above) and comparison with the results of (i) would then establish if there are additional effects due to water in droplet form.

REFERENCES

1	Bertozzi ER	Rubber Chem. & Tech. 41 114 (1968)
2	Southern E & Thomas AG	Water in Polymers, ACS Symp.Series 127 375 (1979)
3	Muniandy K & Thomas AG	TransIMarE(C) 97 Conf2 paper13 87 (1985) and Polymer 28 408 (1987)
4	Fedors RF	Polymer 21 207 (1980)
5	Gregory C & Seegman I	US Patent 2,787,608 (1957)
6	Patrick JC & Mnookin NM	British Patent 302,270 (1927)
7	Patrick JW & Ferguson AR	US Patent 2,466,963 (1949)
8	Panek JR	Polyethers PtII, ed. Gaylord EG Intersci. NY (1962)
9	Mukanyama T & Endo T	Bull. Chem. Soc. Japan 40 2388 (1967)
10	Averko-Antonovich LA, Minkin VS & Kirnichnikov BA	Int. Rubber Conference Kiev (1978) and Poly. Sci. USSR 19 1826 (1977)
11	Stern MD & Tobolsky AV	J. Chem. Phys. 14 93 (1946)
12	Andrews RD & Tobolsky AV	J. Chem. Phys. 11 125 (1945)
13	Colodny PC & Tobolsky AV	J. Am Chem. Soc. 79 4320 (1957)
14	Gee G	Trans. Farad. Soc. 40 468 (1944)
15	Hildebrand J & Scott R	The Solubility of Non-electrolytes Reinhold, NY 3rd ed. (1949)
16	Flory PJ & Rehner J.	J. Chem. Phys. 11 521 (1943)
16a	Flory PJ	J. Phys. Chem. 18 108 (1950)
17	Rodriguez F	Principles of Polymer Systems McGraw Hill (1983)
18	van Amerongen GJ	J. Appl. Phys. 17 972 (1946)
19	Barrer RM, Barrie JA & Rogers MG	J. Poly. Sci. A1 2665 (1963)

20	Barrer RM, Barrie JA & Raman NK	Rubber Chem. & Tech. 36 642 (1963)
21	Kraus G	J. Appl. Poly. Sci. 7 861 (1963)
22	Porter M	Rubber Chem. & Tech. 40 866 (1967)
23	Lorenz O & Parks CR	J. Poly. Sci. 50 299 (1961)
24	Stout RJ	13th SAMPE Tech. Conference (1981)
25	Ramaswamy R & Achery PS	J. Appl.Poly. Sci. 30 3569 (1985)
26	Mueller WJ	Rubber Age 81 982 (1957)
27	Crank J & Park GS (ed.)	Diffusion in Polymers, Academic Press (1968)
28	Fourier JB	Theorie Analytique de la Chaleur, Oeuvres de Fourier 1822
29	Fick A	Ann. der Phys. Lpz. 94 59 (1855)
30	Crank J	Mathematics of Diffusion OUP (1956)
31	Carslaw HS & Jaeger JC	Conduction of Heat in Solids OUP (1956)
32	Einstein A	Zeits fur Electrochemie 14 235 (1908)
33	Eyring H, Glasstone S & Laidler KJ	The Theory of Rate Processes McGraw and Hill (1941)
34	Barrer RM & Skirrow GJ	J. Poly. Sci. 3 549 (1948)
35	Brandt W	J. Phys. Chem. 63 1080 (1959)
36	Bueche F	J. Chem. Phys. 26 1850 (1953)
37	Wilkens JB & Long FA	Trans. Farad. Soc. 53 1454 (1957)
38	Fujita H	Fortsch. Hochpolym. Forsch 3 1 (1961)
39	Fujita H, Kishimoto A & Matsumota K	Trans. Farad. Soc. 56 424 (1960)
40	Meares P	J. Am. Chem. Soc. 76 3145 (1954)
41	Crank J & Park GS	Trans. Farad. Soc. 45 240 (1949)
42	Carpenter AS & Twiss DF	Ind. Eng. Chem. Anal. Ed. 12, 99 (1940)
43	Rogers WA, Buritz RS & Alpert D	J. Appl. Phys. 25 868 (1954)

44 Hartley GS & Crank J — J. Trans. Farad Soc. 45 801 (1949)

45 Mills R — J. Phys. Chem. 67 600 (1963)

46 Bearman RJ — J. Phys. Chem. 65 1961 (1961)

47 Pattle RE, Smith PJA & Hill RW — Trans. Farad. Soc. 63 2389 (1967)

48 Park GS — Trans. Farad. Soc. 48 11 (1952)

49 Daynes HA — Trans. Farad. Soc. 33 531 (1937)

50 Becker R — Trans. Farad. Soc. 29 245 (1937)

51 Petropolous JH — J. Poly. Sci. Phys. 12 35 (1974)

52 Southern E — PhD Thesis U of London (1969)

53 Boltzmann L — Ann. Phys. Lpz. 53 959 (1894)

54 Hayes MJ & Park GS — Trans. Farad. Soc. 52 949 (1956)

55 Garrett TA & Park GS — J. Poly. Sci. C16 601 (1966)

56 Southern E & Thomas AG — Trans. Farad. Soc. 63 1913 (1967)

57 Hansen CM — Poly. Eng. Sci. 20 252,259 (1980)

58 Crank J & Robinson C — Proc. Roy. Soc. A204 549 (1951)

59 Prager S & Long FA — J. Am. Chem. Soc. 73 4072 (1951)

60 Aitken A & Barrer RM — Trans. Farad. Soc. 51 116 (1955)

61 Auerbach I, Miller WR, Kuryla WC & Gehman SD — J. Poly. Sci. 28 129 (1958)

62 Buckley DJ & Berger M — J. Poly. Sci. 56 175 (1968)

63 Koszinowski J — J. Appl. Poly. Sci. 31 1805 (1986)

64 van Amerongen GJ — Rubber Chem. & Tech. 37 1065 (1964)

65 Barrie JA & Platt B — Polymer 4 303 (1963)

66 Gan ST — PhD Thesis U of London 1981

67 Salame M — PRI. Conference diffusion in Polymers (1986)

68 Barrer RM — Chapter 6 of reference 27

69 Maxwell JC — Electricity and Magnetism Vol I Dover Publishing Company (1891)

70 Fricke H — Physics 1 1067 (1931)

71 Bruggeman H — Ann. der Phys. V 24 636 (1936)

72 Meares P J — J. Appl. Poly. Sci. 9 917 (1965)

73 Wroblewski S — Ann. Phys. Lpz. 8 29 (879)

74 Comyn J (ed) — Polymer Permeability Elsevier Applied Science Publishers London (1984)

75 Obach C — Cantor Lecture on Gutta Percha 100 (1898)

76 Lowry HH & Kohmann GT — J. Phys. Chem. 32 23 (1927)

77 Taylor RM, Herriman DB & Kemp AR — Ind. Eng. Chem. 28 1255 (1938)

78 Tester DA — J. Poly. Sci. 19 535 (1956)

79 Barrie JA & Machin D — J. Macromol. Sci. Phys B3(4) 645 (1969)

80 Barrie JA, Machin D & Nunn A — Polymer 16 811 (1975)

81 Briggs GJ, Edwards DC & Storey EB — Proc. 4th Rubber Tech. Conference London 362 (1962)

82 Gent AN & Lindley PB — Proc. Roy.Soc.A 249 195 (1958)

83 Aminabhavi TM, Thomas RW & Cassidy PE — Poly. Eng. Sci. 24 1417 (1984)

84 Helander RD & Tolley WB — Proc. 29th Nat. SAMPE Symposium (1984)

85 Schultz J., Papirer E & Jacquemont C — Eur. Poly. J. 22 499 (1986)

86 Averko-antonovich AL — Kauch.Rezina 27 11 (1968)

87 Mukhurdinova C — Vysok. Soedin. 20 3 (1978)

88 Hanhela PJ, Huang RHE & Brenton Paul D — MRL 658 Australia 1984

89 Hanhela PJ, Huang RHE, Brenton Paul D & Symes TEF — J. Appl. Poly. Sci. 32 5415 (1986)

90 Barrer RM & Ferguson RR — Trans. Farad. Soc. 54 989 (1958)

91 Gillespie T & Williams WM J. Poly. Sci. A1 4 933 (1966)

92 Robinson C Proc. Roy. Soc. A204 339 (1950)

93 Hutcheon AT, Kokes RJ, Hoard JL & Long FA J. Chem. Phys. 20 1232 (1952)

94 Sergeant A & Ashbee ADZ J. Adhesion 18 217 (1985)

95 Grun F Experientia 3 490 (1947)

96 Wang FW & Howell BF Polymer 23 11 (1984)

97 Bartell D & Graessley C J. Poly. Sci. Phys. 24 2057 (1983)

98 Barrer RM, Barrie JA & Slater J J. Poly. Sci. 27 177 (1958)

99 Rosen B J. Poly. Sci. 35 335 (1959)

100 Newns AC J. Textile Inst. 41 T269 (1950)

101 Treloar LRG Physics of Rubber Elasticity Clarendon Press (1975)

102 Orwoll RA Rubber Chem. Tech. 50 451 (1977)

103 Bristow GM & Watson WF Trans. Farad. Soc. 54 1731 (1958)

104 Day J & Thomas DK RAE Tech. Report 75104 (1975)

105 Khan Khadim AH PhD Thesis (CNAA) (1967)

106 Methods of regulating relative humidity ASTM E 104 (1976)

107 Aubrey DW, Welding GN & Wong T J. Appl. Poly. Sci. 13 244 (1969)

108 Fujita H Chapter 3 of ref.27

109 Panek JR (ref. 8) private communication

110 Handbook of Chemistry and Physics Chemical Rubber Pub. Ohio 34th ed. 1952

111 Othmer K Materials & Tech.4 Petroleum Org. Chem. Longman 1972

112 DW Aubrey private communication

113 Hanhela et al MRL 655 Australia (1979)

114 Singh H Rubber World August 32 (1987)

115 Korvezee AE & Mol EA J. Poly. Sci. 2 371 (1947)

116 Ito Y Chem. High Poly. 17 397 (1960)

117 von Schroeder P Z. Phys. Chem. 45 75 (1903)

118 Musty JWG, Pattle RE & Smith PJA J. Appl. Chem. 16 221 (1966)

119 Wolf A Kautschuk & Gummi 36 805 (1985)

120 International Critical Tables NRC McGraw-Hill (1926)

121 Glasstone S Textbook of Physical Chemistry van Nostrand NY 1940

122 Hinkley JA & Holmes BS J. Appl. Poly. Sci. 32 4873 (1986)

123 Frensdorff HK J. Poly. Sci. 2A 341 (1964)

124 Barrer RM Trans. Farad. Soc. 35 628, 644 (1939)

125 Cassidy P & Aminabhavi TM Polymer Communications 27 255 (1986)

126 Park GS Trans. Farad. Soc. 46 684 (1950)